
DOE/ASME NGNP/Generation IV Materials Project DE-FC07-05ID14712

Final report on Task 10 submitted to ASME ST-LLC

# Update and Improve Subsection NH – Alternative Simplified Creep-Fatigue Design Methods

September 30, 2009

Tai Asayama
Japan Atomic Energy Agency

## Record of Revisions

| Revision | Date | Description of change |
|---|---|---|
| 0 | March 31, 2009 | Preliminary daft |
| 1 | April 24, 2009 | Draft for review |
| 2 | August 10, 2009 | Comments partially resolved |
| 3 | September 30, 2009 | Comments resolved |
| 4 | October 26, 2009 | Final report |

## Executive summary

This report described the results of investigation on Task 10 of DOE/ASME Materials NGNP/Generation IV Project based on a contract between ASME Standards Technology, LLC (ASME ST-LLC) and Japan Atomic Energy Agency (JAEA). Task 10 is to Update and Improve Subsection NH – Alternative Simplified Creep-Fatigue Design Methods.

Five newly proposed promising creep-fatigue evaluation methods were investigated. Those are 1) modified ductility exhaustion method, 2) strain range separation method, 3) approach for pressure vessel application, 4) hybrid method of time fraction and ductility exhaustion, and 5) simplified model test approach.

The outlines of those methods are presented first, and predictability of experimental results of these methods is demonstrated using the creep-fatigue data collected in previous Tasks 3 and 5. All the methods (except the simplified model test approach which is not ready for application) predicted experimental results fairly accurately. On the other hand, predicted creep-fatigue life in long-term regions showed considerable differences among the methodologies. These differences come from the concepts each method is based on.

All the new methods investigated in this report have advantages over the currently employed time fraction rule and offer technical insights that should be thought much of in the improvement of creep-fatigue evaluation procedures.

The main points of the modified ductility exhaustion method, the strain range separation method, the approach for pressure vessel application and the hybrid method can be reflected in the improvement of the current time fraction rule. The simplified mode test approach would offer a whole new advantage including robustness and simplicity which are definitely attractive but this approach is yet to be validated for implementation at this point.

Therefore, this report recommends the following two steps as a course of improvement of NH based on newly proposed creep-fatigue evaluation methodologies. The first step is to modify the current approach by incorporating the partial advantages the new method offer, and the second step is to replace the current method by the simplified test approach when it has become technically mature enough.

The recommendations are basically in line with the work scope of the Task Force on Creep-Fatigue of the Subgroup on Elevated Temperature Design of the Standards Committee of the ASME Boiler and Pressure Vessel Committee Section III.

## Acknowledgement

The author is grateful to Mr. Takehiko Kato of Joyo Industries, Ltd. for performing creep-fatigue evaluations according to the newly proposed methods investigated, and for making many valuable and essential technical suggestions that greatly improved the contents of this report.

Table of contents

*Acknowledgement* 4

*1. Introduction* 7

*2. Prerequisites for evaluation* 8

2.1 Evaluated data 8

2.2 Representation of material properties 8

2.3 Prediction using time fraction rule 8

*3. Outline and Predictability of Newly Proposed Creep-Fatigue Evaluation Methods* 14

3.1 Modified ductility exhaustion method 14

3.1.1 Outline 14

3.1.2 Predictability of experimental results 16

3.2 Strain Range Separation Method 36

3.2.1 Outline 36

3.3 Approach for Pressure Vessel Applications 55

3.3.1 Outline 55

3.3.2 Predictability of experimental results 56

3.4 Hybrid Method of Time Fraction and Ductility Exhaustion 74

3.4.1 Outline 74

3.4.2 Predictability of experimental results 75

3.5 Simplified Model Test Approach 90

3.5.1 Outline 90

*4. Potential to deploying the methods investigated to ASME-NH* 100

4.1 Evaluation of creep-fatigue life predictability of the methods investigated in short-term and long-term regions 100

4.1.1 Sensitivity analysis 100

4.1.2 Comparison of predicted creep fatigue life 101

**4.2 Evaluation of basic potential of the methods investigated ____ 120**
4.2.1 Modified Ductility Exhaustion Method ____ 120
4.2.2 Strain Range Separation Method ____ 121
4.2.3 Approach for Pressure Vessel Applications ____ 121
4.2.4 Hybrid method ____ 122
4.2.5 Simplified Model Test Approach ____ 123
4.2.6 Summary ____ 124
**4.3 Evaluation of extendibility of the methods investigated ____ 127**
4.3.1 Extension to higher temperatures ____ 127
4.3.2 Incorporation of thermal aging ____ 127
4.3.3 Incorporation of elastic follow-up ____ 127
4.3.4 Incorporation of geometrical discontinuity ____ 128
4.3.5 Extension to welded joints ____ 128
**4.4 Evaluation of applicability of the methods investigated to ASME-NH ____ 129**
4.4.1 Data generation required ____ 129
4.4.2 Validation tests required ____ 129
4.4.3 Incorporation of safety factors ____ 130
4.4.4 Changes to the ASME-NH code ____ 130
4.4.5 Technical readiness in 2009 ____ 131
**4.5 Recommendations ____ 132**
*5. Conclusions ____ 134*
*References ____ 136*
*Appendix A ____ 138*

# 1. Introduction

The DOE/ASME Generation IV Materials Project Tasks 5 investigated existing creep-fatigue rules to improve the provisions on creep-fatigue evaluation of Mod.9Cr-1Mo steel in Subsection NH of ASME Boiler and Pressure Vessel Code Section III [1]. All the rules investigated in the task were based on the time fraction rules.

The new DOE/ASME NGNP/Generation IV Materials Project Task 10 to which this report is devoted investigates newly proposed creep-fatigue evaluation methods that have not been employed in exiting codes and procedures using the data on Mod.9Cr-1Mo steel collected in Task 5. This report selected the following five promising methods, all of which are more or less different from the conventional time fraction method, for the investigation:

- Modified Ductility Exhaustion Method (MDEM)
- Strain Range Separation Method (SRSM)
- Approach for Pressure Vessel Applications (APVA)
- Hybrid Method of Time Fraction and Ductility Exhaustion (Hybrid)
- Simplified Model Approach (SMT)

This report describes the outline and the predictability of experimental results of the above method, potential to deploying the methods to NH is investigated from the viewpoints of required database, extrapolation strategy and applicability to structural design which is more complex than predicting material test results. Also mentioned is the impact to the provisions of Subsection NH when these methods were to be implemented replacing the current provisions.

This report deals with Mod.9Cr-1Mo steel only. However, it is to be noted that other materials such as 316 stainless steels including low-carbon nitrogen added versions and Alloy 800H are also of interest for the development of New Generation Nuclear Plants.

# 2. Prerequisites for evaluation

## 2.1 Evaluated data

The material dealt with in this report is Mod.9Cr-1Mo steel. The creep-fatigue data evaluated in this report are those collected in previous DOE/ASME Generation IV Materials Project Tasks 3 and 5 [2,3]. Most of the creep-fatigue data were obtained under strain controlled conditions but some of them were obtained under load controlled conditions. Collected data are shown in Figures 2.1 to 2.7. Creep rupture data and fatigue data are also included in the figures. See Appendix A for details.

## 2.2 Representation of material properties

When material properties are needed in evaluation, the equations in DDS [4] procedure were basically employed. In some cases, equations in RCC-MR [5] were used for comparison.

## 2.3 Prediction using time fraction rule

For the basis of comparison, creep-fatigue life predicted by the time fraction rule in the previous Task 5 [3] is shown in Figs. 2.3.1 and 2.3.2. Figure 2.3.1 is the result corresponding to a creep-fatigue damage diagram with an interception point of (0.3, 0.3) and Fig. 2.3.2 indicates, just for reference, the result obtained when creep-fatigue damage diagram with an interception point of (0.5, 0.5) is used.

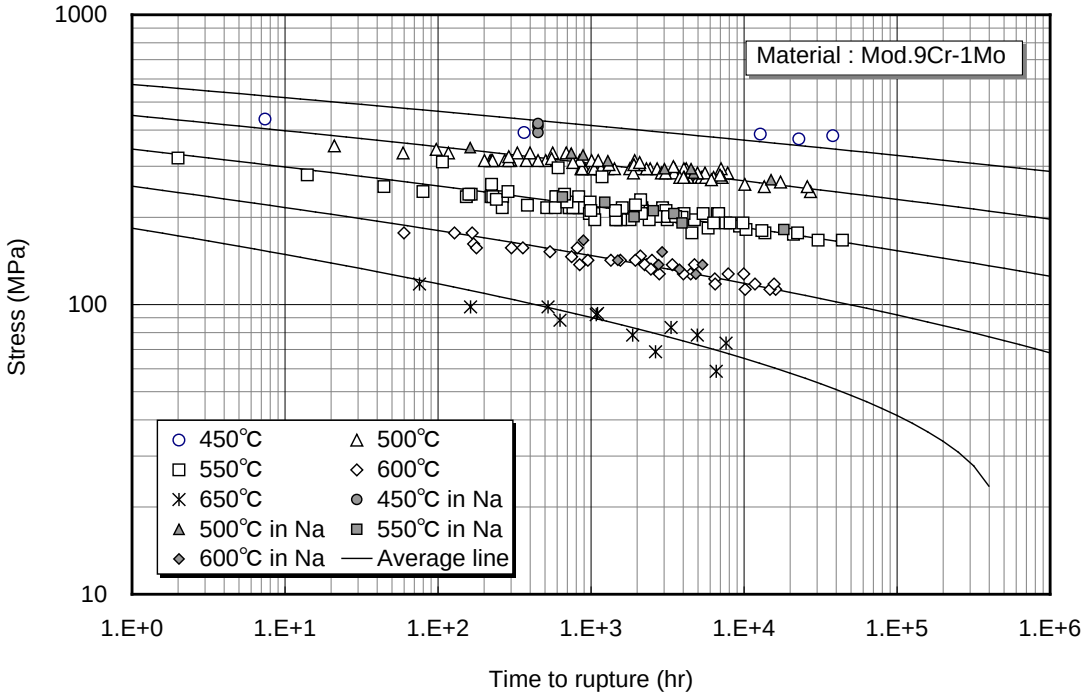


Fig.2.1.1 Creep rupture data at 450-600C

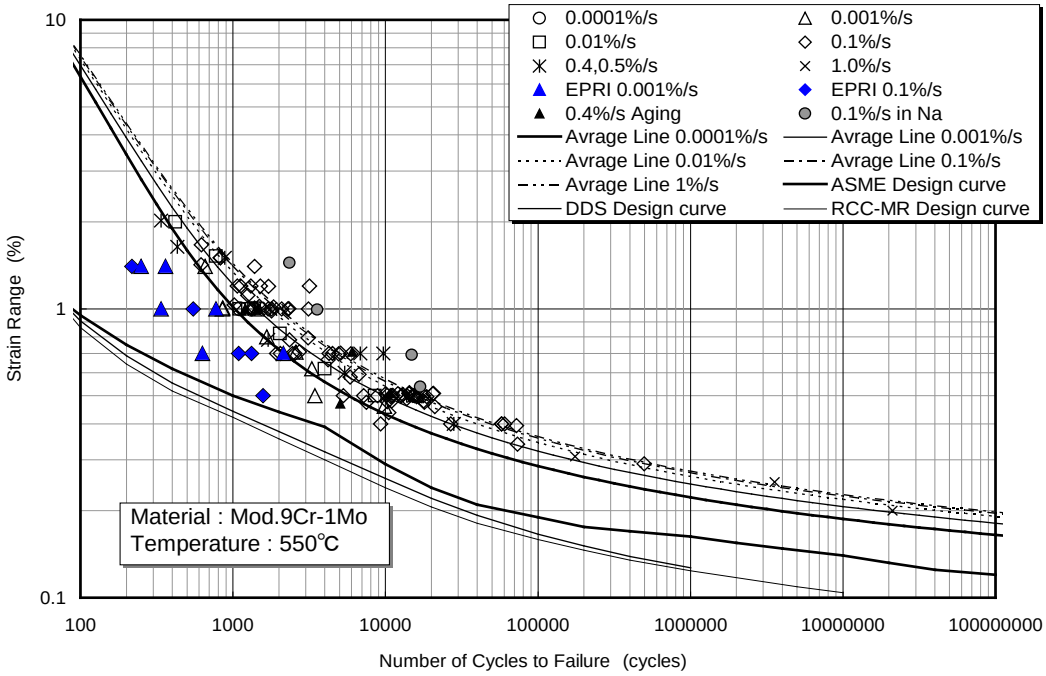


Fig.2.1.2 Fatigue data and design fatigue curves at 550C

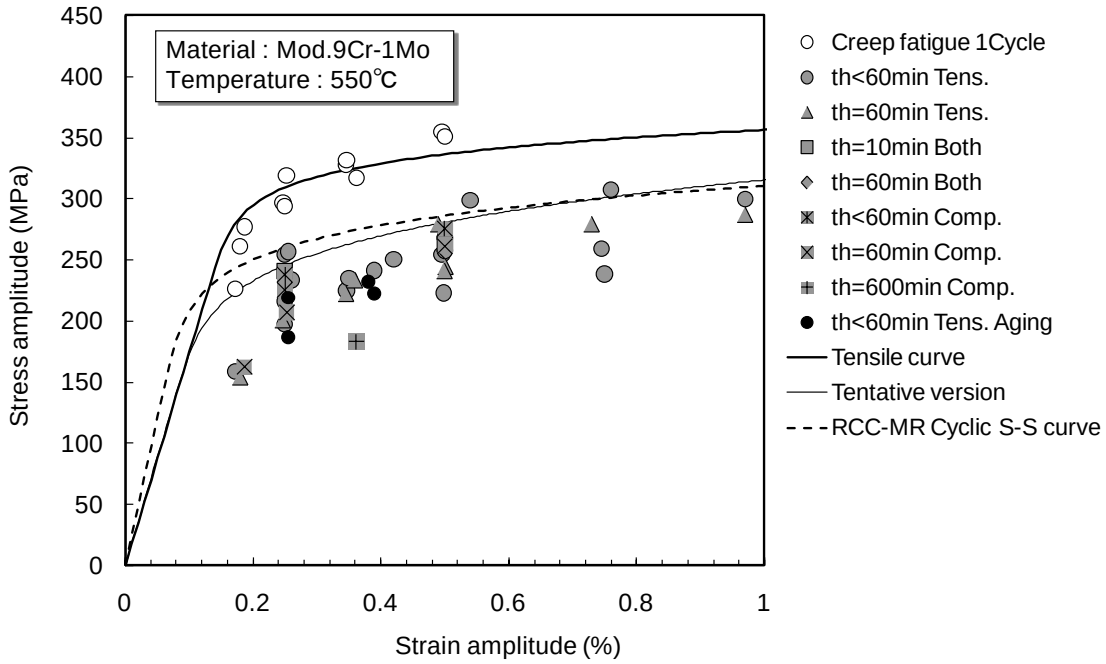


Fig. 2.1.3 Static and cyclic stress-strain curves at 550C

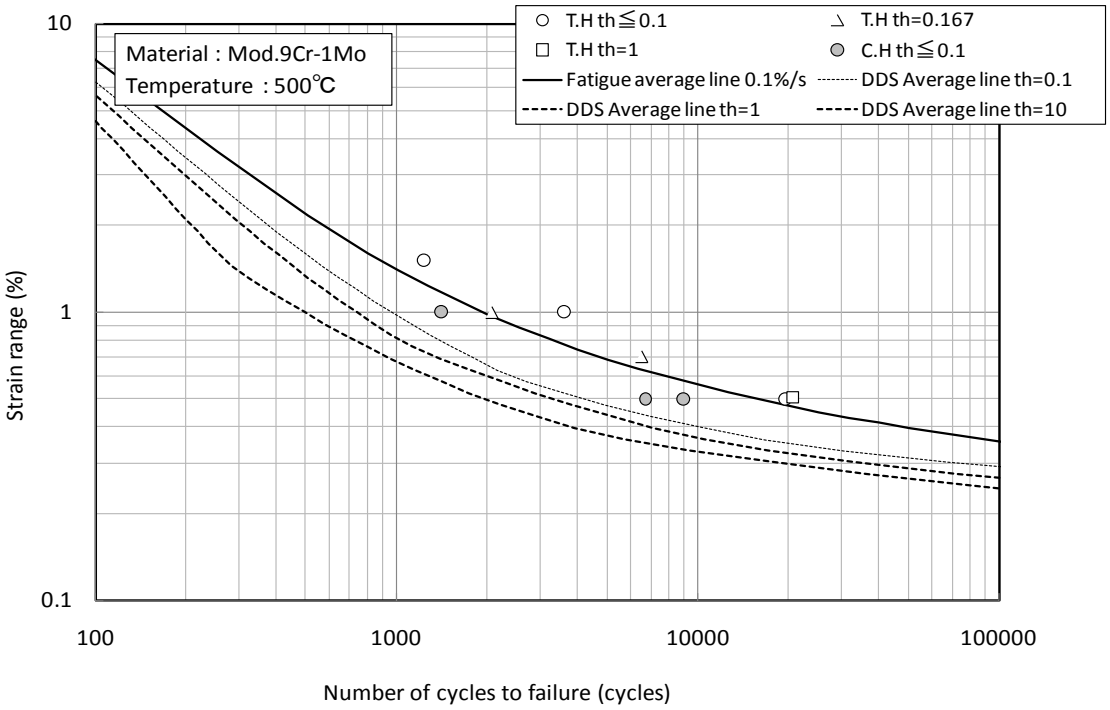


Fig.2.1.4 Creep-fatigue data at 500 C

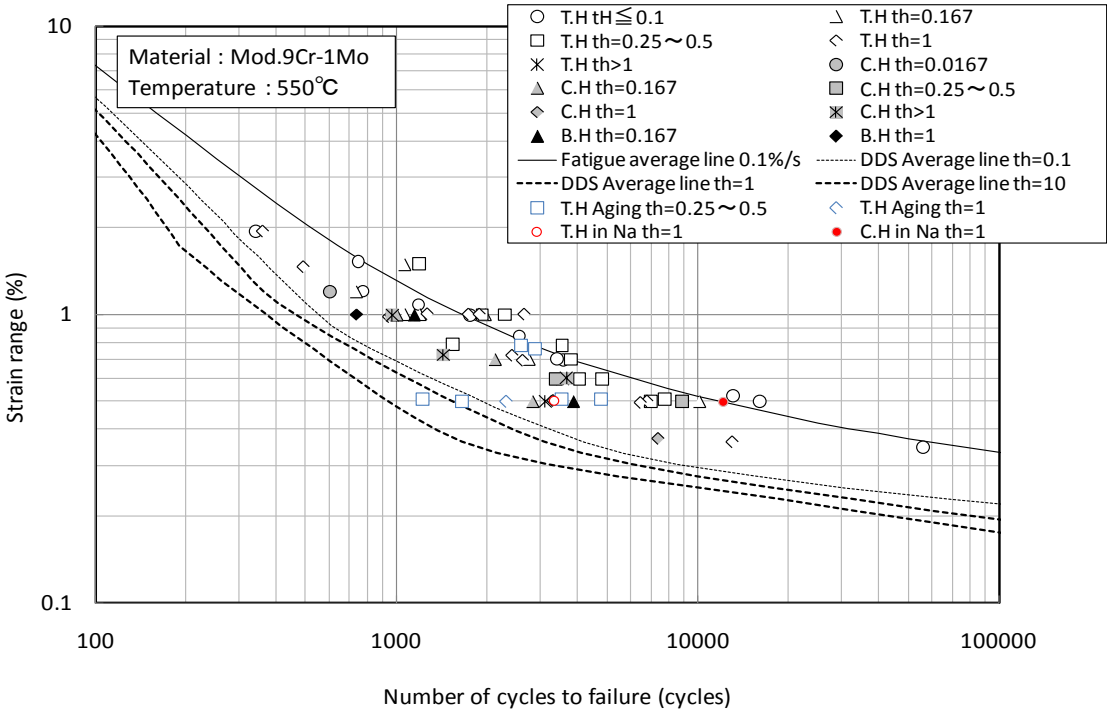


Fig.2.1.5 Creep-fatigue data at 550 C

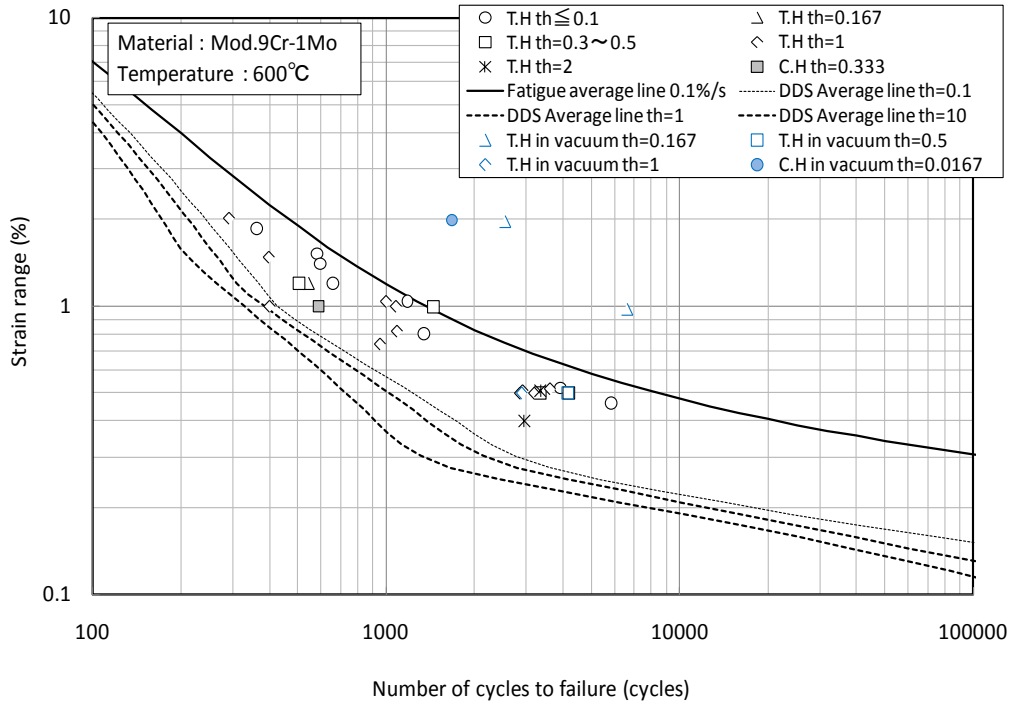


Fig.2.1.6 Creep-fatigue data at 600 C

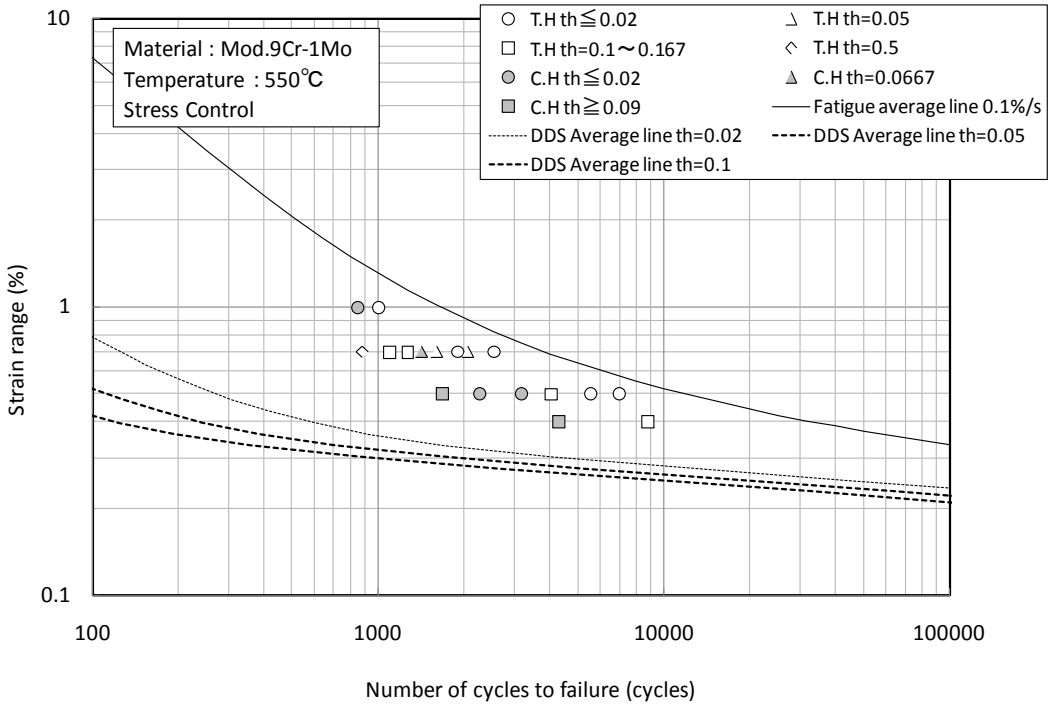


Fig.2.1.7 Creep-fatigue data at 550 C (Stress controlled tests)

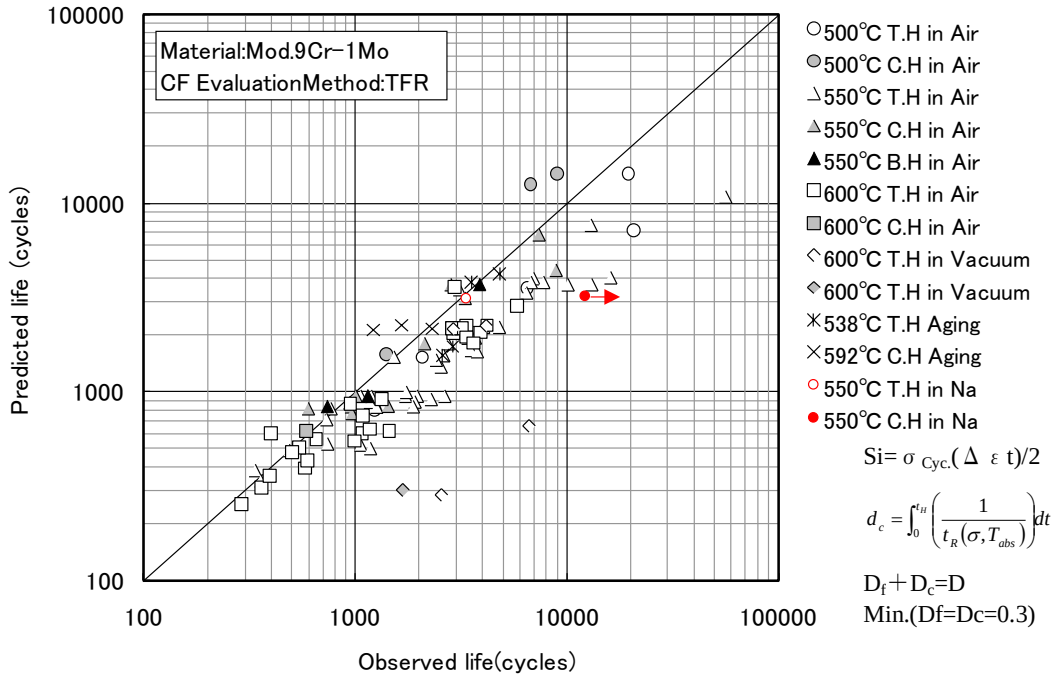


Fig. 2.3.1 Observed and predicted creep-fatigue life with time fraction rule

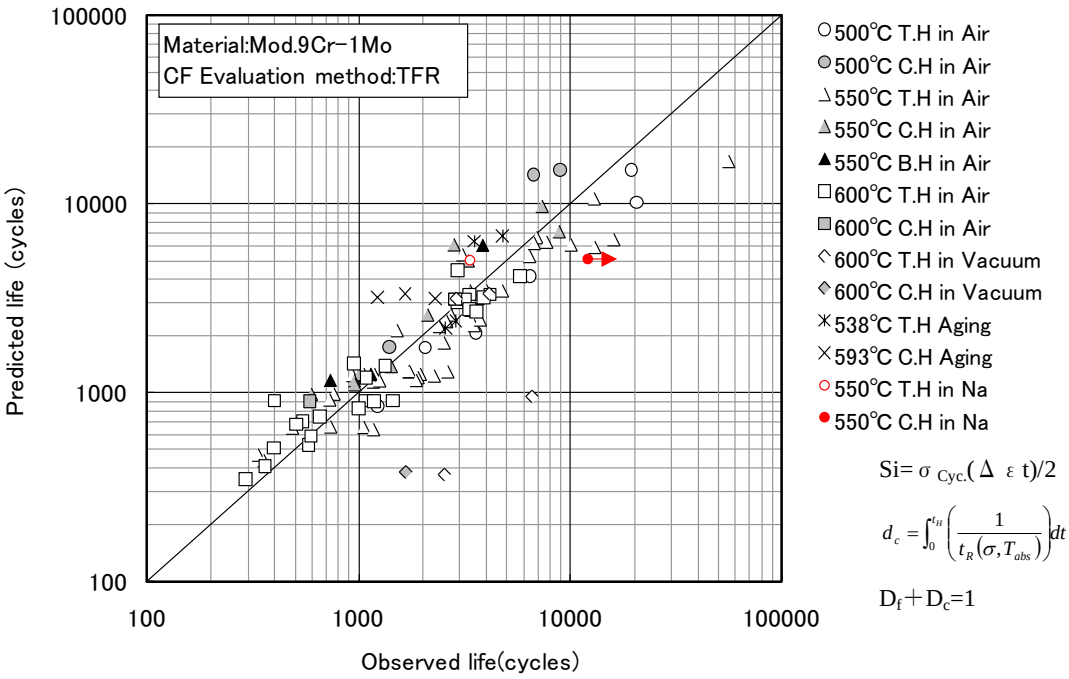


Fig. 2.3.2 Observed and predicted creep-fatigue life with time fraction rule

# 3. Outline and Predictability of Newly Proposed Creep-Fatigue Evaluation Methods

## 3.1 Modified ductility exhaustion method

### 3.1.1 Outline

**1) Concept**

The modified ductility exhaustion method (MDEM) was proposed by Takahashi [6]. Based on the recognition that the conventional ductility exhaustion method (DEM) underestimates creep-fatigue life due to the overestimation of creep damage, the definition of creep damage has been re-examined.

**2) Fatigue damage**

The definition of fatigue damage in this approach is normal minor rule as described by Equation (3.1.1)

$$d_f = \frac{1}{N_{f0}\left(\Delta\varepsilon, \dot{\varepsilon}, T_{abs}\right)} \tag{3.1.1}$$

$d_f$: Fatigue damage per cycle

$N_{f0}$: Fatigue life without hold time

$\Delta\varepsilon$ : Strain range

$\dot{\varepsilon}$ : Strain rate

$T_{abs}$: Temperature

**3) Creep damage**

The definition of creep damage in this approach is described by Equation (3.1.2) and this is unique in that not ductility itself is used but reduction in ductility due to the effect of creep is considered to account for creep damage. Takahashi states in his paper [6] that “in the same way as the ramping periods of the cycles are not considered to be a source of creep damage, inelastic deformation during the early portion of a hold period may be less harmful than the latter portion because of its faster rate. In order to include this effect into life prediction, the definition of creep damage was re-examined. Re-definition of creep damage as an amount of ductility loss caused by inelastic deformation, along with some additional assumptions, leads to the following simple equation for the estimation of creep damage”.

$$d_c = \int_0^{t_H} \left( \frac{1}{\delta(\dot{\varepsilon}_{in}, T_{abs})} - \frac{1}{\delta_0(T_{abs})} \right) \dot{\varepsilon}_{in} dt \tag{3.1.2}$$

$d_c$: creep damage per cycle
$\dot{\varepsilon}_{in}$ : inelastic strain rate
$\delta(\dot{\varepsilon}_{in}, T_{abs})$: creep ductility
$\delta_0(T_{abs})$: ductility at sufficiently high strain rate

$\delta_0(T_{abs})$: is the ductility under a sufficiently high strain rate considered as creep damage free, and the use of the elongation obtained in the conventional tensile tests. The new estimation method always gives smaller creep damage than the conventional method. No creep damage is estimated based on this definition even in creep tests as long as no decrease of ductility occurs.

**4) Creep-Fatigue Interaction**

Although analytical expression for the failure criterion under creep fatigue interaction were derived based on Manson-Coffin relationship, the simplest linear damage summation rule proved to be a fairly good approximation to those under regularly repeated loading cycles.

$$D_f + D_c = 1 \tag{3.1.3}$$

$$N_f = \frac{1}{d_f + d_c} \tag{3.1.4}$$

$D_f$: Accumulated fatigue damage
$D_c$: Accumulated creep damage

**5) Required material properties**

The material properties required to perform evaluation based on this method are as follows:

- Fatigue curve (number of cycles to failure vs total strain range)
- Stress-strain curve
- Inelastic strain rate vs ductility (obtained by both tensile tests and creep tests)

Figure 3.1.1 shows the relationship between creep rupture time and fracture elongation. Figures

3.1.2 to 3.1.4 show the relationships between inelastic rate and rupture elongation encompassing tensile and creep data for the temperature of 500C, 550C and 600C. Regression is performed for air data and sodium data separately. Figure 3.1.5 shows fracture elongation obtained by tensile tests under various temperature levels.

**6) Miscellaneous**

For compression hold tests a method different from that for tensile tests is proposed as the following equations.

$$R = \frac{N_f}{N_{f0}} = \frac{1}{1 + BN_{f0}{}^{N} \log\left(1 + t_H{}^{p}\right)} \tag{3.1.5}$$

$$\frac{N_{f0}/N_f}{\log\left(1 + t_H{}^{p}\right)} = BN_{f0}{}^{N} \tag{3.1.6}$$

### 3.1.2 Predictability of experimental results

**1) Creep-fatigue life prediction**

First, creep-fatigue life prediction is performed using data of which stress relaxation history is available. Figure 3.1.6 and 3.1.7 show the result of creep-fatigue life prediction based on the "conventional ductility exhaustion" method. Life prediction tends to be significantly conservative as creep-fatigue life increases. Figures 3.1.8, 3.1.9 and 3.1.10 show the result of the modified ductility exhaustion method. Conservativeness in the long-term region is improved but still remains to some extent.

Secondly, test data of which stress relaxation histories are not available are also included in evaluation. In this case, the initial stress and stress relaxation behavior were estimated using the cyclic stress-strain curves and creep strain curves determined in the DDS procedure [3]. Figures 3.1.11, 3.1.12 and 3.1.13 show the result of creep-fatigue life prediction of strain controlled tests. Predictability is fairly good except for the data obtained in vacuum environments, of which creep-fatigue life is significantly longer than those in air due to the absence of air environmental effects. In these figures, compression hold tests are evaluated in a manner same as tensile hold tests as if they are tensile hold tests. Figure 3.1.14 and 3.1.15 show the result of creep-fatigue life

prediction of stress controlled tests. In these figures, the creep-fatigue life predicted by time fraction rule is also plotted for comparison. The modified ductility exhaustion method gives unconservative life prediction under stress controlled conditions.

Figure 3.1.16 summarizes the ratio of predicted creep-fatigue life to observed life under tensile hold conditions. Both strain controlled and stress controlled tests are included. The ration varied from 0.2 to 2.0 for strain controlled tests and it varied from 1.5 to 4.0 for stress controlled tests.

Figure 3.1.17 shows the result of regression analysis to obtain the materials constants *B* and *N* in Equations (3.1.5) and (3.1.6) with the value of *p* fixed to 0.1. Figure 3.1.18 shows the result when *p* is fixed to 0.5. Figures 3.1.19 and 3.1.20 show the result of creep-fatigue life prediction when *p* is 0.1 and 0.5, respectively. It is to be noted that stress-controlled tests show tendencies different from those of strain controlled tests and that predicted creep-fatigue life coincides well with observed life when materials constants are determined for stress-controlled tests and strain-controlled tests independently.

**2) Sensitivity to parameters**

Sensitivity of predicted creep-fatigue life to various parameters used in the evaluation by the modified ductility exhaustion method was investigated. Figure 3.1.21 shows the result of creep-fatigue life prediction using the static stress-strain curve instead of the cyclic stress-strain curve. The difference (see Fig.3.1.11) is small. Figure 3.1.22 shows the result of creep-fatigue life prediction using the creep strain curve of RCC-MR instead of that of DDS. Again, the difference is small. Figure 3.1.23 compares the results of creep-fatigue life prediction at 550C using three different values for ductility at sufficiently high strain rate $\delta_0$ corresponding to the average value, the upper limit and 103% of the upper limit, considering the possibility that data higher than existing ones will be obtained in future. The result shows the predicted creep-fatigue life is fairly sensitive to the value of $\delta_0$. This can be explained by the fact that creep damage in the modified ductility exhaustion method depends on the value of $\delta_0$ significantly as shown in Figures 3.1.24 and 3.1.25.

**3) Extrapolation to long-terms**

Figures 3.1.26, 3.1.27 and 3.1.28 show predicted creep-fatigue life for a wide range of time for both the modified ductility exhaustion method and the time fraction method. It is observed that in the

long-term region, the modified ductility exhaustion method gives longer predicted creep-fatigue life than the time fraction approach does. It is because the increase of creep damage tends to saturate in the long term region because stress relaxation saturates. Figures 3.1.29, 3.1.30 and 3.1.31 show the ratio of predicted creep-fatigue life by the modified ductility exhaustion method and the time fraction method.

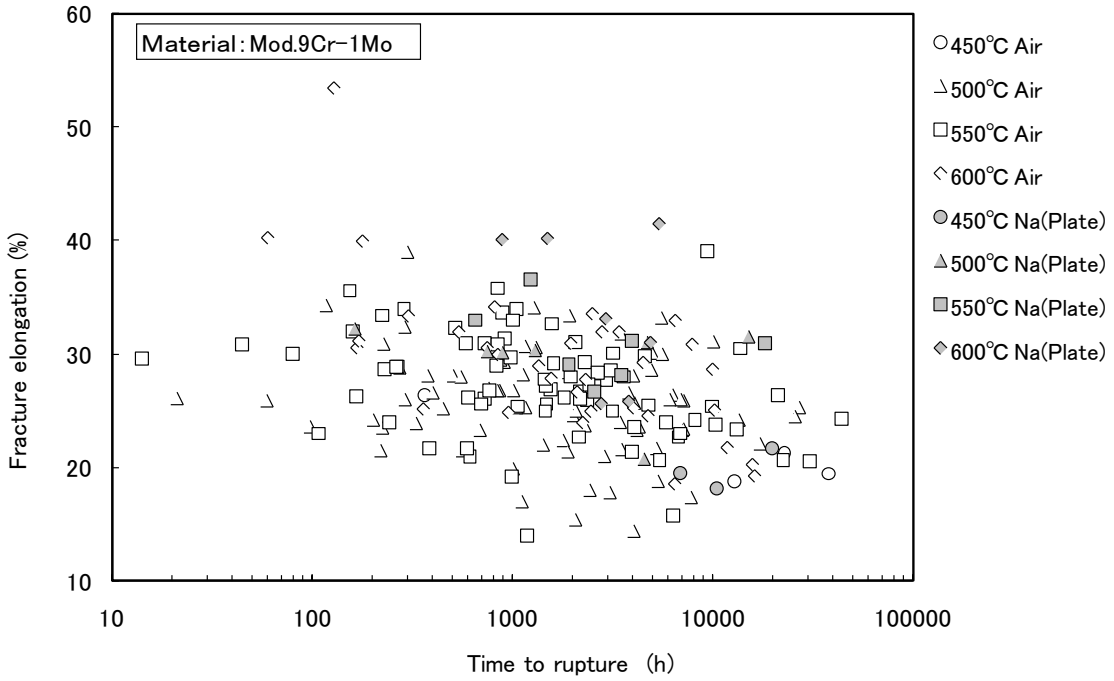


Fig. 3.1.1 Relation between creep rupture time and fracture elongation

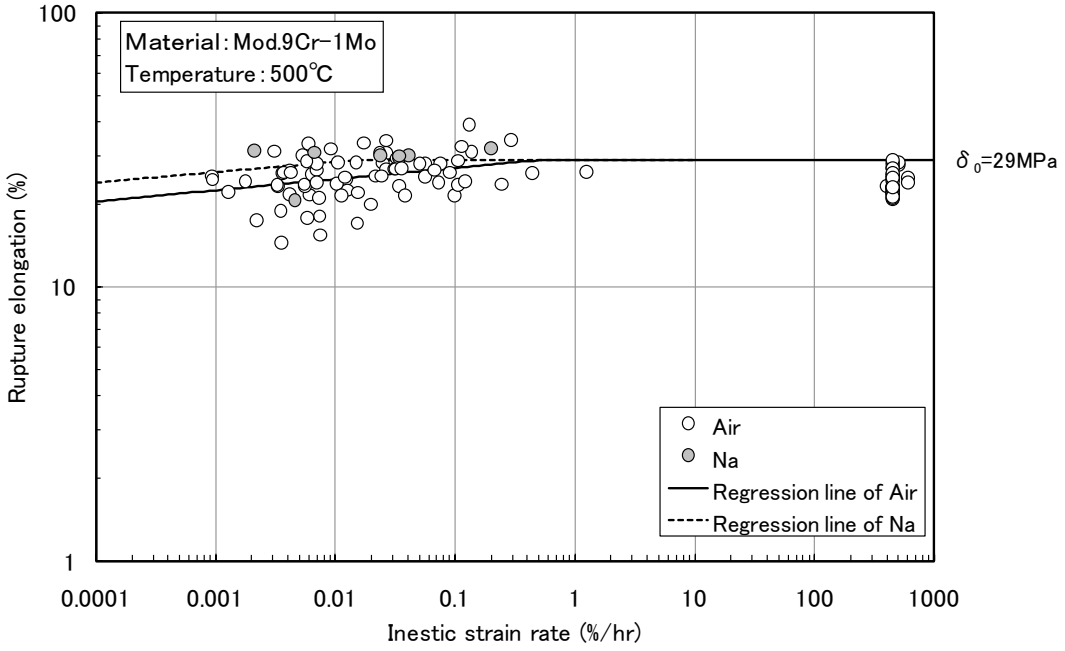


Fig. 3.1.2 Relation between inelastic strain rate and creep rupture elongation at 500 C

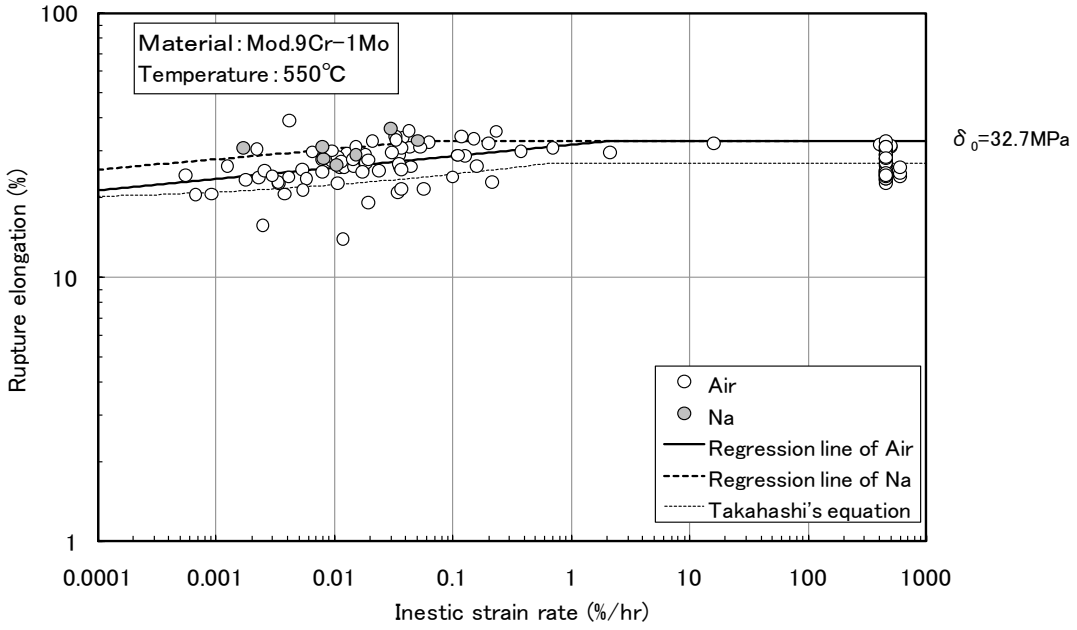


Fig. 3.1.3 Relation between inelastic strain rate and creep rupture elongation at 550 C

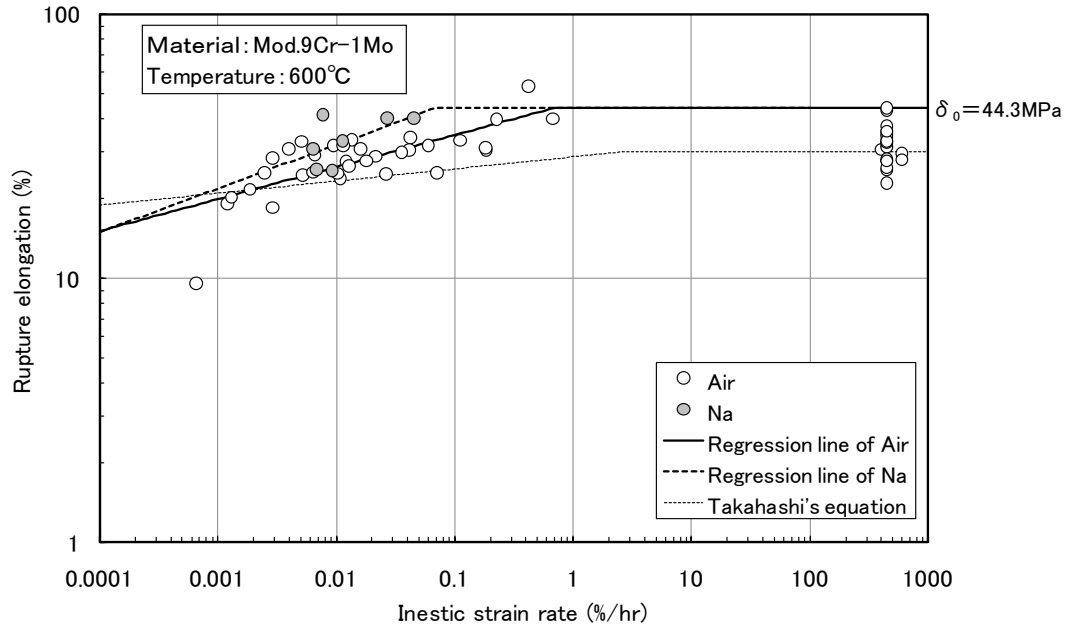


Fig. 3.1.4 Relation between inelastic strain rate and creep rupture elongation at 600 C

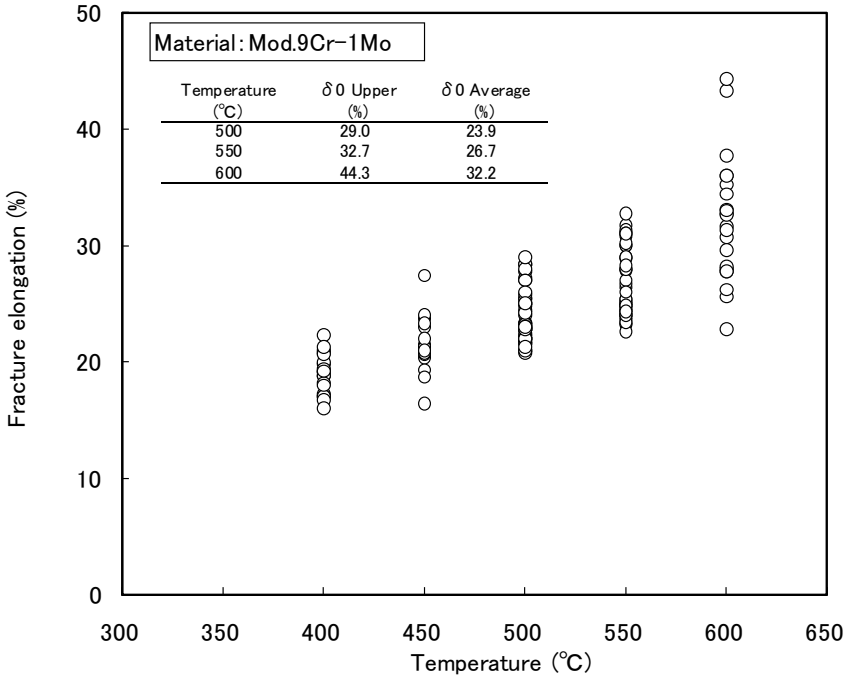


Fig. 3.1.5 Relation between temperature and tensile fracture elongation

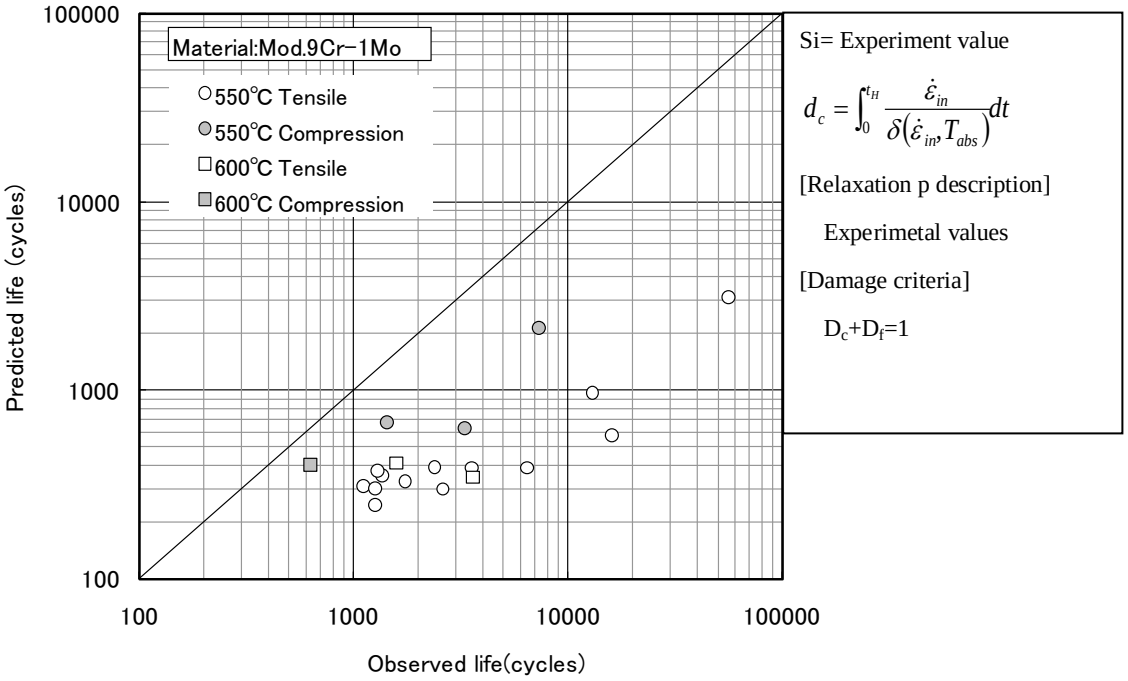


Fig. 3.1.6 Observed and predicted creep-fatigue life by ductility exhaustion method

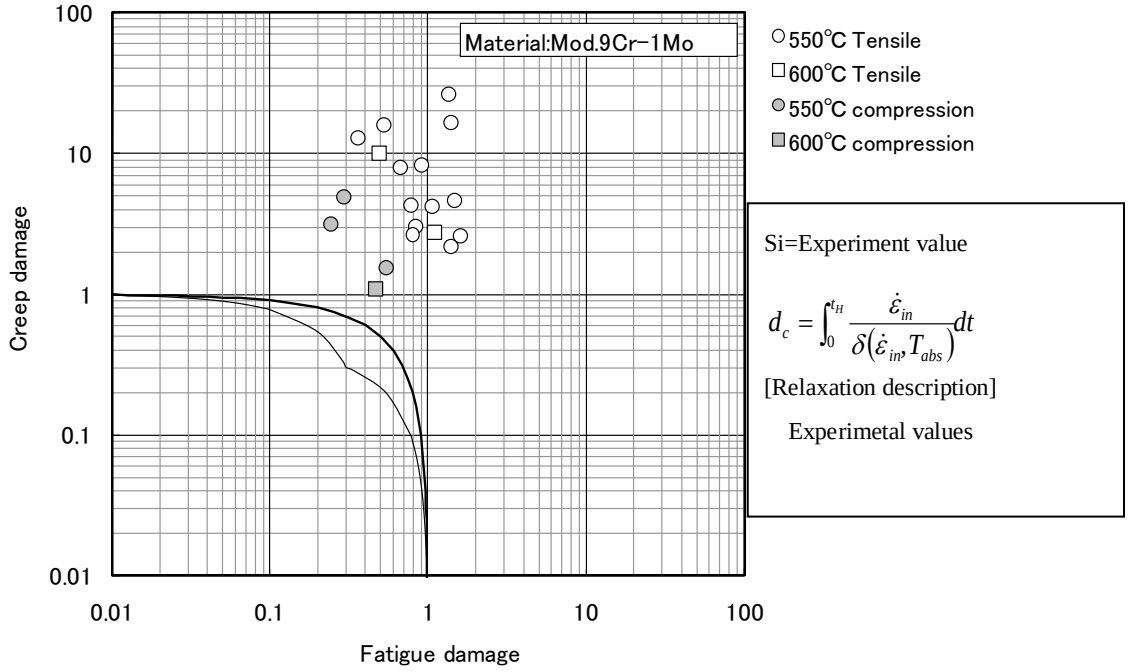


Fig. 3.1.7 Creep-fatigue damage calculated by ductility exhaustion method

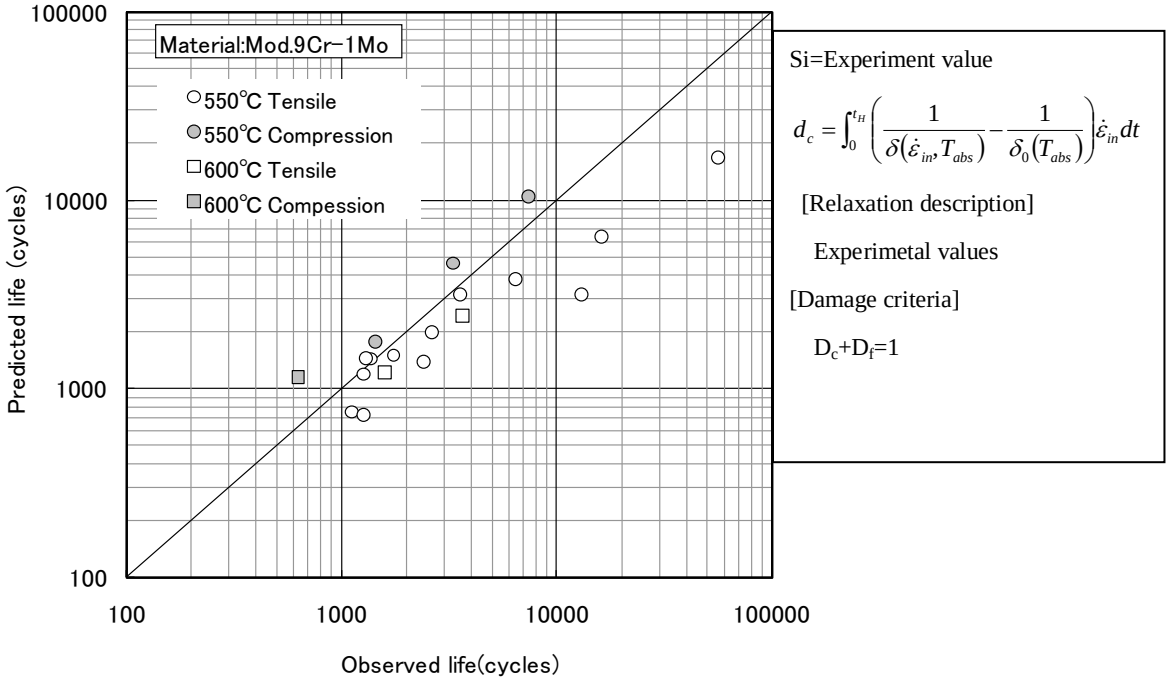


Fig.3.1.8 Observed and predicted creep-fatigue life by modified ductility exhaustion method

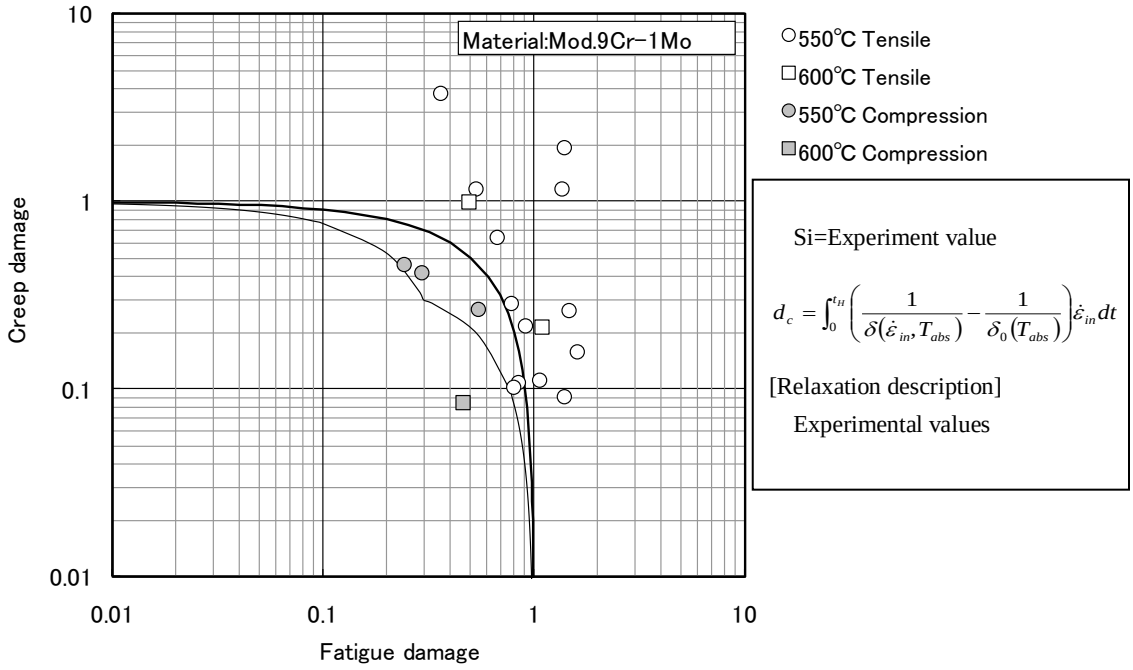


Fig. 3.1.9 Creep-fatigue damage calculated by modified ductility exhaustion method

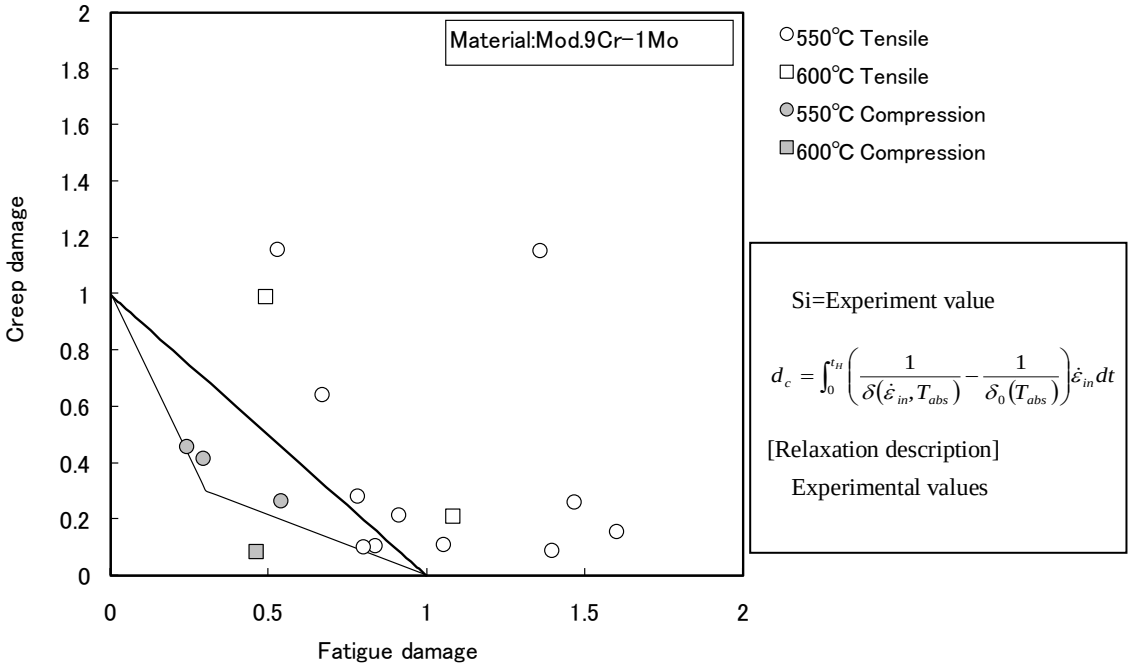


Fig. 3.1.10 Creep-fatigue damage calculated by modified ductility exhaustion method

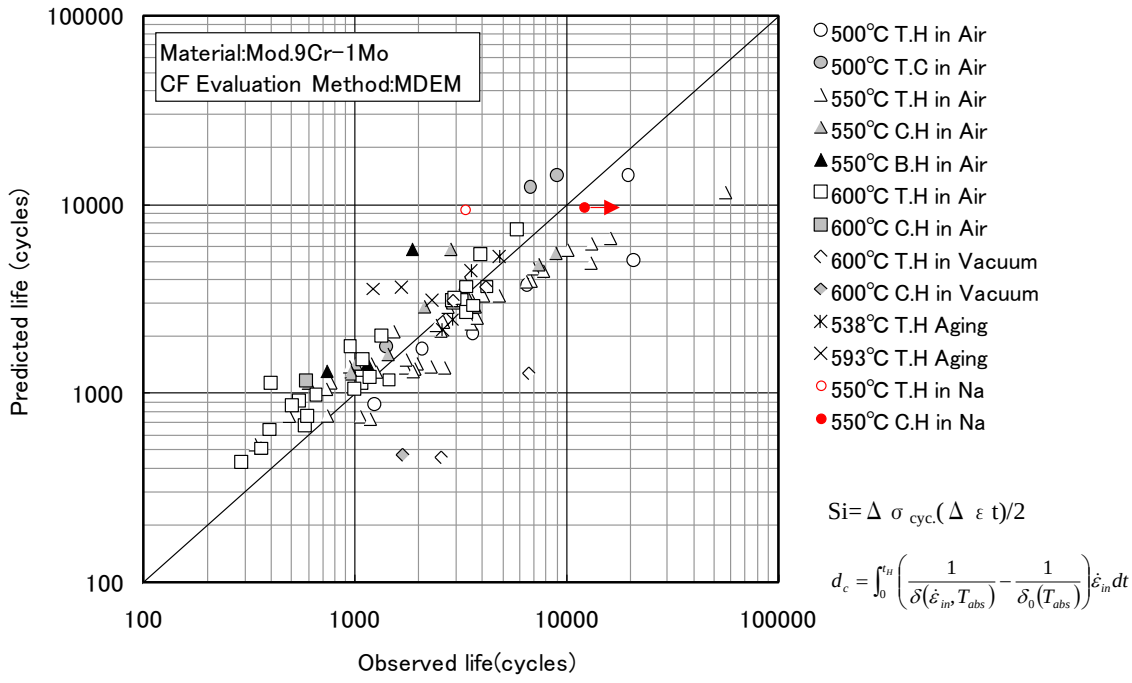


Fig. 3.1.11 Observed and predicted creep-fatigue life by modified ductility exhaustion method

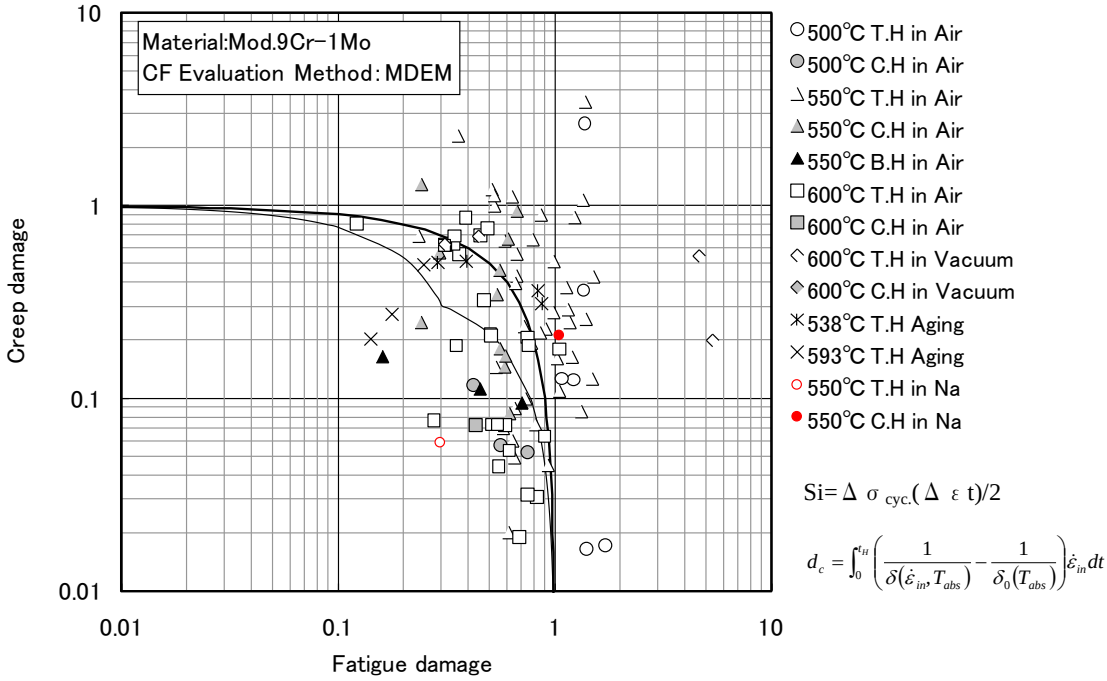


Fig. 3.1.12 Creep-fatigue damage calculated by modified ductility exhaustion method

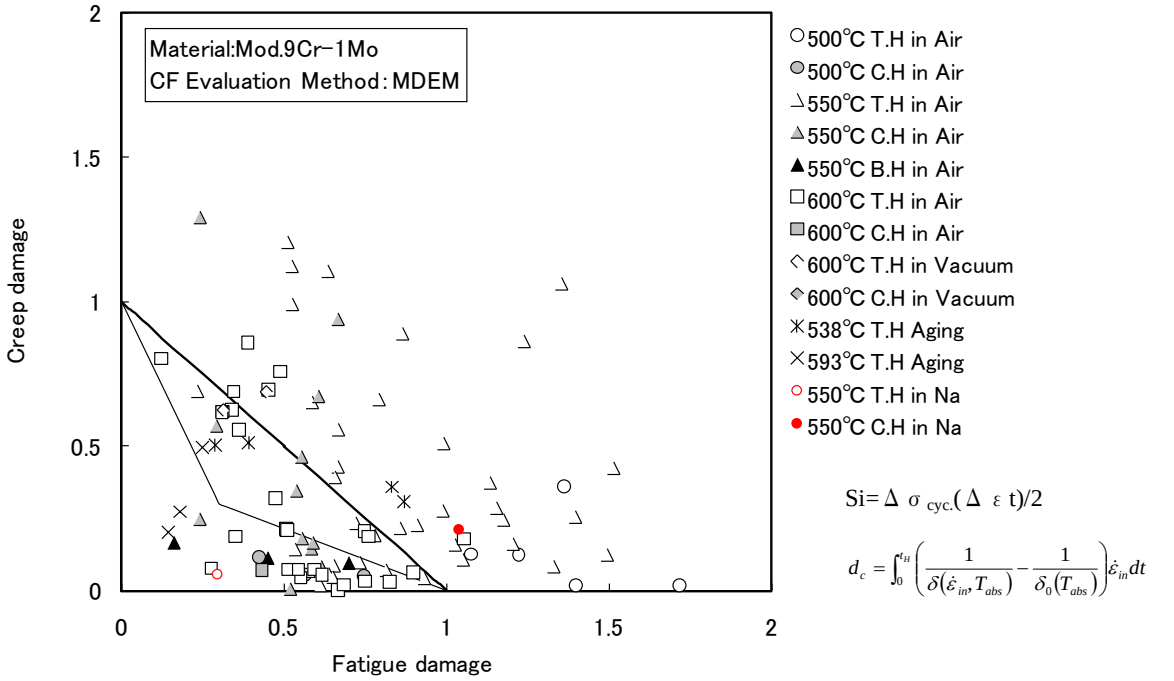


Fig. 3.1.13 Creep-fatigue damage calculated by modified ductility exhaustion method

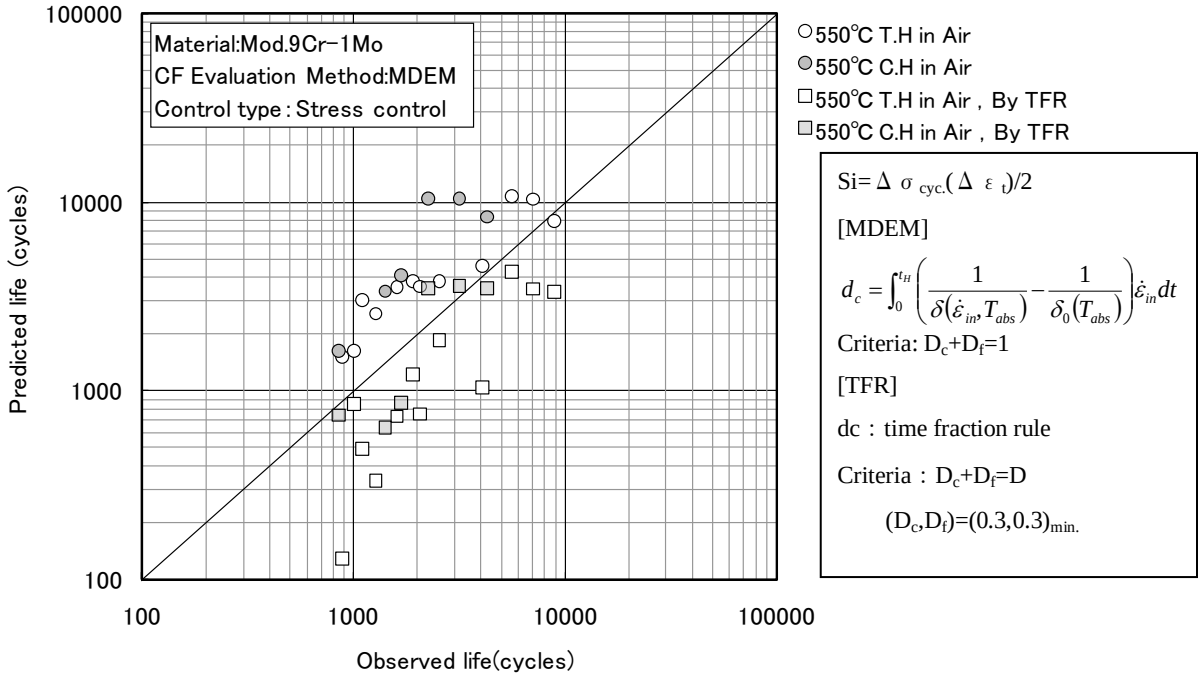


Fig. 3.1.14 Observed and predicted creep-fatigue life with modified ductility exhaustion method for stress controlled tests

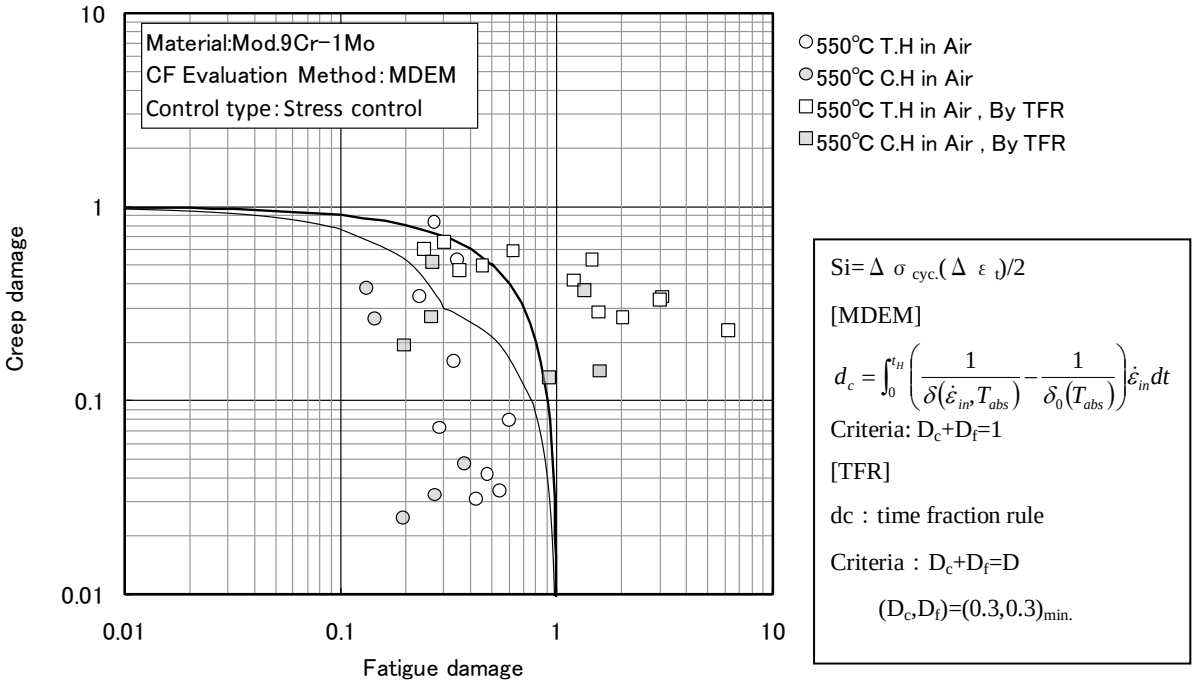


Fig. 3.1.15 Creep-fatigue damage calculated by modified ductility exhaustion method for stress controlled tests

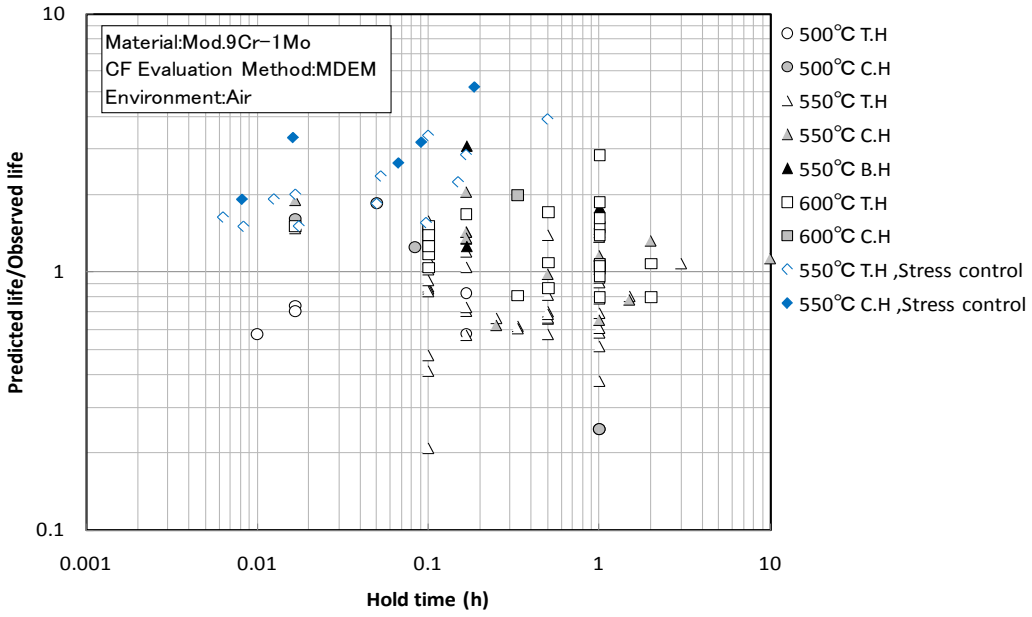


Fig. 3.1.16 Ratio of predicted life to observed life against hold time

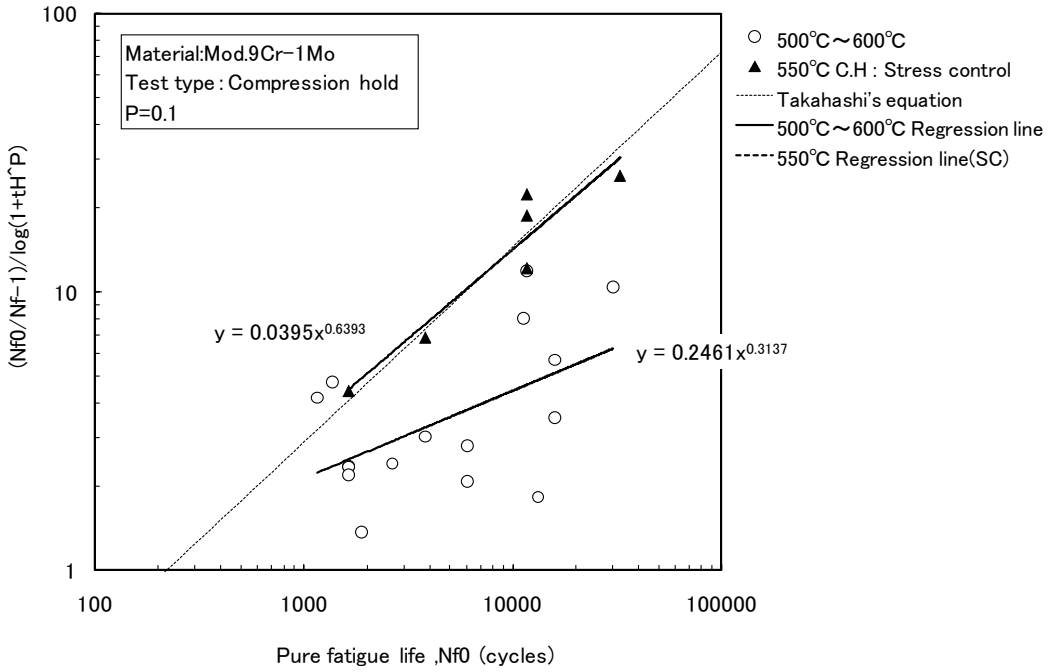


Fig. 3.1.17 Life reduction coefficient as a function of pure fatigue life when *p* is 0.1

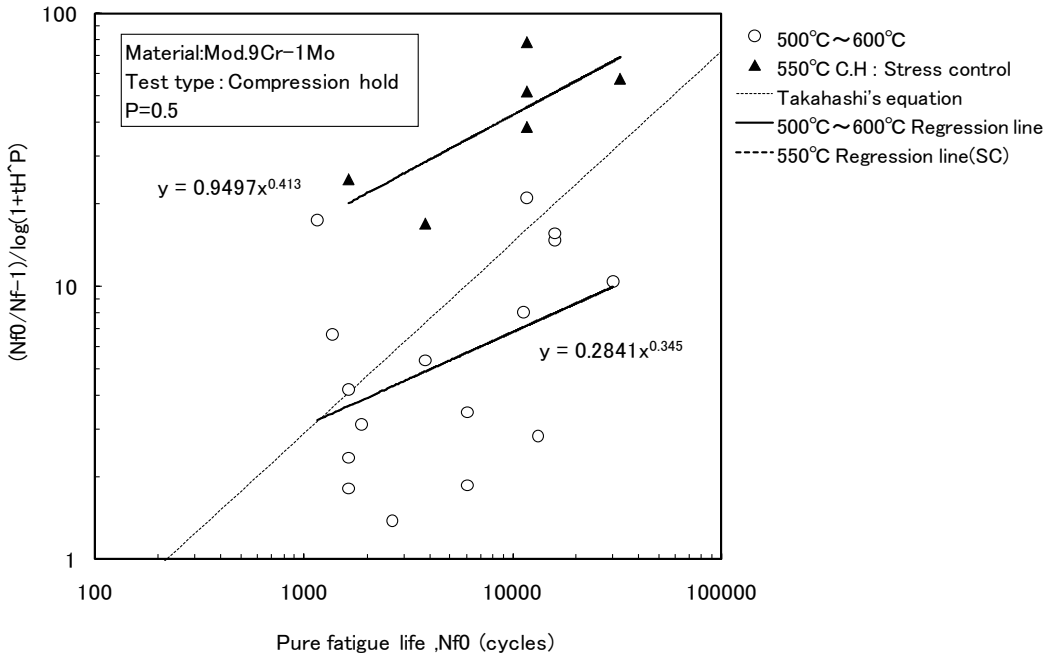


Fig. 3.1.18 Life reduction coefficient as a function of pure fatigue life when *p* is 0.5

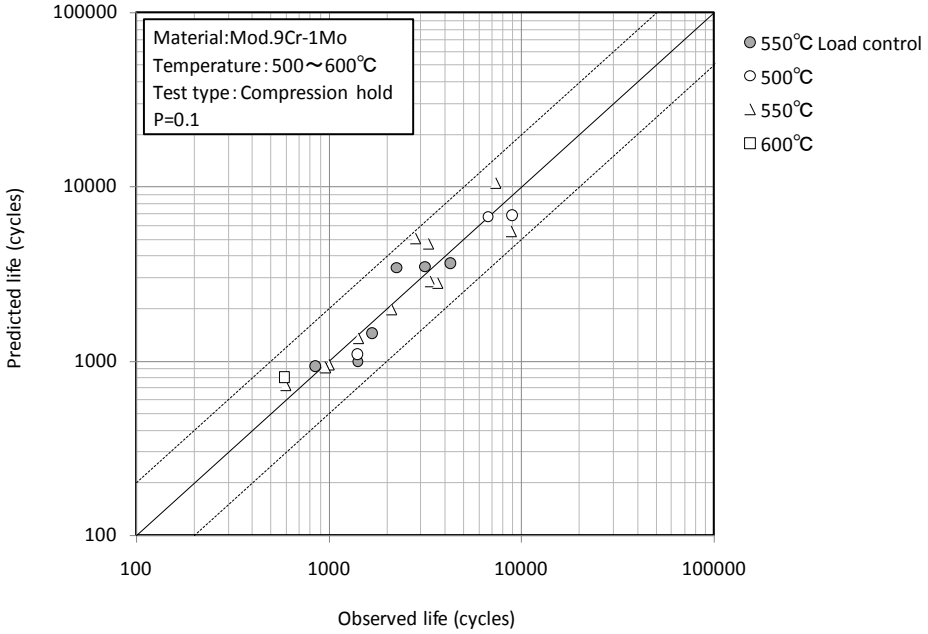


Fig. 3.1.19 Observed and predicted creep-fatigue life by modified ductility exhaustion method for compressive hold tests

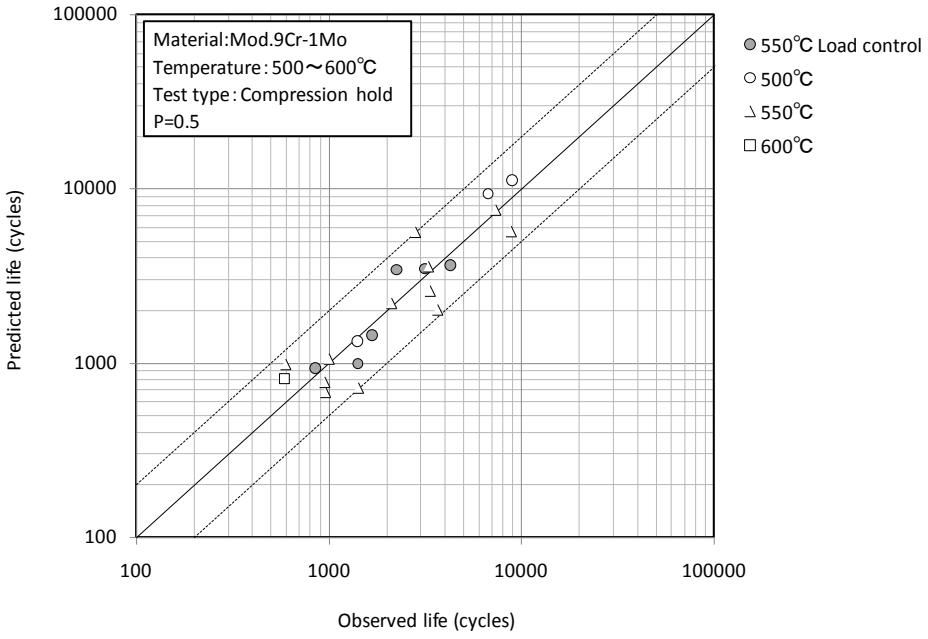


Fig. 3.1.20 Observed and predicted creep-fatigue life by modified ductility exhaustion method for compressive hold tests

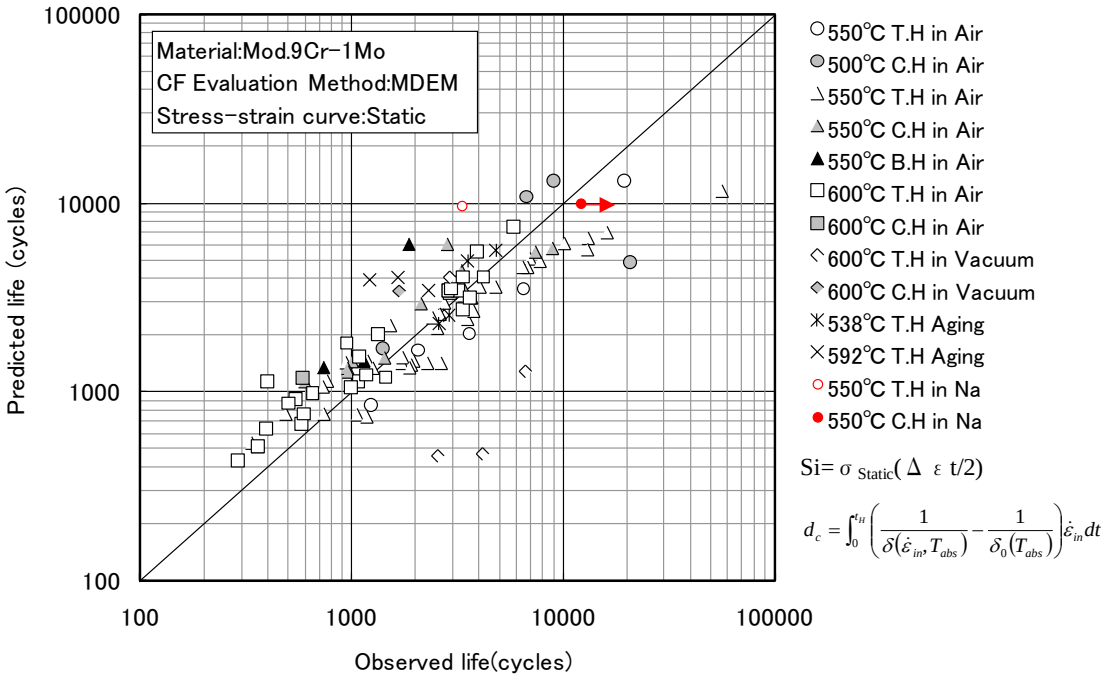


Fig. 3.1.21 Observed and predicted creep-fatigue life by modified ductility exhaustion method

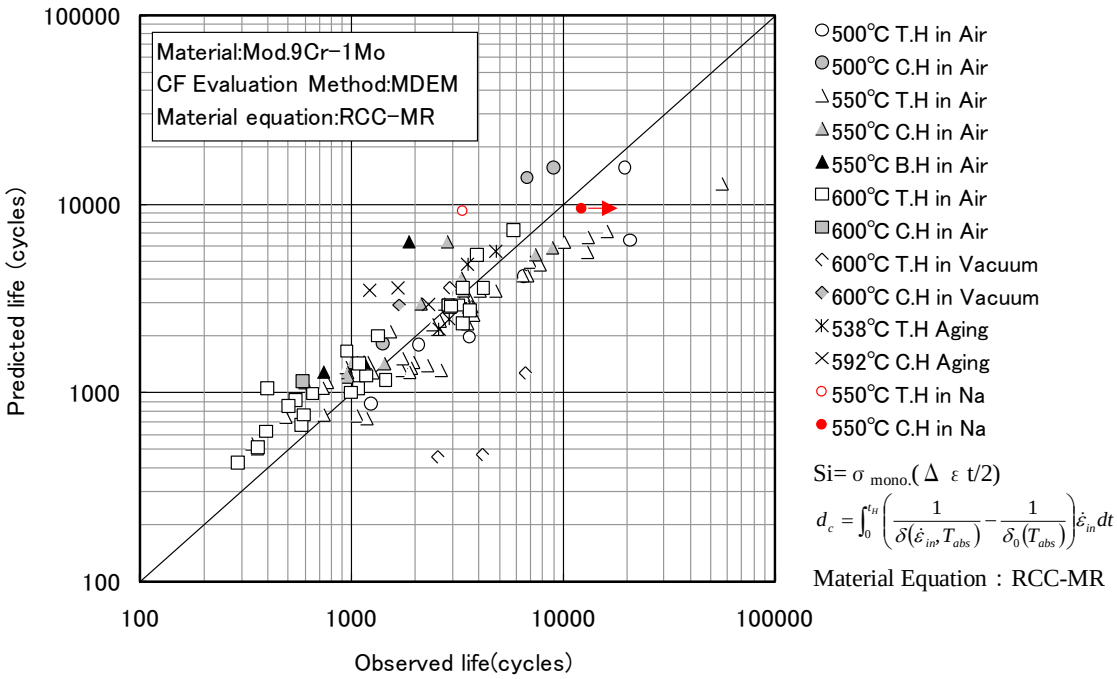


Fig. 3.1.22 Observed and predicted creep-fatigue life by modified ductility exhaustion method

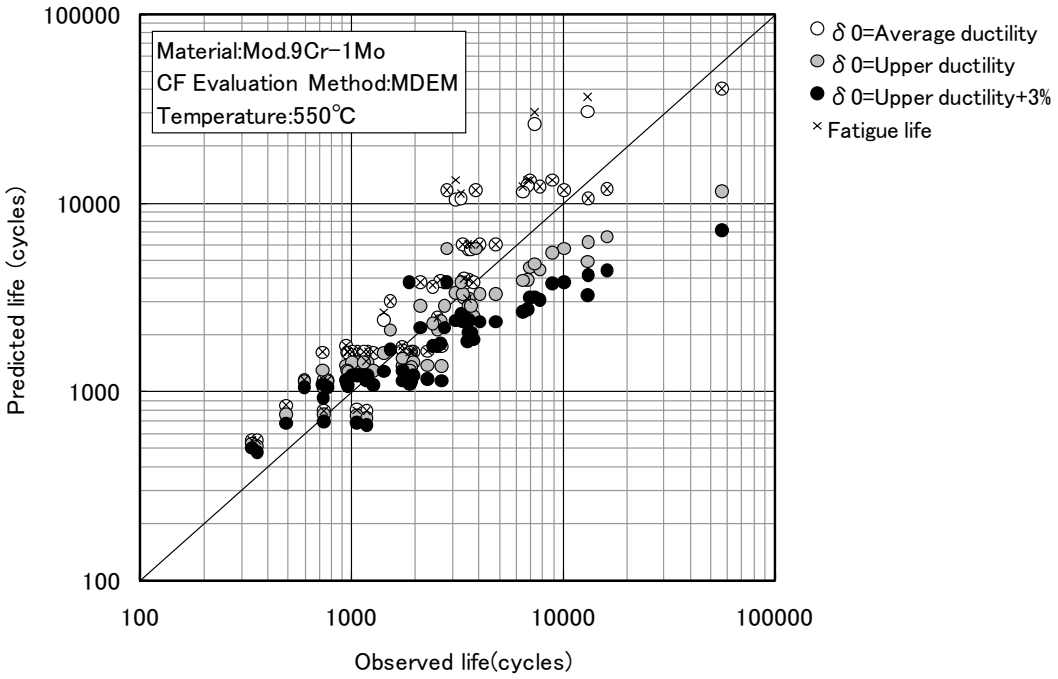


Fig. 3.1.23 Observed and predicted tensile fracture elongation $\delta_0$ at 550℃

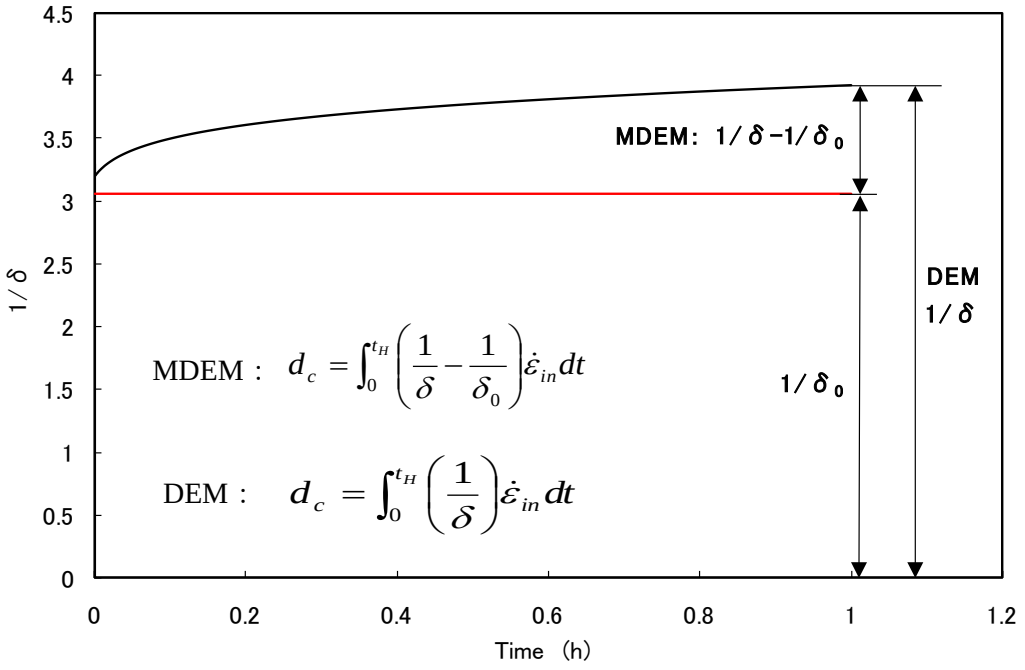


Fig. 3.1.24 Comparison of estimation of creep damage between MDEM and DEM

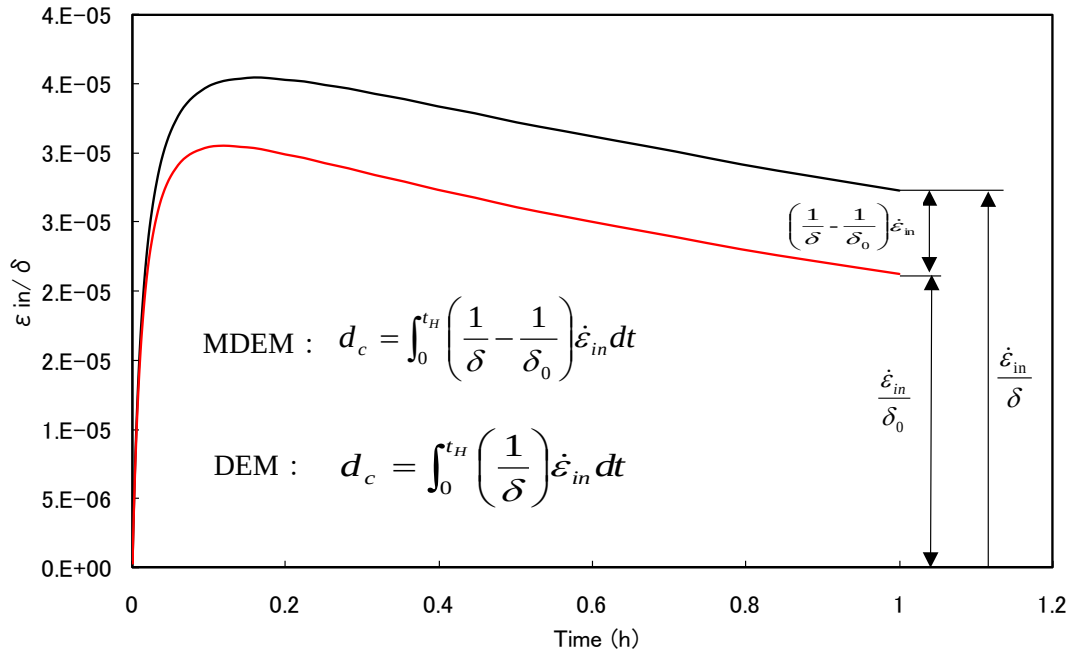


Fig. 3.1.25 Comparison of estimation of creep damage between MDEM and DEM

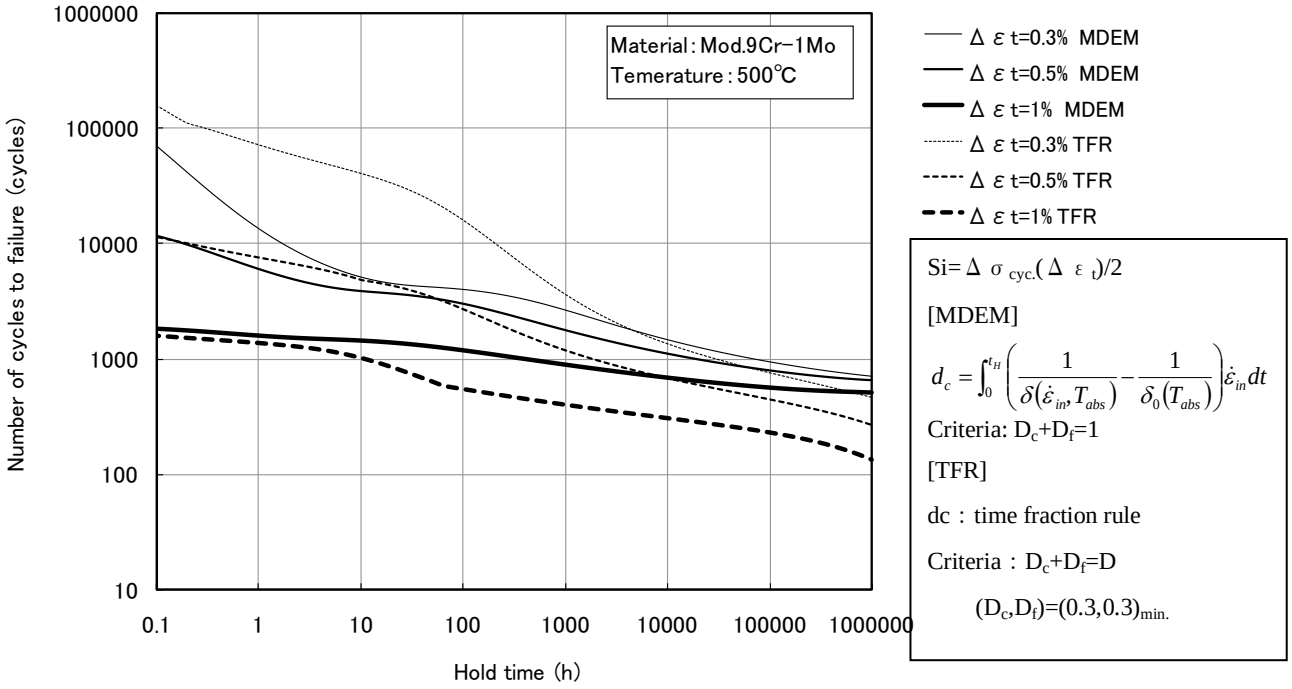


Fig. 3.1.26 Comparison of creep-fatigue life between MDEM and TFR at 500 C

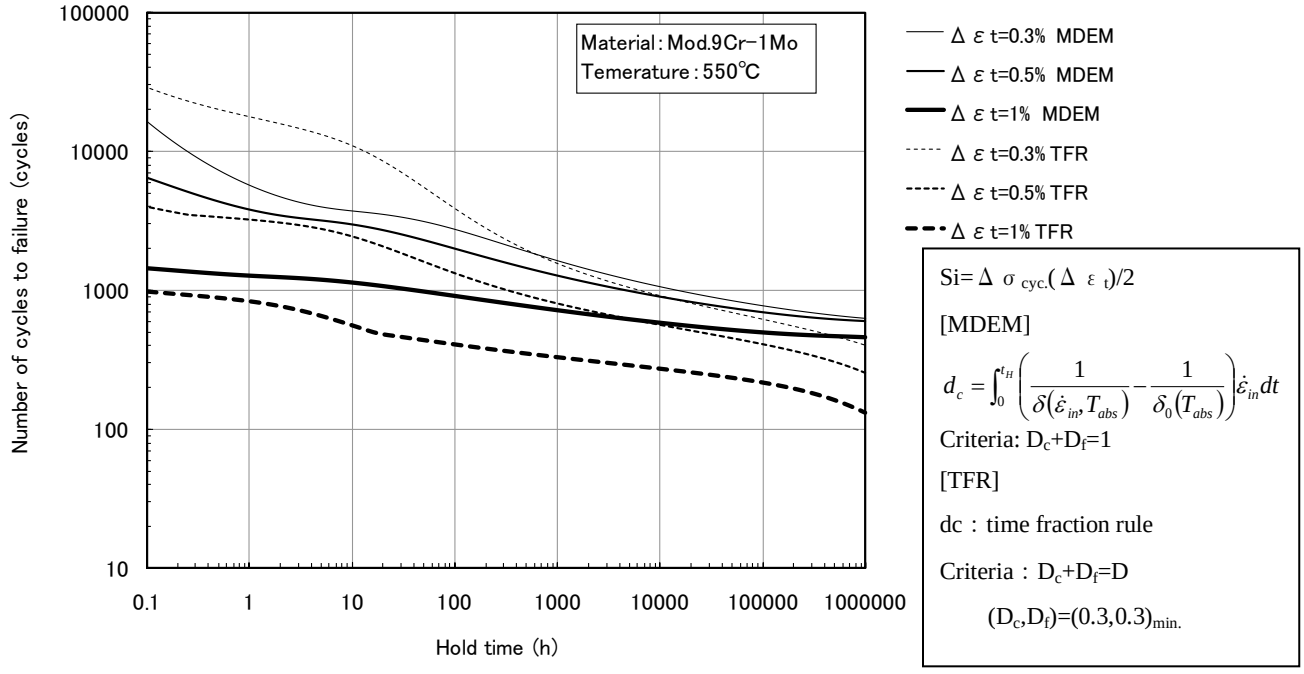


Fig. 3.1.27 Comparison of creep-fatigue life between MDEM and TFR at 550 C

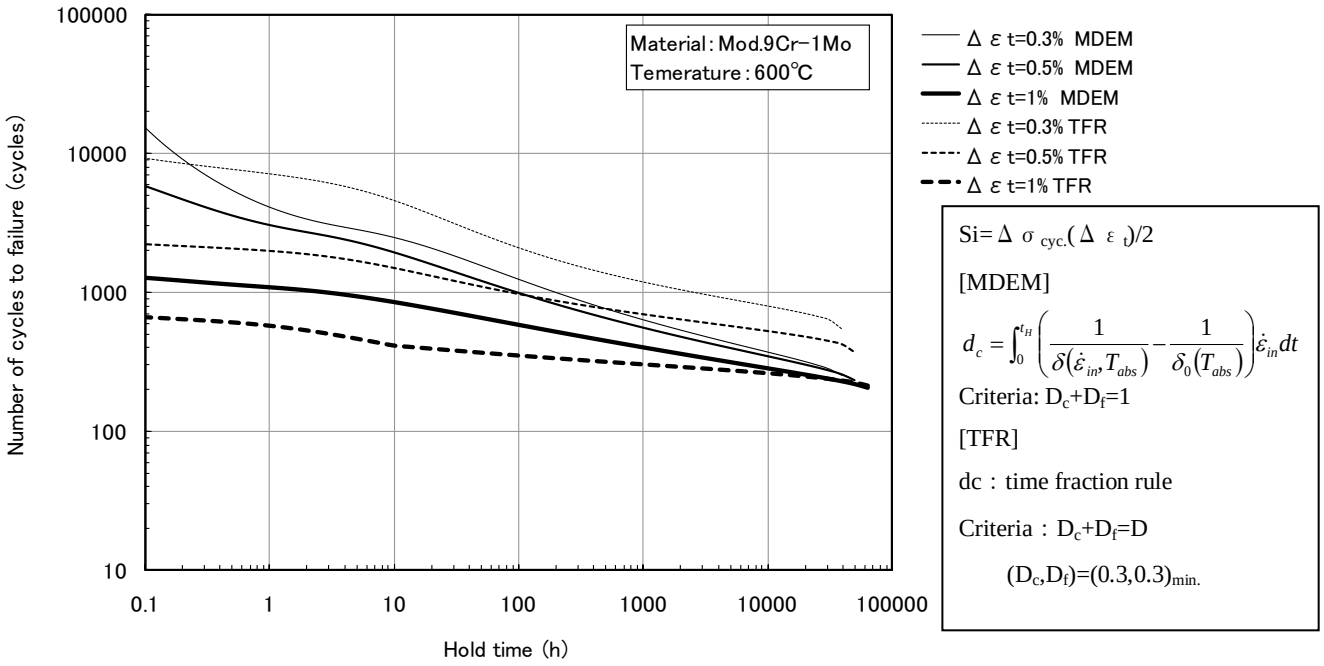


Fig. 3.1.28 Comparison of creep-fatigue life between MDEM and TFR at 600 C

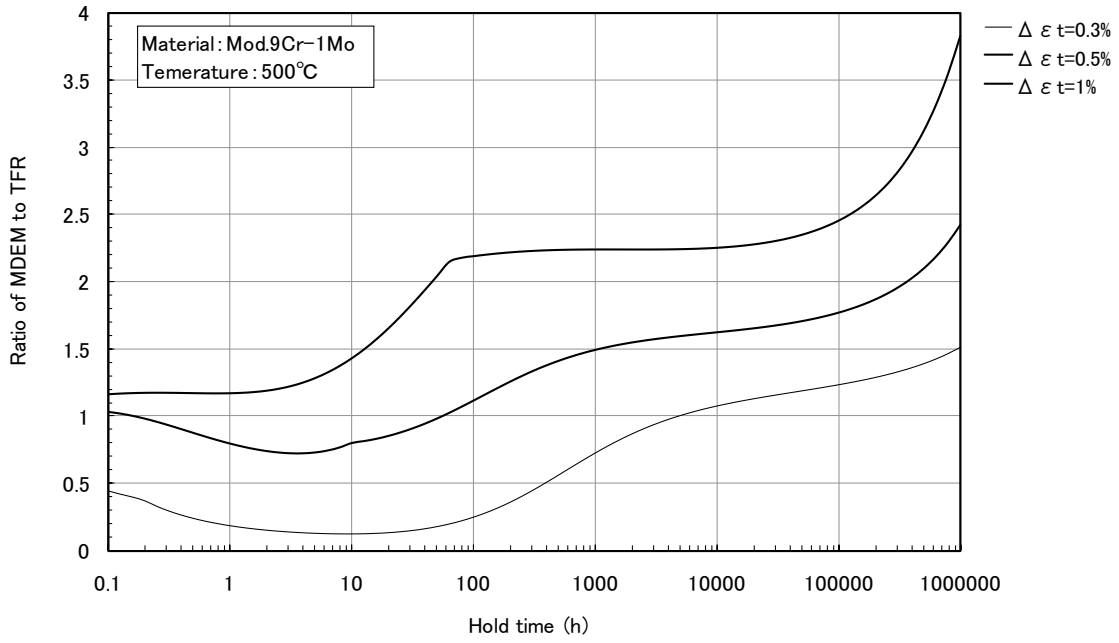


Fig.3.1.29 Ratio of creep-fatigue life predicted by MDEM to that predicted by TFR at 500C

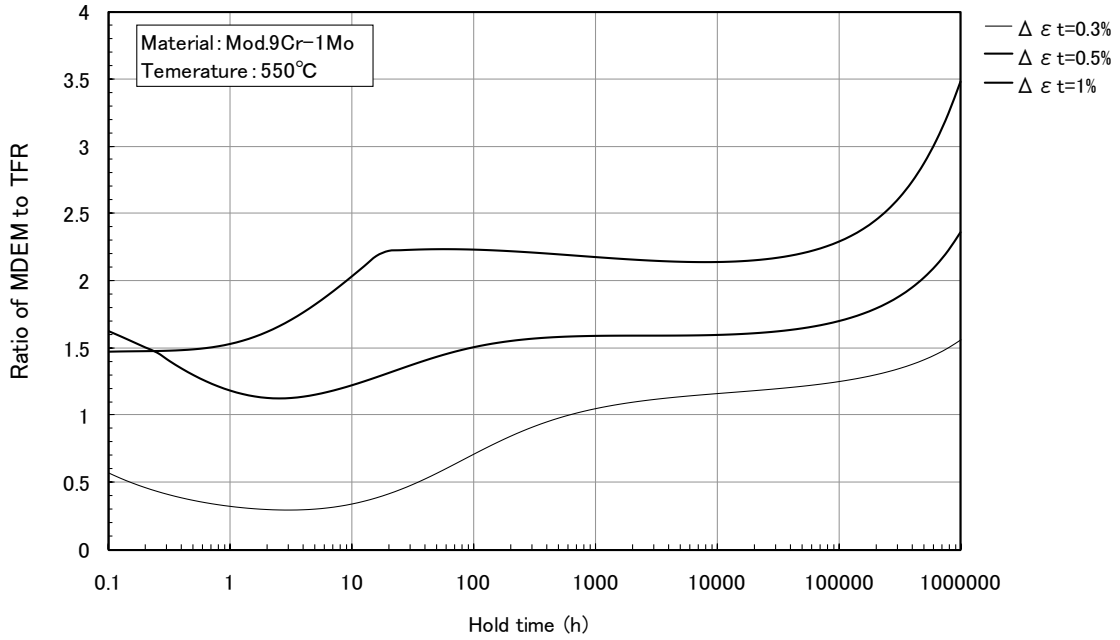


Fig.3.1.30 Ratio of creep-fatigue life predicted by MDEM to that predicted by TFR at 550C

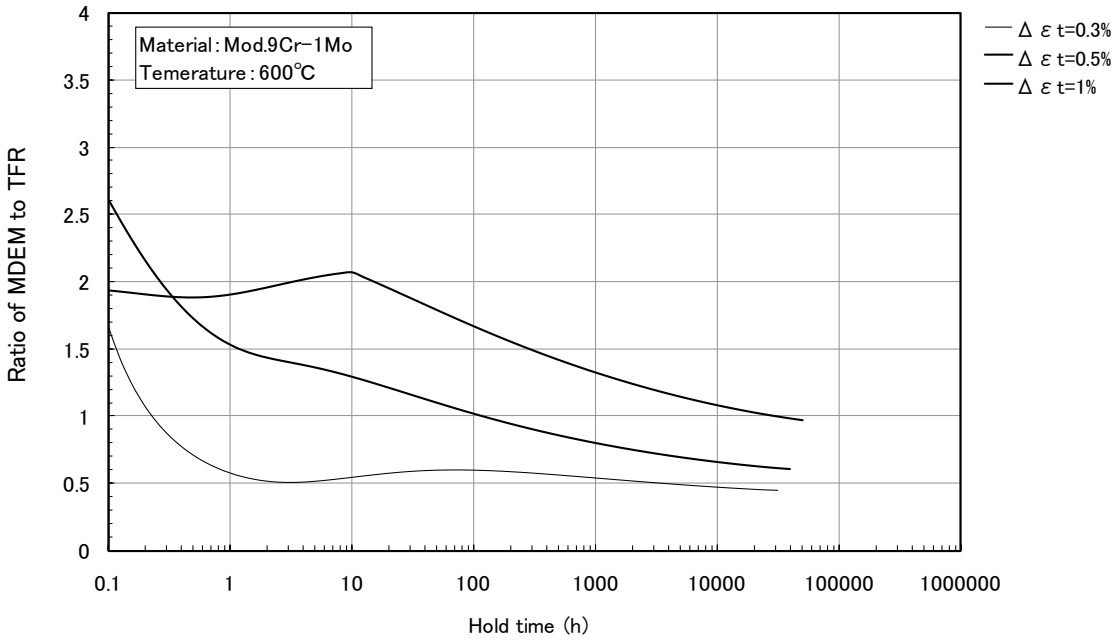


Fig.3.1.31 Ratio of creep-fatigue life predicted by MDEM to that predicted by TFR at 600C

## 3.2 Strain Range Separation Method

### 3.2.1 Outline

**1) Concept**

The Strain Range Separation Method (SRSM) was proposed by Hoffelner [7]. It basically follows the traditional scheme of strain range partitioning method but formulation is simplified and creep damage is calculated based on stress relaxation history. The effect of cyclic softening on creep properties are accounted for by correction of initial stress of relaxation by a magnitude that corresponds to the difference in yield stress before and after cyclic softening.

A strain range is divided into four components, plastic strain range $\Delta\varepsilon_{pp}$, creep strain range $\Delta\varepsilon_{cc}$, plastic-creep strain range (plastic strain in tension and creep strain in compression) $\Delta\varepsilon_{pc}$ and creep-plastic strain range (creep strain in tension and plastic strain in compression) $\Delta\varepsilon_{cp}$. It is assumed that for each of strain ranges, Coffin-Manson law holds. $\Delta\varepsilon_{pp}$ is obtained by fatigue tests without hold time and other strain ranges are obtained from creep-fatigue tests.

$$N_{ik} = A_{ik}\left(\Delta\varepsilon_{ik}\right)^{\alpha_{ik}} \qquad \text{With } i,k=p \text{ and/or } c \tag{3.2.1}$$

Creep-fatigue life $N_f$ can be obtained by the following equation:

$$\frac{1}{N_f} = \frac{1}{N_{pp}} + \frac{1}{N_{pc}} + \frac{1}{N_{cp}} + \frac{1}{N_{cc}} \tag{3.3.2}$$

If we consider creep-fatigue cycles with hold times in tension or compression side only, life corresponding to fatigue and life corresponding to creep are expressed by Equation (3.2.3) and (3.2.4) where suffix *p* and *c* indicating *pp* and *cc* in Equation (3.2.1).

$$N_p = A_p\left(\Delta\varepsilon_{\mathrm{p}}\right)^{\alpha_p} \tag{3.2.3}$$

$$N_{\mathrm{c}} = A_{\mathrm{c}}\left(\Delta\varepsilon_c\right)^{\alpha_c} \tag{3.2.4}$$

Creep-fatigue life $N_f$ is expressed by the following equation:

$$\frac{1}{N_f} = \frac{1}{A_p(\Delta\varepsilon_p)^{\alpha_p}} + \frac{1}{A_c(\Delta\varepsilon_c)\alpha_c} \tag{3.2.5}$$

Inelastic strain range $\Delta\varepsilon_{in}$ is expressed by the following equation:

$$\Delta\varepsilon_{in} = \Delta\varepsilon_p + \Delta\varepsilon_c \tag{3.2.6}$$

Creep damage is calculated by "Spera approach, Equation (3.2.7), which is essentially similar to the definition of creep damage in the time fraction rule.

$$N_{f,AC} = \frac{1}{D_c(\tau)} = \left[\int_0^\tau \frac{1}{t_{f(\sigma,T)}} dt\right]^{-1} \tag{3.2.7}$$

Creep strain is expressed by the following equation:

$$\varepsilon(\tau) = \int_0^\tau \frac{d\varepsilon}{dt}(\sigma,T)dt \tag{3.2.8}$$

**2) Relationships necessary for creep-fatigue life prediction**

There are several necessary relationships for creep-fatigue life prediction other than the cyclic stress-strain curve and the creep strain curve which are described below.

a) Plastic strain range vs $N_p$

Figures 3.2.1 and 3.2.2 show the relationships between plastic strain range and fatigue life ($N_p$) at 550C and 600C, respectively. These relationships can be expressed by the following equation:

$$\Delta\varepsilon_t = \Delta\varepsilon_e + \Delta\varepsilon_p = \frac{\Delta\sigma}{E} + \left(\frac{\Delta\sigma - 2\sigma_p}{K}\right)^{1/m} \tag{3.2.9}$$

b) Creep strain range vs $N_c$

Figures 3.2.3 and 3.2.4 show the relationships between creep strain range and creep life ($N_c$) 550C and 600C, respectively. Creep strain range can be calculated by the following equation where $\Delta\varepsilon_{in}$ indicated elastic strain range:

$$\Delta\varepsilon_p = \Delta\varepsilon_t - \left(\Delta\varepsilon_e + \Delta\varepsilon_p\right) \tag{3.2.10}$$

**3) Creep-fatigue life prediction**

Predicted creep-fatigue life based on the relationships obtained in the previous section is shown in Fig. 3.2.5. Fairly good agreement was obtained. Figure 3.2.6 shows fatigue and creep damage.

The SRS method proposes a method to predict creep damage analytically, in addition to the method which estimates creep damage by curve fitting as described above. Creep damage analytically predicted using Equation (3.2.7) is platted together with creep damage determined from curve fitting (shown in Figs. 3.2.2 and 3.2.3) in Figs 3.2.7 and 3.2.8 for 550C and 600C, respectively. Both of them show almost same slopes which is approximately unity, but the values corresponding to a same creep strain range differ by two orders of magnitude.

The SRS method adjusts the difference by adding the difference of stresses in the monotonic stress-strain curve and cyclic stress-strain curve ("additive stress") to the cyclic stress-strain curve. That is, "additive stress" is added to the initial stress of relaxation and stress relaxation curve is estimated. Then, thus obtained stress relaxation curve is "shifted" downwards by the magnitude of the "additive stress". Stress relaxation is accelerated due to the additive stress. The difference between the monotonic stress-strain curve and the cyclic stress-strain curve is shown in Figs. 3.2.9 and 3.2.10 for 550C and 600C, respectively.

Creep damage is calculated by the shifted stress relaxation curve and original creep rupture properties. Therefore, the additive stress has an effect to decrease estimated creep damage which means that is has an effect to increase predicted creep-fatigue life.

Table 3.2.1 shows the values of additive stress used in this report. The values of the additive stress at 500C and 550C of Case-1 are from reference [7] and other values were taken from the monotonic and cyclic stress-strain curves at relevant temperatures shown in Figs. 3.2.9 and 3.2.10. Figures 3.2.11 and 12 show predicted creep-fatigue life for strain controlled tests based on Case-1 and Case-2, respectively. Predicted life based on Case-1 tends to be unconservative in long-term region and that based on Case-2 showed the opposite tendency. Figure 3.2.13 shows those for stress controlled tests. In the case of stress controlled tests, predicted creep-fatigue life is same for both

cases because stress rupture curves used in the life prediction is not affected by the “additive stress”. Figures 3.2.14 and 3.2.15 show creep damage obtained for Case-1 and Figs. 3.2.16 and 3.2.17 show creep damage obtained for Case-2. The former is smaller than latter. Calculated creep damage is affected by the amount of “additive stress”.

**4) Extrapolation to long-terms**

Figures 3.2.18, 3.2.19 and 3.2.20 show the relationships between hold time and predicted creep-fatigue life for Case-1 and Case-2. The ratio of creep-fatigue life predicted by this method to that predicted by TFR is shown in Figs. 3.2.21 and 3.2.22. The SRS method tends to give longer creep-fatigue life in long-term regions compared to the TFR. Moreover, the SRS method predicts almost constant creep-fatigue (or very small further life reduction) for hold times that exceed a certain level.

In order to interpret the results, estimated stress relaxation behaviors are shown in Figs. 3.2.23 and 3.2.24. In general, as the additive stresses gets larger, larger amount of stress relaxation is predicted. Again generally, when stress becomes lower than a certain level after relaxation, increase of creep damage becomes negligible and life reduction due to the increase of hold time also becomes negligible. This situation is illustrated in Fig. 3.2.25 which shows the relationship between hold time and predicted creep-fatigue life for various values of additive stress. It is observed that the larger the additive stress, the longer the predicted creep-fatigue life. However, when the additive stress becomes larger than 60 MPa, the effect is not so pronounced.

**5) Discussion**

When the analytical method represented by Equation (3.2.7) is used for the estimation of creep damage, the basic flow of the SRS method coincides with that of TFR as shown by Equation (3.2.11).

$$\left.\begin{aligned} &\frac{1}{N_f}=\frac{1}{N_p}+\frac{1}{N_c} \\ &\frac{1}{N_f}=d_f+d_c^* \\ &N_f\left(d_f+d_c^*\right)=N_f d_f+N_f d_c^*=1 \\ &D_f+D_c=1 \end{aligned}\right\} \qquad (3.2.11)$$

The difference in specific points is that creep damage is calculated using only steady state creep rate (the relationship between stress and steady state creep rate). Therefore, very rapid relaxation in the beginning of strain hold dwell is not reproduced in the evaluation. This leads to very conservative prediction of stress relaxation behavior. This might be the reason why the additive stress must be introduced for more realistic prediction of stress relaxation behavior. When the additive stress is introduced, the amount of stress relaxation becomes larger for a certain level of initial stress of relaxation. If the proposed value in reference [7] is adopted, fairly large relaxation is predicted and predicted creep-fatigue life becomes much larger than that predicted by TFR. This situation is shown in Fig. 3.2.26.

Table 3.2.1 Additive stress in the rupture curve

| Temperature (C) | Additive stress (MPa) | |
|---|---|---|
| | Case-1 | Case-2 |
| 500℃ | 107 | 69 |
| 550℃ | 107 | 60 |
| 600℃ | 50 | 50 |

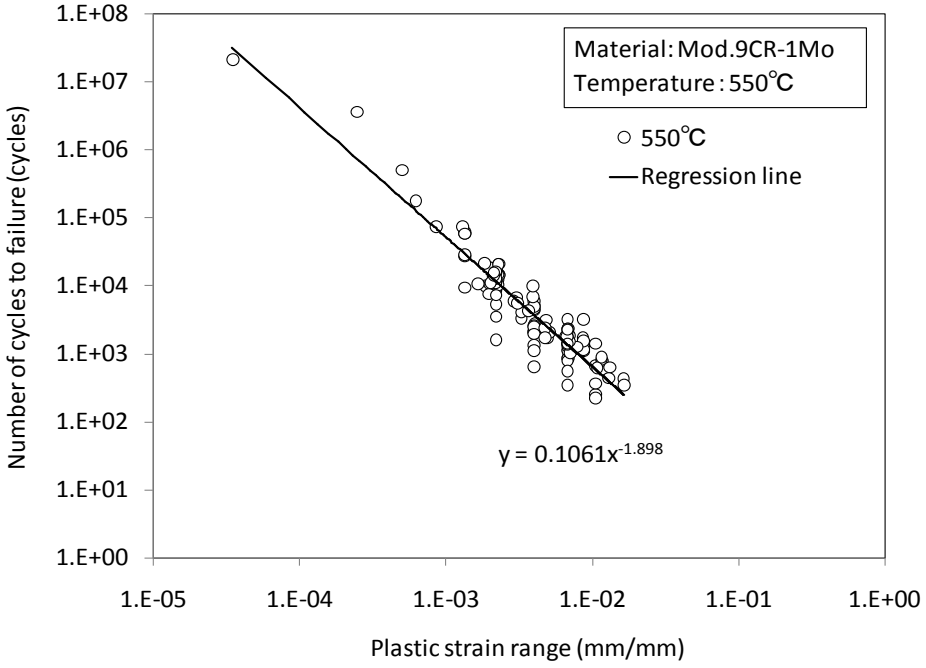


Fig.3.2.1 Formulation of Manson-Coffin type relation $N_p = A_p\left(\Delta\varepsilon_p\right)^{\alpha_p}$ at 550C

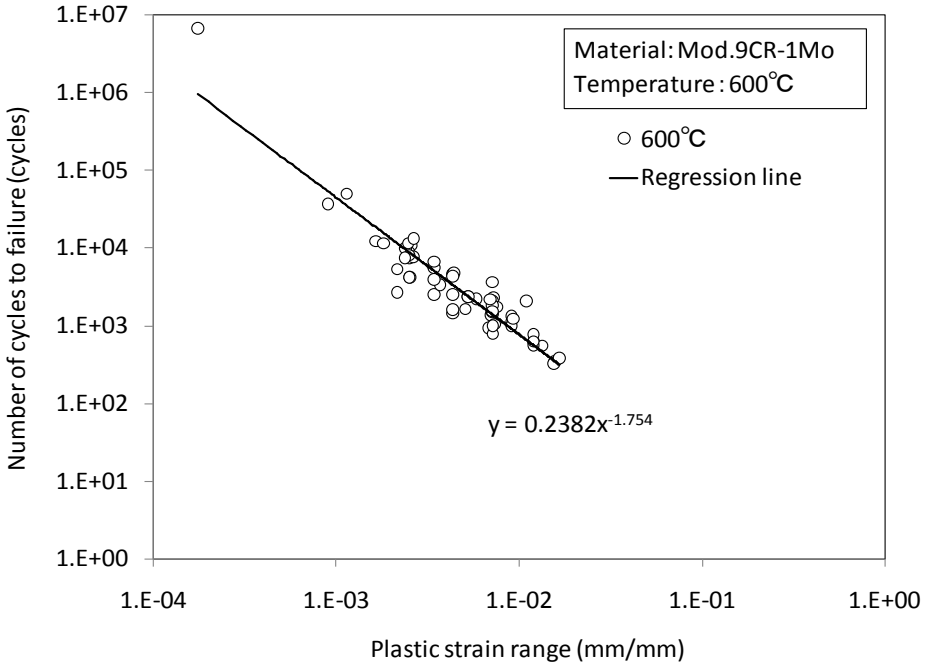


Fig.3.2.2 Formulation of Manson-Coffin type relation $N_p = A_p\left(\Delta\varepsilon_p\right)^{\alpha_p}$ at 600C

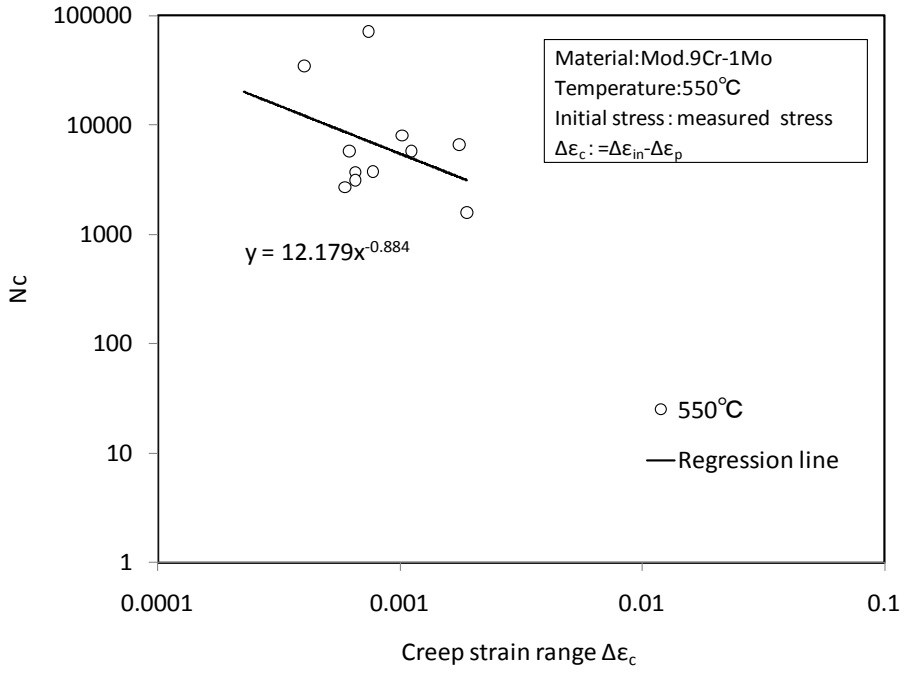


Fig.3.2.3 Formulation of Manson-Coffin type relation $N_c = A_c(\Delta\varepsilon_c)^{\alpha_c}$ at 550C

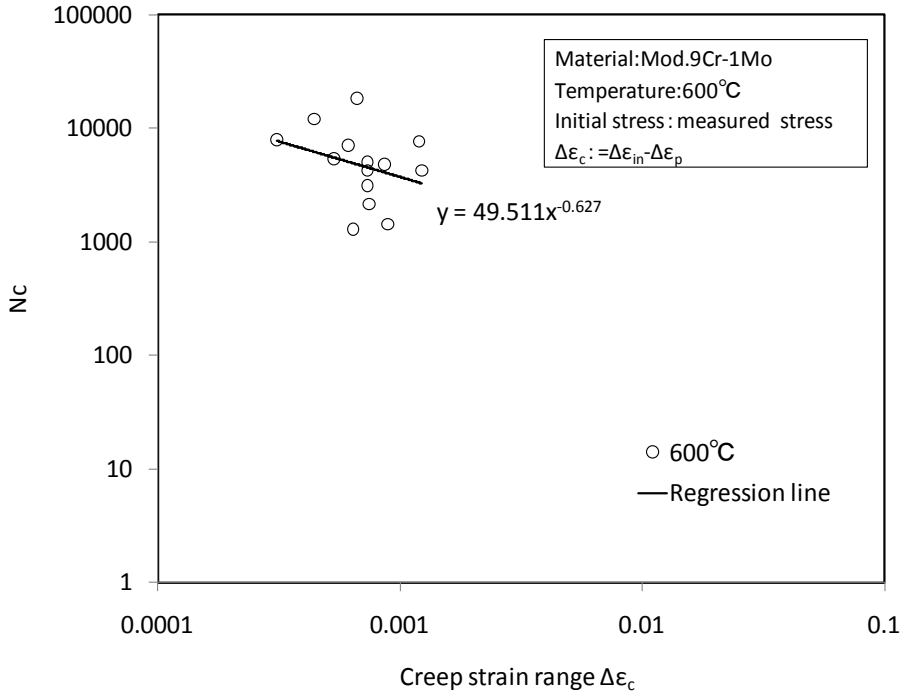


Fig.3.2.4 Formulation of Manson-Coffin type relation $N_c = A_c(\Delta\varepsilon_c)^{\alpha_c}$ at 600C

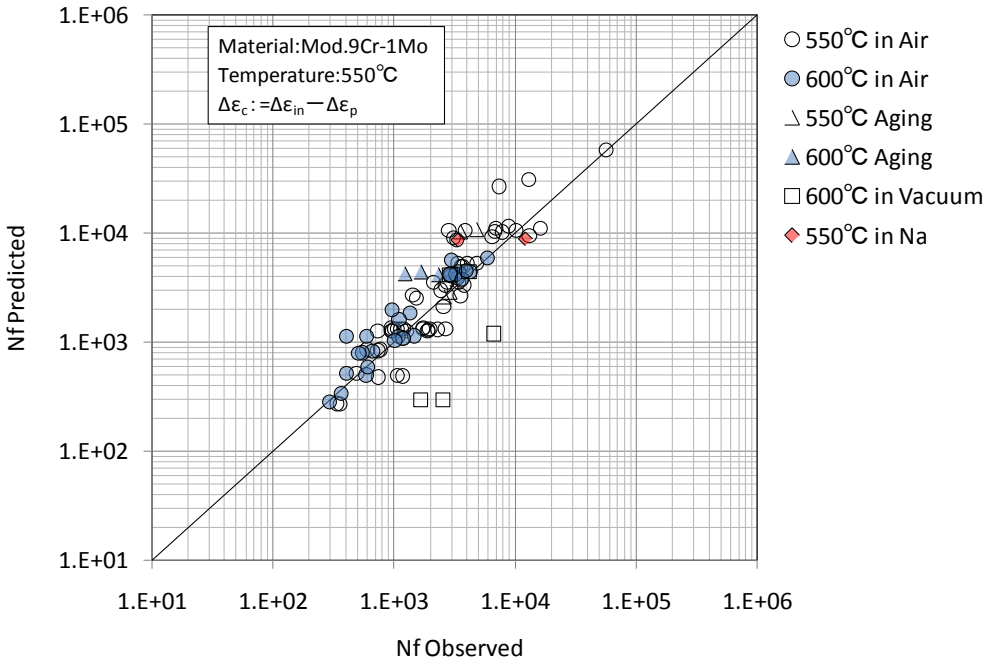


Fig.3.2.5 Observed and predicted creep-fatigue life by SRS method

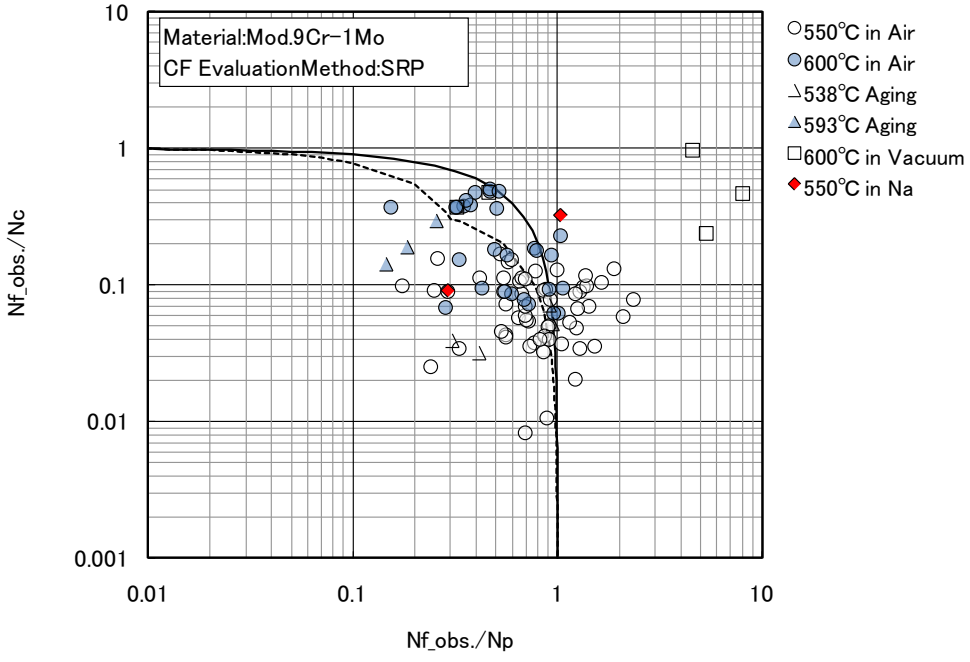


Fig.3.2.6 Creep-fatigue damage calculated by SRS method

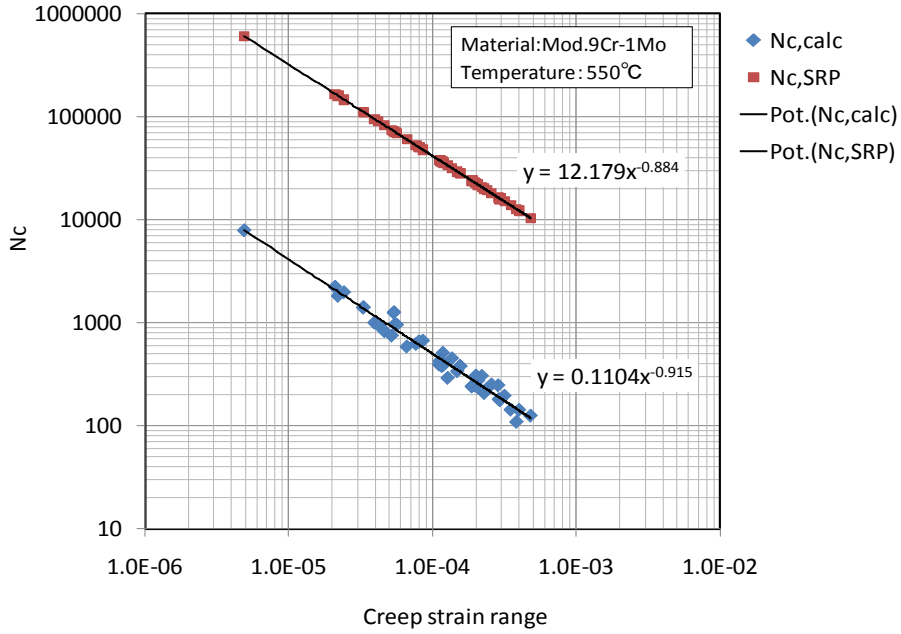


Fig.3.2.7 Comparison of pure cyclic creep life determined by curve fitting and that determined by numerical integration of creep damage at 550C

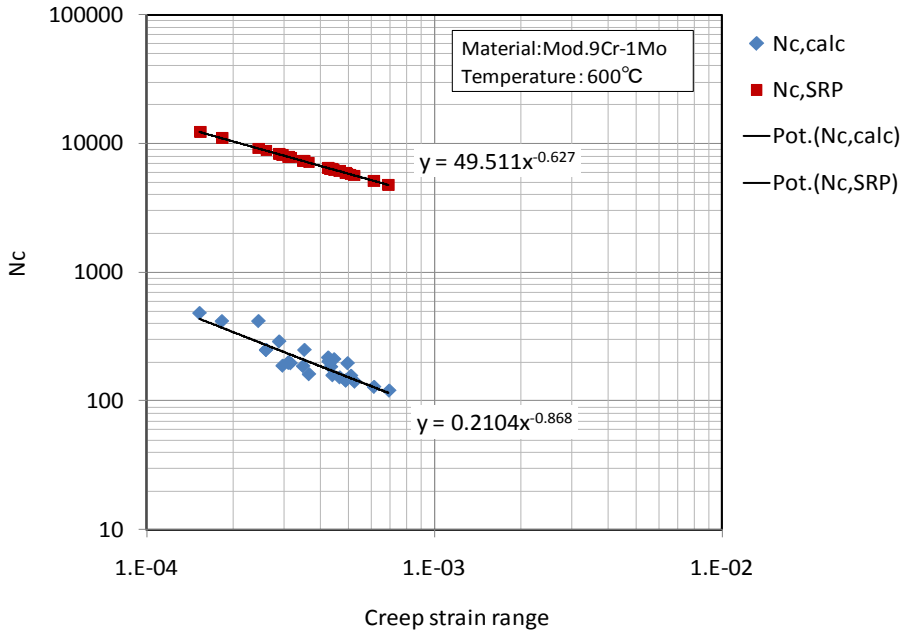


Fig.3.2.8 Comparison of pure cyclic creep life determined by curve fitting and that determined by numerical integration of creep damage at 600C

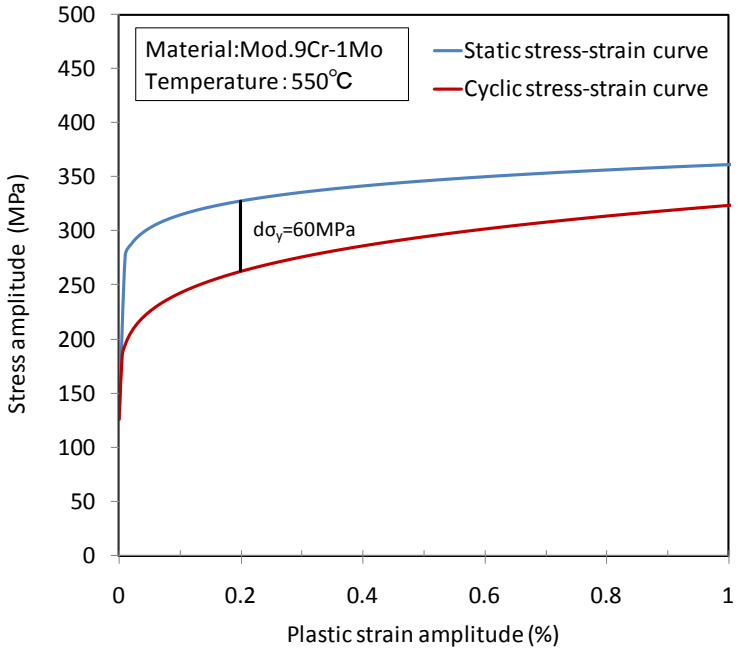


Fig. 3.2.9 Difference of yield stress between static and cyclic stress-strain relations at 550 C

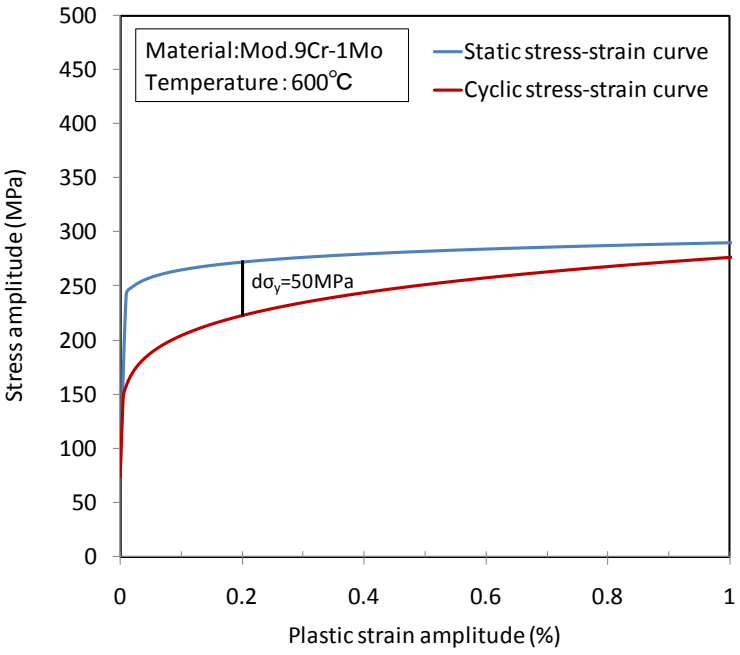


Fig. 3.2.10 Difference of yield stress between static and cyclic stress-strain relations at 600 C

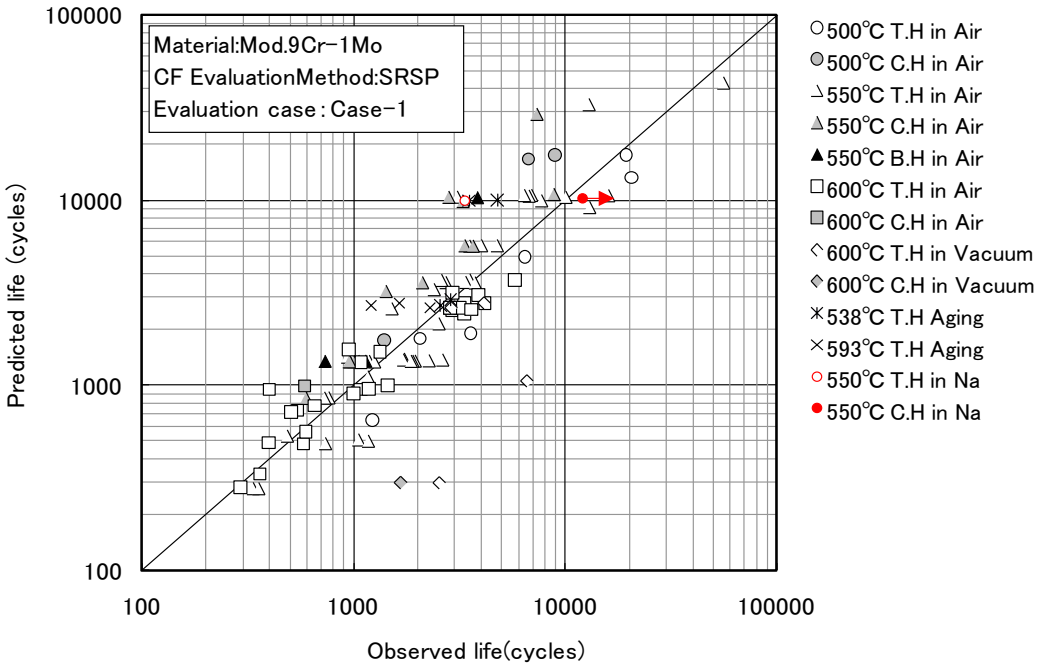


Fig.3.2.11 Observed and predicted creep-fatigue life by SRS method (Case-1)

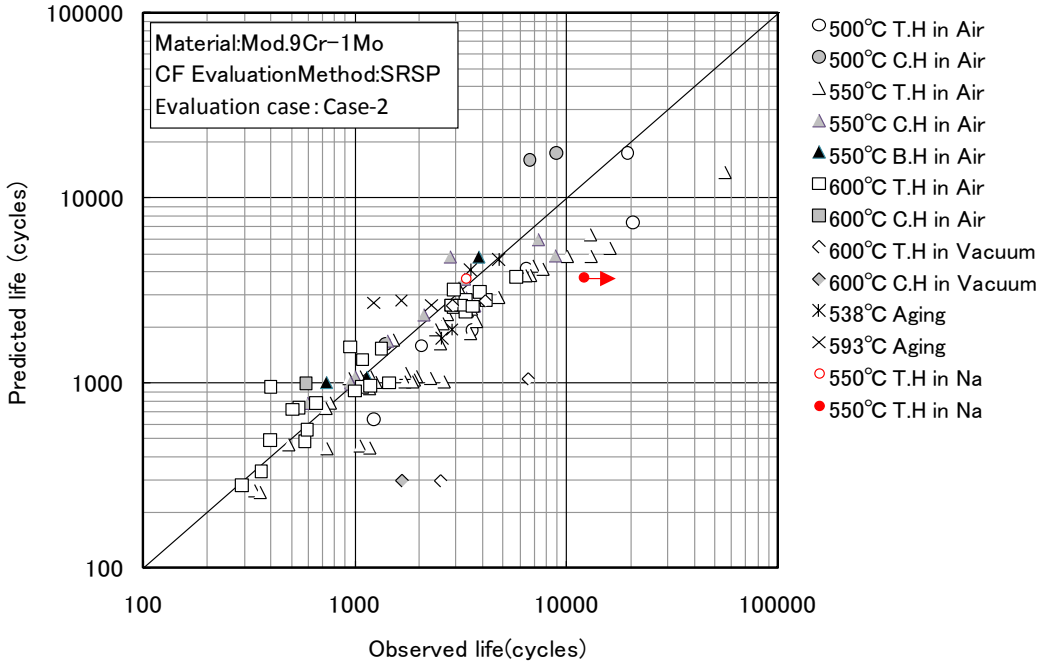


Fig.3.2.12 Observed and predicted creep-fatigue life by SRS method (Case-2)

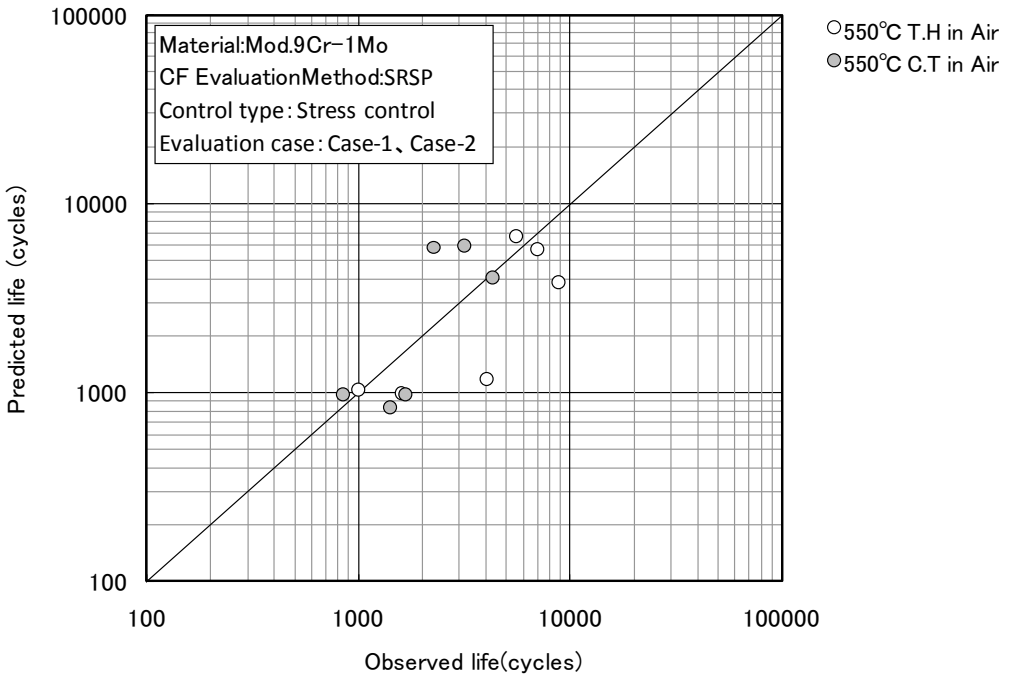


Fig.3.2.13 Observed and predicted creep-fatigue life by SRS method for stress controlled tests (Case-1 and 2)

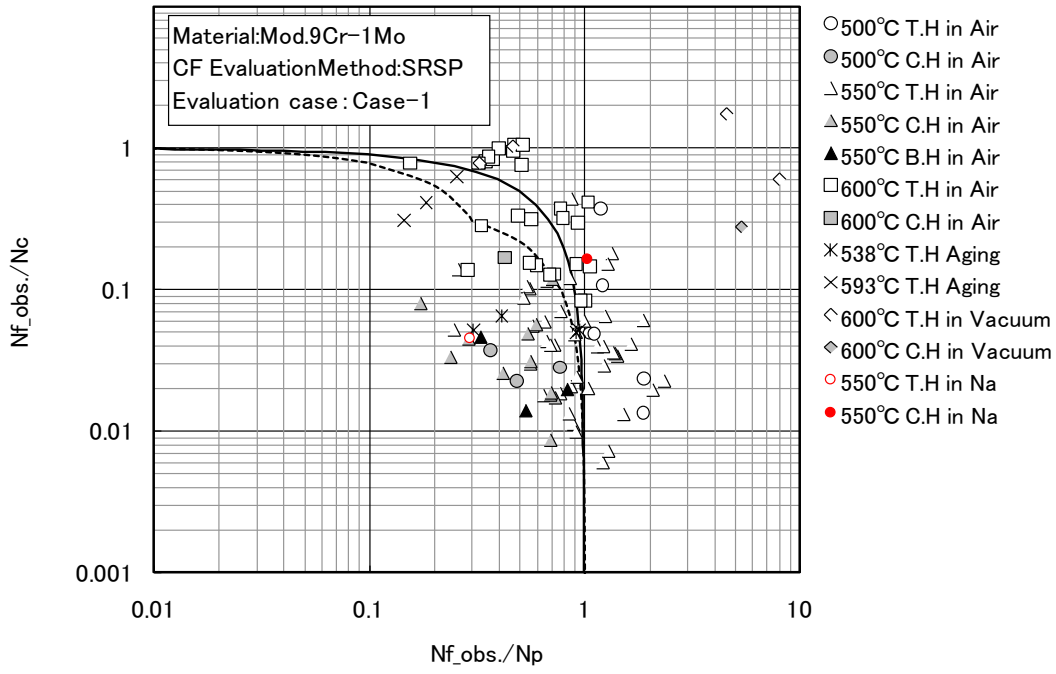


Fig.3.2.14 Creep-fatigue damage calculated by SRS method (Case-1)

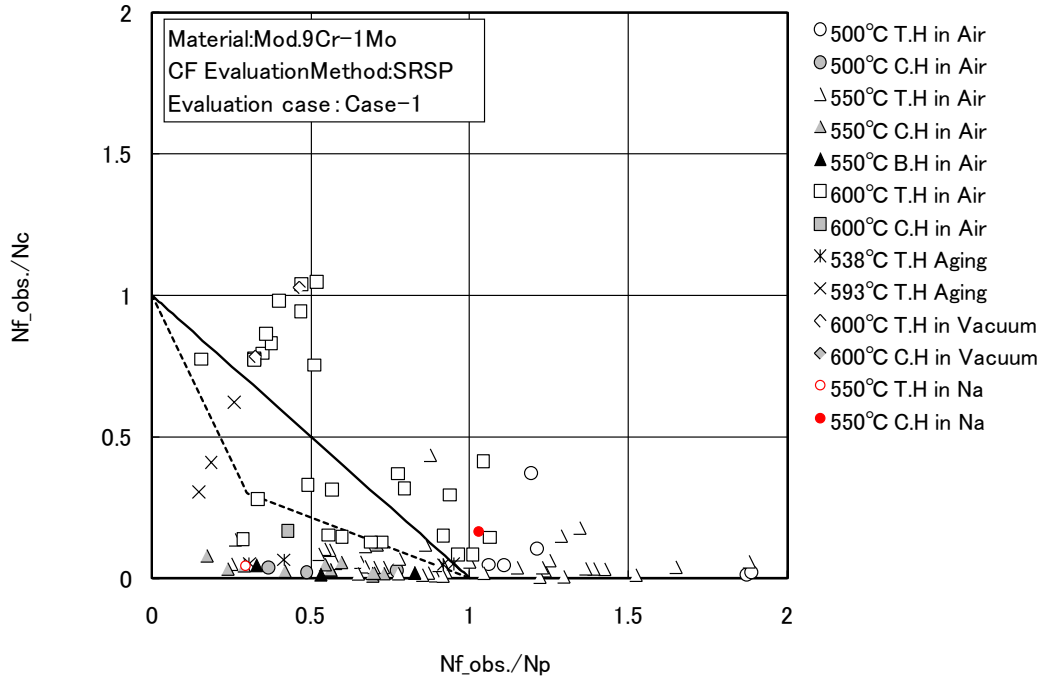


Fig.3.2.15 Creep-fatigue damage calculated by SRS method shown in normal scale (Case-1)

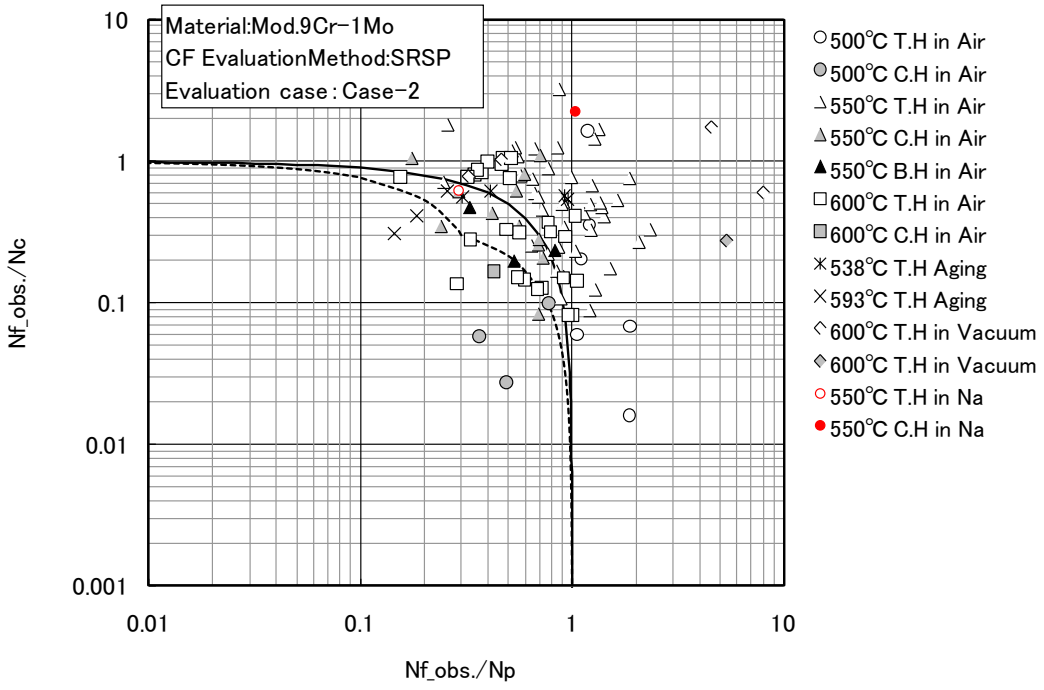


Fig.3.2.16 Creep-fatigue damage calculated by SRS method (Case-2)

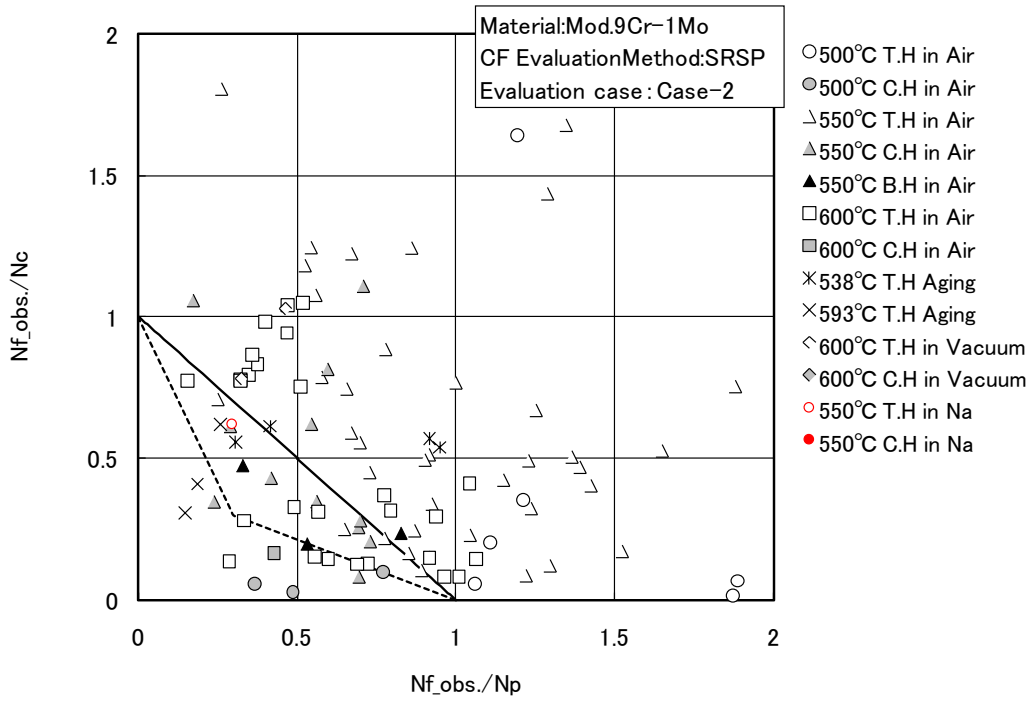


Fig.3.2.17 Creep-fatigue damage calculated by SRS method shown in normal scale (Case-2)

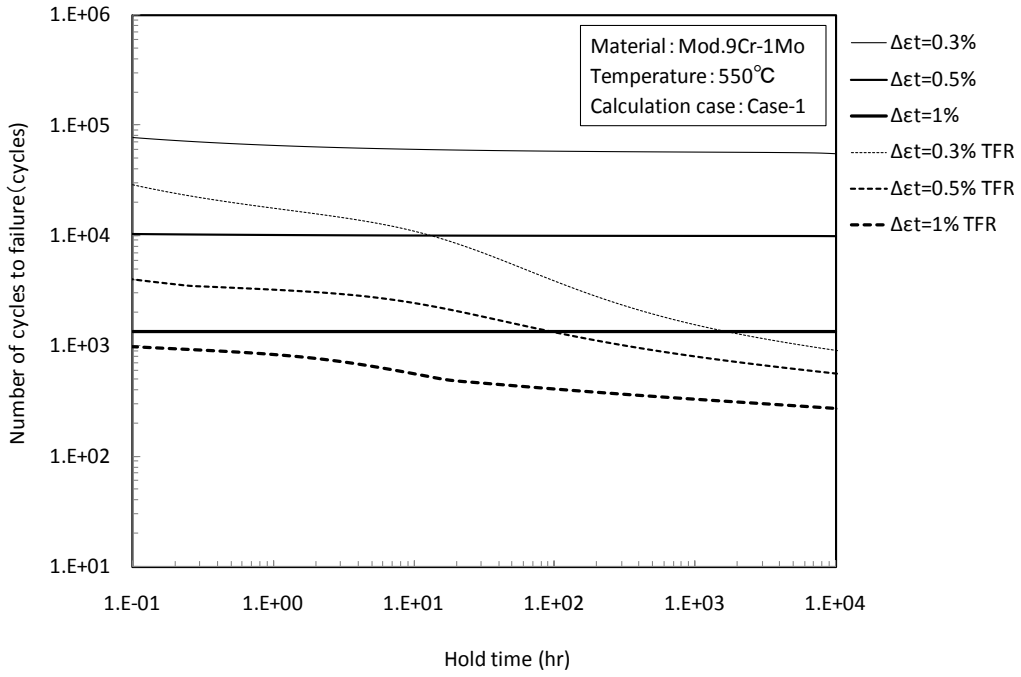


Fig.3.2.18 Comparison of creep-fatigue life between SRS (Case-1) and TFR at 550 C

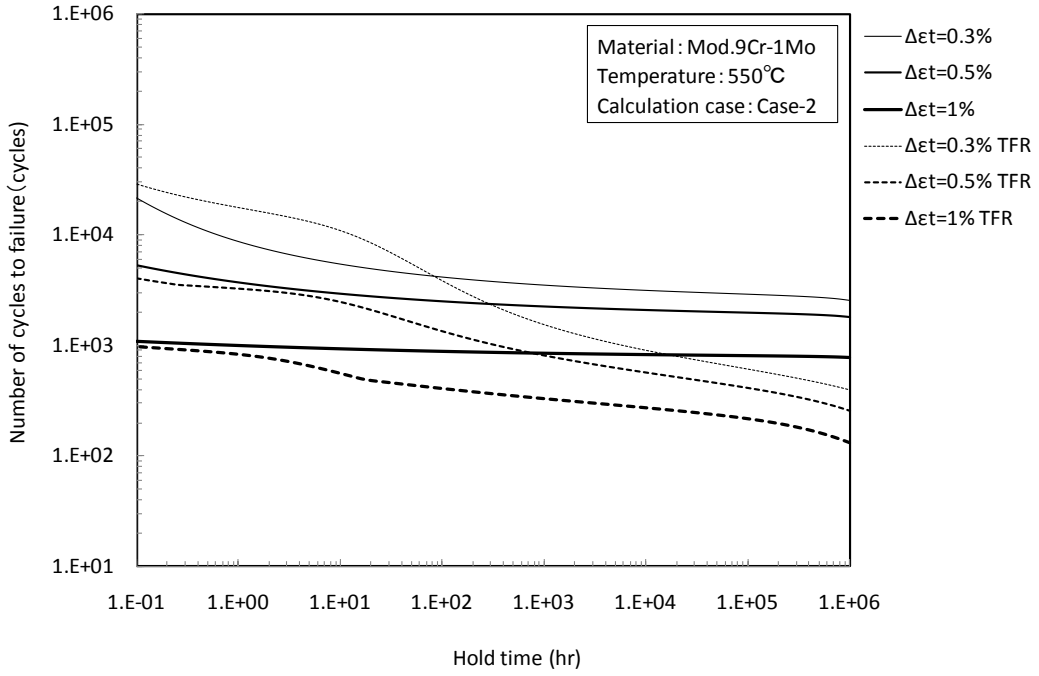


Fig.3.2.19 Comparison of creep-fatigue life between SRS (Case-2) and TFR at 550 C

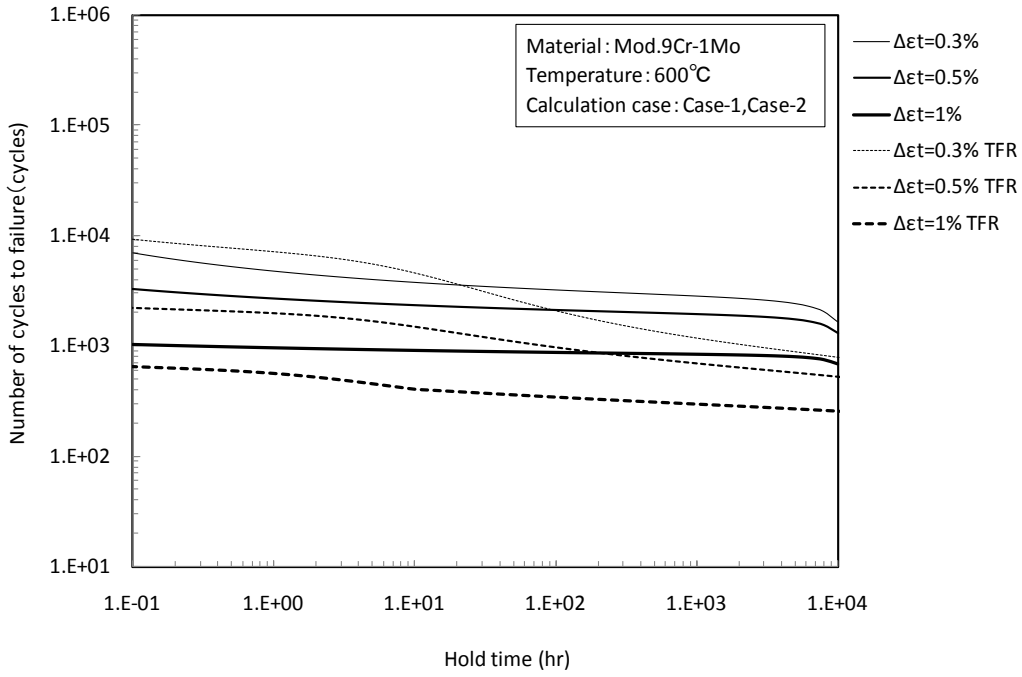


Fig.3.2.20 Comparison of creep-fatigue life between SRS (Case-1 and Case-2) and TFR at 600 C

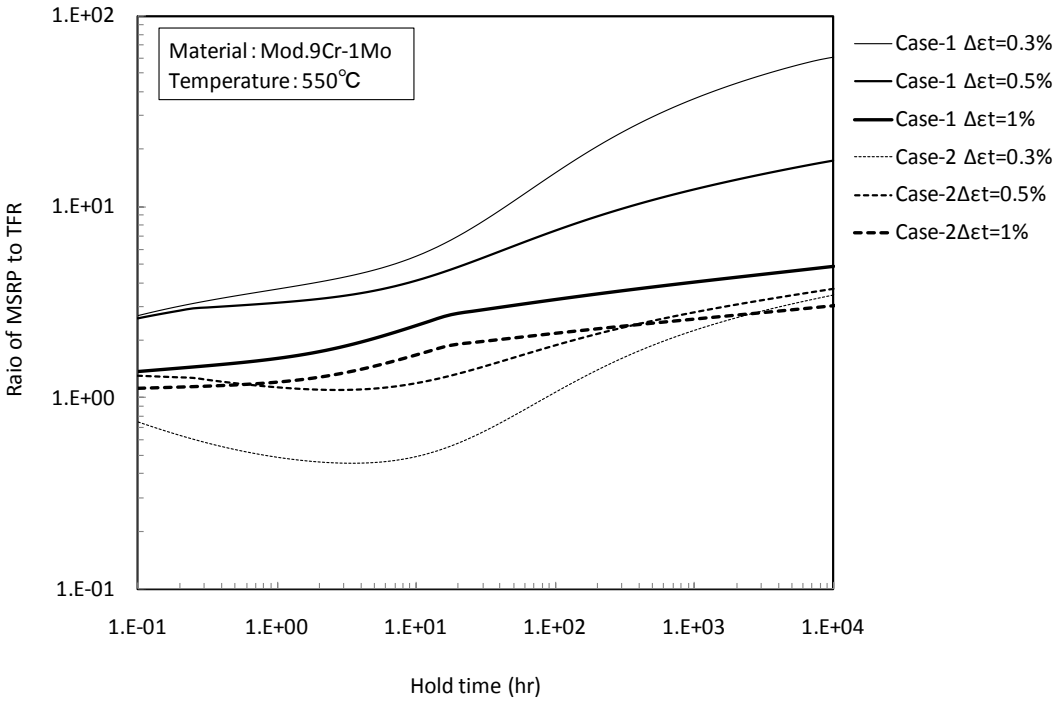


Fig.3.2.21 Ratio of predicted creep-fatigue life by SRS method to that predicted by TFR at 550C

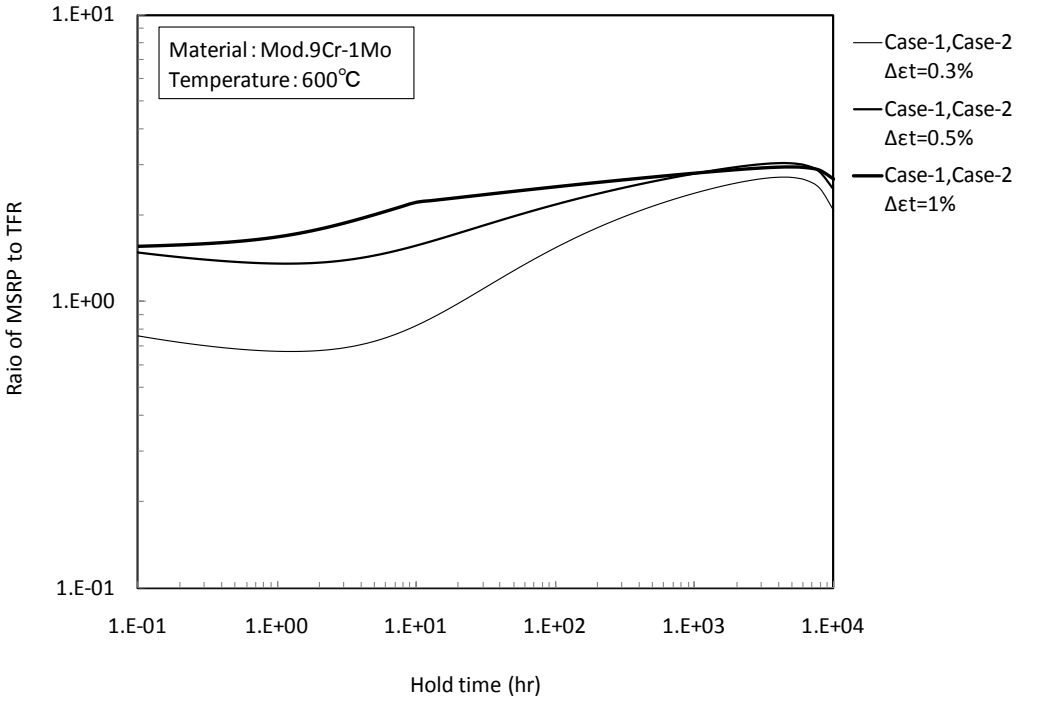


Fig.3.2.22 Ratio of predicted creep-fatigue life by SRS method to that predicted by TFR at 600C

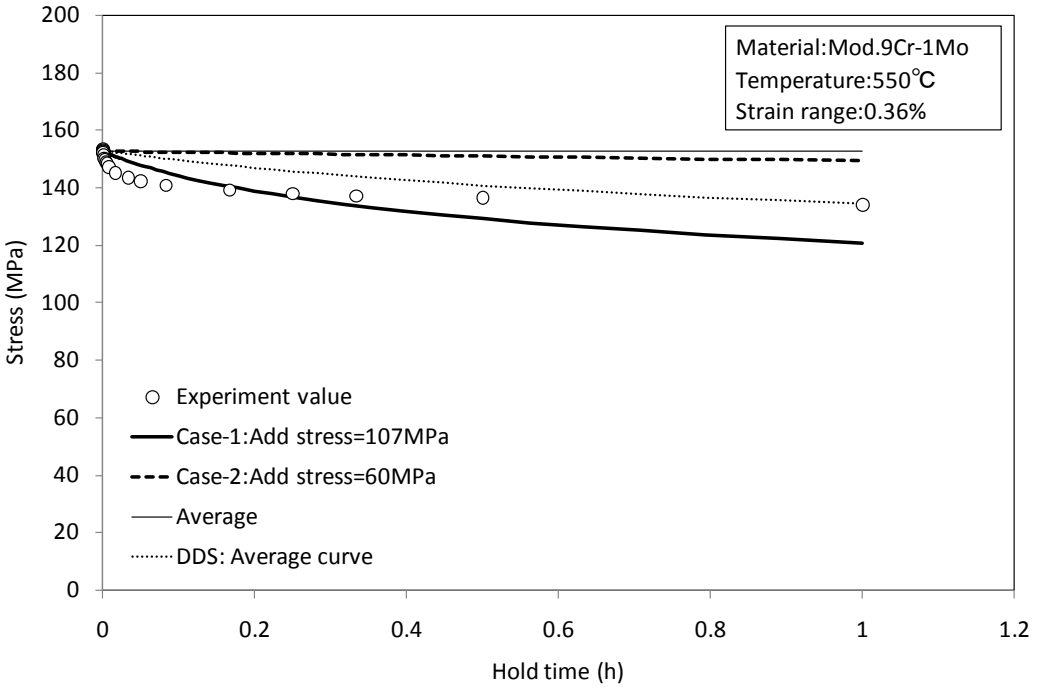


Fig.3.2.23 Effect of additive stress on stress relaxation behavior (Example-1)

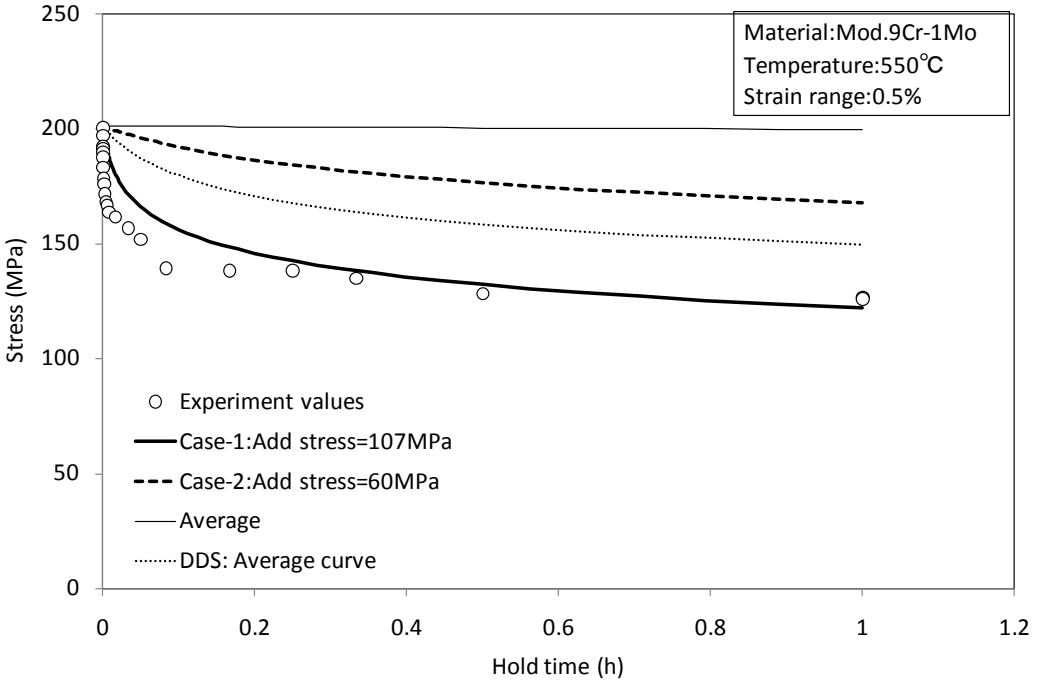


Fig.3.2.24 Effect of additive stress on stress relaxation behavior (Example-2)

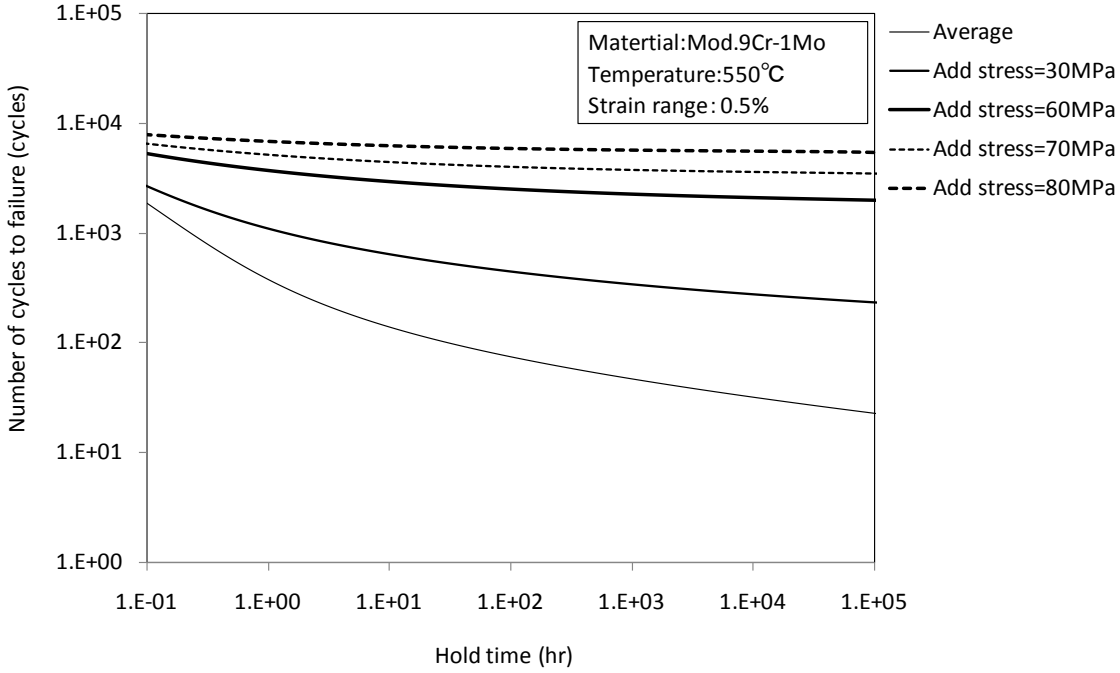


Fig.3.2.25 Effect of additive stress on predicted creep-fatigue life

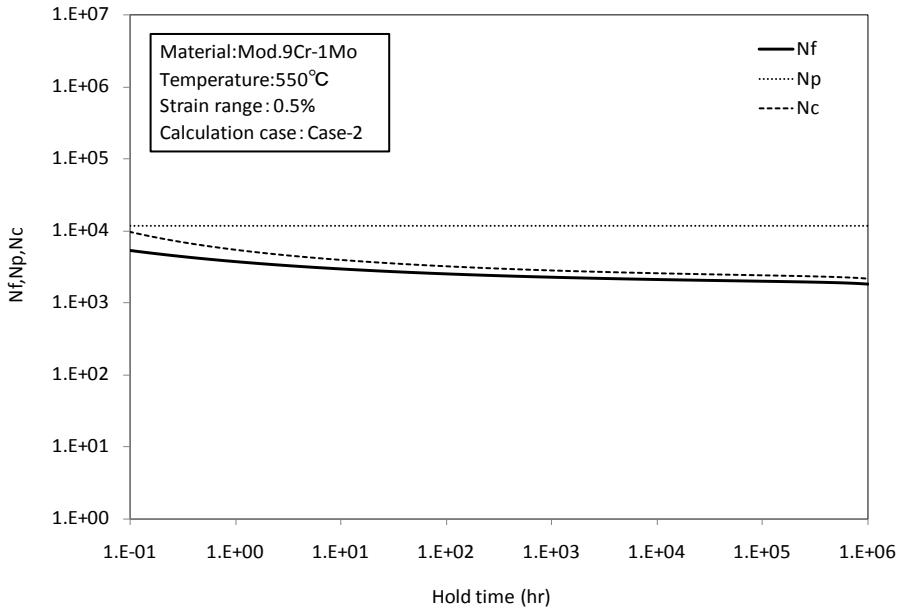


Fig.3.2.26 Comparison of $N_p$, $N_c$, and $N_f$ (Case-2, 550C, $\Delta\varepsilon_t$ =0.5%)

## 3.3 Approach for Pressure Vessel Applications

### 3.3.1 Outline

**1) Concept**

This method was proposed by M. Prager [9] for the application to pressure vessels. This method has been incorporated in a Code Case of the ASME Boiler and Pressure Vessel Code Section VIII. The basic idea is that creep strain and strain rate are increased by cyclically imposed plastic strain and hold time.

Fatigue damage is defined using usual Minor's rule as described in Equation (3.3.1).

$$D_f = \frac{N}{N_f} \tag{3.3.1}$$

$D_f$ : Accumulated fatigue damage

$N$ : Number of cycles imposed

$N_f$ : Fatigue life absent creep

Creep damage is defined by Equation (3.3.2). This is the essential part of the method.

$$D_c = \frac{T_f}{T_r} \tag{3.3.2}$$

$T_f$ : Life with fatigue

$T_r$ : Life absent fatigue

Creep-fatigue interaction is automatically evaluated by the above equations depending on loading conditions as investigated in the discussion section and there is no fixed diagram or envelope to estimate it.

### 3.3.2 Predictability of experimental results

**1) Creep-fatigue life prediction procedure**

Creep life with fatigue (creep-fatigue life, hereafter) is predicted by Equation (3.3.3) by characterizing the rate strain increase with creep strain absent fatigue.

$$T_f = \frac{\ln\left(\beta\varepsilon_p N' T_r + 1\right)}{\beta\varepsilon_p N'} \tag{3.3.3}$$

$\beta$ : Material constant determined from creep-fatigue tests

$\varepsilon_p$ : Plastic strain per cycle

$N'$ : Cycle frequency or 1/hold time

$t_H$ : Hold time per one cycle

$\beta$ represents the extent of creep-fatigue interaction. The larger the $\beta$, the larger the interaction, and $\beta = 0$ indicates there is no creep-fatigue interaction. Dividing Equation (3.3.3) by creep time (hold time per one cycle $t_H$), we get creep-fatigue life as shown in Equation (3.3.4).

$$\begin{aligned} N_{cf} &= \frac{T_f}{t_H} \\ &= \frac{T_r D_c}{t_H} \\ &= \frac{T_r \ln\left(\beta\varepsilon_p N' T_r + 1\right)}{\beta\varepsilon_p N' t_H T_r} \\ &= \frac{\ln\left(\beta\varepsilon_p N' T_r + 1\right)}{\beta\varepsilon_p} \end{aligned} \tag{3.3.4}$$

$N_{cf}$ : Creep-fatigue life in cycles

This method focuses on the effect of plastic strain on creep-fatigue. When there is no fatigue, life (life absent fatigue) coincides with creep life itself. This can be confirmed from the viewpoint of life with fatigue from the following consideration.

$$\lim_{\varepsilon_p \to 0} N_{cf} = \lim_{\varepsilon_p \to 0} \frac{\ln\left(\beta\varepsilon_p N' T_r + 1\right)}{\beta\varepsilon_p}$$
$$= \lim_{\varepsilon_p \to 0} \frac{\dfrac{\beta N' T_r}{\beta\varepsilon_p N' T_r + 1}}{\beta}$$
$$= N' T_r$$
$$= 1$$

The following consideration confirms that no creep-fatigue interaction is considered when .

$$\lim_{\beta \to 0} N_{cf} = \lim_{\beta \to 0} \frac{\ln\left(\beta\varepsilon_p N' T_r + 1\right)}{\beta\varepsilon_p}$$
$$= \lim_{\varepsilon_p \to 0} \frac{\dfrac{\varepsilon_p N' T_r}{\beta\varepsilon_p N' T_r + 1}}{\varepsilon_p}$$
$$= N' T_r = \frac{T_r}{t_H}$$

**2) Predicted creep-fatigue life**

As we can see from Equation (3.3.4), creep-fatigue life depends on the material constant $\beta$. Therefore, the effects when $\beta$ takes a value between 0.05 and 4 were investigated for the following four cases where life absent fatigue $T_r$ was determined in deferent ways.

**Case-1:** For each test data, take measured creep-fatigue life times hold time per hour as a value of $T_r$.

$$T_r = N_{f\_fat} \cdot t_H \qquad (3.3.5)$$

$N_{f\_fat}$ : Measured creep-fatigue life

**Case-2:** Take the longest value of measured creep-fatigue life times hold time per hour among the creep-fatigue data. In this case, $T_r = 2 \times 10^4$ hours.

**Case-3:** Use the product of fatigue life (absent creep) and hold time per cycle as $T_r$. This $T_r$ becomes always larger than the one used in Case-1 which is measure creep-fatigue life time.

**Case-4:** Use $T_r = 1\times10^6$ hours as a value obtained by multiplying a service period (of fossil plants) of $1x10^5$ hours by a factor of safety 10.

Figures 3.3.1 shows the creep-fatigue life predicted by the method of Case-1. As $\beta$ becomes closer to 0, predicted creep-fatigue life approaches to measured creep-fatigue life. This can be explained as follows. We start with Equation (3.3.4).

$$N_{cf} = \ln\left(\beta\varepsilon_p N' T_r + 1\right) / \beta\varepsilon_p$$

We set $T_r$ by Equation (3.3.5).
Then,

$$\begin{aligned} N_{cf\_pred} &= \frac{\ln\left(\beta\varepsilon_p N' T_r + 1\right)}{\beta\varepsilon_p N' t_H} \\ &= \frac{\ln\left(\beta\varepsilon_p N' N_{cf\_obs} \cdot t_H + 1\right)}{\beta\varepsilon_p N' t_H} \\ &= \frac{\ln\left(\beta\varepsilon_p N_{cf\_obs} + 1\right)}{\beta\varepsilon_p} \end{aligned} \qquad (3.3.6)$$

When $\beta$ approaches zero, we obtain the following which shows that predicted creep-fatigue and measured creep-fatigue life coincide.

$$\lim_{\beta\to 0} N_{cf\_pred} = \lim_{\beta\to 0} \frac{\ln\left(\beta\varepsilon_p N_{cf\_obs} + 1\right)}{\beta\varepsilon_p}$$
$$= \lim_{\beta\to 0} \frac{\dfrac{\varepsilon_p N_{cf\_obs}}{\beta\varepsilon_p N_{cf\_obs} + 1}}{\varepsilon_p}$$
$$= \lim_{\beta\to 0} \frac{N_{cf\_obs}}{\beta\varepsilon_p N_{cf\_obs} + 1}$$
$$= N_{cf\_obs} \qquad (3.3.7)$$

Figure 3.3.2 shows fatigue damage and creep damage obtained by this method. A Campbell type diagram of which interception is (0.3, 0.3) is plotted just for comparison. It is to be noted that these "interaction diagrams" are not used for life prediction by this method and that the estimation of creep-fatigue interaction is considered to depend on loading conditions (strain range and hold time, etc) as shown in the discussion section of this chapter.

Figures 3.3.3 shows the creep-fatigue life predicted by the method of Case-2. In this case, $\beta = 1$ gave the best result. However, prediction tends to be more conservative as creep-fatigue becomes longer. Figure 3.3.4 shows fatigue damage and creep damage.

Figure 3.3.5 shows the creep-fatigue life predicted by the method of Case-3. In this case, difference in life prediction due to the value of $\beta$ is not so large. Figure 3.3.6 shows fatigue damage and creep damage. What is specific to this case is that fatigue damage and creep damage show identical values. This can be shown by Equations (3.3.1), (3.3.2), (3.3.4) and the definition of $T_r$ in Case-3.

Figures 3.3.7 shows the creep-fatigue life predicted by the method of Case-4. In this case, $\beta = 2$ gave the best result. However, prediction tends to be more conservative as creep-fatigue becomes longer. Figure 3.3.8 shows fatigue damage and creep damage.

Figures 3.3.9 and 3.3.10 summarize the result with $T_r$=1x10$^6$ hours and $\beta = 2$. Although it is considered that appropriate values of $T_r$ should be selected to predict creep-fatigue life corresponding to various different conditions by this method, $T_r$=1x10$^6$ was used to predict all the experimental results for simplicity. It is observed that creep-fatigue life prediction tends to be more

conservative as life becomes longer, however scatter is within reasonable extent.

Figures 3.3.11 and 3.3.12 show creep-fatigue life prediction results for stress controlled tests using the assumptions of Case-2. Figures 3.3.13 and 3.3.14 show those obtained using the assumptions of Case-3. Figures 3.3.15 and 3.3.16 show those obtained using the assumptions of Case-4. In both cases, prediction seems to be better compared to Figs 3.3.1, 3.3.3 and 3.3.7 which correspond to strain controlled creep-fatigue tests. It may be because the method is originally proposed for fossil power plants where normal load is generally constant. However, it should be noted that there are few data with long tensile hold tensile data.

**3) Extrapolation of creep-fatigue life**

As we can see from Equation (3.3.4), creep-fatigue life depends on the material constant $\beta$. Therefore, the effects of $\beta$ between 0.05 and 4 were investigated for the following three cases where life absent fatigue $T_r$ was determined in different ways. Figure 3.3.17 shows predicted creep-fatigue life as a function of hold time per cycle when is 2 and $T_r$ is $1x10^6$ hours. Creep-fatigue life predicted by the time-fraction method is also plotted for comparison. The present method gives similar results to the one by the time fraction method in short term region but in long term region it tends to give a more conservative and at $1x10^6$ hours the predicted creep-fatigue life becomes 1. Figure 3.3.18 shows the result with $\beta$ is 4 and $T_r$ is $1x10^6$ hours. Predicted creep-fatigue life becomes slightly more conservative compared to Fig. 3.3.17.

Figure 3.3.19 shows the effect of $\beta$ when it varies from 1 to 4 with $T_r$ fixed to $1x10^6$ hours. Figure 3.3.20 shows the effect of $T_r$ when it varies from $1x10^5$ hour$1x10^8$ hours.

**4) Discussion**

In the present method, the estimation of plastic strain amplitude that is used for creep-fatigue life evaluation is very important. Figure 3.3.21 shows cyclic stress-strain curves for with and without hold times. Hold time generally reduces stress range and thus plastic strain range is affected accordingly. For precise evaluation, it is considered that plastic strain amplitude for hold time for which creep-fatigue life is to be predicted should be used.

Another important point regarding this method is that the degree of creep-fatigue interaction depends on loading conditions, unlike other methods such as the time fraction method in which the “interaction diagram” is fixed and used for all the conditions. In order to see the situation of

creep-fatigue interaction in the present method, the resultant creep-fatigue “interaction diagram” evaluated is given in Figs. 3.3.22 and 3.3.23. The lines in the figures are the relationships between fatigue damage and creep damage at creep-fatigue fail lure. Each line corresponds to a specific combinations of $\beta$ and $T_r$, with plastic strain range being a parameter which varies to obtain locus. It is understood that the degree of creep-fatigue interaction becomes severer when $\beta$ becomes larger and if $T_r$ is fixed, and it becomes severer when $T_r$ becomes shorter when $\beta$ is fixed. The concept that creep-fatigue interaction depends on loading conditions seems to be reasonable when that fact that what is happening in materials depends on temperature, strain range and hold time.

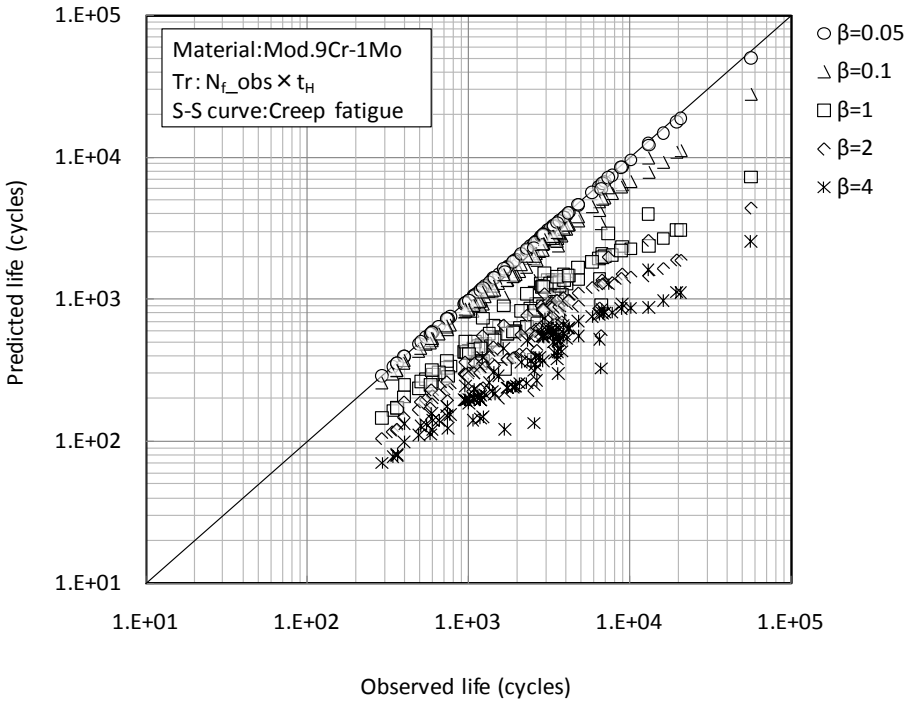


Fig.3.3.1 Observed and predicted creep-fatigue life with $T_r$=$N_{f_obs.}$x $t_H$ (Case-1)

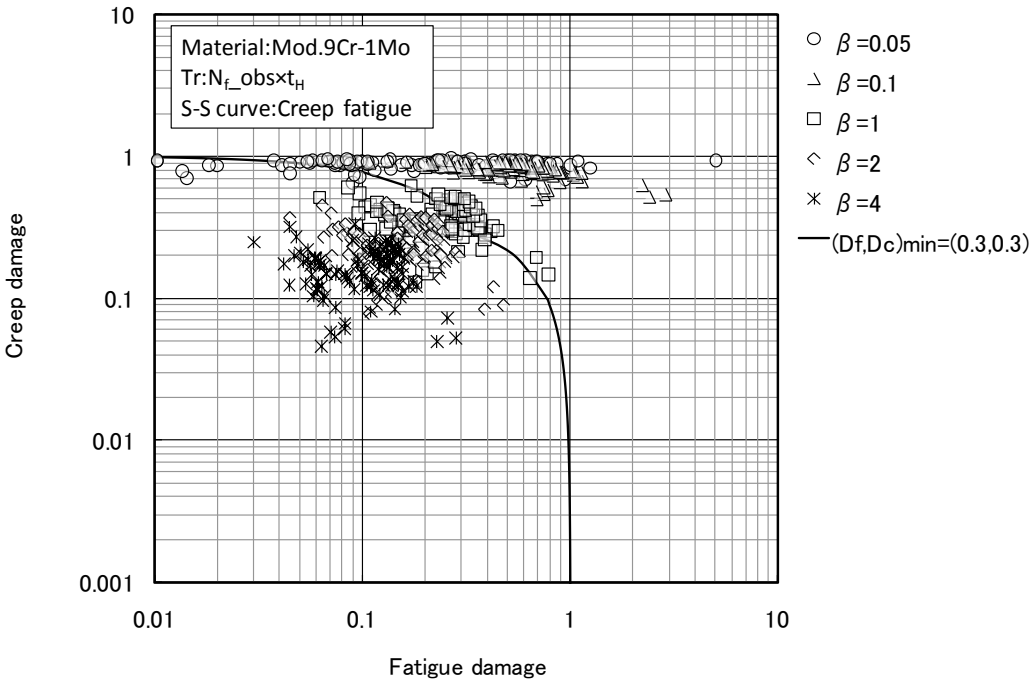


Fig.3.3.2 Creep-fatigue damage calculated with $T_r$=$N_{f_obs.}$x $t_H$ (Case-1)

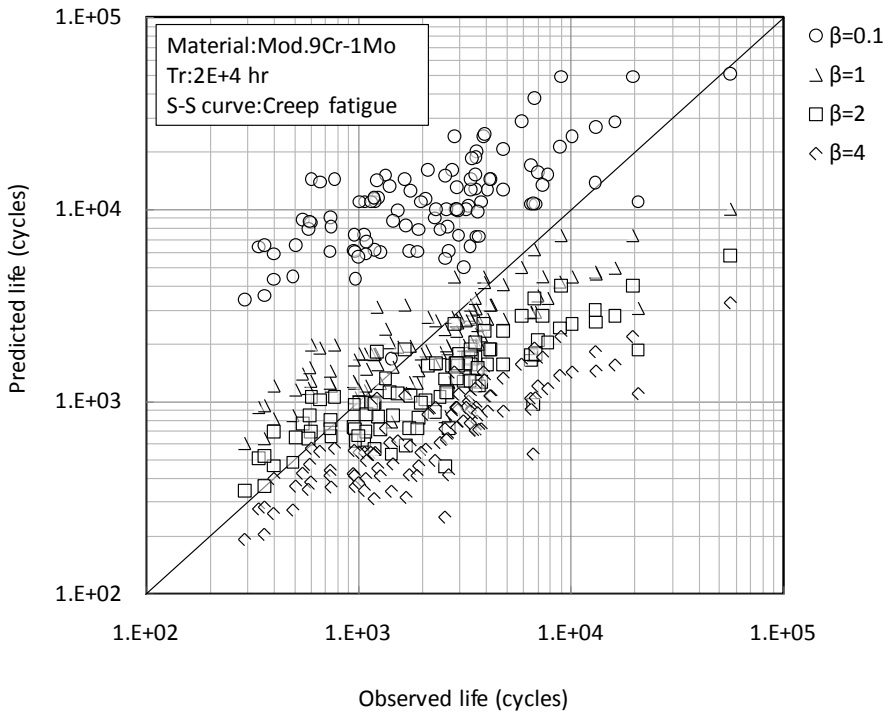


Fig.3.3.3 Observed and predicted creep-fatigue life with $T_r$=2x10$^4$ hours (Case-2)

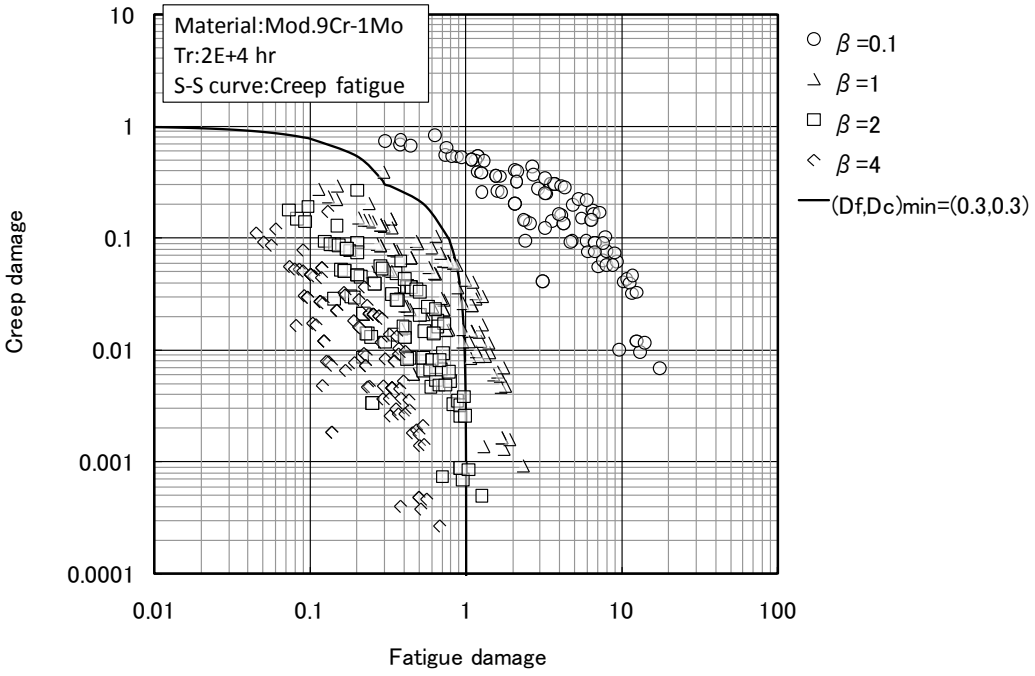


Fig.3.3.4 Creep-fatigue damage calculated with $T_r$=2x10$^4$ hours (Case-2)

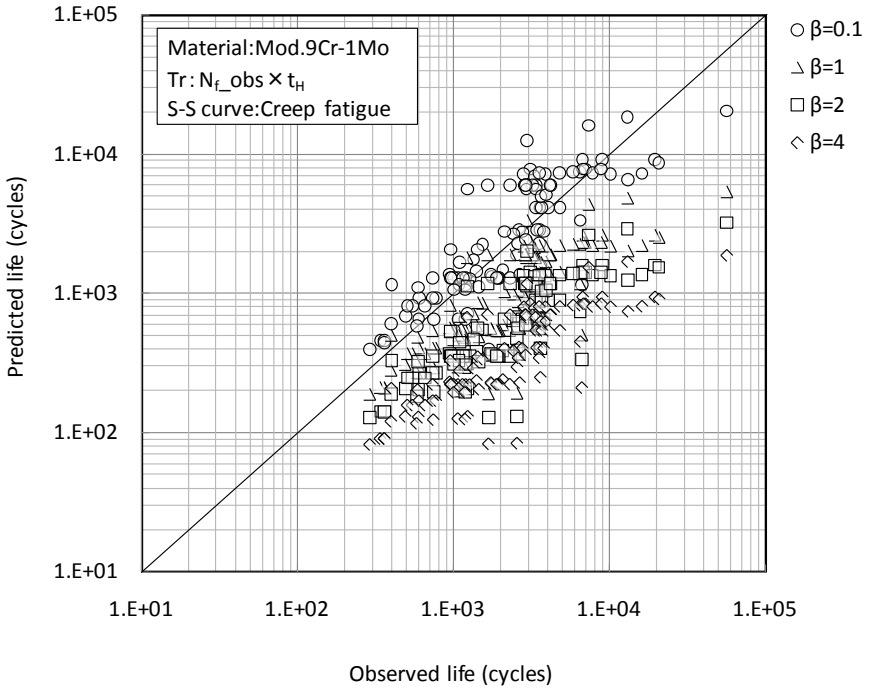


Fig.3.3.5 Observed and predicted creep-fatigue life with $T_r$=fatigue life x $t_H$ (Case-3)

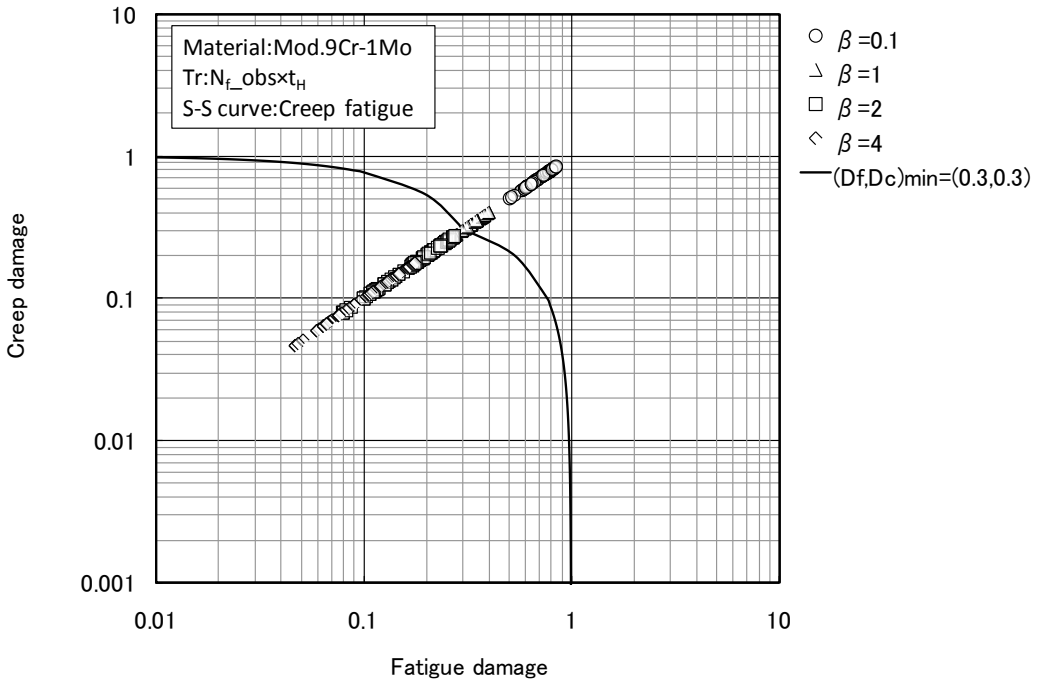


Fig.3.3.6 Creep-fatigue damage calculated with $T_r$=fatigue life x $t_H$ (Case-3)

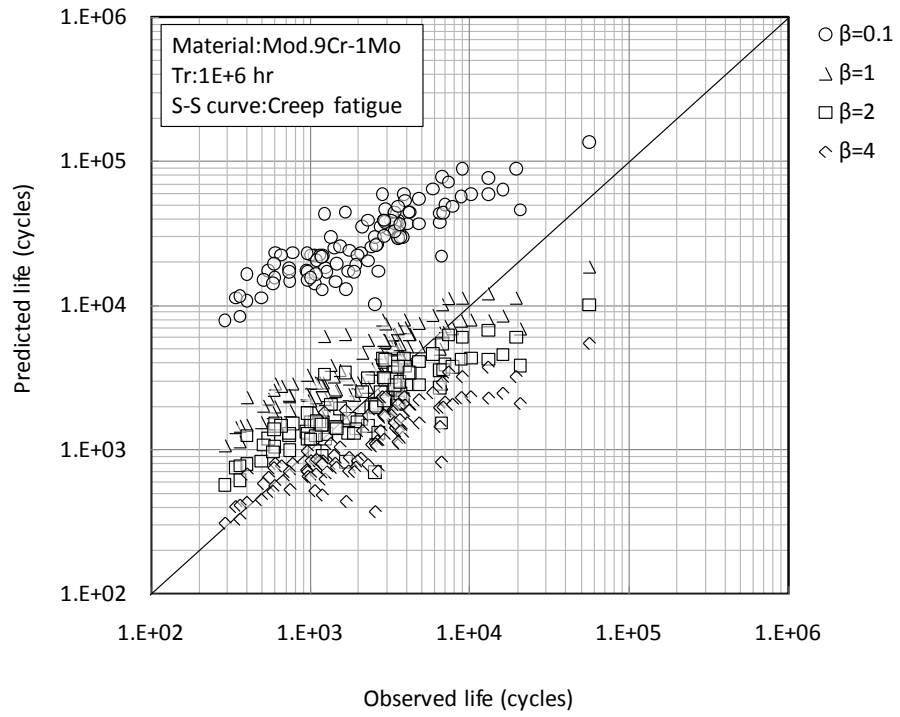


Fig.3.3.7 Observed and predicted creep-fatigue life with $T_r$=1x10$^6$ hours (Case-4)

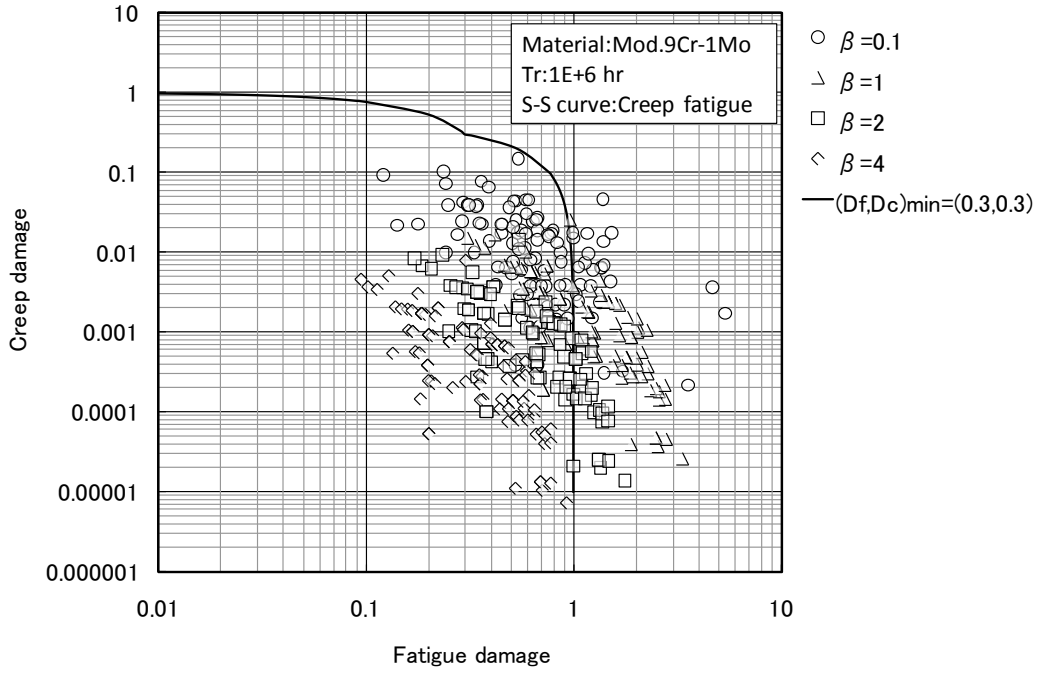


Fig.3.3.8 Creep-fatigue damage calculated with $T_r$=1x10$^6$ hours (Case-4)

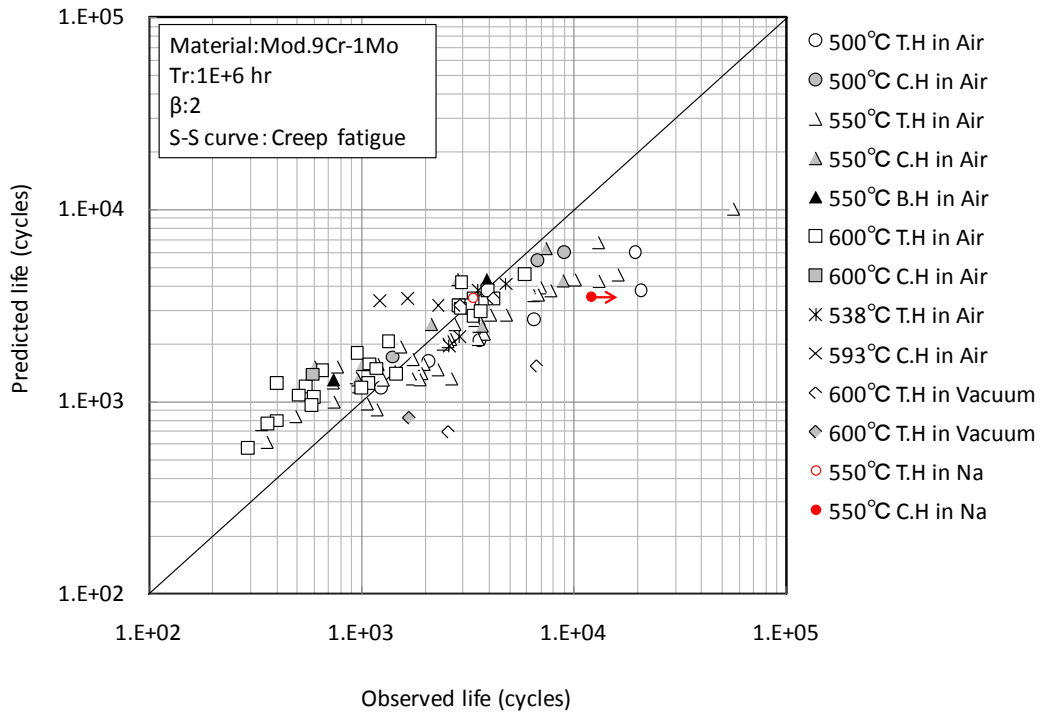


Fig.3.3.9 Observed and predicted creep-fatigue life with $T_r$=1x10$^6$ hours and $\beta = 2$

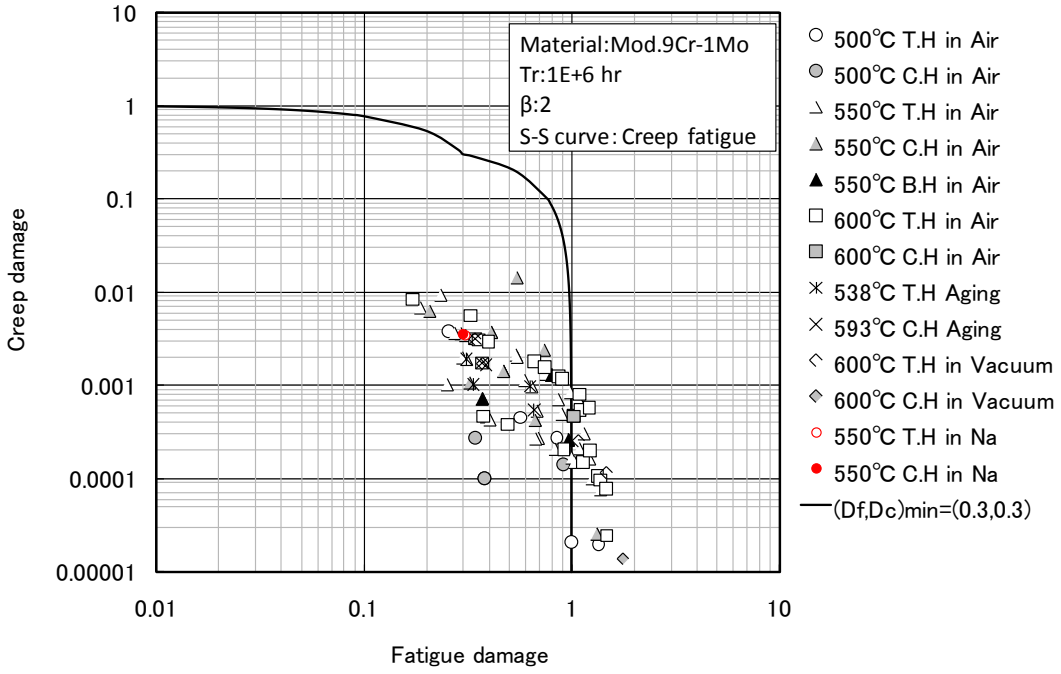


Fig.3.3.10 Creep-fatigue damage with $T_r$=1x10$^6$ hours and $\beta = 2$

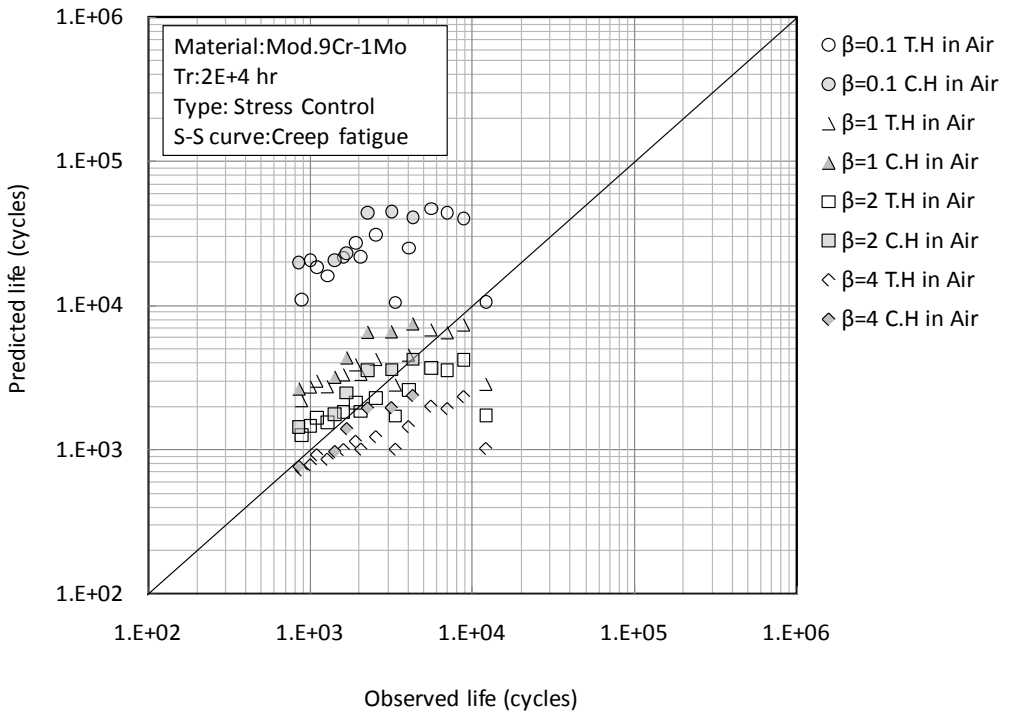


Fig. 3.3.11 Observed and predicted creep-fatigue life under stress controlled conditions (Case-2)

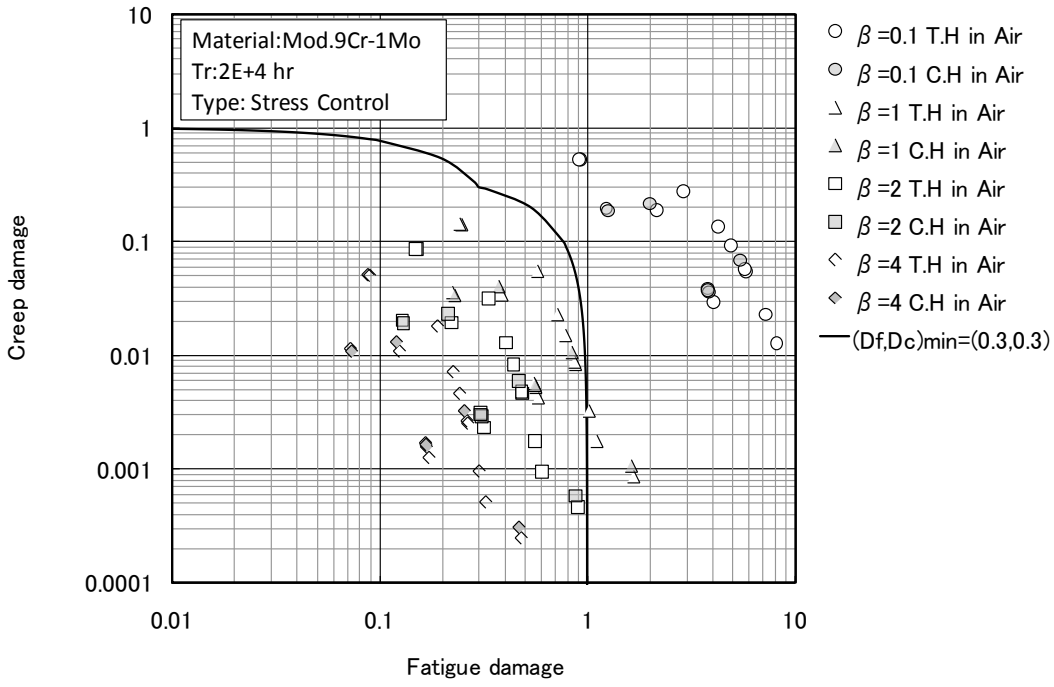


Fig. 3.3.12 Creep-fatigue damage under stress controlled conditions (Case-2)

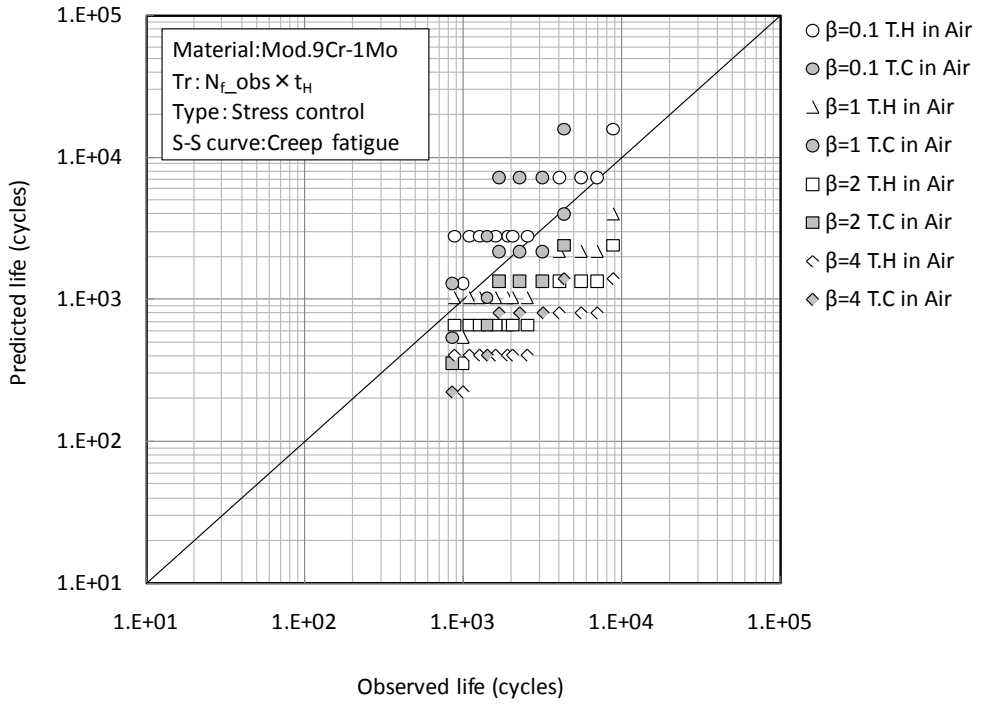


Fig. 3.3.13 Observed and predicted creep-fatigue life under stress controlled conditions (Case-3)

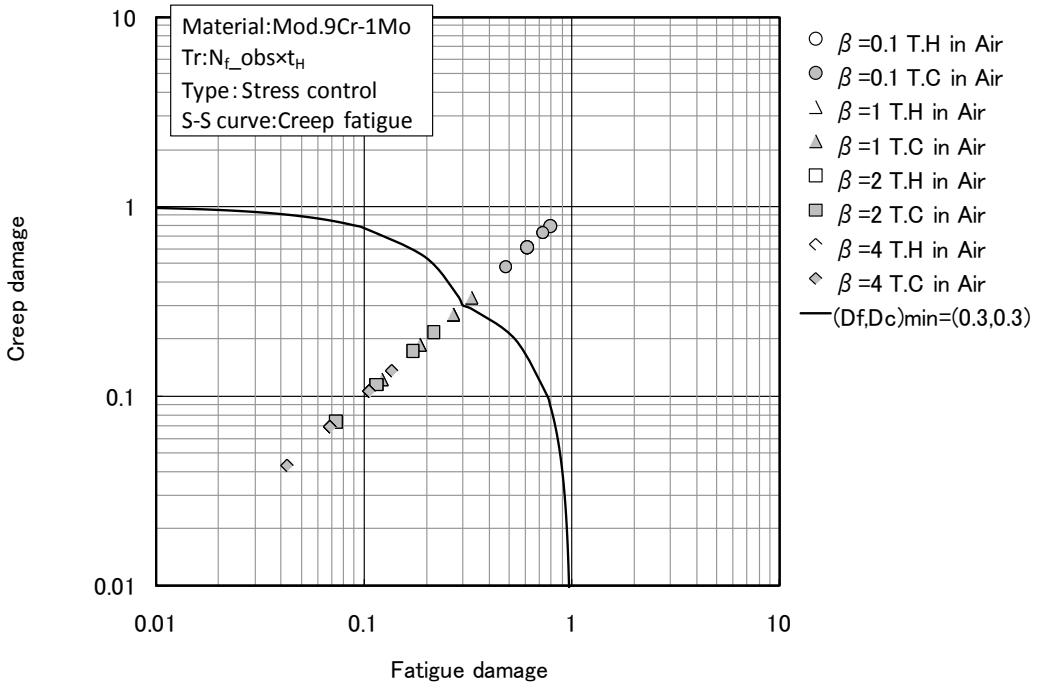


Fig. 3.3.14 Creep-fatigue damage under stress controlled conditions (Case-3)

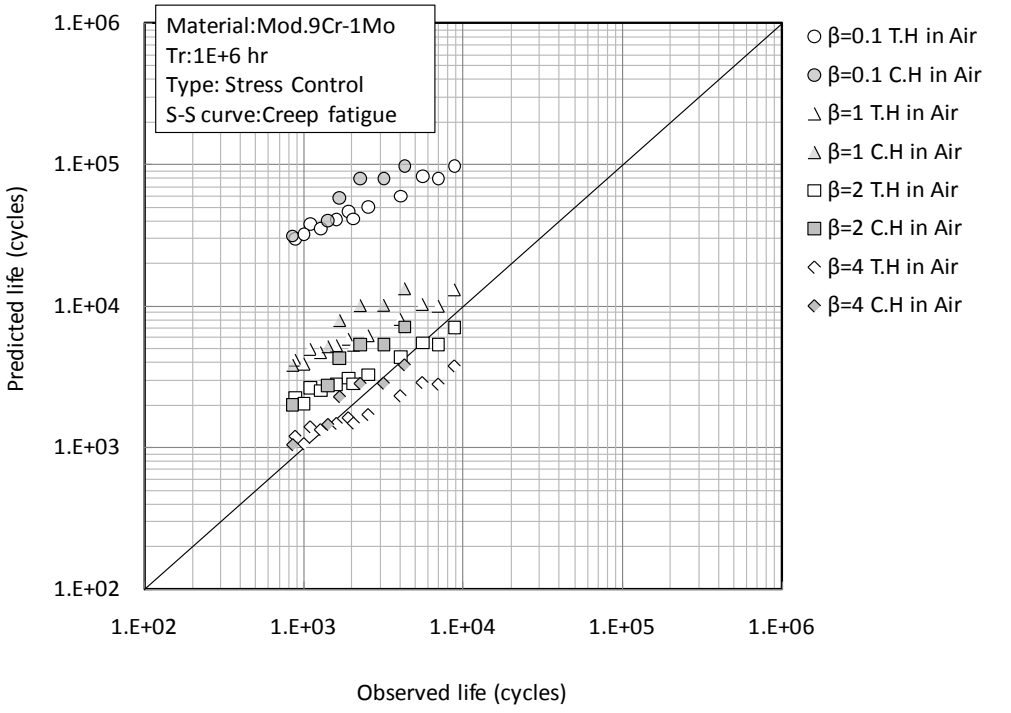


Fig.3.3.15 Observed and predicted creep-fatigue life under stress controlled conditions (Case-4)

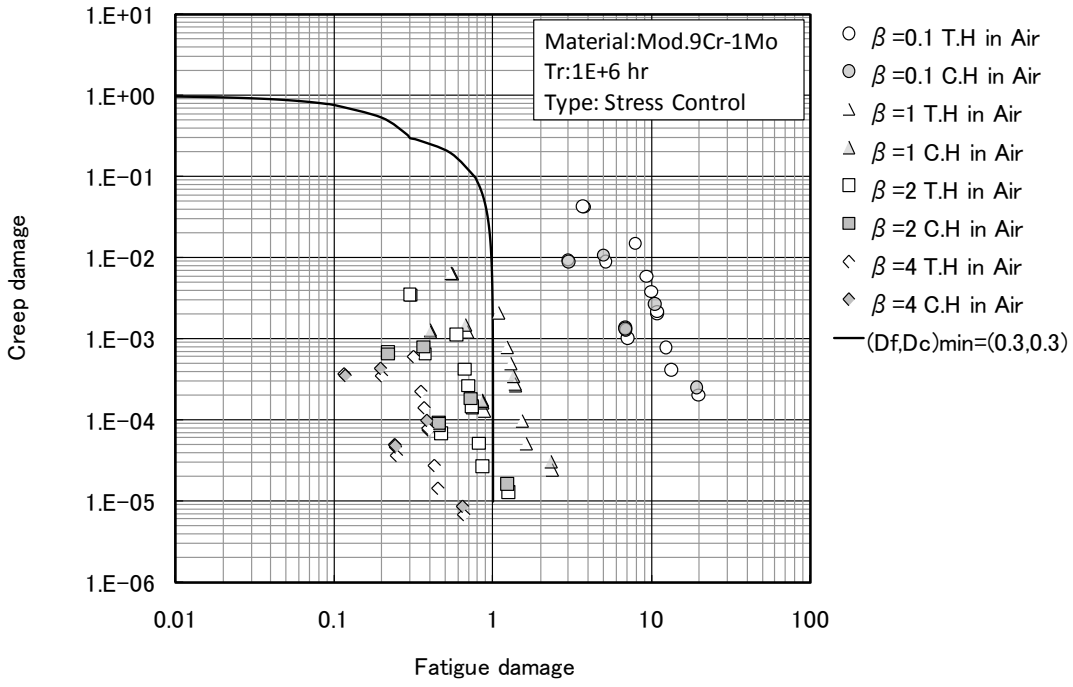


Fig.3.3.16 Creep-fatigue damage under stress controlled conditions (Case-4)

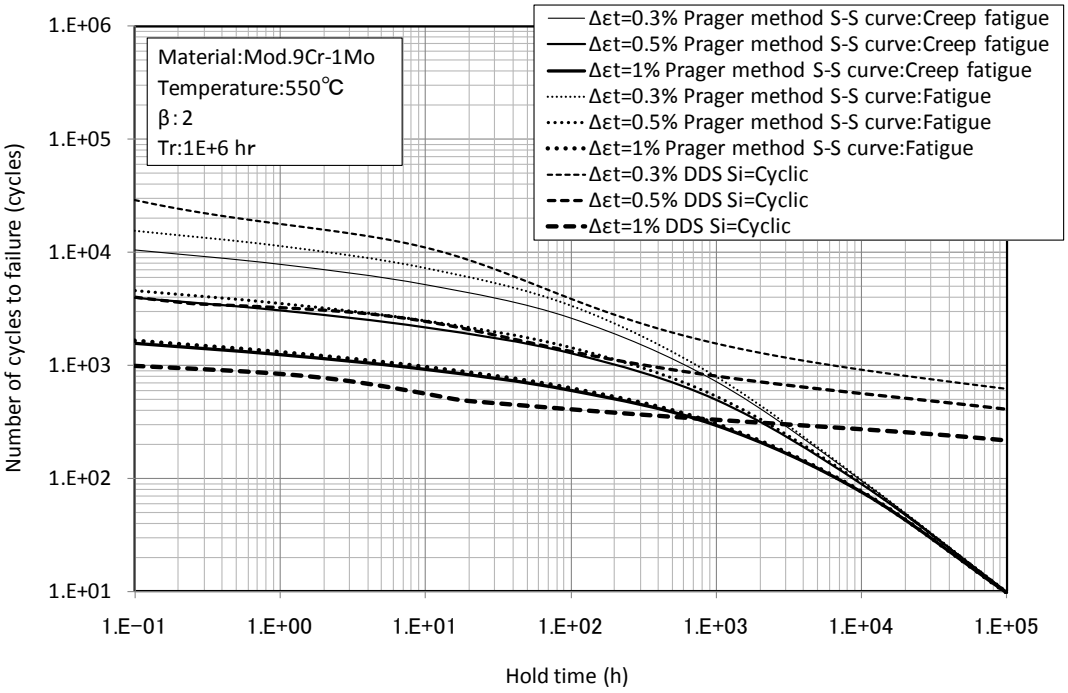


Fig3.3.17 Relationship between hold time and number of cycles to failure ( $\beta = 2$ )

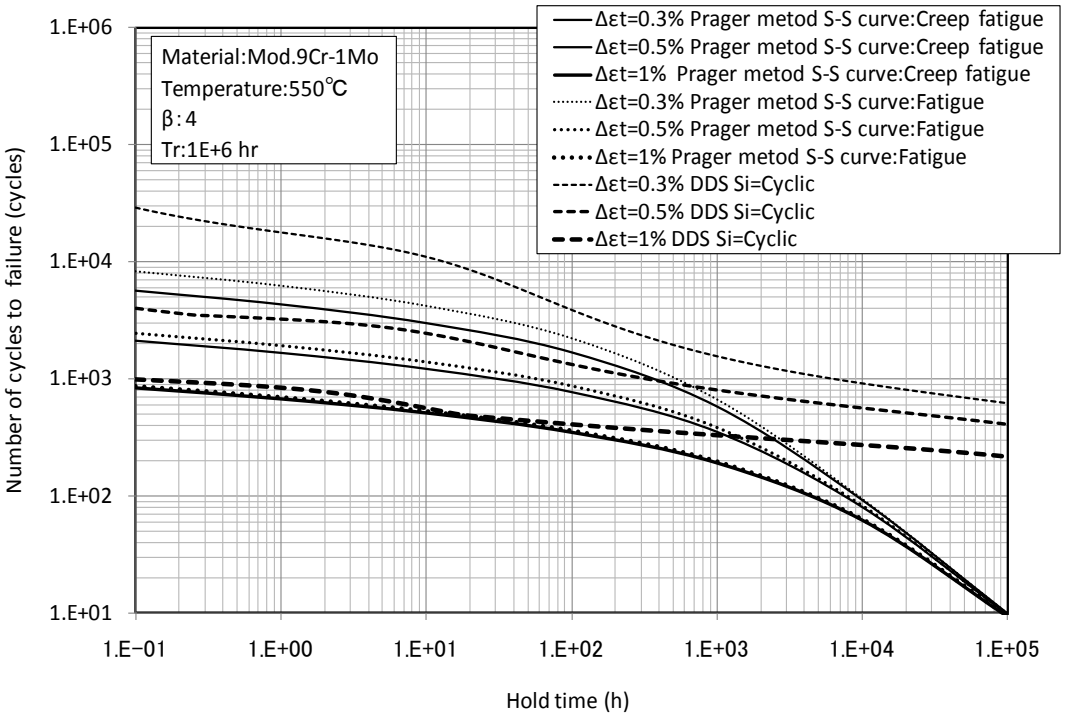


Fig3.3.18 Relationship between hold time and number of cycles to failure ( $\beta = 4$ )

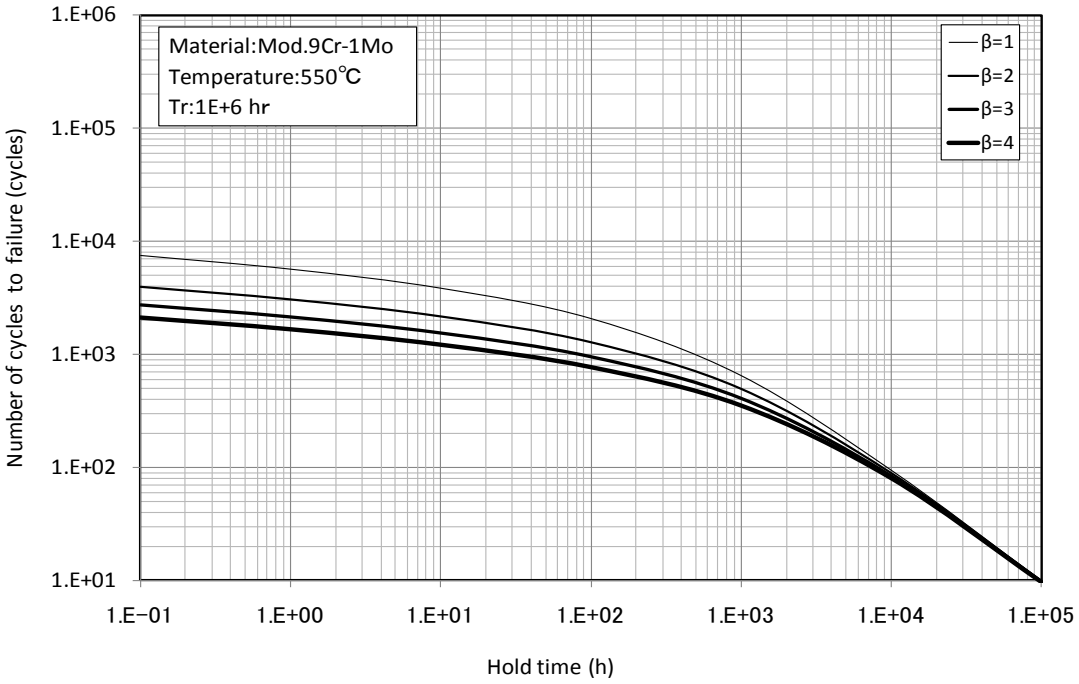


Fig.3.3.19 Relationship between hold time and number of cycles to failure ($T_r$=1x10$^6$ hours)

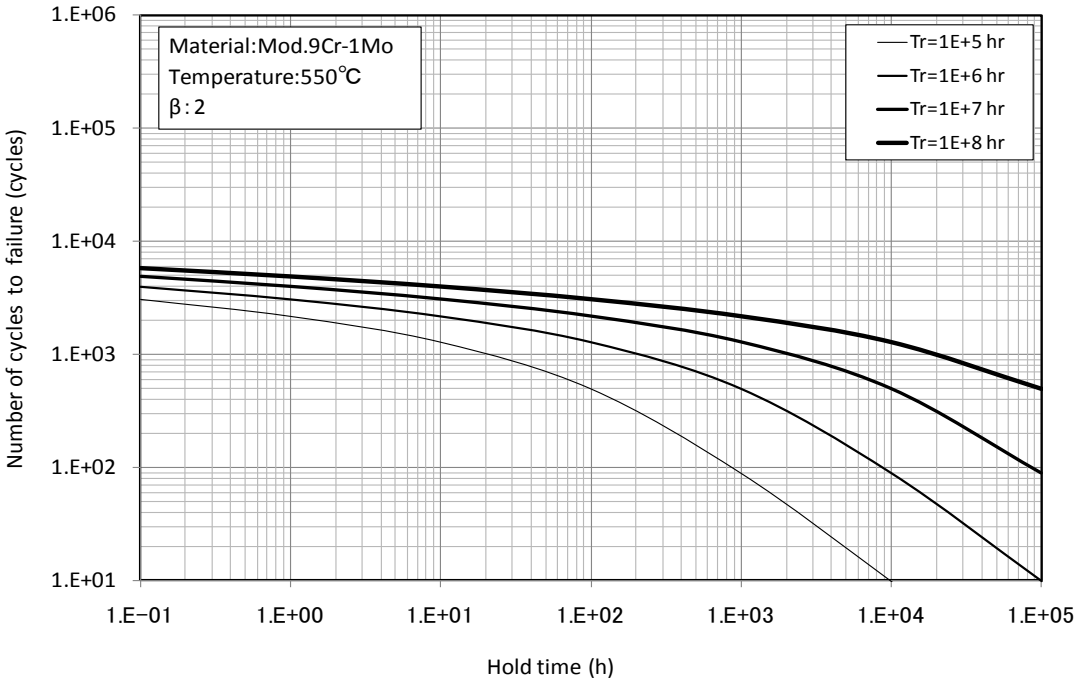


Fig.3.3.20 Relationship between hold time and number of cycles to failure ( $\beta = 2$ )

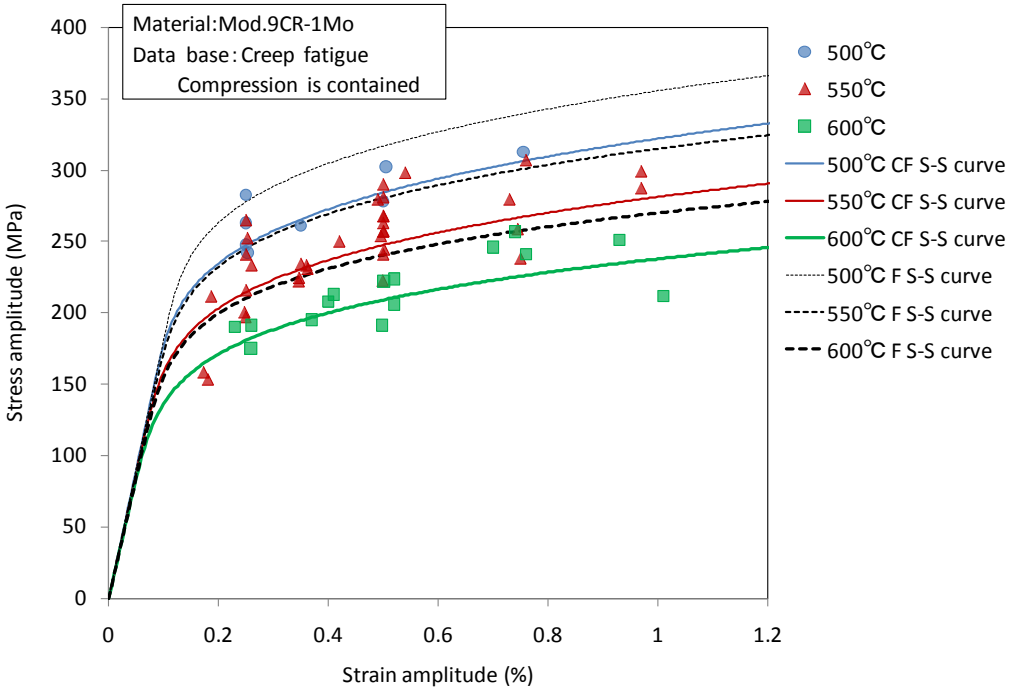


Fig.3.3.21 Cyclic stress-strain relations and effects of hold time on them

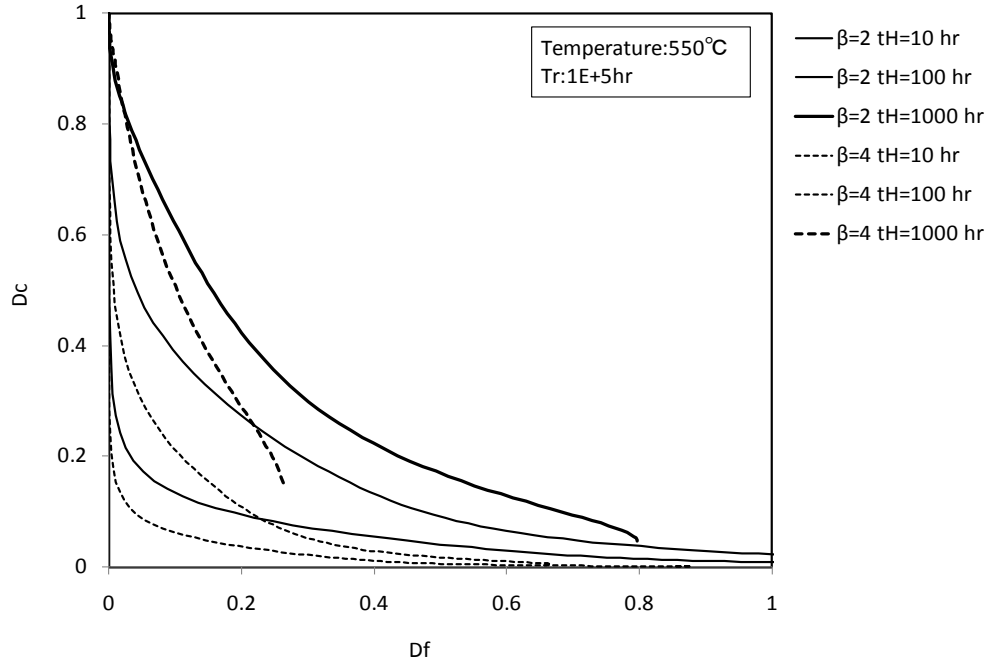


Fig.3.3.22 Creep-fatigue damage interaction ($T_r$=1x10$^5$ hours)

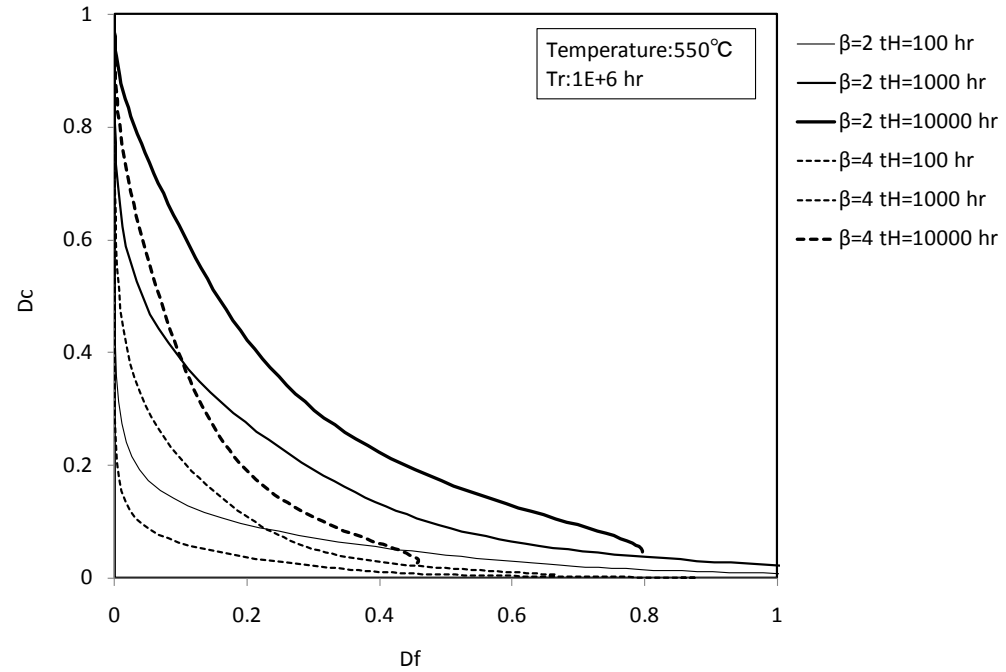


Fig.3.3.22 Creep-fatigue damage interaction ($T_r$=1x10$^6$ hours)

## 3.4 Hybrid Method of Time Fraction and Ductility Exhaustion

### 3.4.1 Outline

**1) Concept**

This method in implemented in a standard published by High Pressure Institute of Japan [10] and it is mentioned that this method is for plant operated at high temperatures such as fossil power generation plants or petrochemical plants.

The outstanding character of this method is that it uses both time fraction approach and ductility exhaustion approach for creep damage evaluation. The ratio of the both terms is to be determined based on experimental result and it is considered to be a material constant. The basic scheme can be described as follows:

Fatigue damage is defined using Minor's rule as usual.

$$D_f = \sum\left(\frac{n_i}{N_{fi}}\right) \tag{3.4.1}$$

Creep damage is defined using two terms corresponding to ductility exhaustion approach and time fraction approach, respectively. Ductility exhaustion employed here is a "classical one" and not the modified ductility exhaustion method described in Section 3.1 of this report.

$$D_c = k\sum_j\left(\frac{\varepsilon_{cj}}{\varepsilon_f}\right) + (1-k)\sum_j\int_0^{t_H}\frac{dt}{T_r} \tag{3.4.2}$$

$$D_f + D_c \le D \tag{3.4.3}$$

where,

$n_i$: Number of imposed cycles at strain range of $\Delta\varepsilon_i$

$N_{fi}$: Number of cycles to failure at strain range of $\Delta\varepsilon_i$

$t_H$: High temperature hold time

$T_r$: Creep rupture time corresponding to stress during relaxation

$\varepsilon_{cj}$: Creep strain induced during hold time

$\varepsilon_f$: Creep rupture ductility as a function of temperature and accumulated high temperature

hold time

*D*: Limit of accumulated creep-fatigue damage

*k*: Material constant

Creep rupture ductility is calculated from Equation (3.4.4)

$$\varepsilon_f = \ln\left(\frac{100}{100-\phi}\right) \tag{3.4.4}$$

$\phi$: Reduction of area at creep rupture

### 3.4.2 Predictability of experimental results

**1) Creep-fatigue life prediction**

Figure 3.4.1 shows creep rupture ductility used for the subsequent evaluation. Figures 3.4.2 to 3.4.6 show the result of creep-fatigue life prediction with *k*=0, 0.25, 0.50, 0.75, 1.0. The creep-fatigue life prediction was performed using the measured history of stress relaxation. As the value of *k* increases, creep-fatigue life prediction moves from an unconservative trend to a conservative trend. Figure 3.4.7 shows creep-fatigue damage predicted with various values of *k*. Figure 3.4.8 shows the standard deviation of the ratio of predicted creep-fatigue life to observed life as a function of constant *k*. The minimum of standard deviation was observed when *k* was 0.33. Figure 3.4.9 shows the result of creep-fatigue life prediction with the optimum value of *k*, i.e., 0.33. Figure 3.4.10 shows the calculated creep-fatigue damage with different values of *k*.

Figures 3.4.11, 3.4.12 and 3.4.13 show the result of creep-fatigue life prediction using material properties determined in the DDS [4] with different values of *k*. These results involve tests of which stress relaxation histories were not available. Figure 3.4.14 shows the standard deviation of the ratio of predicted creep-fatigue life to observed life as a function of constant *k*. In this case, 0 was the optimum value of *k*. Figure 3.4.15 shows the calculated creep-fatigue damage with different values of *k*.

Figures 3.4.16, 3.4.17 and 3.4.18 show the result of creep-fatigue life prediction under stress controlled tests. In this case, 1.0 was the optimum value of *k*. Figure 3.4.19 shows creep-fatigue damage predicted with various values of *k*.

**2) Extrapolation to long-terms**

Figures 3.4.20, 3.4.21 and 3.4.22 show the relationships between hold time and predicted number of cycles to failure with different values of *k* for 500C, 550C and 600C, respectively. When hold time is relatively short, ductility exhaustion method gives more conservative prediction but as hold time becomes longer, the trend becomes opposite. This tendency is common to all the temperatures. Figures 3.4.23, 3.4.24 and 3.4.25 show the ratio of predicted creep-fatigue life with *k* of 0.5 and 1.0 to the predicted creep-fatigue life with *k* of 0. Again the tendency described above is observed.

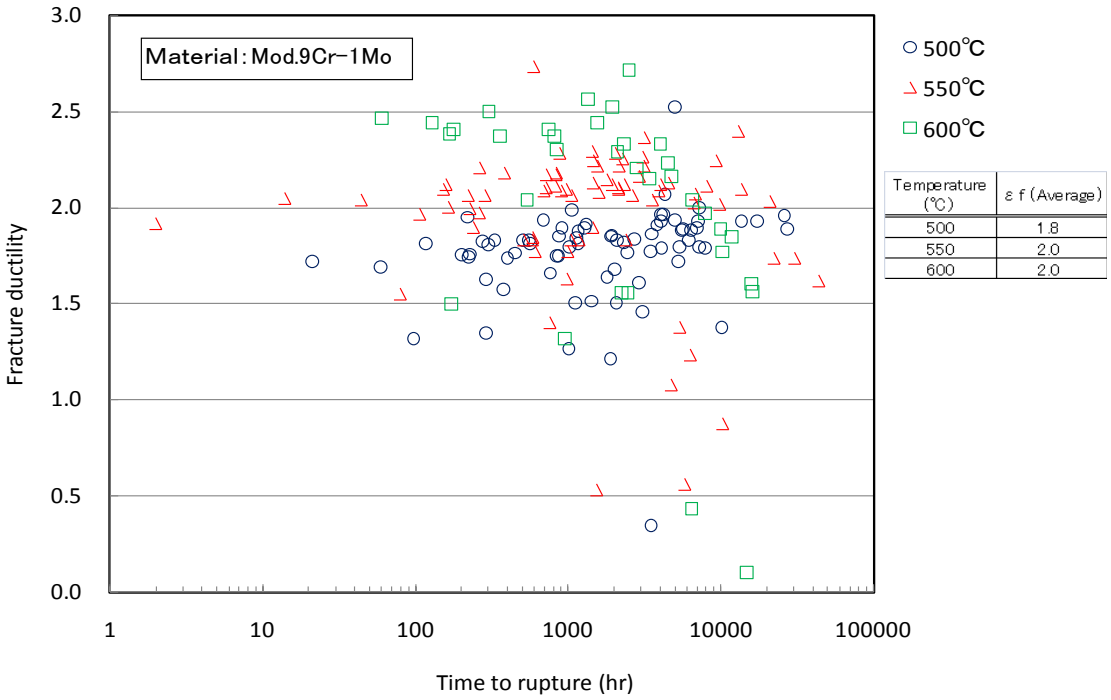


Fig.3.4.1 Creep rupture ductility at various temperatures

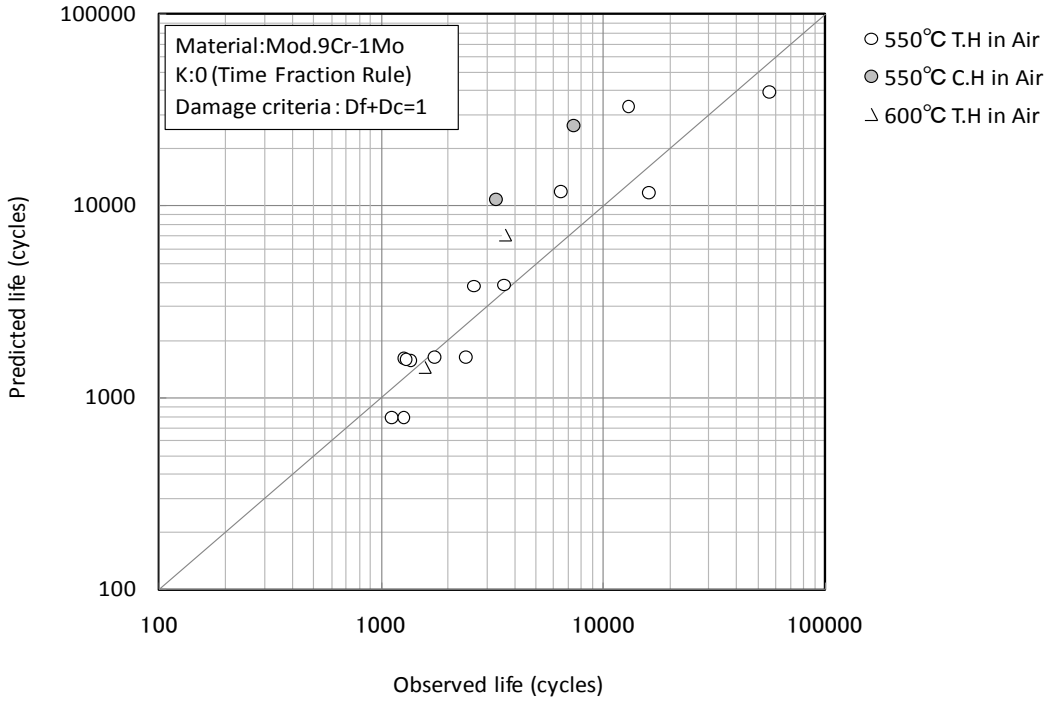


Fig.3.4.2 Observed and predicted creep-fatigue life by Hybrid method, *k*=0

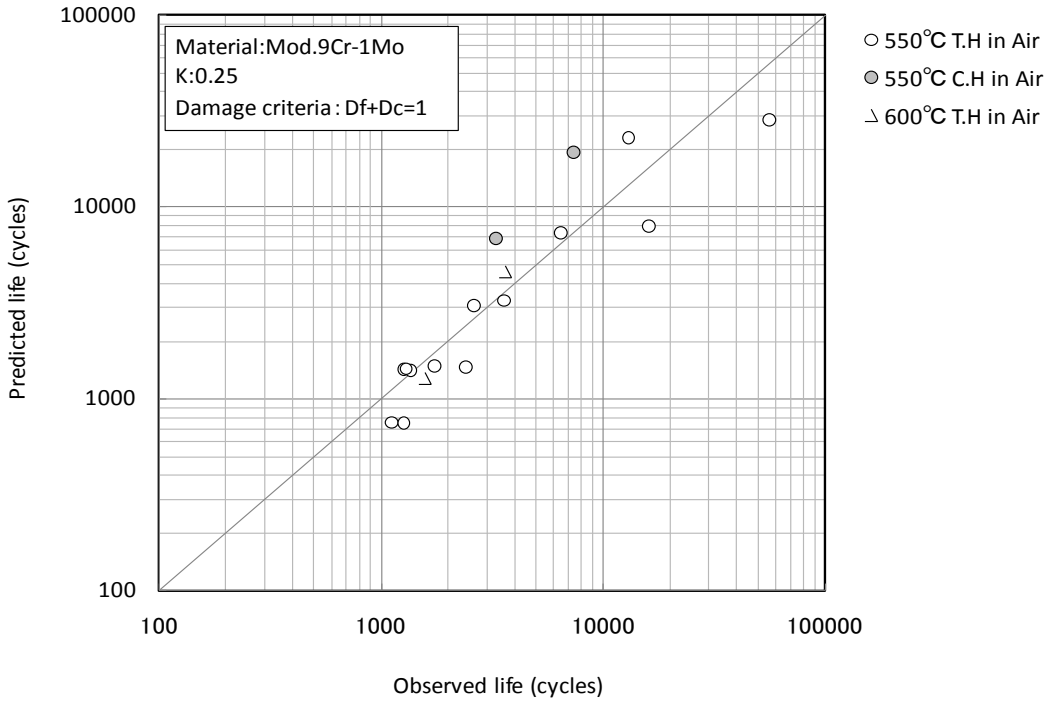


Fig.3.4.3 Observed and predicted creep-fatigue life by Hybrid method, *k*=0.25

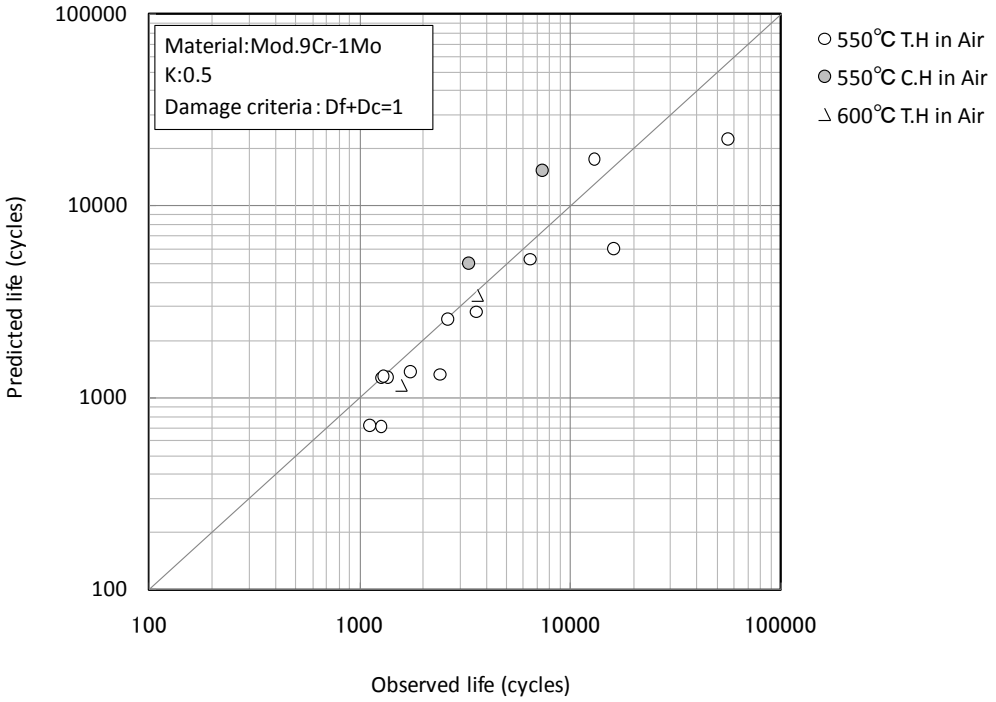


Fig.3.4.4 Observed and predicted creep-fatigue life by Hybrid method, *k*=0.5

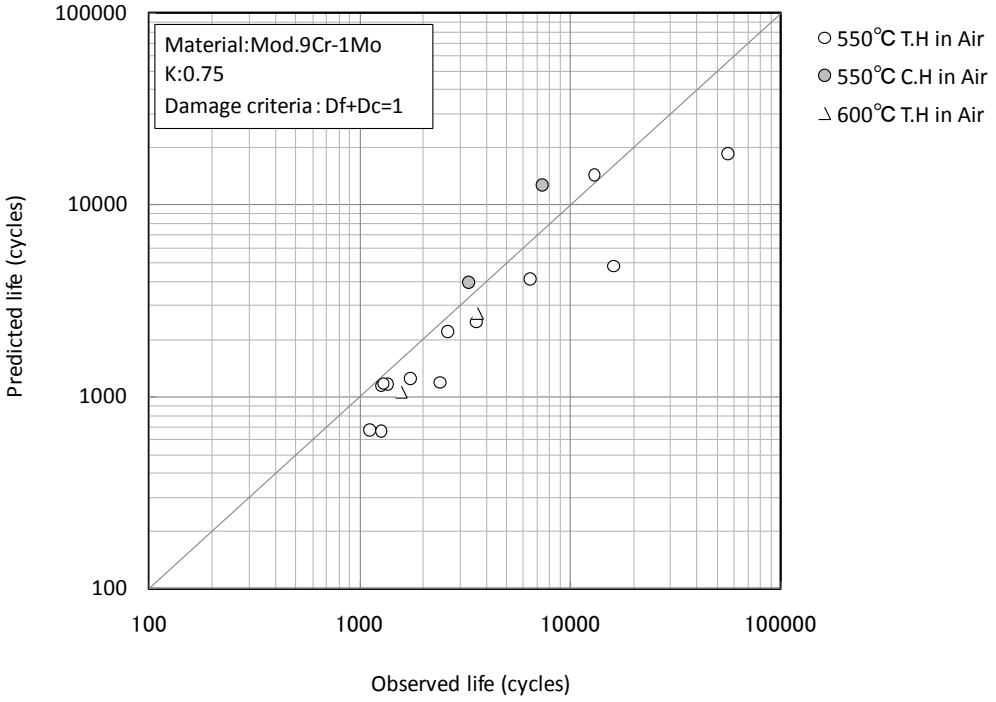


Fig.3.4.5 Observed and predicted creep-fatigue life by Hybrid method, *k*=0.75

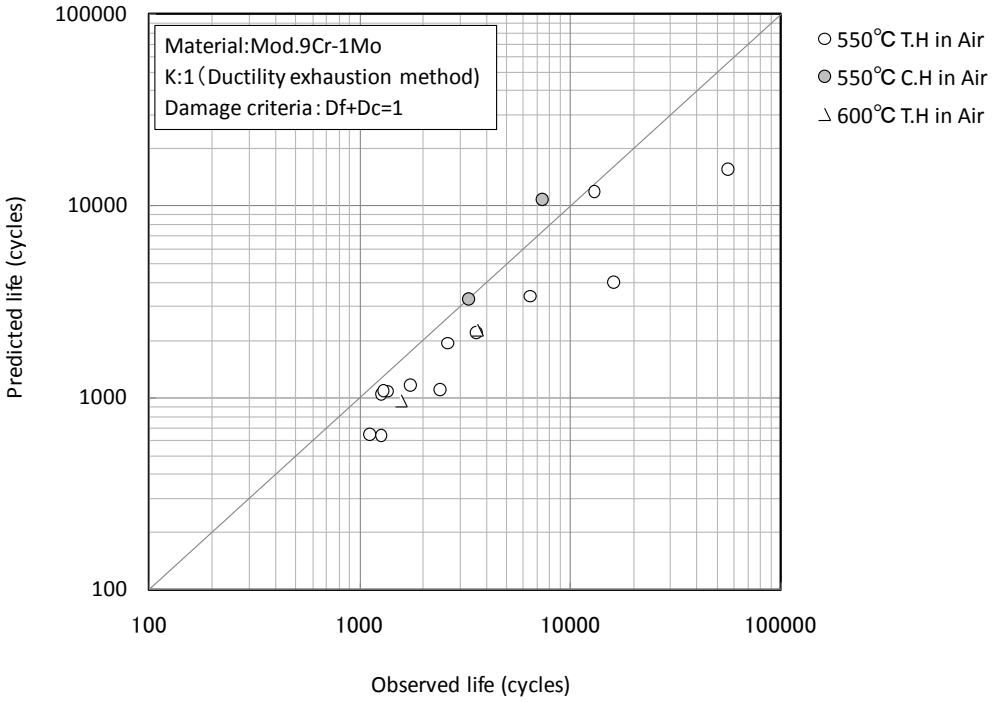


Fig.3.4.6 Observed and predicted creep-fatigue life by Hybrid method, *k*=1

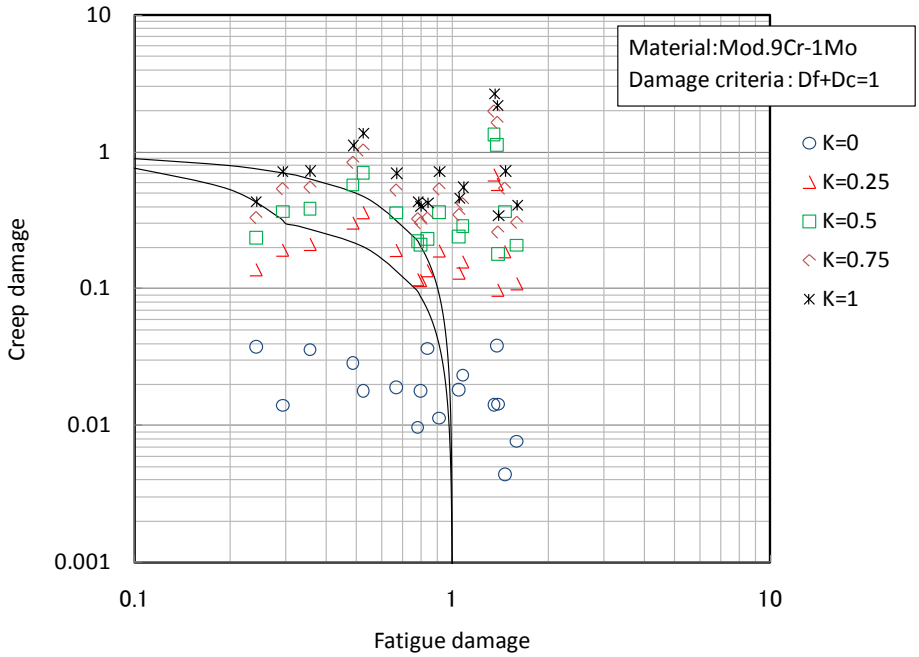


Fig.3.4.7 Creep-fatigue damage calculated by Hybrid method, all conditions

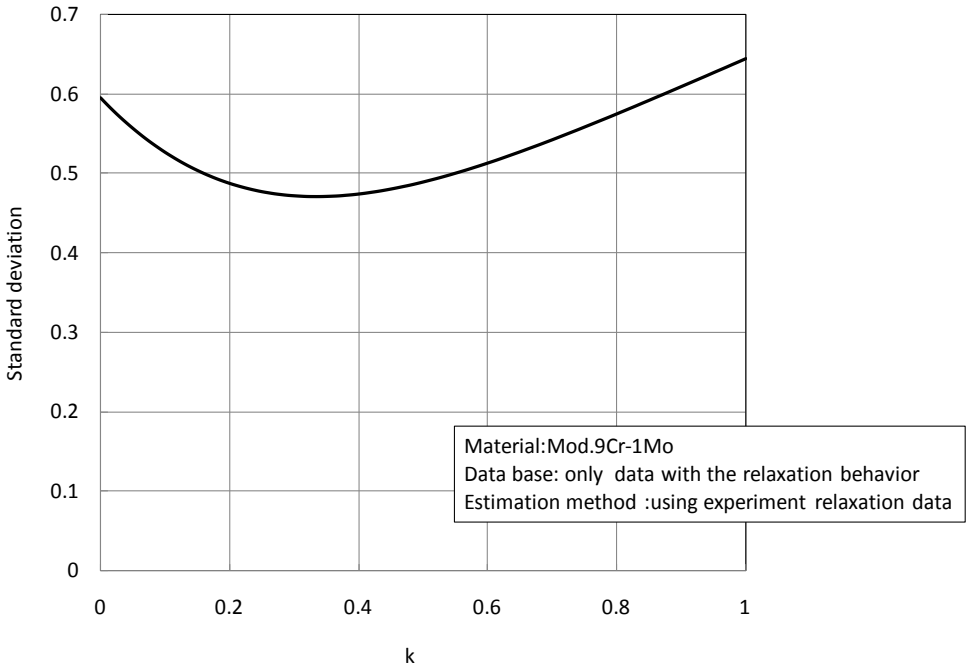


Fig.3.4.8 Relation between *k* and standard deviation of life prediction

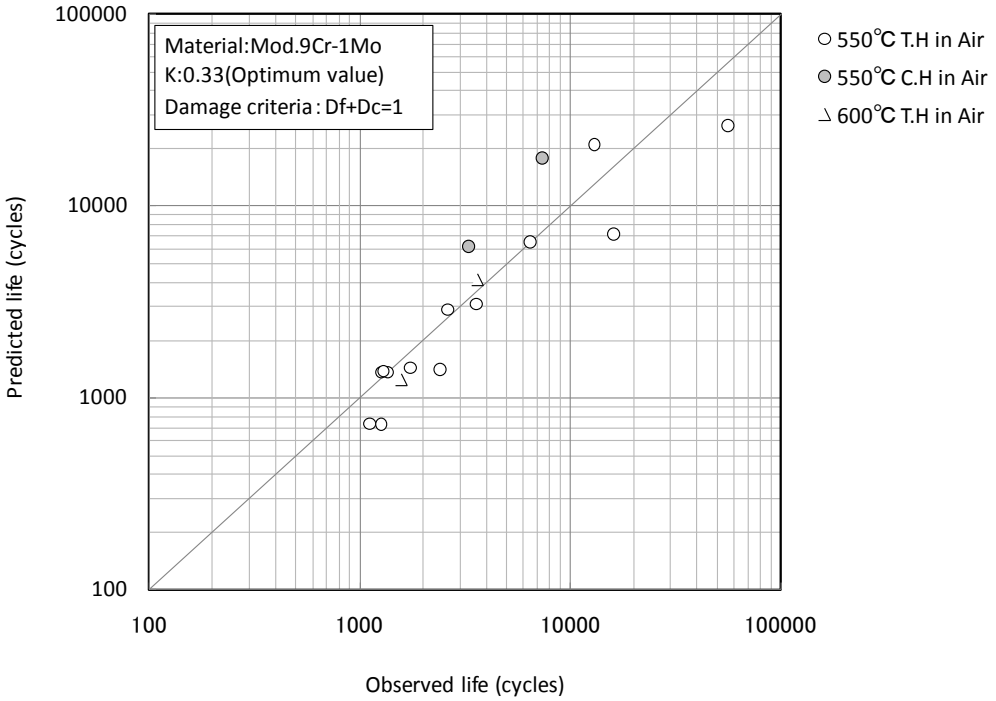


Fig.3.4.9 Observed and predicted creep-fatigue life by Hybrid method, *k*=0.33

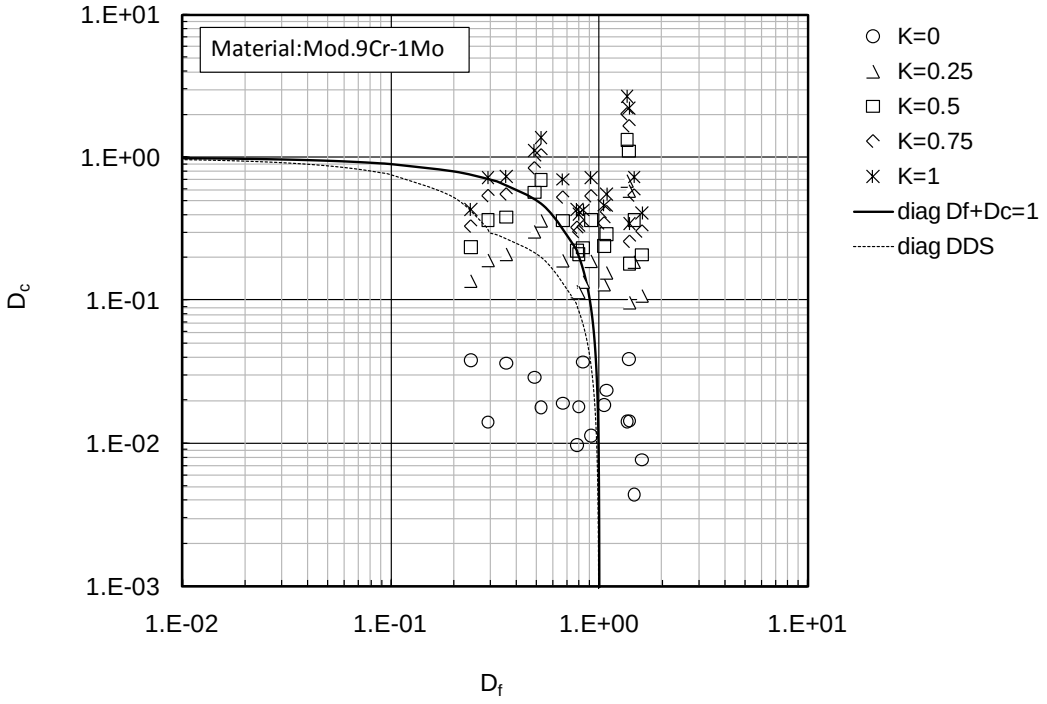


Fig.3.4.10 Creep-fatigue damage calculated by Hybrid method, all conditions

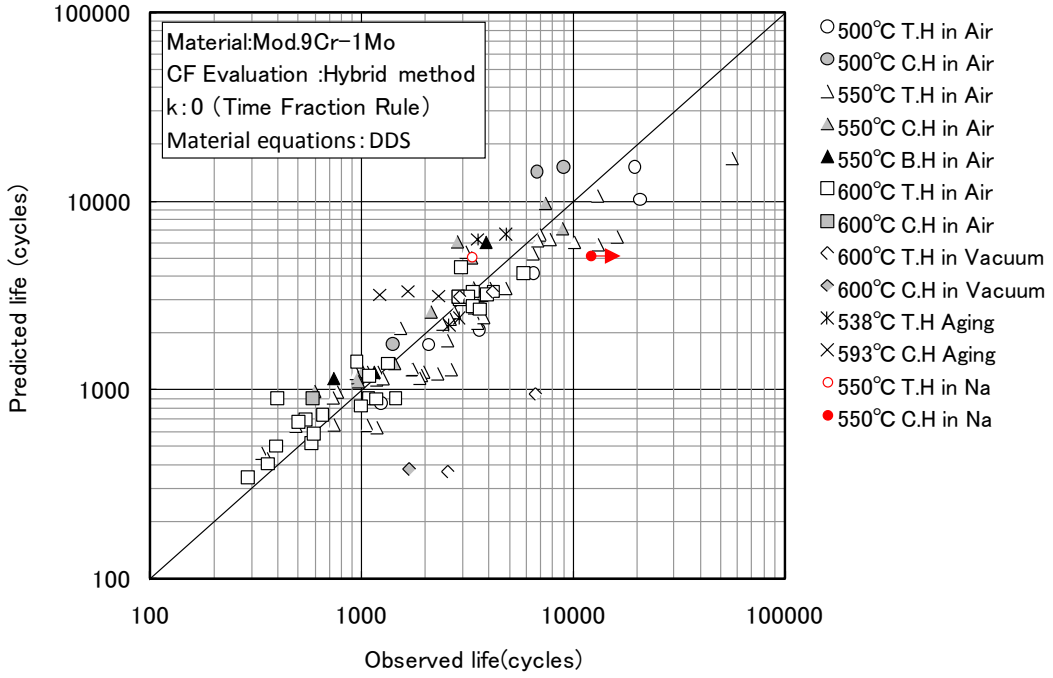


Fig.3.4.11 Observed and predicted creep-fatigue life by Hybrid method, *k*=0

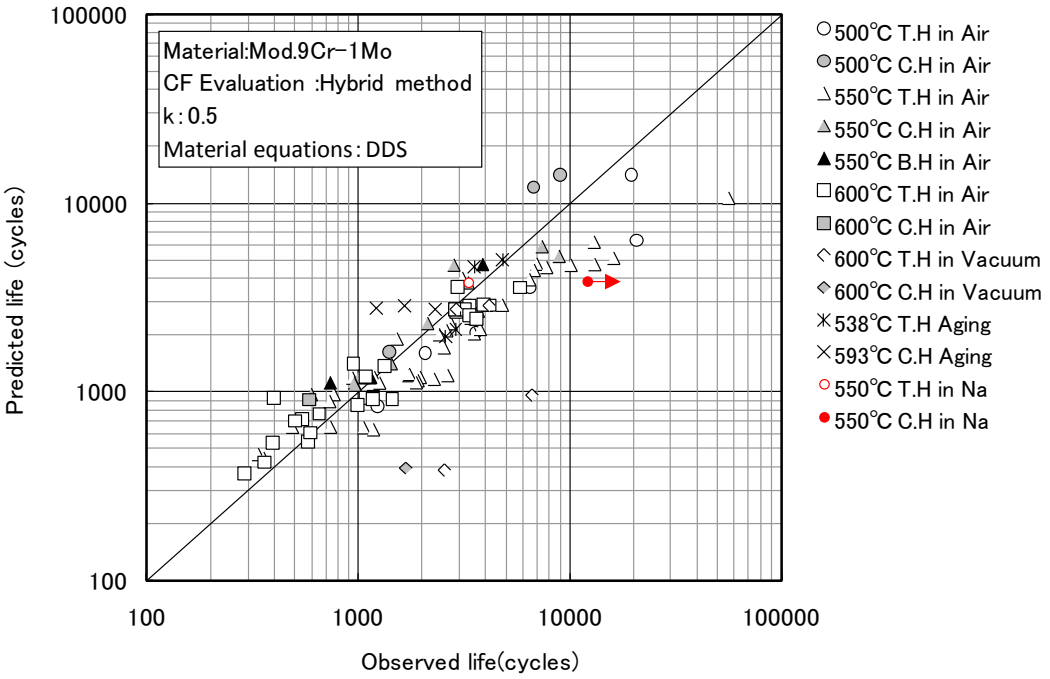


Fig.3.4.12 Observed and predicted creep-fatigue life by Hybrid method, *k*=0.5

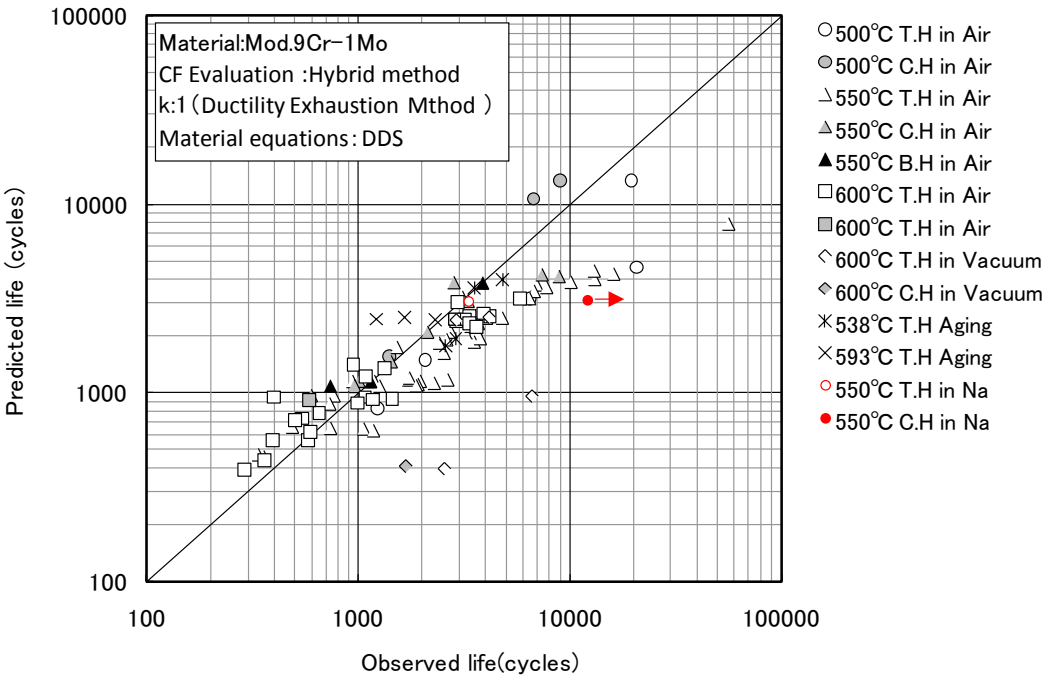


Fig.3.4.13 Observed and predicted creep-fatigue life by Hybrid method, *k*=1

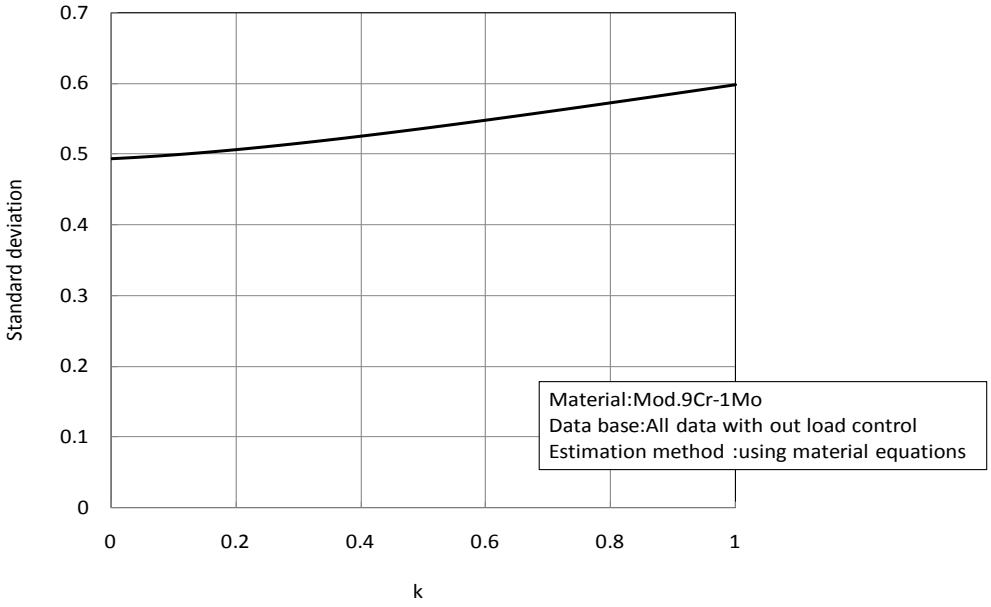


Fig.3.4.14 Relation between *k* and standard deviation of life prediction

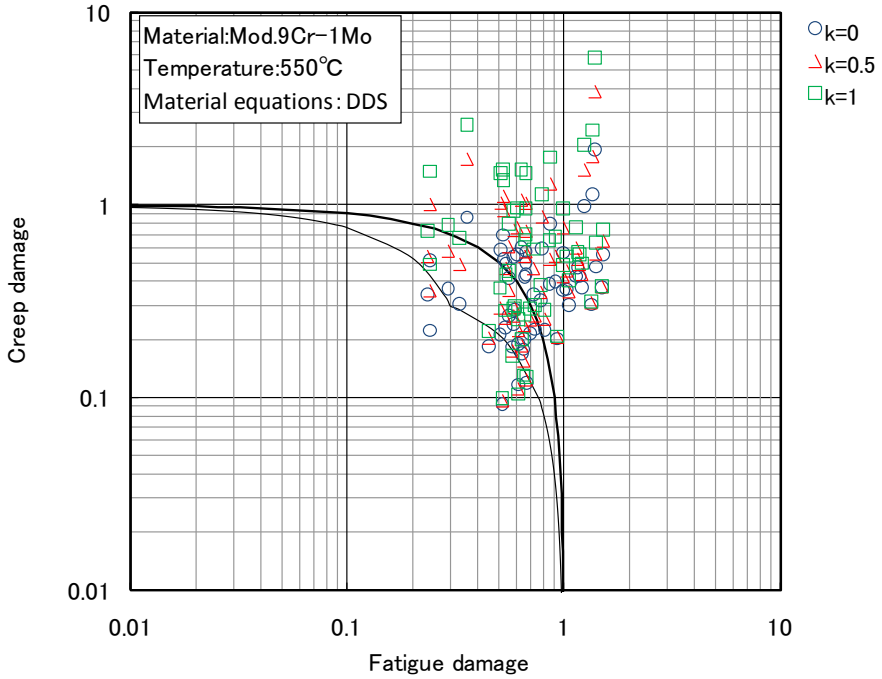


Fig.3.4.15 Creep-fatigue damage calculated by Hybrid method

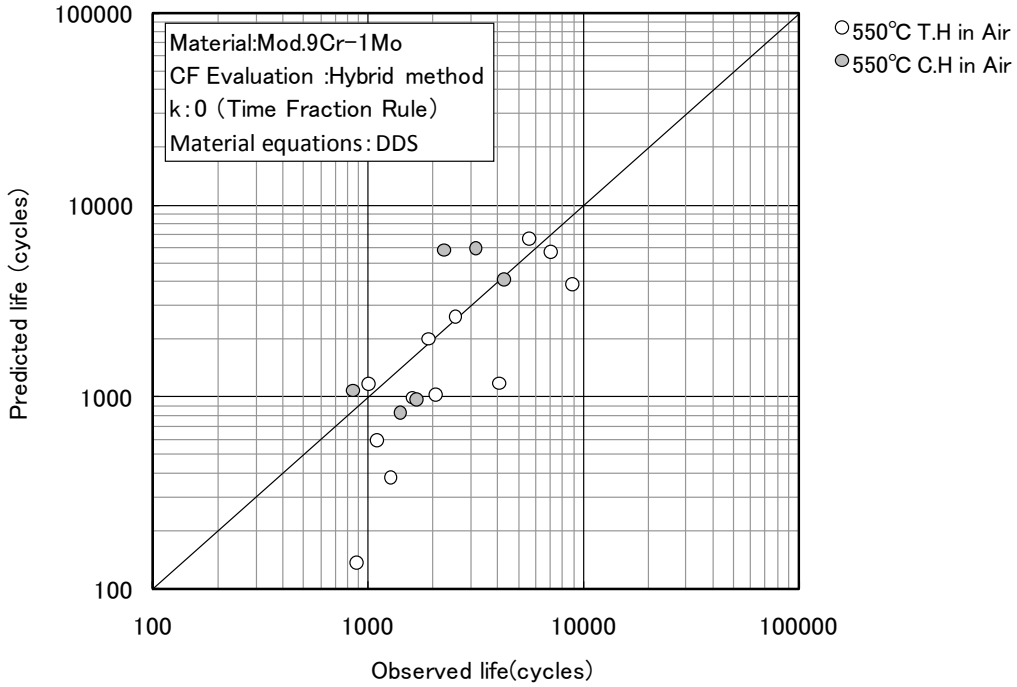


Fig.3.4.16 Observed and predicted creep-fatigue life by Hybrid method under stress control, *k*=0

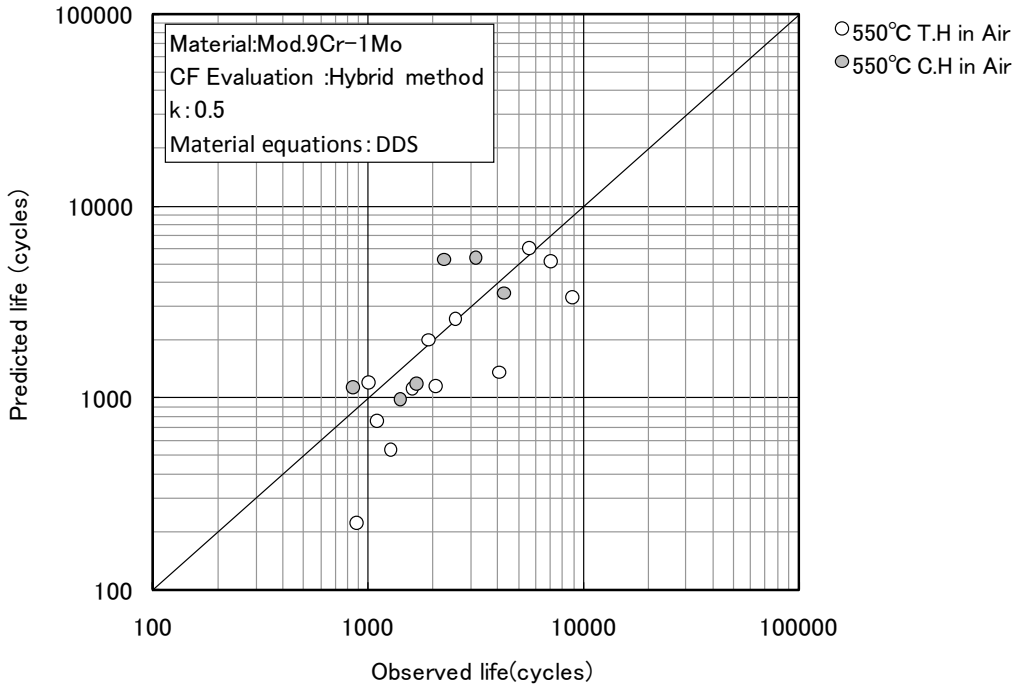


Fig.3.4.17 Observed and predicted creep-fatigue life by Hybrid method under stress control, *k*=0.5

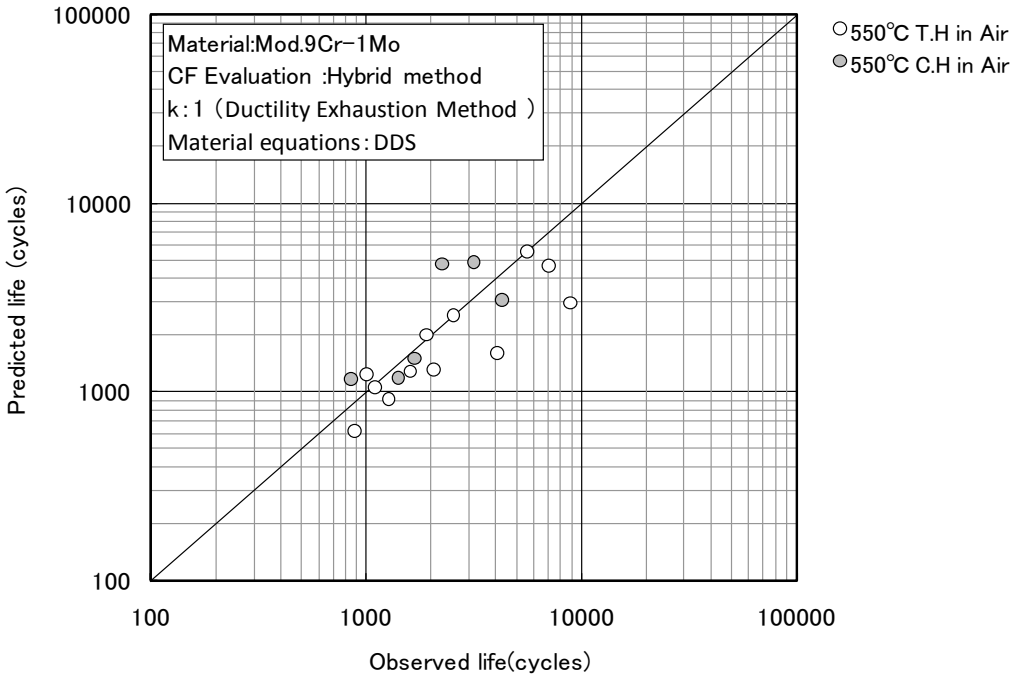


Fig.3.4.18 Observed and predicted creep-fatigue life by Hybrid method under stress control, *k*=1

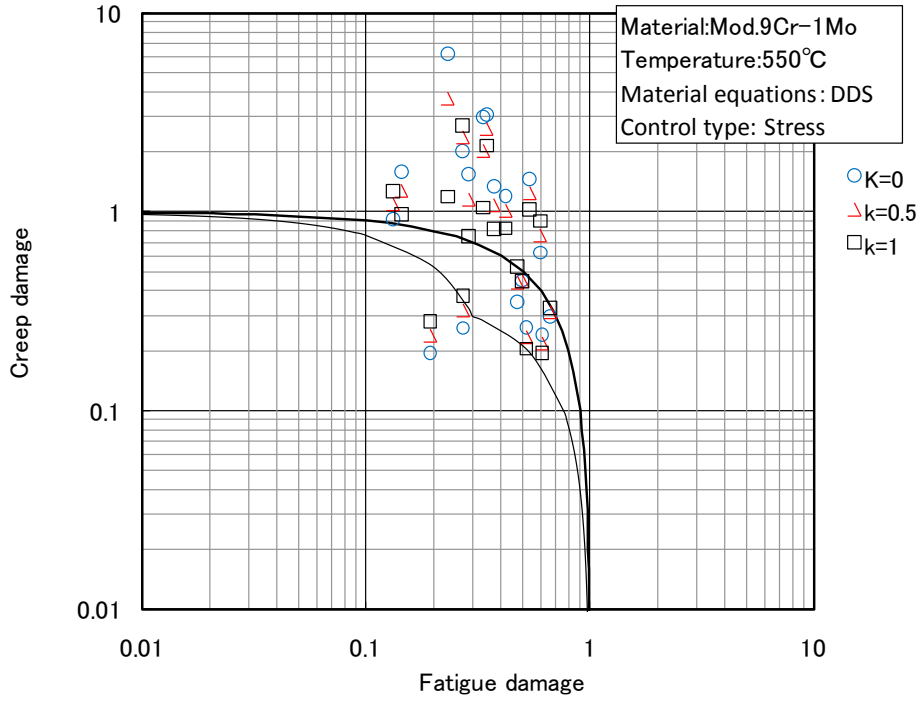


Fig.3.4.19 Creep-fatigue damage calculated by Hybrid method under stress controlled conditions

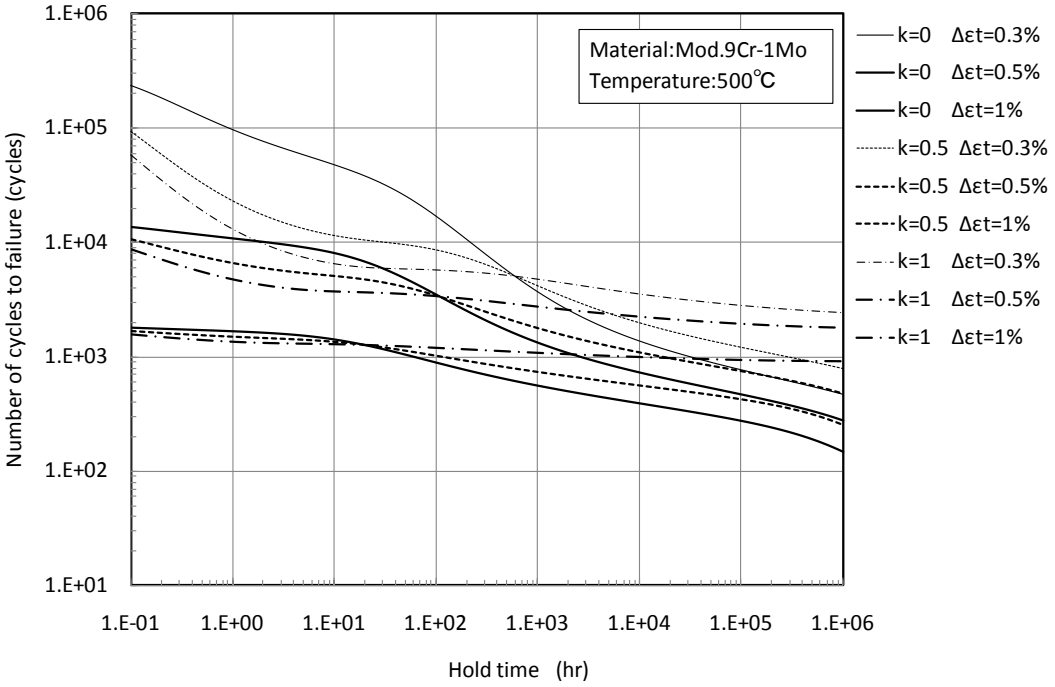


Fig. 3.4.20 Comparison of creep-fatigue life at various strain ranges at 500 C

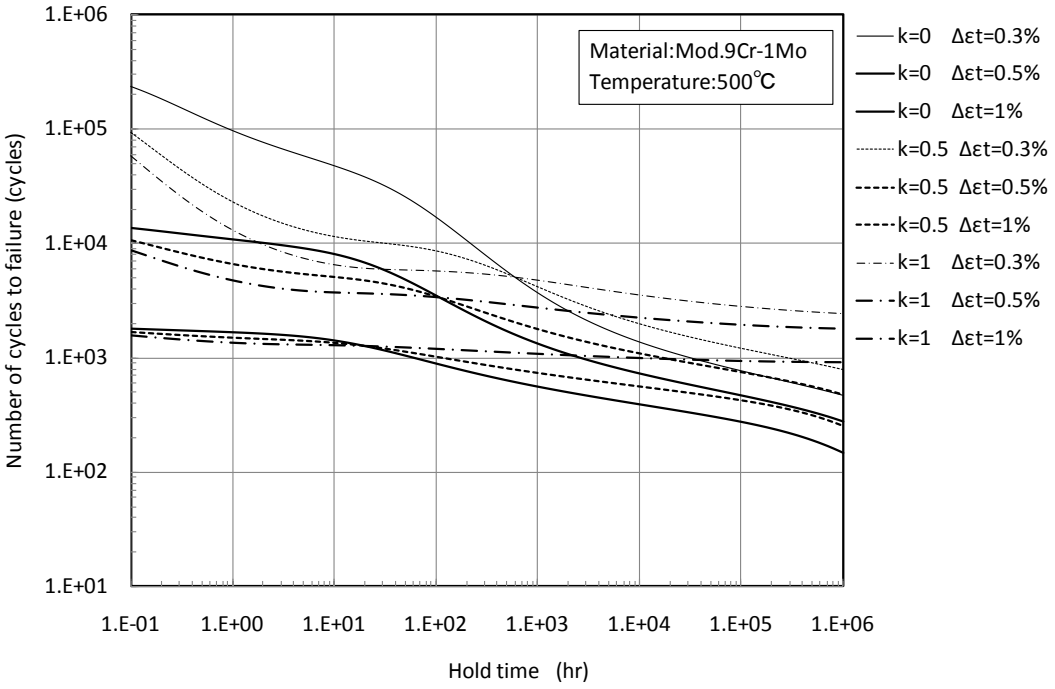


Fig. 3.4.21 Comparison of creep-fatigue life at various strain ranges at 550 C

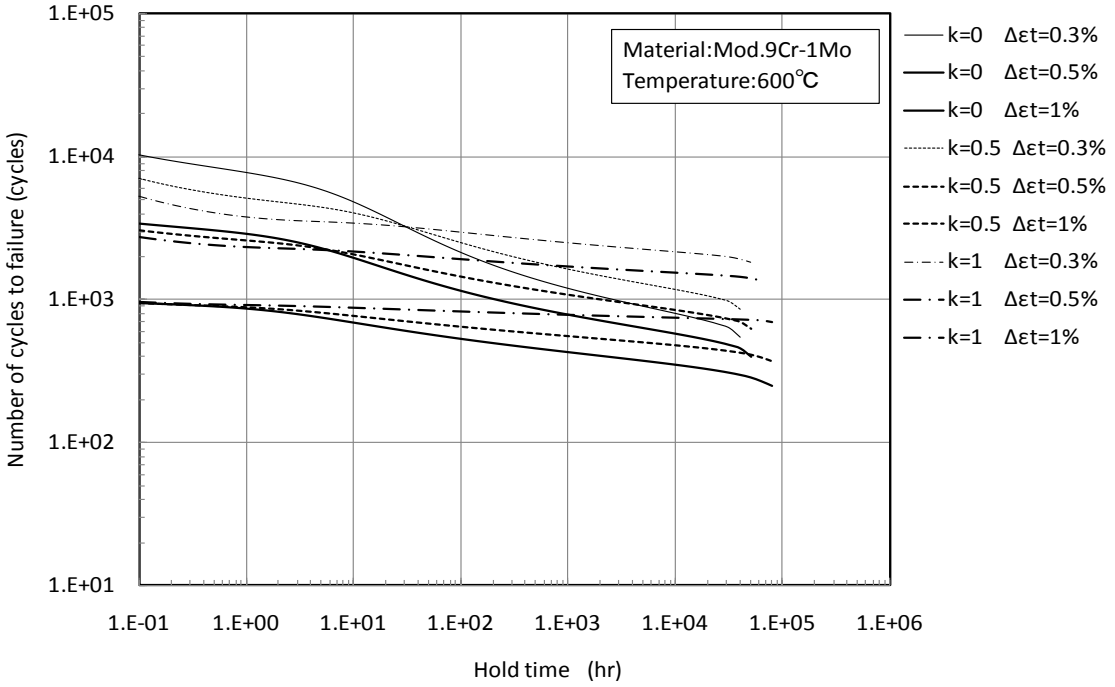


Fig. 3.4.22 Comparison of creep-fatigue life at various strain ranges at 600 C

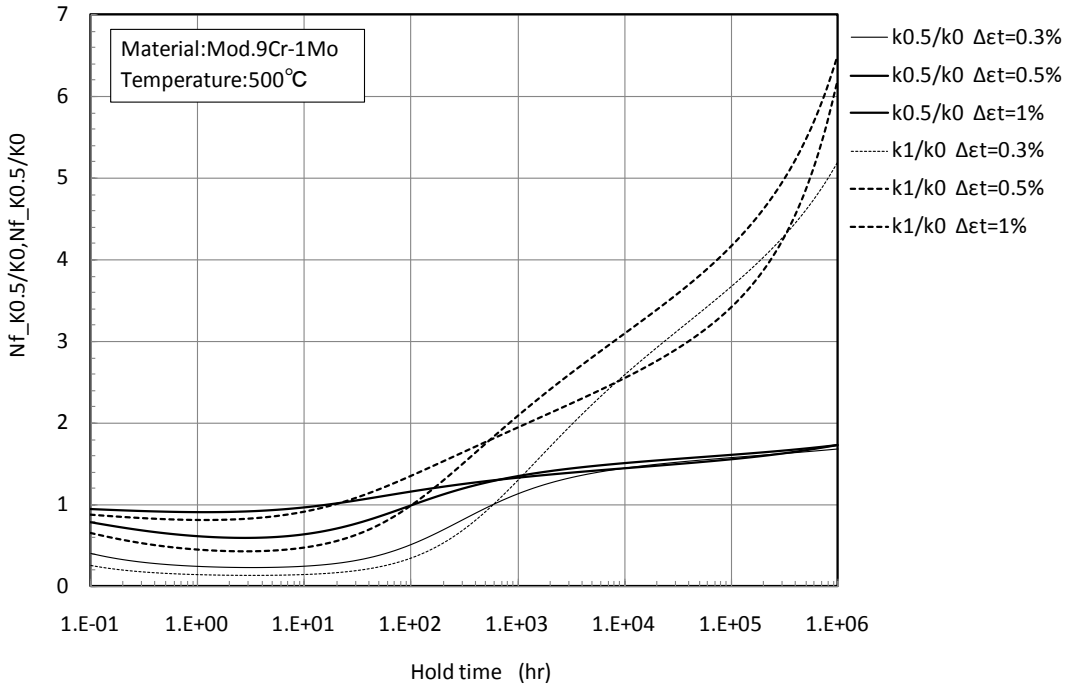


Fig.3.4.23 Ratio of predicted creep-fatigue life by Hybrid method to that predicted by TFR at 500C

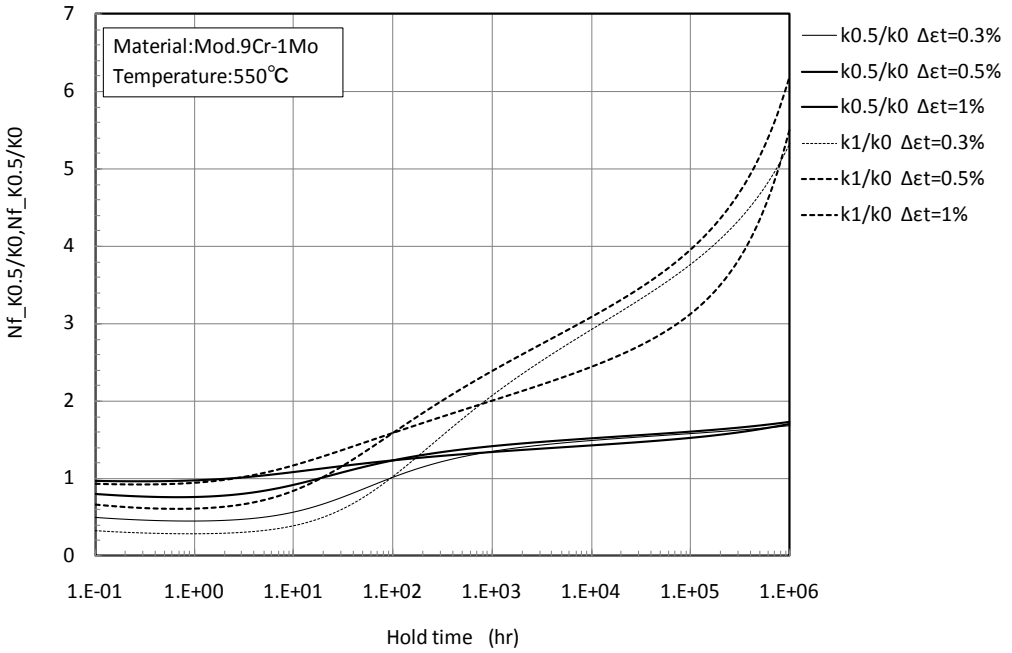


Fig.3.4.24 Ratio of predicted creep-fatigue life by Hybrid method to that predicted by TFR at 550C

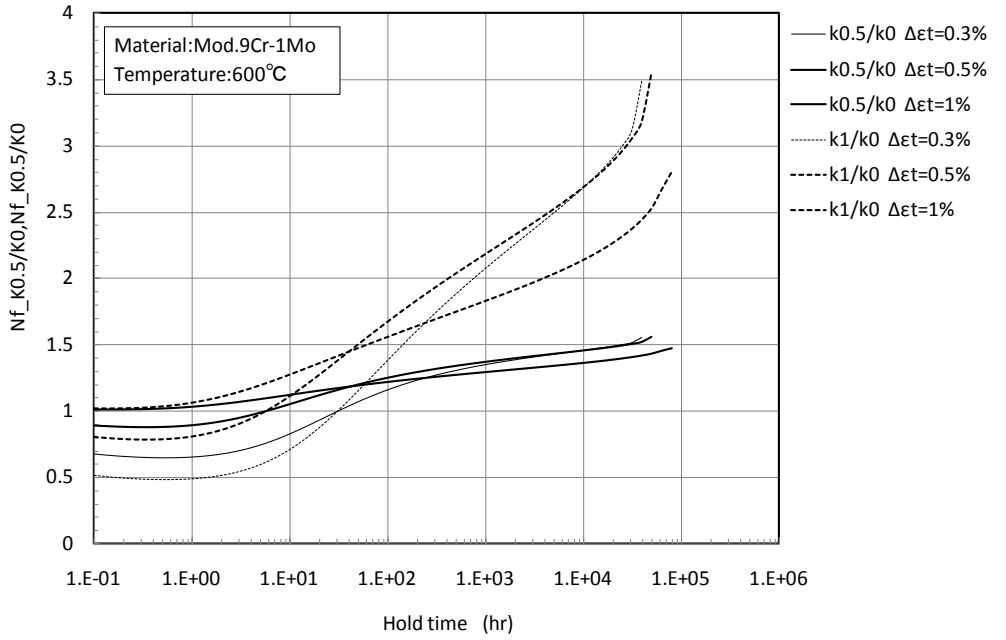


Fig.3.4.25 Ratio of predicted creep-fatigue life by Hybrid method to that predicted by TFR at 600C

## 3.5 Simplified Model Test Approach

### 3.5.1 Outline

**1) Concept**

This method was proposed by Jetter [11, 20].

In the report of the DOE/ASME Generation IV Materials Project Task 5, the advantages and disadvantages of current creep-fatigue evaluation methods have been highlighted. Briefly, in these methods cyclic damage is separated into two components, creep damage and fatigue damage. Conceptually straightforward, implementation of these methods can be difficult. While evaluation of fatigue damage is relatively direct, the number of cycles to failure can be counted, creep damage is a computed, not directly measured quantity. In ASME-NH there are two basic routs to evaluation of creep-fatigue damage, inelastic analysis and elastic analysis. Conceptually, the use of inelastic analysis to predict the stress and strain history is straight forward, however, its implementation requires detailed modeling of material time dependent behavior under cyclic loading conditions. Development of these material models is complex and their verification with test data is well beyond the scope of this discussion. Evaluation procedures based on the use of the results of elastic analysis use much simpler material models, thus avoiding one of the significant limitations to the implementation of inelastic analyses, but elastic analysis methods also have significant disadvantages. Because the stress and strain computed with an elastic material model does not represent the actual stress and strain in the component, various mechanistic models are incorporated to enable the elastically computed parameters to be used to bound the effects of time dependent stress and strain redistribution on creep and fatigue damage. The background and guidelines for the use of these mechanistic models in ASME- NH can be found in Chapter 12 of the Companion Guide to the ASME Boiler & Pressure Vessel Code [12]. To avoid these difficulties, an alternate approach, called the Simplified Model Test (SMT) approach has been identified [13].

The SMT approach is based on the use of creep-fatigue hold time test data with elastic follow-up. Cyclic damage is no longer separated into a creep component and a fatigue component, a major source of difficulty in current approaches. Instead, the effects of stress and strain redistribution and the combined effects of creep and fatigue damage are accounted for a simplified model test specimen suitably sized to ensure that the cyclic damage in the test bounds the damage in an actual structure when subjected to comparable loading.

The basic concept of the SMT approach is shown in Fig. 3.5.1. Both the test specimen and the "real" component it represents are subjected to a displacement which results in an elastically calculated stress and strain. The SMT specimen needs to be suitably sized such that when subjected to a relative displacement of the ends of the specimen resulting in an elastically calculated strain, $\varepsilon E$, test , the resulting life, e. g. cycles-to-failure, is greater than the cyclic life of the real component with an applied load that results in an equivalent elastically calculated strain, $\varepsilon E$, comp . Thus, in order to be effective, the 2-bar SMT model must be sized to provide a histeresis loop which envelopes the histeresis loop of the component(s) under consideration. The approach used to develop this relationship was to start with the 4-bar representation suggested by [14] to represent a generalized structure and then develop the necessary conditions and restrictions such that a 2-bar model would bound the 4-bar model's response and be representative of real structures.

**2) Analytical development**

In the 4-bar model shown in Fig. 3.5.2, the elastic stress in bar 1 represents the maximum stress at the stress concentration, $(P_L + P_B + Q + F)$, and the follow up in the 2- bar system, $q_{12}$ , represents the component's local follow up, $q_L$ , due to the local stress concentration, K. The stress in bar 3 represents the stress corresponding to the primary plus secondary stress range, $(P_L + P_B + Q)$, and the follow up in the 2-bar system, $q_{34}$ , represents the component's global follow-up, $q_n$ ,due to the interaction of the two cylinders. For a given choice of area ratios, the 4-bar model can be sized from the following relationships for elastic stress distribution and follow-up:

$$K = l_3/[l_1 + l_2(a_1/a_2)] \tag{3.5.1}$$

$$q_L = q_{12} = [1 + (l_2/l_1)(a_1/a_2)]/ [1 + (l_2/l_1)(a_1/a_2)^m] \tag{3.5.2}$$

$$q_n = q_{34} = [1 + (l_4/l_3)(a_3/a_4)]/ [1 + (l_4/l_3)(a_3/a_4)^m] \tag{3.5.3}$$

where m = creep exponent in the Norton law expression for strain rate. Representing the local follow-up as a function of K and m:

$$q_L = q_{12} = K^{(m-1)/(m+1)} \tag{3.5.4}$$

and using expressions from reference [14] for stress relaxation, the following requirement for the follow-up in the SMT specimen can be developed [13], for a range of practical values for K and $q_n$ :

$$q_{test} \leq K\, q_n \qquad (3.5.5)$$

This expression agrees with the peak elastic follow-up recommended by reference [15].

There is a further limitation on based on the allowable magnitude of the local stress concentration when combined with the effects of global elastic follow-up. This criterion is required to ensure that local peak stresses are not prevented from relaxing due to the strain transferred to the stress field surrounding the local discontinuity by the follow-up from the global discontinuity. Again using relaxation expressions from reference [14], the following expression was developed for the limiting relationship between K and $q_n$:

$$K \leq q_n/(\, q_n - 1) \qquad (3.5.6)$$

Equation (3.5.6) for the limiting relationship between allowable stress concentration and global elastic follow-up agrees with good design practice. For example, for a representative global follow-up of q = 2, the limiting value of K = 2 from Eq. (3.5.6) roughly corresponds to a corner radius of 20% of the cylinder wall thickness in Fig. 3.5.1. It is also only slightly smaller than the minimum corner radius of 25% of the wall thickness required by the design by rule provisions of Section VIII, Div 1 of the ASME B&PV Code, Fig., UG-34 (b-2).

Based on a series of analytical studies reported by reference [15] and [16], the DDS incorporates a maximum global follow-up factor, $q_n$ = 3.0. Substituting Eq. (3.5.6) into Eq. (3.5.5) then yields a maximum required value for the SMT specimen:

$$q_{test} \leq 4\ 5 \qquad (3.5.7)$$

However, some comparative analyses by [13] indicate that a follow-up factor of 3.0 may be more appropriate.

**3) Design application**

In the original description of the SMT approach [13], there were other consideration addressed in addition to the development of the criteria for representation of real structures by a 2-bar model

with elastic follow-up. Among these considerations were loading limitations, e. g. primary plus secondary stress limits, welds, the effect of sustained loading and extrapolation of relatively short time test data to the hold times representative of plant operation. An issue not previously addressed is the impact of peak thermal stresses due to rapid thermal transients.

Regarding loading limitations, it was suggested that the maximum primary stress intensity plus the range of secondary stress intensity be limited as follows:

$$(P_L + P_B/K)_{max} + (Q_R)_{max}/4 \leq S_t \qquad (3.5.8)$$

where the symbols follow the usual definition. This relationship is based a linear approximation of the ratcheting boundary shown on Fig. T-1332-2 of ASME-NH, and the use of $S_t$ to limit strain accumulation rather than working through the yield strength normalization, core stress, and isochronous stress-strain curves. An alternate approach would have been to use the creep modified shakedown requirement currently invoked by ASME-NH, T-1431(a)(2) for creep-fatigue limits using elastic analysis. However, that approach requires use of the relaxation strength, which, as previously described, has significant uncertainties and for which there is generally insufficient data.

Welds were addressed based largely on the work of reference [17] involving a test of a 304SS vessel with representative FBR design features subjected to 1330 cycle of severe thermal transients producing cracking at all points of interest including welds. For weld joints, they introduced a composite strain concentration factor which was the product of three factors representing strain and shape concentrating mechanisms and a metallurgical concentration factor of Kmat = 1.5. The strain and shape factors are already included in the SMT approach. Based on the consideration that welds in compliance with the weld joint requirements of ASME-NH will most likely have a global elastic follow-up of less than two, a weld joint geometry with a recommended shape concentration factor, Kshape $\leq$ 1.5, times a metallurgical factor, Kmat = 1.5 will satisfy Eq. (3.5.6) for qn $\leq$ 1.8 and also satisfy Eq. (3.5.5) and (3.5.7) considering the combined concentration factors.

The effect of sustained loading was addressed previously in the sense that it was rationalized to have little practical impact. There were several rationale presented:

(a) The limit on primary stress plus secondary stress range in combination with the limit on peak stress concentration insures that primary stresses are high, the maximum strain range will be low and vice versa.

(b) In the creep regime, secondary stresses due to pressure will be included as primary in Eq. (3.5.8).

(c) The criteria for St will keep the damage fraction from sustained loads to a relatively low level.

It would be advantageous to have an SMT test specimen that it would enable experimental confirmation of the above rationale.

Extrapolation of relatively short hold time test data to the much longer hold times representative of actual plant operation is an important issue for all creep-fatigue evaluation methodologies. Perhaps the most promising approach for the SMT methodology is to use a best fit direct extrapolation of test data backed up with theory based extrapolation such as the time fraction and ductility exhaustion approaches discussed above. The theory based extrapolations would be used to correlate and extend the SMT test data and not as a damage evaluation in a design methodology. An example of direct data extrapolation was discussed previously [13]. Based on a review of several sources of creep-fatigue data, it was concluded that cycles to failure were reduced a fraction of 2/3 to 1/3 for each factor of 10 increase in hold time. Thus the cycles to failure at a given strain range for a 1 hr hold time would be reduced by a factor of approximately 2 – 10 for a hold time of 1000 hr, which would be more representative of actual plant operation. This extrapolation assumes the cyclic life continues to decrease at the same exponential rate as the hold time increases. Generally the lower the strain range, the more rapid is the rate of decrease in cyclic life with hold time. However, in some materials, e. g. Alloy 880H at 850$^{o}$C, the effects of hold time saturate in less than 30 min [18].

The impact of peak thermal stresses on the criteria development was not previously considered. Such stresses would, of course, be included in the calculated elastic strain of the real structure. The concern is that peak thermal stresses might have a potentially destabilizing effect analogous to the destabilizing effect of a high local stress concentration collocated with region with high global follow-up. That later concern is addressed by Eq. (3.5.6). Pending further analytical studies of representative structures, it is suggested that in the presence of significant peak thermal stresses, an equivalent thermal plus geometric stress concentration factor should be developed and limited by

Eq. (3.5.6). The equivalent concentration factor can be determined from the ratio of primary plus secondary plus peak stress to the primary plus secondary stress:

$$Keq = (P + Q + F)/(P + Q) \quad (3.5.9)$$

**4) Testing**

Reference [19] reported on a series of elastic follow-up tests conducted on 304 SS specimens at 550°C. They tested a stepped bar specimen, shown in Fig. 3.5.3 and a notched bar specimen by machining a groove in the stepped bar specimen as shown in Fig. 3.5.4. The tests were also intended to support the SMT approach although the calculated follow-up in the stepped bar specimen was only $q_n$ = 1.64 for a creep exponent of m =5. Tests were conducted in both a conventional strain controlled mode based on the strain in the reduced diameter section and a stroke controlled, SMT, mode based on the relative displacement of the ends the specimen. The tests were conducted with and without a hold time. The hold time was 600 sec. in tension.

The results of the stepped bar tests are shown in Fig. 3.5.5 and the 0.8mm radius notched bar tests in Fig. 3.5.6; plotted as a function of calculated elastic strain. The tabulated results are also presented in the referenced paper. Comparing the strain controlled, $q_n$ = 1.0, and stroke controlled, $q_n$ = 1.64, results for a 600 sec. hold time, the stroke controlled specimen fails in a factor of about 3 to 7 fewer cycles with the cyclic ratio decreasing as the strain range decreases. A similar comparison of the notched specimen results shows a factor of 3 reduction of cyclic life at a calculated strain slightly less than 2%, but, in this case the difference in life is increasing as the strain range decreases. The lower cyclic life for the stroke controlled test can be attributed to the combined effect of the increase in strain range due to follow-up and the increase in creep damage for a given strain range due to the slower stress relaxation rate due to elastic follow-up.

Another relevant comparison is between the cyclic life of the notched and un-notched stepped cylinder specimens. At a calculated elastic strain of about 1% the cycles to failure are about a factor of 2 lower in the stepped cylinder specimen as compared to the notched specimen. The difference increases to about a factor of 3 as the strain range decreases to about 0.75%. This is a somewhat unexpected result since the follow-up of the notched specimen is greater than the un-notched; however, it does indicate confirmation of the ability of an SMT type specimen to bound the behavior of a more complex structure – a key point.

Additional tests based on the SMT approach are currently in the early planning stage. The proposed specimen shown in Fig. 3.5.7 is somewhat different in that it is composed of tubular sections. The tubular specimen has two advantages. First, by maximizing the cross-section moment of inertia for a given area, it permits longer specimens without experiencing stability problems. Longer specimens are desirable for two reasons: (a) it is possible to achieve higher values of elastic follow-up in specimens with a larger ratio of the length of the lower stressed bar to the higher stressed bar, ($l_2/l_1$) and, (b), the longer the specimen the easier it is to accurately control the end displacements. The second advantage of the tubular specimen is that it can be internally pressurized, thus permitting an assessment of the impact of sustained loading on the cyclic life under displacement controlled loading.

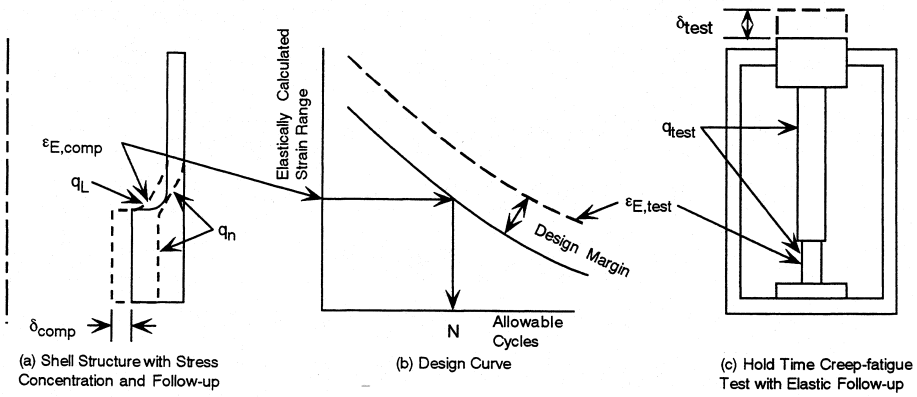


Fig. 3.5.1 SMT Methodology

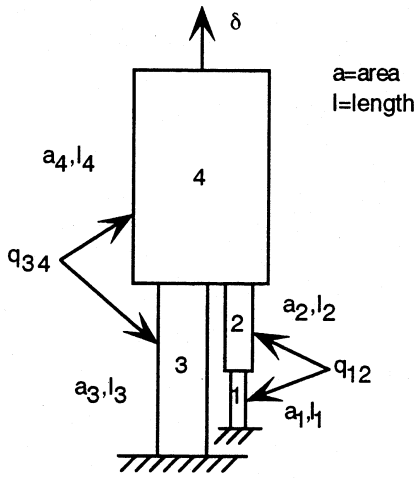


Fig. 3.5.2 4 Bar Model

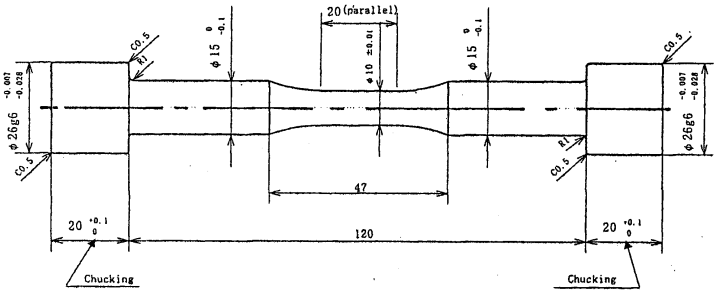


Fig. 3.5.3 Stepped bar test specimen

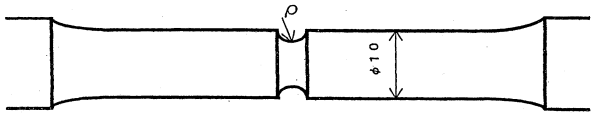


Fig. 3.5.4 Notched bar specimen

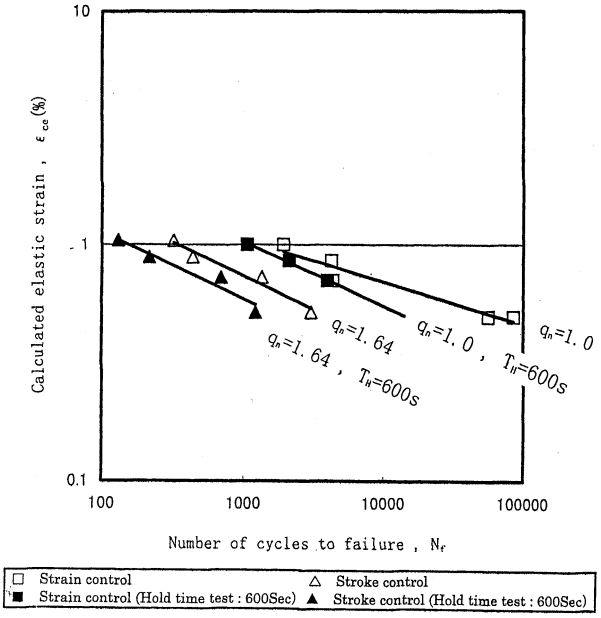


Fig. 3.5.5 Stepped bar test results

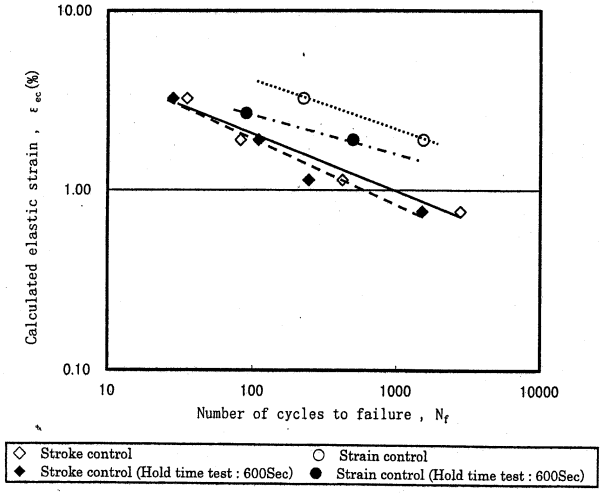


Fig. 3.5.6 Notched bar test results

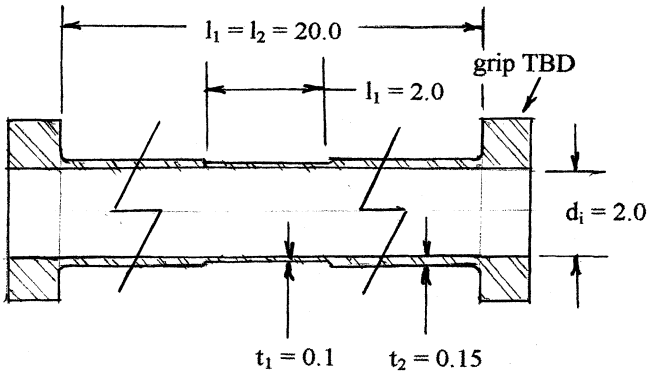


Fig. 3.5.7 Proposed SMT specimen, q ≈ 3.7

# 4. Potential to deploying the methods investigated to ASME-NH

## 4.1 Evaluation of creep-fatigue life predictability of the methods investigated in short-term and long-term regions

This section evaluated creep-fatigue life predictability of the methods investigated in this report in short term and long-term regions. The evaluation was performed from two standpoints: one is sensitivity to parameters used in the method and the other is comparison of predicted creep-fatigue life. Predicted creep-fatigue life was compared with experimental results in short-term region and in long term region, predicted life was compared among the methods.

### 4.1.1 Sensitivity analysis

Parameters employed in the methods were employed for the sensitivity analysis. These are;

1) creep rupture time,
2) creep rupture elongation,
3) tensile fracture elongation,
4) initial stress of relaxation (stress-strain curve),
5) steady state creep rate,
6) creep strain equation, and
7) elastic follow-up parameter.

The ranges for each parameter in this sensitivity analysis were determined so that the upper limit and the lower limit of the parameters roughly bound the scatters that are expected in evaluation of experimental results and practical applications. The ranges for the creep rupture time, creep rupture elongation, creep ductility, tensile elongation, cyclic stress-strain curve and stress relaxation behavior are shown in Figs. 4.1.1, 4.1.2 (definition of fracture ductility is given by Equation (3.4.4)), 4.1.3, 4.1.4, 4.1.5, 4.1.6, 4.1.7 and 4.1.8. Not all of the above parameter are involved in every method. Some methods are completely insensitive to some parameters. For the strain range separation method, the additive stress of 60 MPa was employed to perform calculation.

The results of the analyses are shown in Figs. 4. 1. 7 to 4.1.34. The figures show the upper limit and the lower limit for each evaluation methods and they correspond to the upper limit and the lower

limit of the parameters described in Figs. 4.1.1 to 4.1.8. These results will be referred to in the discussions in the following sections. In the figures predicted creep-fatigue life by the time fraction method obtained in Task 5 is also plotted for comparison.

### 4.1.2 Comparison of predicted creep fatigue life

Figure 4.1.35 and 4.1.36 compares predicted creep-fatigue life by the methods investigated (For the strain range separation method, the values shown in Table 3.2.1 were used as additive stress). With regards to the prediction of the experimental data, all the newly proposed methods investigated in this report (except the SMT approach which is not yet ready for life prediction) and the time fraction method investigated in Task 5 give satisfactory results as shown in Fig. 4.4.1. The difference in predicted life among the methods in short and mid-term regions where experimentally creep-fatigue data are available is fairly small.

On the contrary, the tendency in long-term region is significantly different depending on method. As shown in Fig. 4.1.36 shows the relationship between strain hold time and predicted creep-fatigue life for strain ranges of 0.3% and 0.5%. When hold time is 10,000 hours, the strain range separation method gives the longest creep-fatigue predicted life, and the modified ductility exhaustion method, the time fraction method, Hybrid method which is identical to the time fraction method follow. The approach for pressure vessel application gave the most conservative results if constant $T_r$ is $1x10^5$ hours[1] The magnitude of the difference can be as much as two orders.

[1] This might not be the most appropriate value of $T_r$ to make such a comparison. The most appropriate value should be investigated further

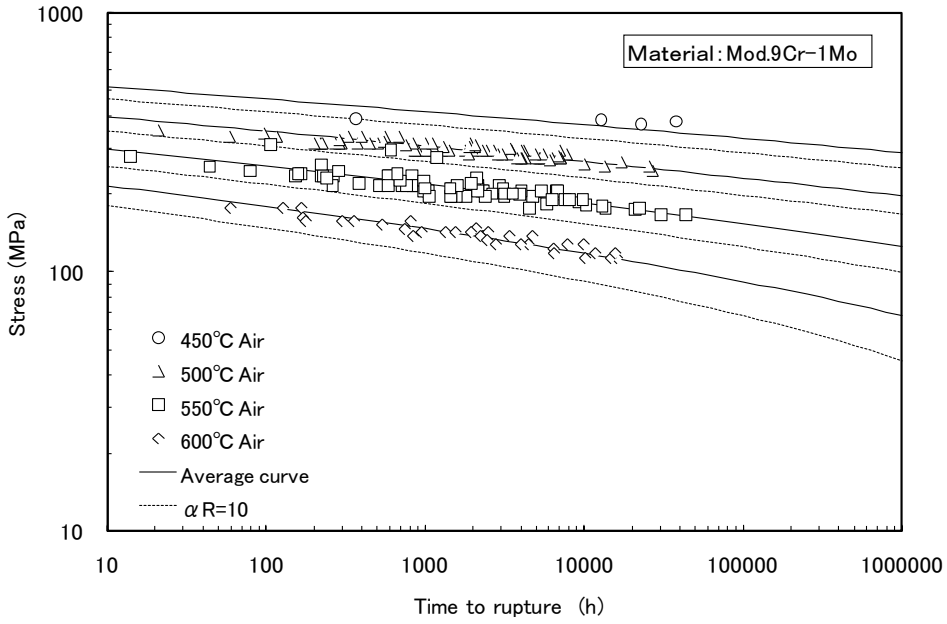


Fig. 4.1.1 Parameter for creep rupture time

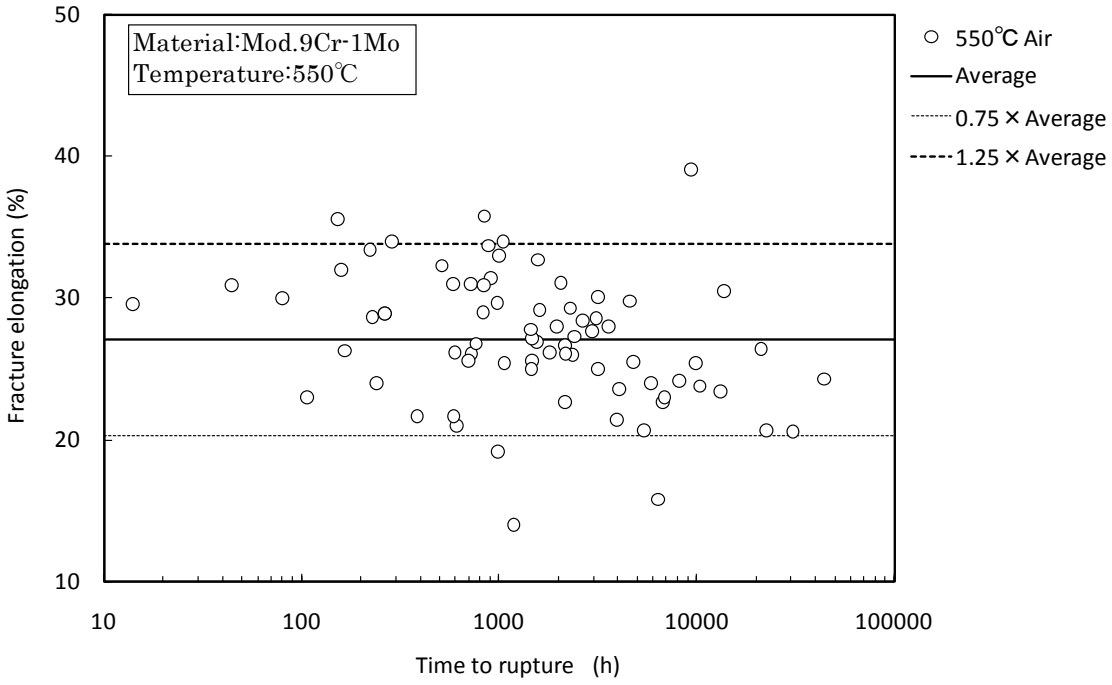


Fig. 4.1.2 Parameter for creep rupture elongation

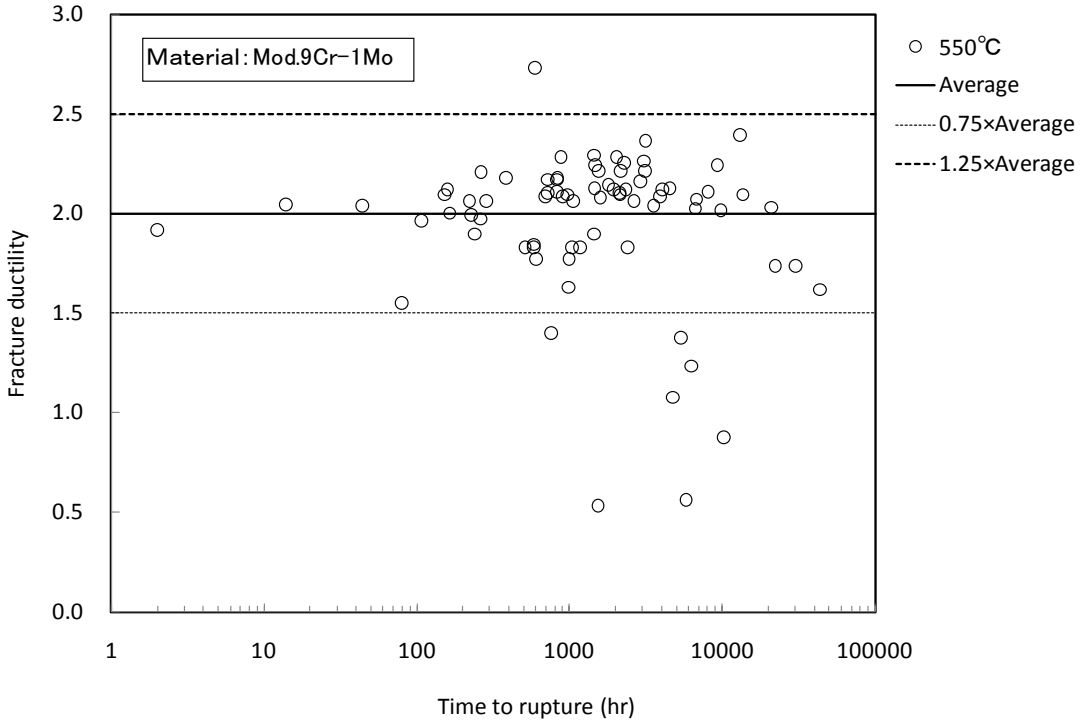


Fig. 4.1.3 Parameter for creep rupture ductility

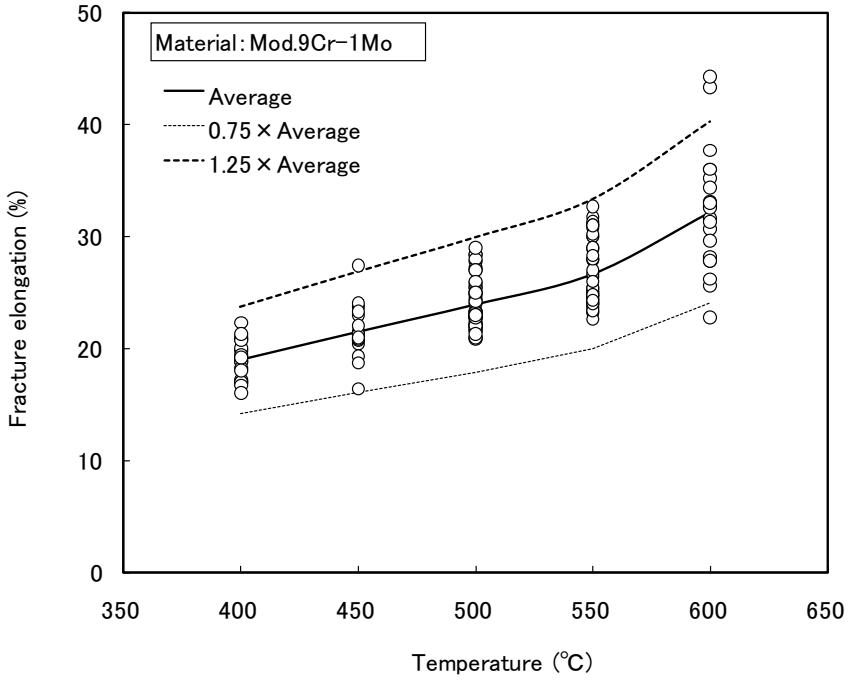


Fig. 4.1.4 Parameter for tensile elongation

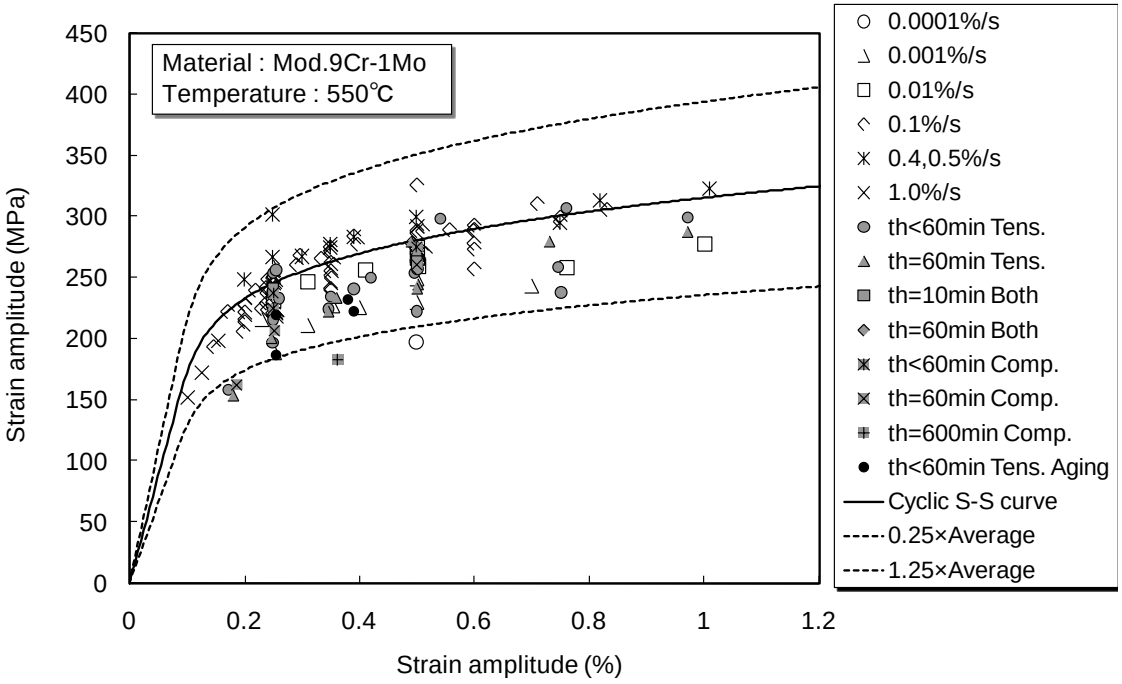


Fig. 4.1.5 Parameter for cyclic stress-strain curve

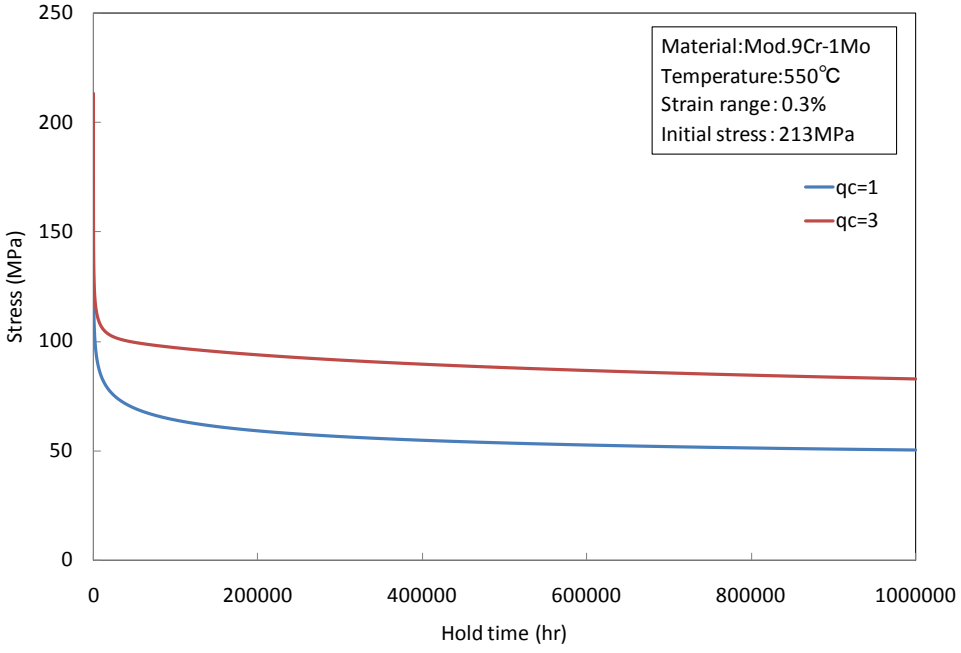


Fig. 4.1.6 Parameter for stress relaxation behavior

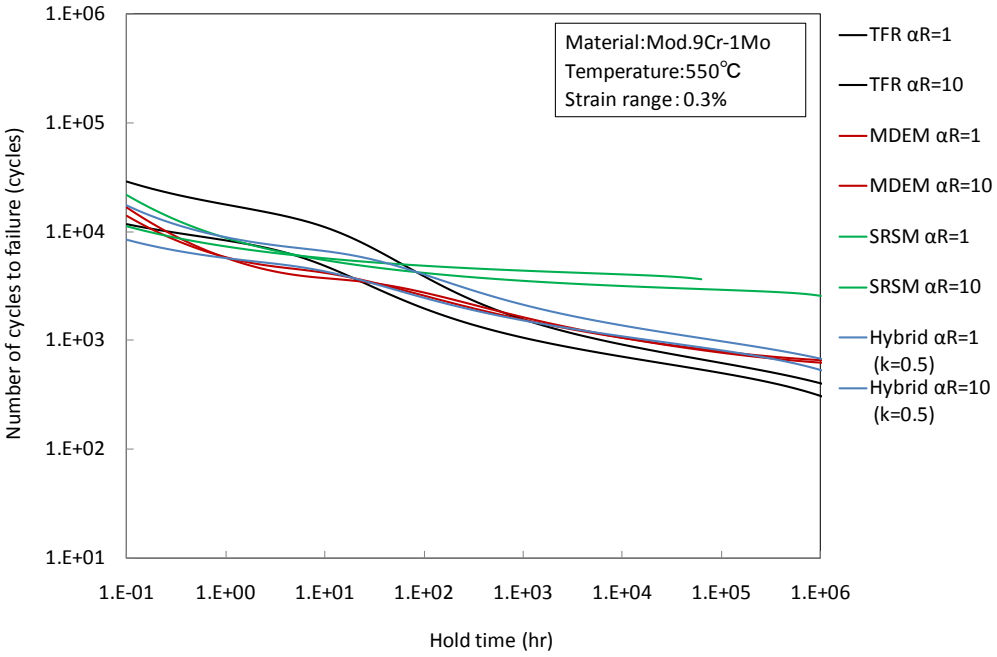


Fig. 4.1.7 Relationship between hold time and creep-fatigue life at 550C, $\Delta\varepsilon_t$ =0.3% (Parameter: time to rupture)

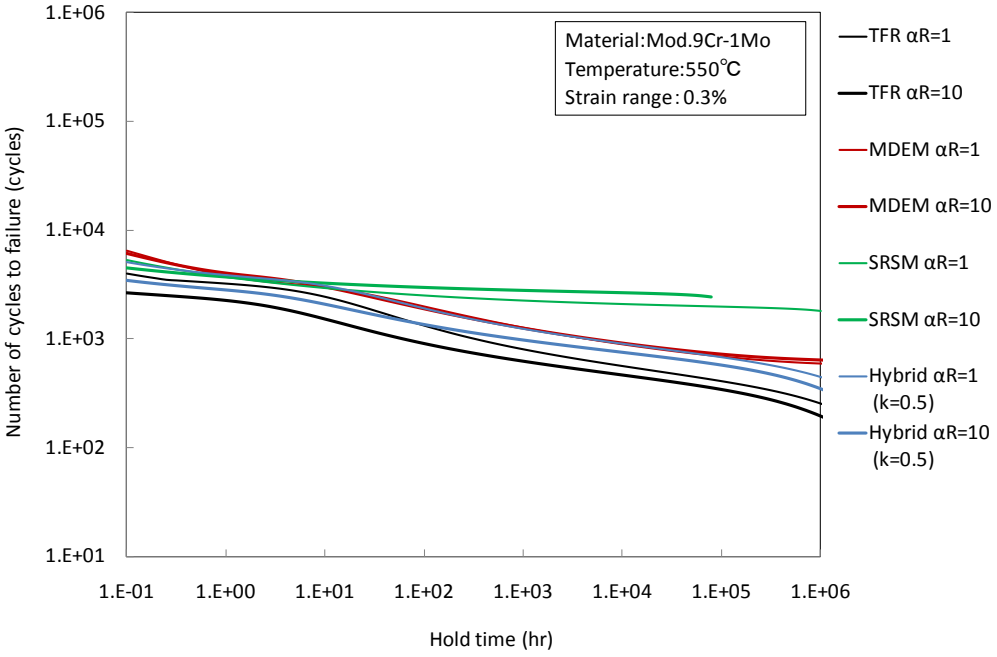


Fig. 4.1.8 Relationship between hold time and creep-fatigue life at 550C, $\Delta\varepsilon_t$ =0.5% (Parameter: time to rupture)

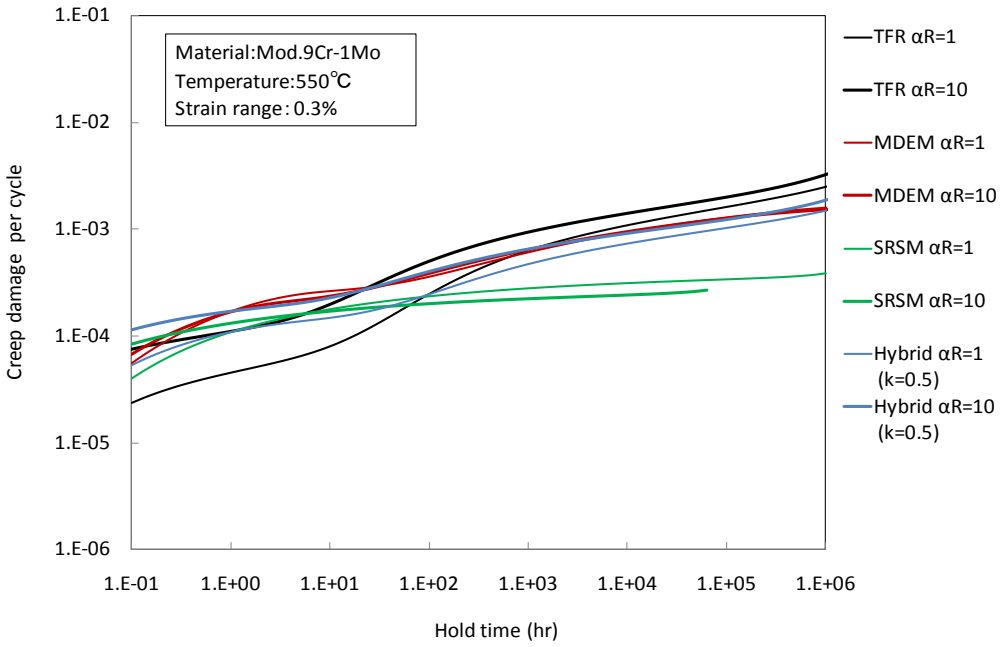


Fig. 4.1.9 Relationship between hold time and creep damage at 550C, $\Delta\varepsilon_t$ =0.3%
(Parameter: time to rupture)

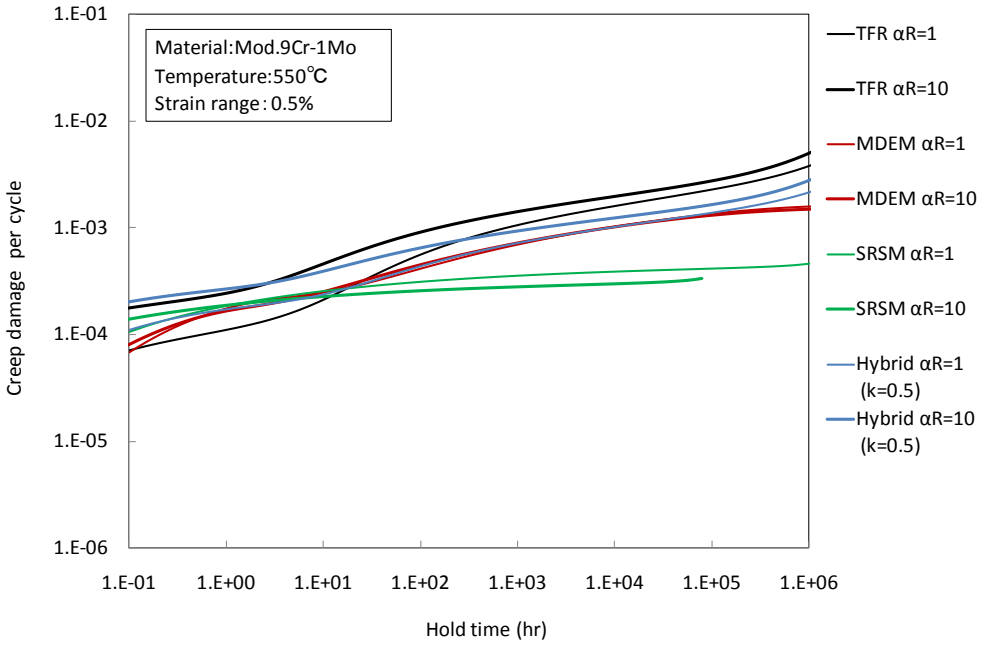


Fig. 4.1.10 Relationship between hold time and creep damage at 550C, $\Delta\varepsilon_t$ =0.5%
(Parameter: time to rupture)

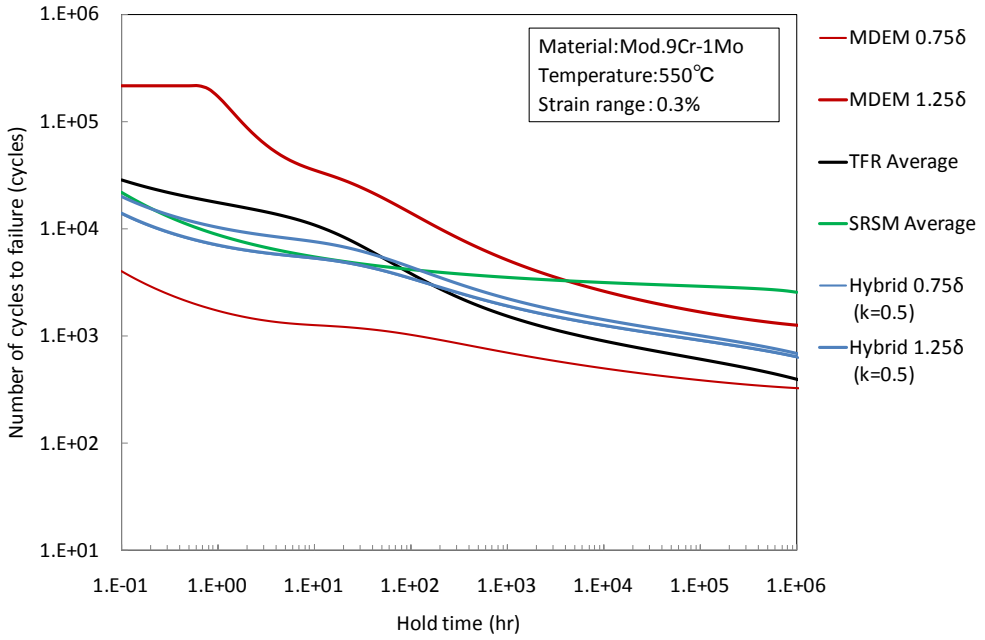


Fig. 4.1.11 Relationship between hold time and creep-fatigue life at 550C, $\Delta\varepsilon_t$ =0.3% (Parameter: creep rupture elongation)

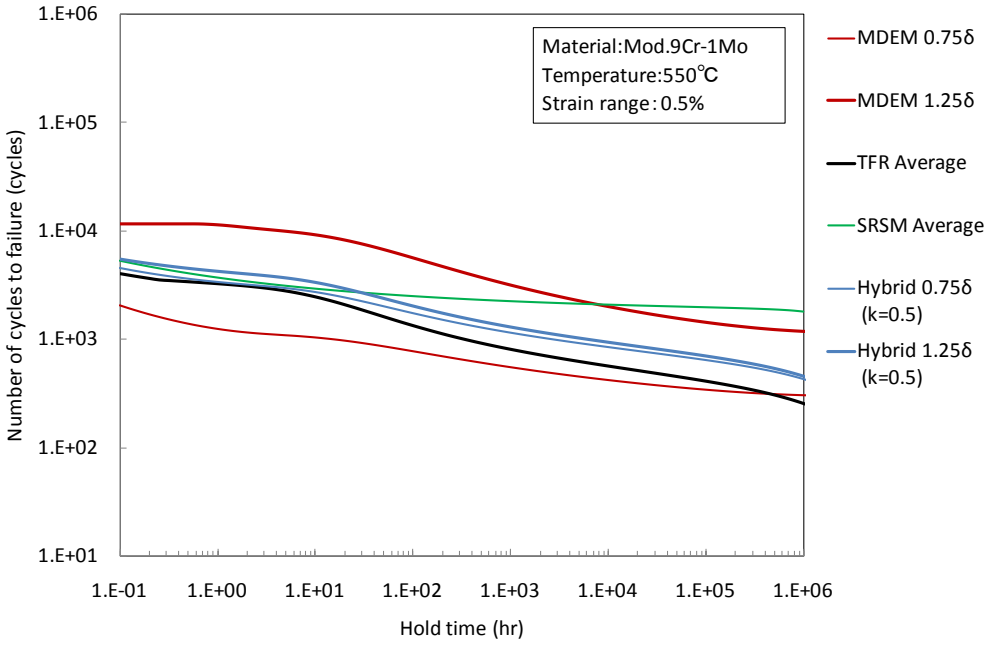


Fig. 4.1.12 Relationship between hold time and creep-fatigue life at 550C, $\Delta\varepsilon_t$ =0.5% (Parameter: creep rupture elongation)

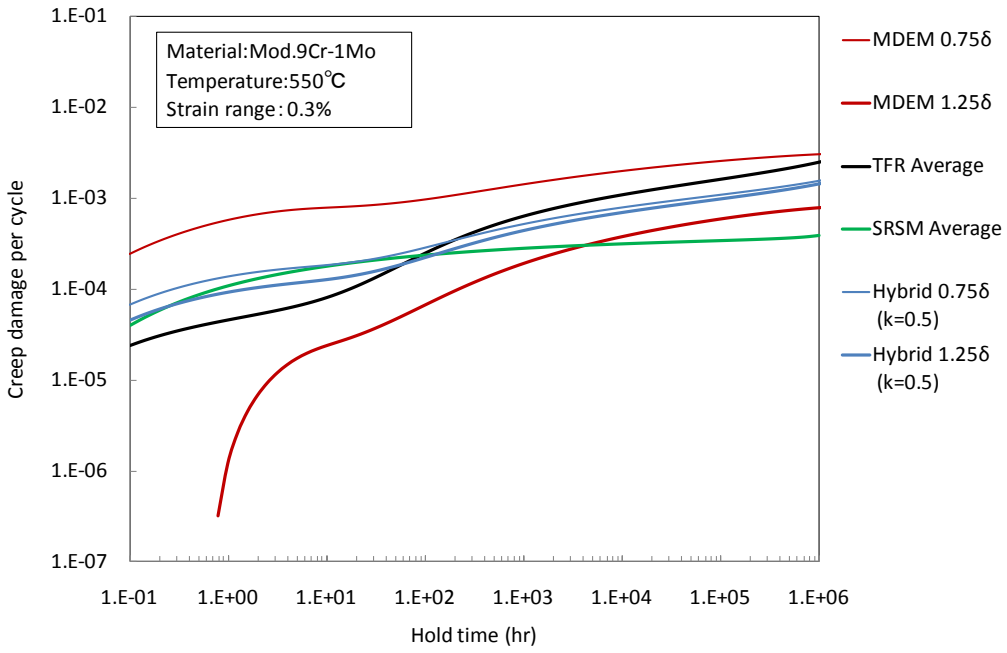


Fig. 4.1.13 Relationship between hold time and creep damage at 550C, $\Delta\varepsilon_t$ =0.3% (Parameter: creep rupture elongation)

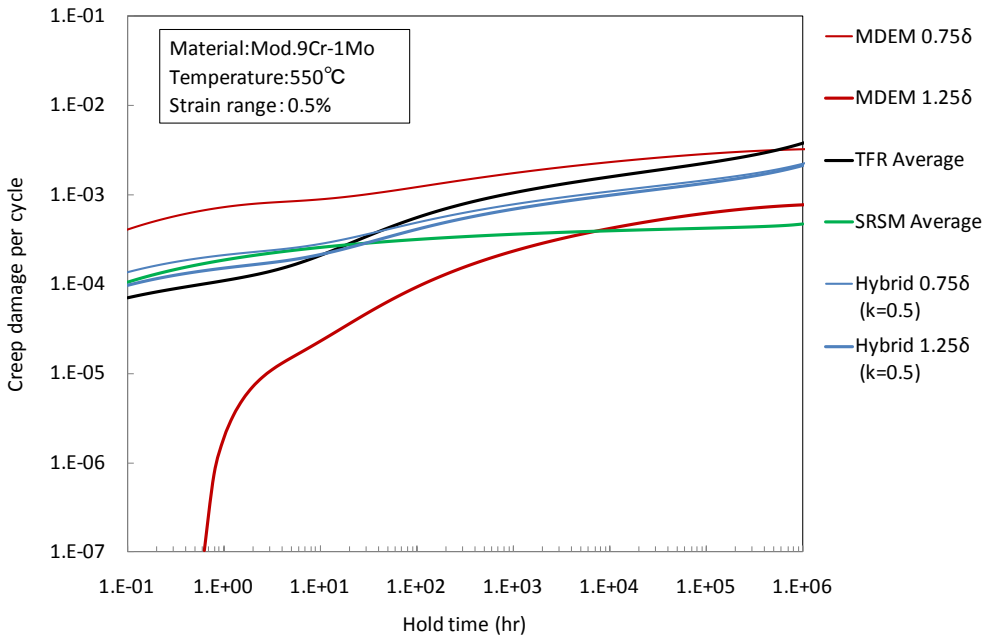


Fig. 4.1.14 Relationship between hold time and creep damage at 550C, $\Delta\varepsilon_t$ =0.5% (Parameter: creep rupture elongation)

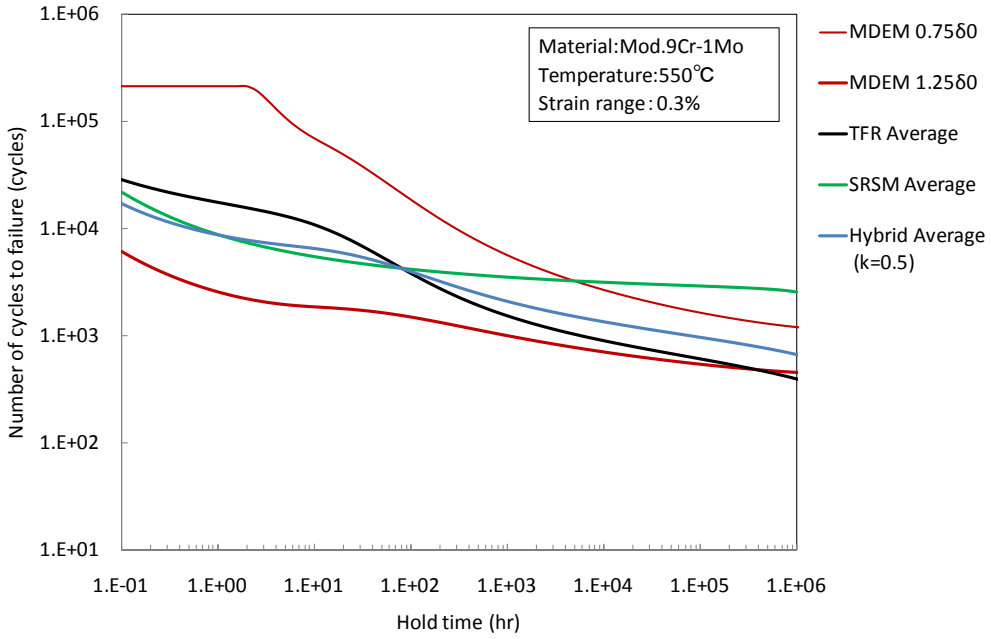


Fig. 4.1.15 Relationship between hold time and creep-fatigue life at 550C, $\Delta\varepsilon_t$ =0.3% (Parameter: Tensile rupture elongation)

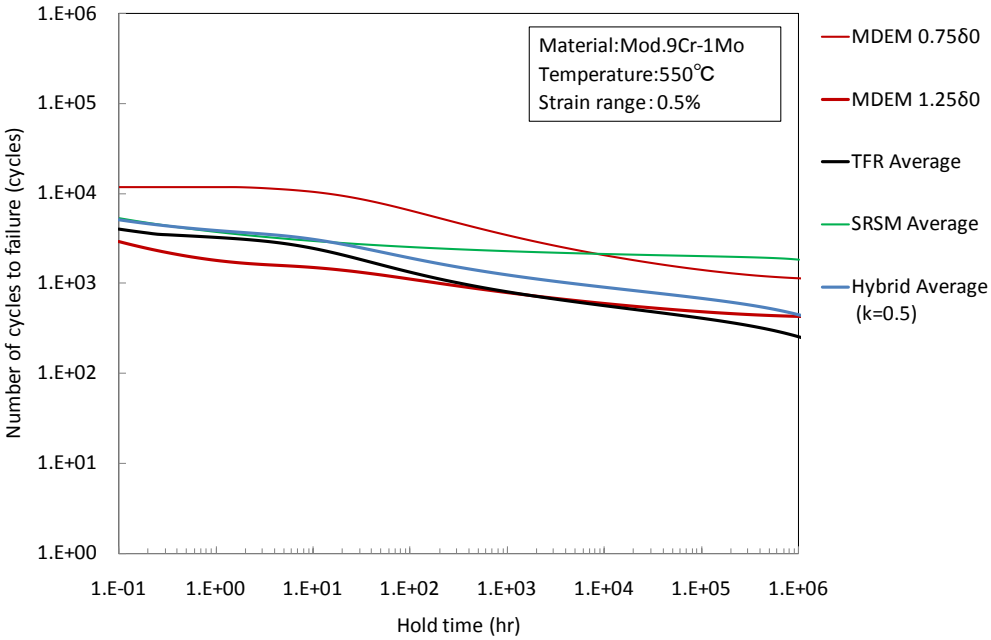


Fig. 4.1.16 Relationship between hold time and creep-fatigue life at 550C, $\Delta\varepsilon_t$ =0.5% (Parameter: Tensile rupture elongation)

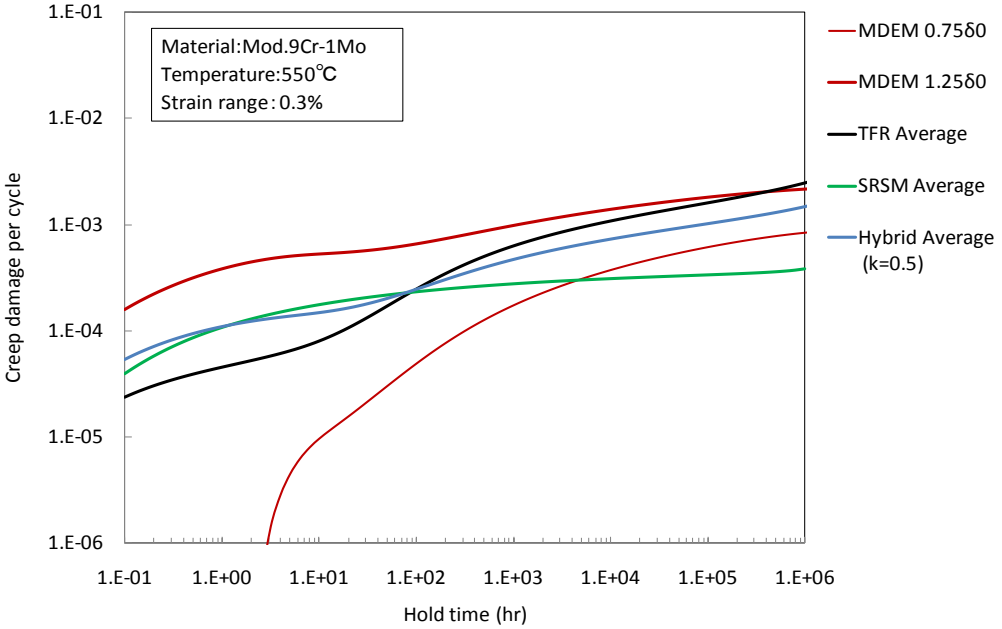


Fig. 4.1.17 Relationship between hold time and creep damage at 550C, $\Delta\varepsilon_t$ =0.3%
(Parameter: Tensile rupture elongation)

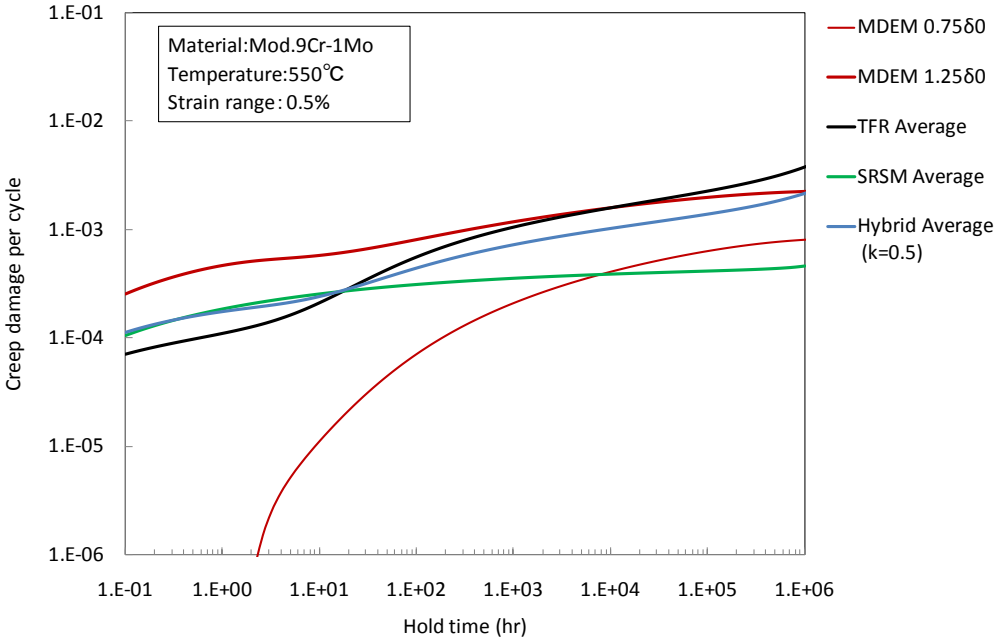


Fig. 4.1.18 Relationship between hold time and creep damage at 550C, $\Delta\varepsilon_t$ =0.5%
(Parameter: Tensile rupture elongation)

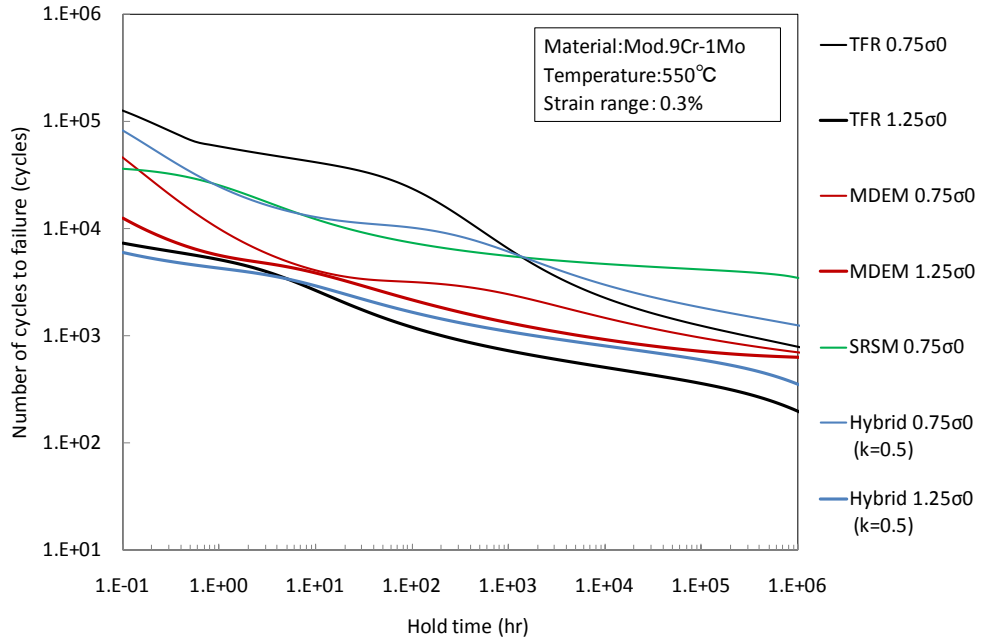


Fig. 4.1.19 Relationship between hold time and creep-fatigue life at 550C, $\Delta\varepsilon_t$ =0.3%
(Parameter: initial stress of relaxation)

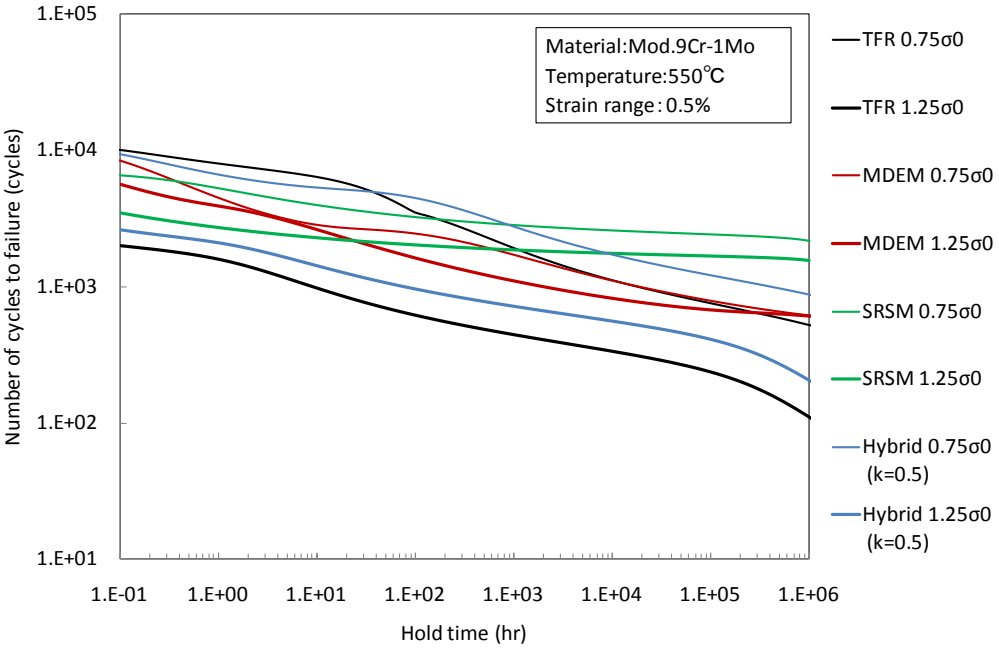


Fig.4.1.20 Relationship between hold time and creep-fatigue life at 550C, $\Delta\varepsilon_t$ =0.5%
(Parameter: initial stress of relaxation)

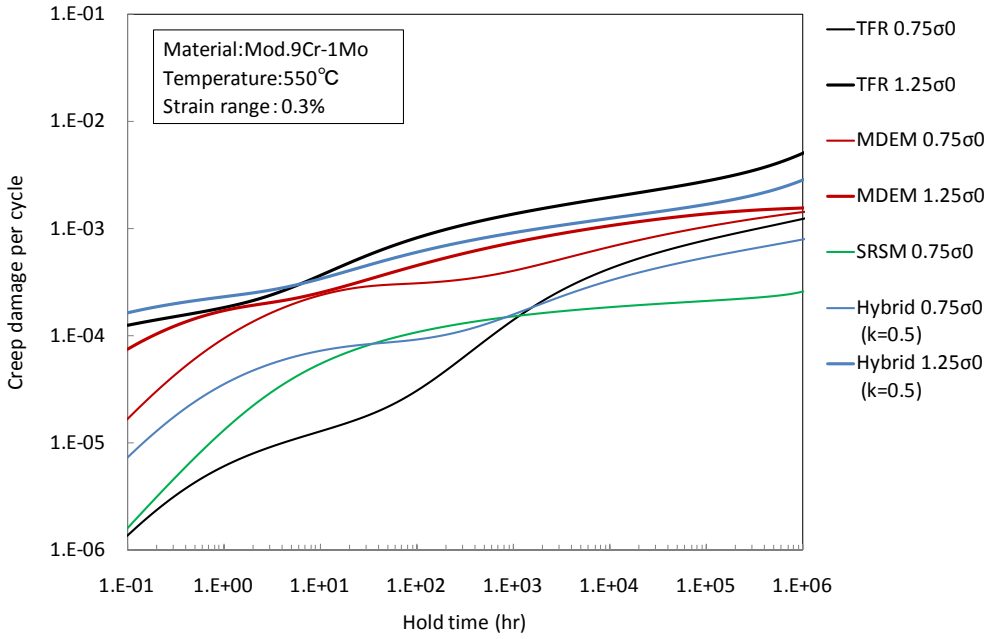


Fig. 4.1.21 Relationship between hold time and creep damage at 550C, $\Delta\varepsilon_t$ =0.3% (Parameter: initial stress of relaxation)

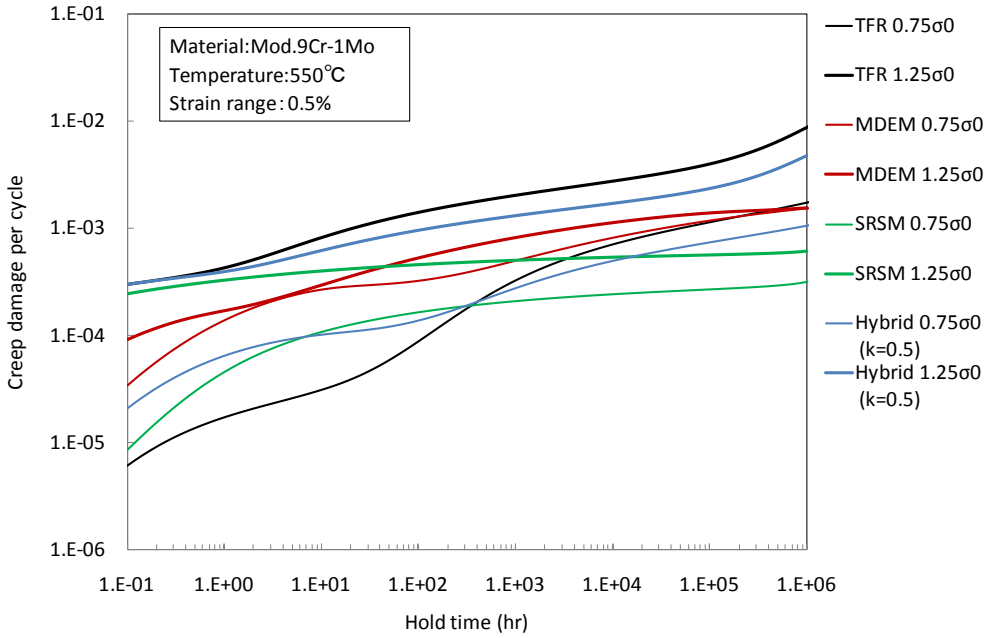


Fig. 4.1.22 Relationship between hold time and creep damage at 550C, $\Delta\varepsilon_t$ =0.5% (Parameter: initial stress of relaxation)

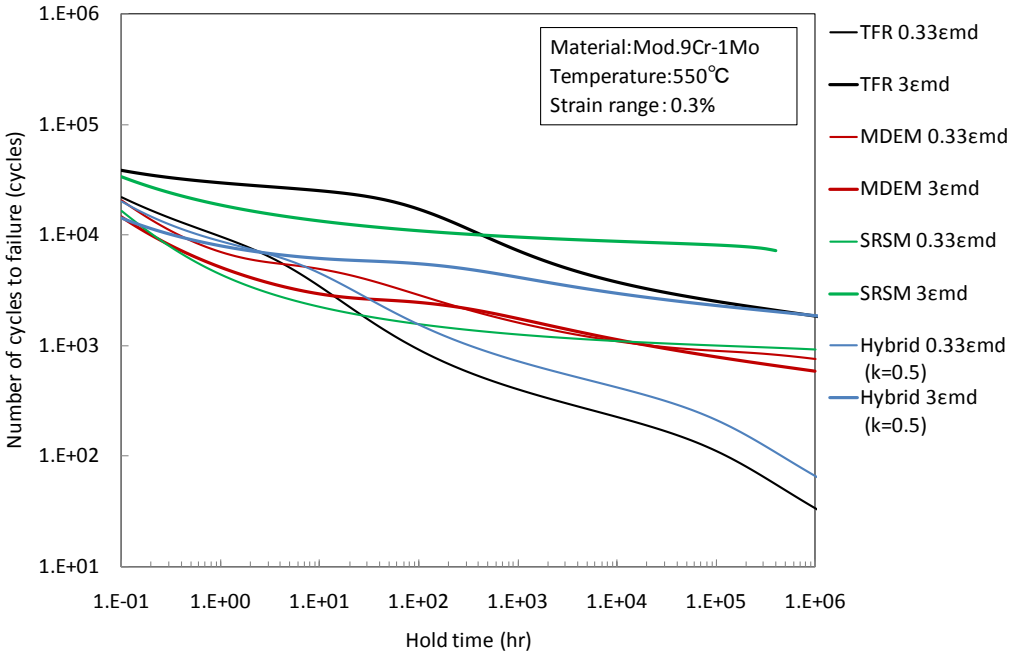


Fig. 4.1.23 Relationship between hold time and creep-fatigue life at 550C, $\Delta\varepsilon_t$ =0.3%
(Parameter: steady state creep rate)

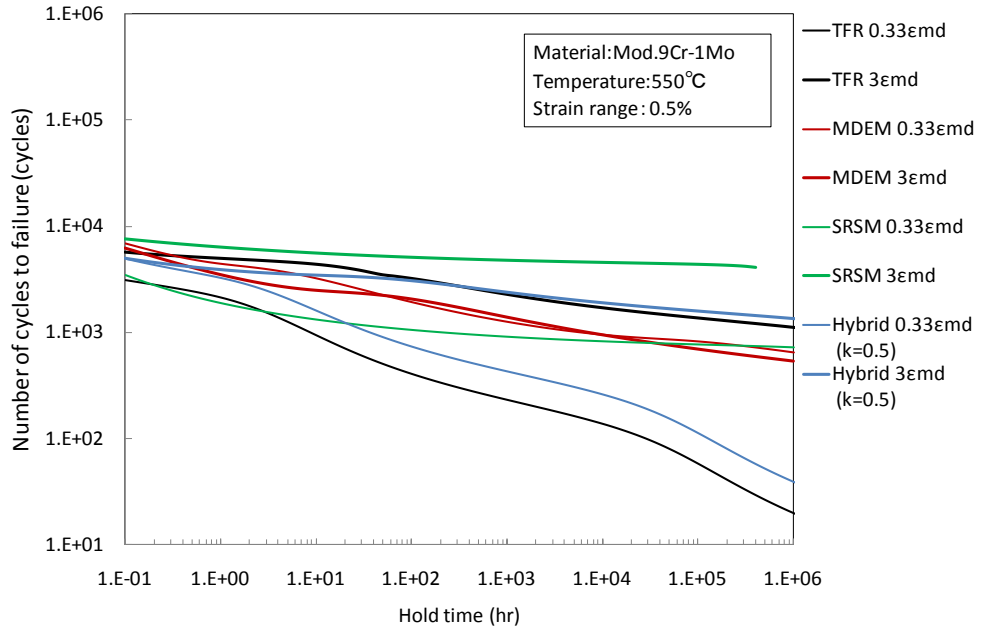


Fig. 4.1.24 Relationship between hold time and creep-fatigue life at 550C, $\Delta\varepsilon_t$ =0.5%
(Parameter: steady state creep rate)

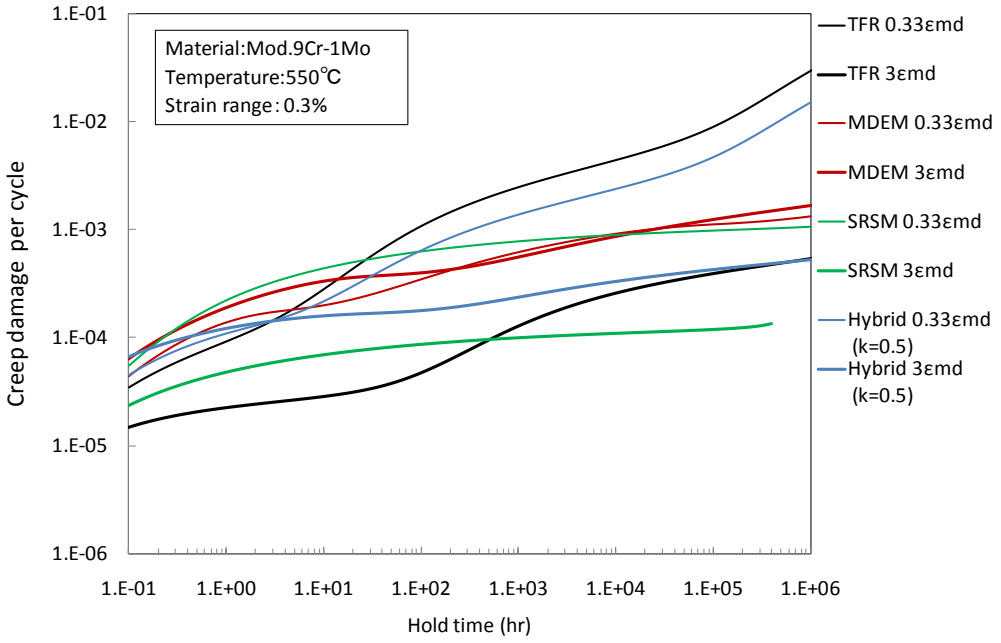


Fig. 4.1.25 Relationship between hold time and creep damage at 550C, $\Delta\varepsilon_t$ =0.3% (Parameter: steady state creep rate)

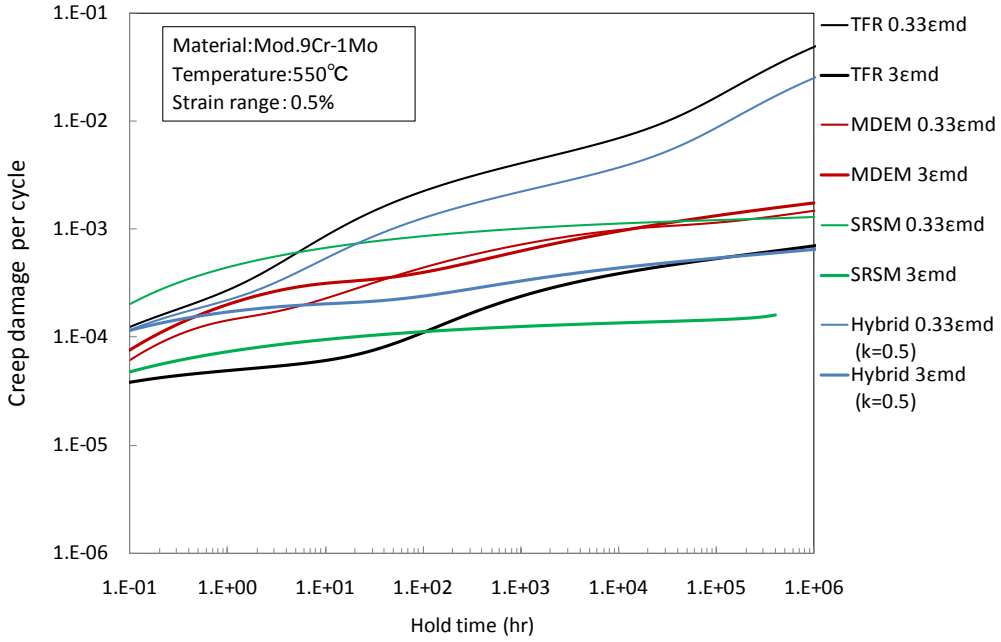


Fig. 4.1.26 Relationship between hold time and creep damage at 550C, $\Delta\varepsilon_t$ =0.5% (Parameter: steady state creep rate)

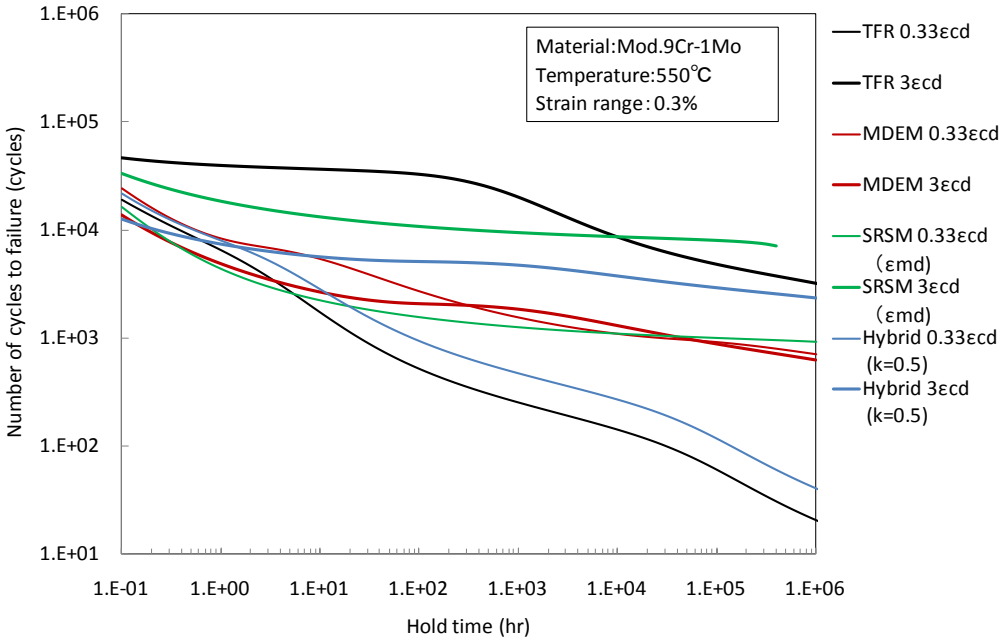


Fig. 4.1.27 Relationship between hold time and creep-fatigue life at 550C, $\Delta\varepsilon_t$ =0.3%
(Parameter: creep strain equation)

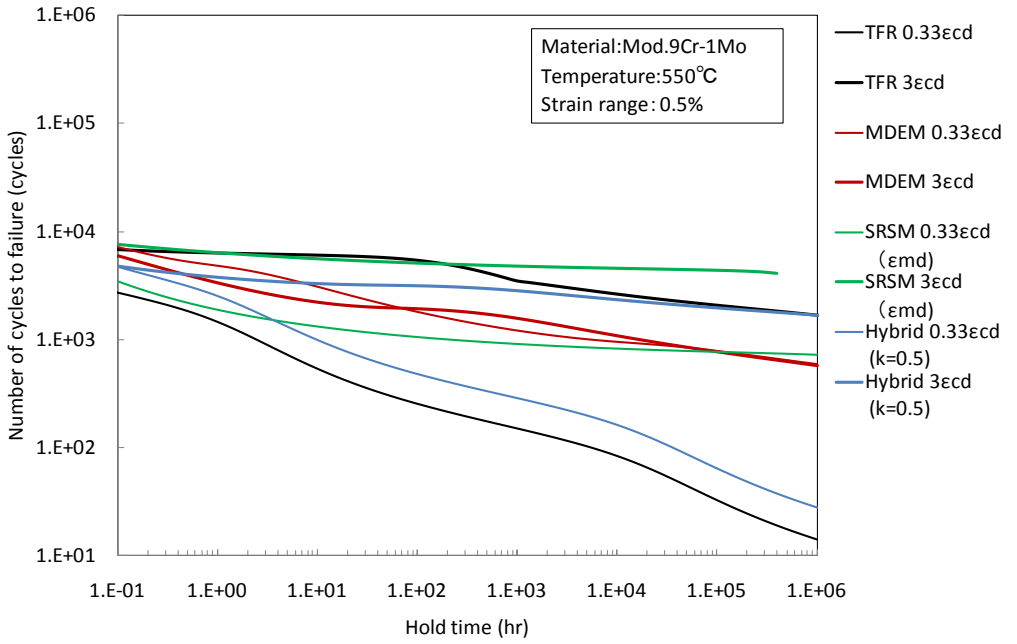


Fig. 4.1.28 Relationship between hold time and creep-fatigue life at 550C, $\Delta\varepsilon_t$ =0.5%
(Parameter: creep strain equation)

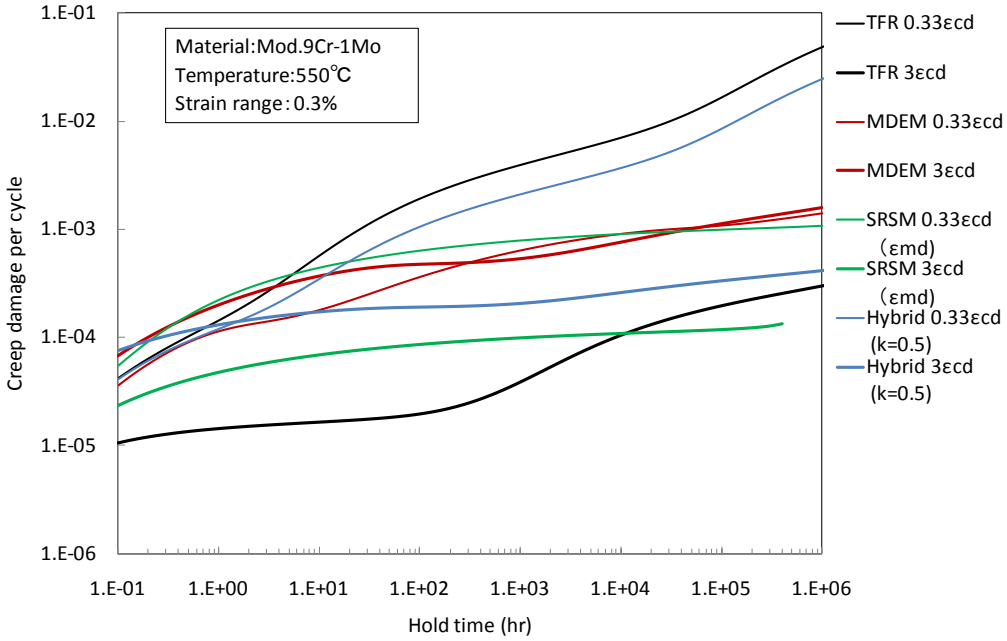


Fig. 4.1.29 Relationship between hold time and creep damage at 550C, $\Delta\varepsilon_t$ =0.3%
(Parameter: creep strain equation)

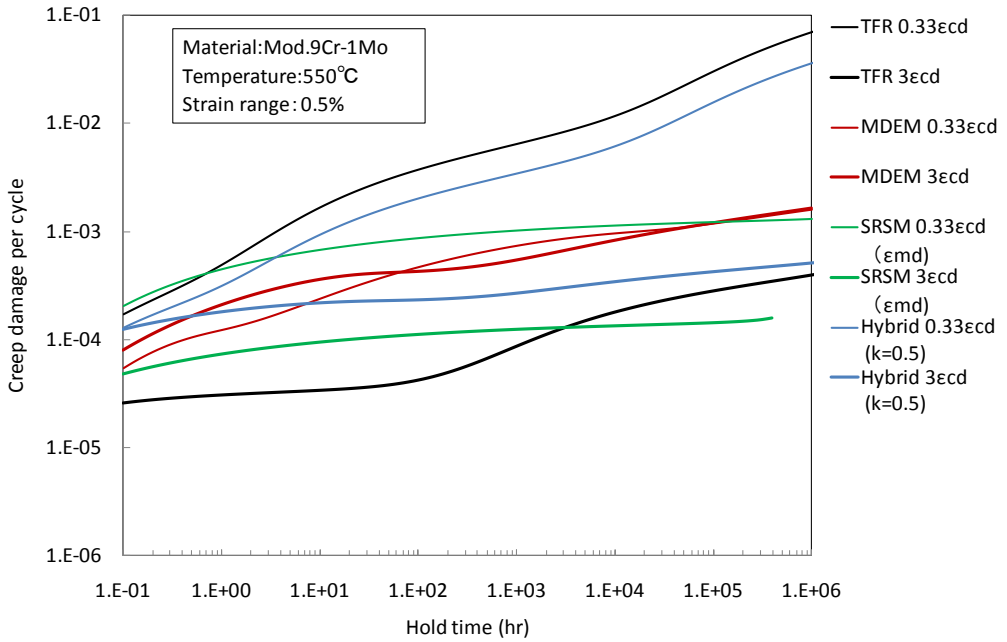


Fig. 4.1.30 Relationship between hold time and creep damage at 550C, $\Delta\varepsilon_t$ =0.5%
(Parameter: creep strain equation)

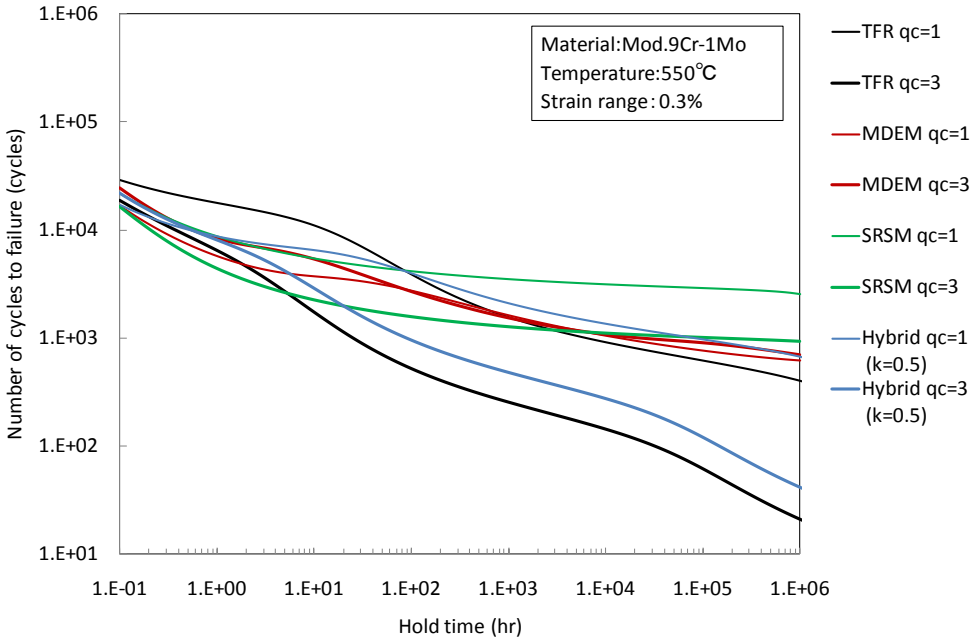


Fig. 4.1.31 Relationship between hold time and creep-fatigue life at 550C, $\Delta\varepsilon_t$ =0.3% (Parameter: elastic follow-up parameter)

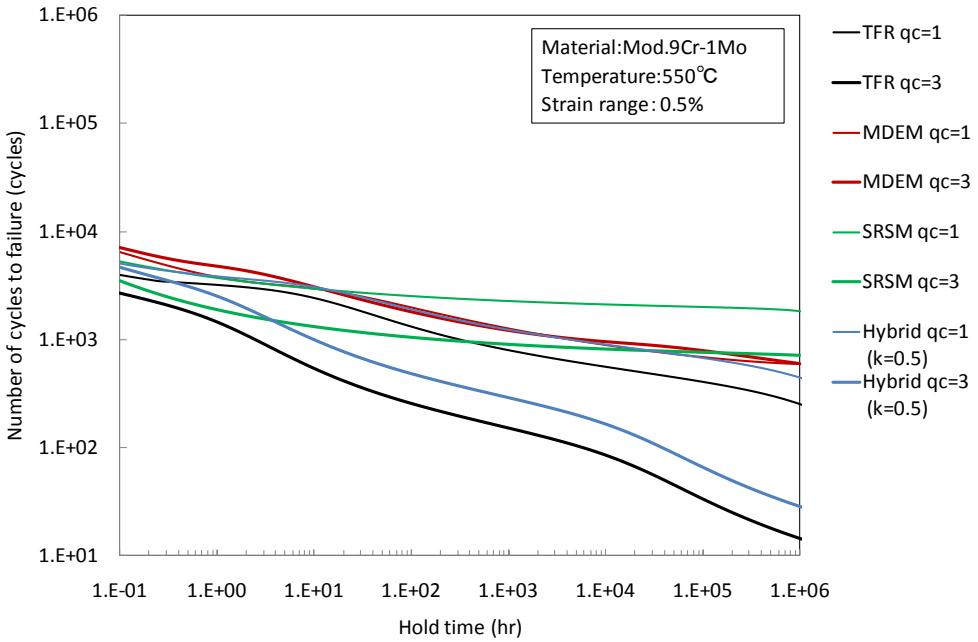


Fig. 4.1.32 Relationship between hold time and creep-fatigue life at 550C, $\Delta\varepsilon_t$ =0.5% (Parameter: elastic follow-up parameter)

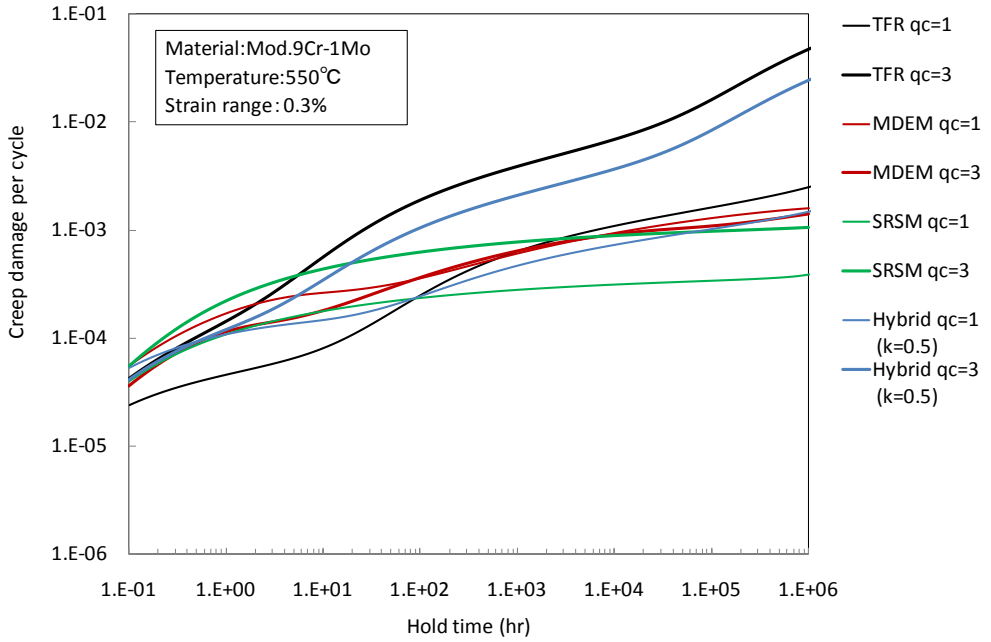


Fig. 4.1.33 Relationship between hold time and creep damage at 550C, $\Delta\varepsilon_t$ =0.3%
(Parameter: elastic follow-up parameter)

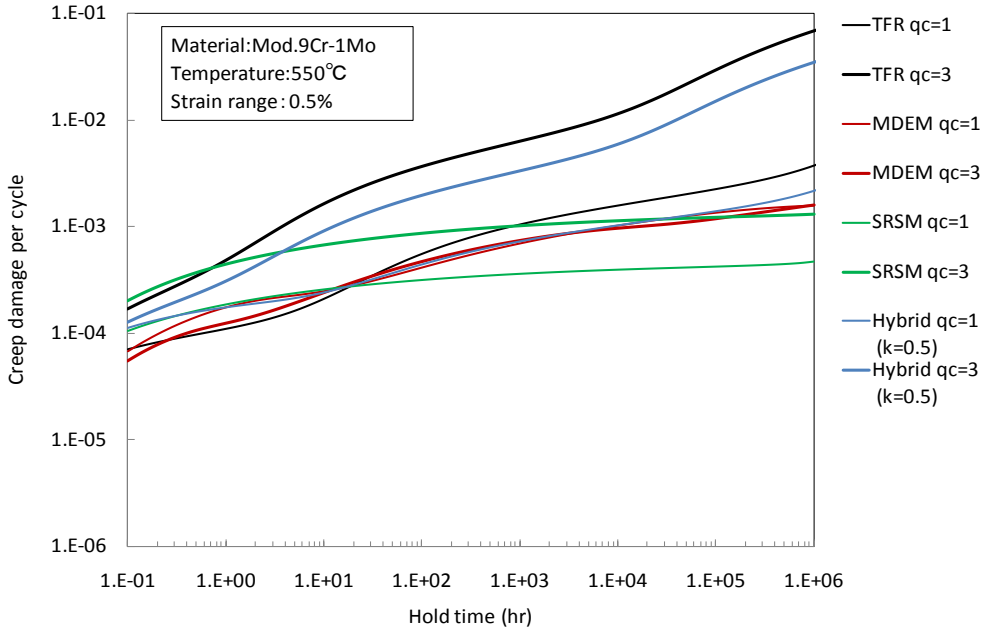


Fig. 4.1.34 Relationship between hold time and creep damage at 550C, $\Delta\varepsilon_t$ =0.5%
(Parameter: elastic follow-up parameter )

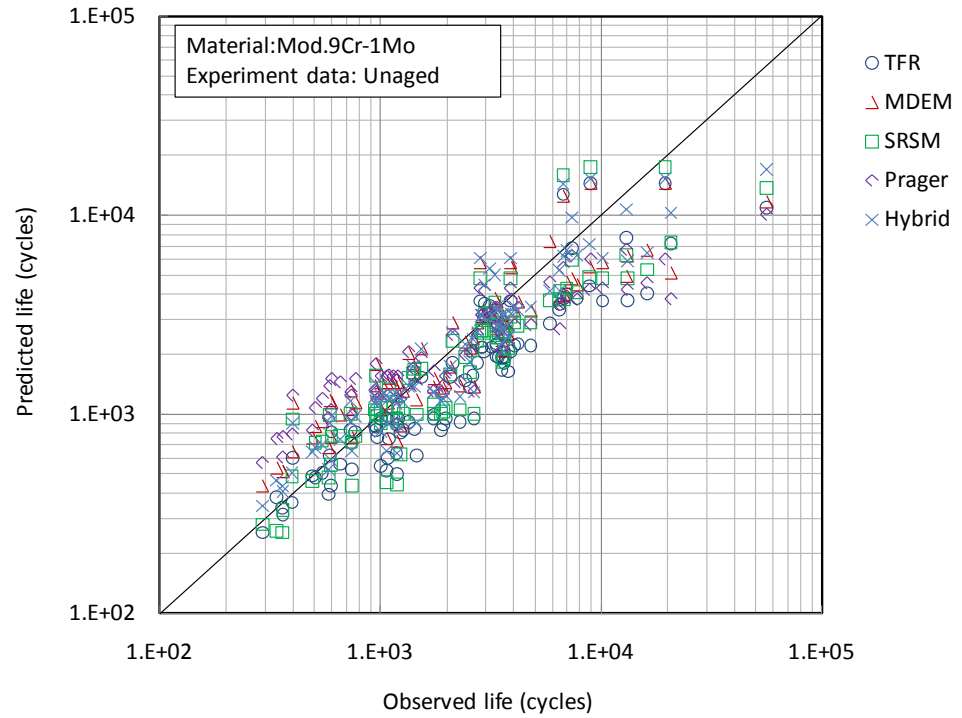


Fig. 4.1.35 Creep-fatigue life prediction of experimental results by various methods

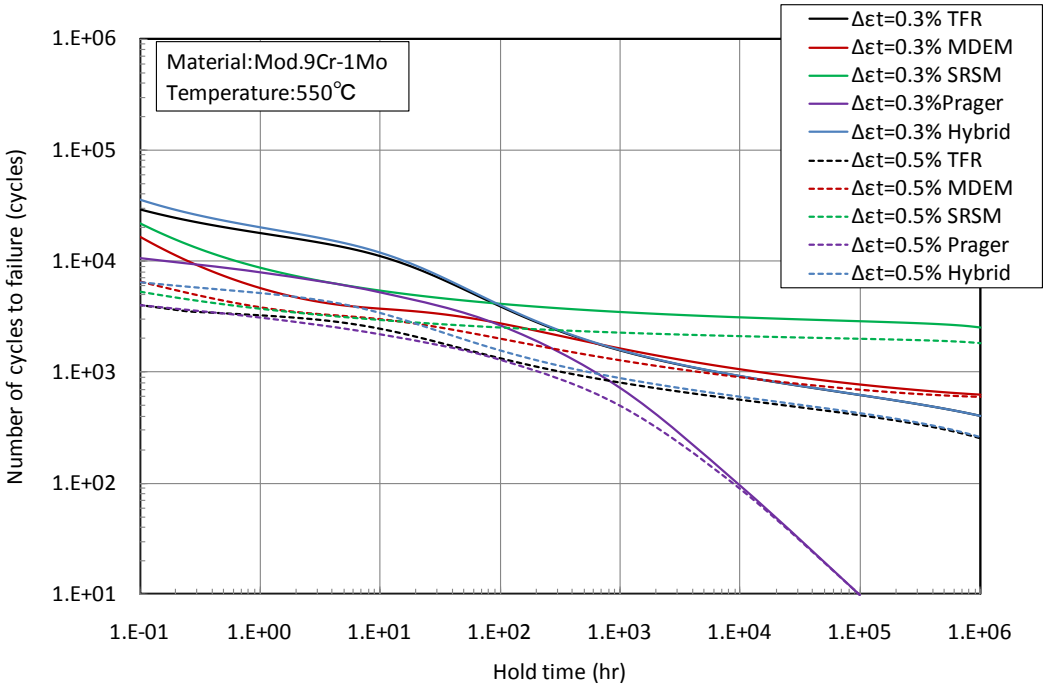


Fig. 4.1.36 Extrapolation of creep-fatigue life prediction to longer terms

## 4.2 Evaluation of basic potential of the methods investigated

This section evaluates the basic potential of the methods investigated from the viewpoints of scientific relevance, in anther word, technical advantage over the time fraction rule.

### 4.2.1 Modified Ductility Exhaustion Method

The advantage of the modified ductility exhaustion method is that creep-fatigue life prediction result is insensitive to creep rupture time, initial stress of relaxation and description of stress relaxation behavior (i.e., creep strain equation, steady state creep rate and elastic follow-up parameter), which is contrary to the case of time fraction rule. For example, two different creep strain curves, i.e. creep strain curves of DDS and RCC-MR give almost identical results. However, this method is very sensitive to creep rupture elongation and tensile rupture elongation. Therefore, one should be very careful in formulating the relationships between inelastic strain rate and creep and tensile elongation. The above observations can be confirmed by Figs. 4.1.7 to 4.1.34.

Regarding the formulation of relationships between inelastic strain rate and tensile and creep rupture elongation, the reason why the upper limit should be used for time independent ductility while an average trend is used for time-dependent portion of this relationship is not clear. Moreover, it is not easy to determine the upper limit of time-independent rupture ductility relevantly because it significantly depends on a database used for the determination of the upper limit. In addition, scatter of creep rupture elongation is generally fairly large and formulation of temperature dependency might not be an easy task as shown in Fig. 4.2.1, where cross cutting of relationships for different temperatures, which does not seem to be natural, is observed.

However, this method gives fairly good creep-fatigue life prediction under conditions where experiments are possible, but prediction in longer time regions tends to be unconservative compared to time fraction rule. It is because estimated creep damage tends to saturate under 550 C due to the saturation (slow down of strain rate) of stress relaxation. Although there is no scientific way is available to determine which prediction is more appropriate, this point should be noted when implementation of the method to code rules is discussed.

Simplicity of the method is comparable to the time fraction rule.

### 4.2.2 Strain Range Separation Method

The main point of strain range separation method is that creep damage is calculated based on a simple characteristic, the Monkman-Grant relationship only, but that accuracy of prediction is appropriately maintained by accounting for the effects of cyclic softening on stress relaxation behaviors, taking account of "additive stress". The method results in a procedure very similar to that of the time fraction rule when creep life fraction $N_c$ is formulated as $N_c=1/D_c$ and $D_c$ is calculated by Spera method, which is integration of creep damage during a hold time.

However, the selection of the additive stress that accounts for the effects of cyclic softening affects predicted creep-fatigue life significantly as shown in Section 3.2. In the sensitivity analysis described in Section 4.1, 60MPa was used as the additive stress. In this case, the SRS method is insensitive to creep rupture elongation and tensile rupture elongation, and is rather insensitive to creep rupture time, steady state creep rate, creep strain equation and elastic follow-up parameter, and is sensitive to initial stress of relaxation. The above observations can be confirmed by Figs. 4.1.7 to 4.1.34.

A concern regarding the SRS method is that although selection of additive stress can have significant effect on predicted creep-fatigue life, methods to determine the value of additive stress is not necessarily clear in light of practical application. Since the adoption of the additive stress comes from the fact that only steady state creep rate is considered in the evaluation of stress relaxation, this problem seems to be solved when creep equations that describe primary creep which accounts for very rapid stress relaxation in addition to the secondary creep. An equation in DDS procedure is such an example. In this case, the SRS method would be identical to the time fraction rule. Anyway this method emphasizes the importance of considering the effects of cyclic softening in creep-fatigue life prediction.

Simplicity of the method is comparable to the time fraction rule.

### 4.2.3 Approach for Pressure Vessel Applications

The main point of this approach is that this method focuses on the effect of cyclic plastic strain on creep rupture life, not vice versa. Therefore, when number of plastic cycles is unity, corresponding life in time (hold time) becomes $T_r$, which is life absent fatigue expressed in time. In this sense, concept of extrapolation of creep-fatigue life is very clear and it seems that application to plants

whose design is basically performed by referencing stress allowable $S$ (conceptually stress level corresponding to creep rupture time of $1x10^5$ hours) would be fairly practical.

However, applications to creep-fatigue accompanied by significant stress relaxation under strain controlled conditions which are expected in fast breeder reactors for example, a step-by-step procedure to apply the present method (for example, how to select appropriate values of constants such as $T_r$ and beta) is yet to be established.

The most interesting point of the method that could be reflected to the improvement of the current time fraction rule is that the fact that the estimated degree of creep-fatigue interaction depends on loading conditions such as strain range and hold time. Other creep-fatigue evaluation methods such as time fraction rule, ductility exhaustion method (including the modified ductility exhaustion method), the degree of creep-fatigue interaction is expressed uniquely by a "damage diagram (damage envelope)" which prescribes the degree of creep-fatigue interaction depending only on the ratio of creep damage to fatigue damage regardless of other loading conditions. This point should be further looked into when other methods' application is discussed.

Simplicity of the method is better than the time fraction rule.

### 4.2.4 Hybrid method

The main point of this Hybrid method is that it takes into account of both stress and strain in evaluating creep damage through using formulations used in the time fraction rule and the conventional ductility exhaustion method. Consequently, this method could be one that takes advantage of the merits of both time fraction rule and ductility exhaustion method.

However, there are some technical difficulties associated determining the constant $k$ which defines the respective contribution of time fraction term and ductility exhaustion term. First, necessary condition for this approach to be meaningful is that the predicted life by the time fraction rule and ductility exhaustion rule show the opposite trend, i.e., if one of them gives conservative results, result by the other method should be unconservative. This is the case as shown in Figs. 4.2.2 and 4.2.3. Second, the relationships of creep damage estimated by the time fraction method and the ductility exhaustion method become vice-versa at a certain hold time that depends on temperature. This means that the value of constant $k$ could be time-dependent, and that not only short-term

experimental data but also insights on long-term creep-fatigue predictions should be taken account for the determination of the value of *k*.

Another point is that the creep-fatigue damage envelope should be identical for the two methods, the time fraction rule and the conventional ductility exhaustion method. Generally speaking, the creep-fatigue damage envelope combined with the time fraction approach employs an interception point more conservative than (0.5, 0.5). Therefore, this method is not a simple combination of the two methods but some kind of modification would be necessary.

In addition, that logical (or physical) background is not sufficiently provided could be an obstacle to practical implementation. In order to deploy this method to design code, justification of this approach and the value of *k* become necessary. The most efficient way to determine the value of *k* would be regression analysis. However, results of regression analysis tend to be sensitive to database used. Also, the most appropriate value of *k* could depend on creep equations as shown in Figs. 4.2.2 and 4.2.3. Metallurgical investigations might help but how this could be done is not clear. Determining a value of *k* which is most appropriate for practically expected conditions could be an issue.

What we can learn from this method is that methods have own bias in long-term regions and this fact should always be kept in mind.

This method is more complex than the time fraction method because a ductility exhaustion term is added.

### 4.2.5 Simplified Model Test Approach

From a designer's perspective, the main advantage of the proposed SMT approach is that it is based on the use of the results of elastic analyses in procedures similar to the current procedures used below the creep regime, e. g. ASME – Subsection NB. Clearly, and as noted in the main text under some topics, there is additional work to be done before implementing the SMT approach. A number of additional representations of actual geometry, materials and operating conditions need to be evaluated to verify the conservatism of the approach.

Although there is initial encouraging test data, more data need to be generated with particular attention to extending the hold time as long as economically feasible. An additional advantage of obtaining additional SMT data on materials of interest is that they would also provide a valuable basis for evaluation and development of the analytical models and constitutive equations used to predict material behavior using inelastic analysis. Correlation with SMT results would be a valuable requirement for any inelastic analysis and design procedure.

This is the simplest method among those investigated.

### 4.2.6 Summary

From the above discussions, it is summarized that the modified ductility exhaustion method, the strain range separation method, the approach for pressure vessel applications and the hybrid method offers advantages and insights that could be reflected to improve the currently used time fraction rule. The simplified model test approach offers whole new advantage particularly from the viewpoint of robustness and simplicity of procedure.

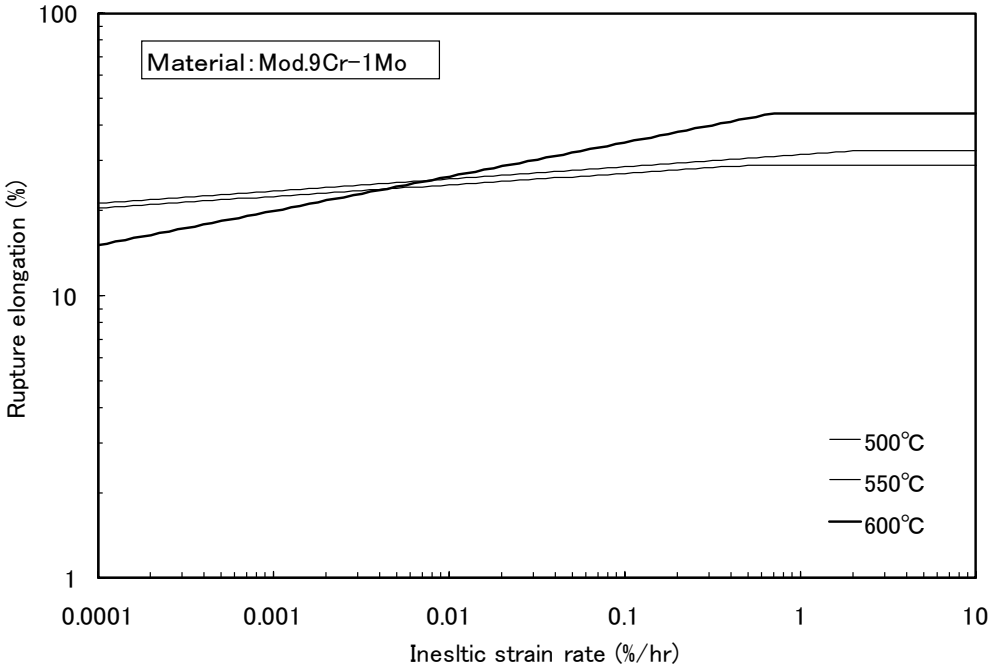


Fig. 4.2.1 Comparison of regression line between inelastic strain rate and rupture elongation at each temperature

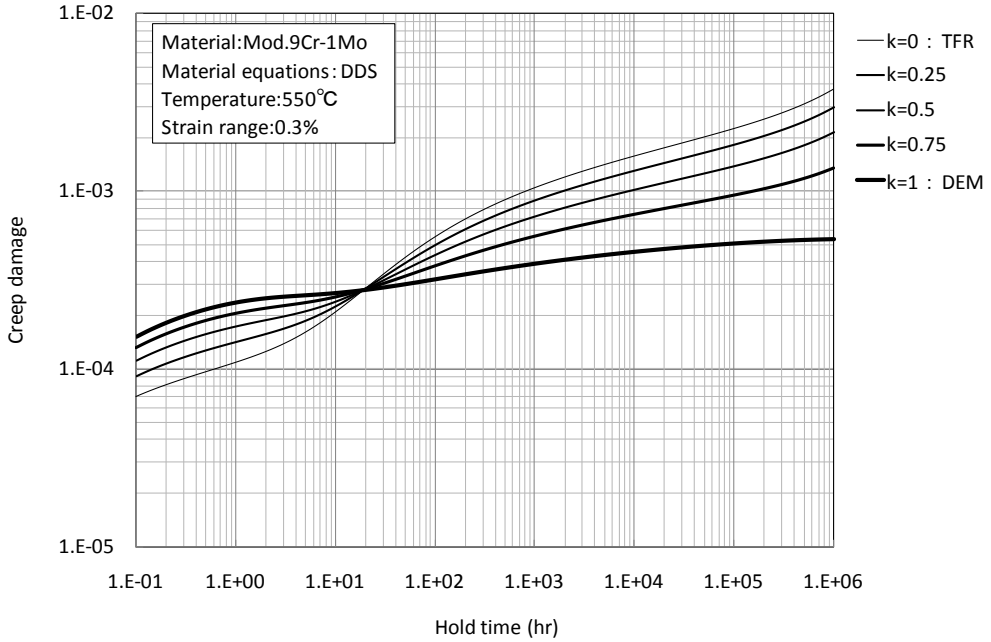


Fig. 4.2.2 Relationship between hold time and creep damage by DDS at 550C, 0.3%

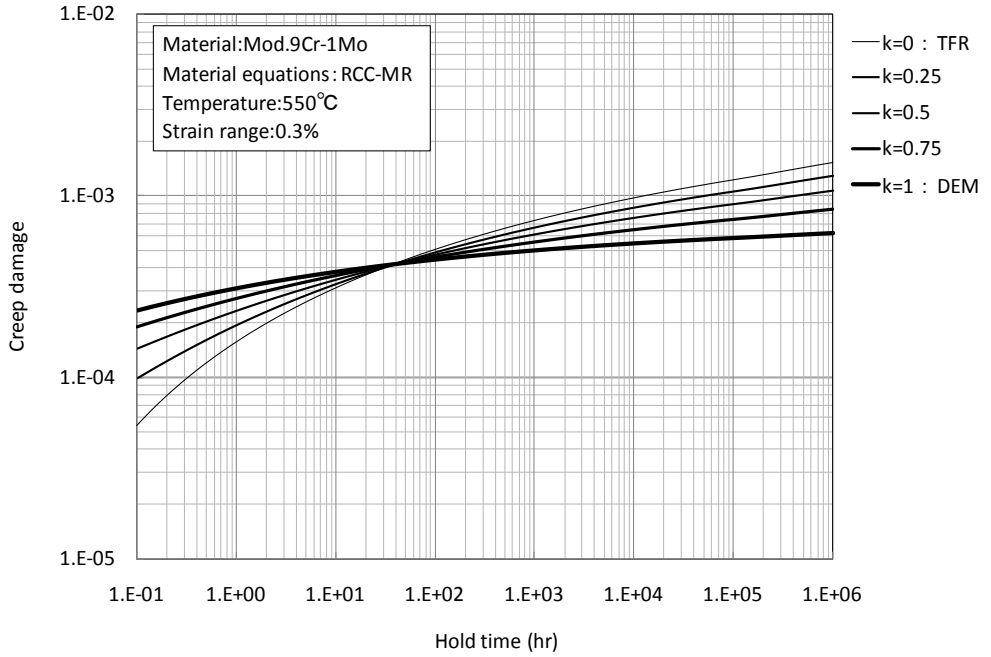


Fig. 4.2.3 Relationship between hold time and creep damage by RCC-MR at 550C, 0.3%

## 4.3 Evaluation of extendibility of the methods investigated

This section summarizes the evaluation of extendibility of the methods investigated. Factors that can affect creep-fatigue life which are not necessarily explicitly taken account of when the methods were developed are picked up and how each method could deal with them is discussed.

### 4.3.1 Extension to higher temperatures

All the methods use material data (including equations concerning material strength and properties) at temperatures where creep-fatigue life prediction is to be performed. All the methods investigated will require relevant additional test data when they are to be applied to higher temperatures. None of the methods propose an approach that enables temperature extrapolation without corresponding data.

### 4.3.2 Incorporation of thermal aging

As all the methods use material data at temperatures where creep-fatigue life prediction is performed, if the effect of thermal aging is included in the data, the methods can take account of thermal aging. Needless to say, the effects of thermal aging on properties not used in evaluation can not be reflected in creep-fatigue life prediction (for example, the time fraction rule does not account for the effect of thermal aging on ductility which is not used in evaluation).

### 4.3.3 Incorporation of elastic follow-up

In creep-fatigue life prediction, the effect of elastic follow-up is generally accounted for in the course of estimation of strain range and stress relaxation behavior during strain hold.

The modified ductility exhaustion method, the strain range separation method, the hybrid method can account of the effect of elastic follow-up through estimation of strain range stress relaxation behavior. The approach for pressure vessel application can do so through estimation o f strain range. This method does not deal with stress relaxation. However, considering that this approach was originally proposed for stress controlled situations, it might be possible to interpret that the effect of elastic follow-up has been incorporated in the most conservative way.

The SMT approach is constructed based on specimens that reproduce elastic follow-up. Therefore, the creep-fatigue life prediction curves based on the SMT approach automatically account for elastic follow-up.

### 4.3.4 Incorporation of geometrical discontinuity

Geometrical discontinuity can be taken into consideration through factoring strain range.

The modified ductility exhaustion method, the strain range separation method, the hybrid method and the approach for pressure vessel application can take the effects of geometrical discontinuity into account through estimation of strain range. The SMT approach is constructed based on specimens that represent geometrical discontinuity in practical components.

### 4.3.5 Extension to welded joints

Two main factors associated with creep-fatigue life prediction of welded joints is to take account of 1) (possible) inferior strength or ductility of weld metal and head affected zone, and 2) strain distribution raised by combination of different inelastic behaviors of base metal, weld metal and heat affected zone with in welded joint. The latter point can be analyzed by the finite element method and the result are input for creep-fatigue life prediction.

The modified ductility exhaustion method, the strain range separation method, the hybrid method and the approach for pressure vessels application may predict the creep-fatigue life of welded joints by predicting each part of welded joints such as base metal, weld metal, and heat affected zone using corresponding material properties obtained by experiments. For precise prediction, it is desirable that material properties are obtained for weld metal and heat affected zone. This will require performing test such as tensile tests, creep tests and fatigue tests for both of them.

Strain concentration and/or stress concentration need to be evaluated beforehand separately.

The SMT approach will require creep-fatigue tests of welded joints.

## 4.4 Evaluation of applicability of the methods investigated to ASME-NH

This section summarizes the applicability to ASME-NH of the methods investigated. Viewpoints are additional data generation required to deploy the method to NH, validation tests required, way of incorporation of safety factors and necessary change required to NH.

It should be noted that how respective design methodologies go about determining the relevant design parameters applicable to a specific configuration and set of operating conditions is equally important or perhaps subject to even greater viability. However, this will require another round of investigation.

### 4.4.1 Data generation required

The modified ductility exhaustion method, the strain range separation method and the hybrid method basically require the same data that are needed in the case of the time fraction method. In this regard, data have been already acquitted. For the modified ductility exhaustion method, ductility should be determined as a function of strain rate. However, available data can be limited because strain rate is not necessarily recorded in creep tests and additional data generation would be necessary.

The SMT approach requires a whole new set of creep-fatigue data using the specimen uniquely designed for this purpose as described in Chapter 3. Generation of such data could require a lot of time and resource. A practical approach could be to explore possibility of using the vast amount of “conventional data” such as smooth bar fatigue and creep data together with the newly obtained SMT data that can determine the shift of life due to elastic follow-up. This could enable most efficient use of SMT data of which amount would be relatively limited.

### 4.4.2 Validation tests required

Generally, creep-fatigue evaluation methods are developed based on smooth bar specimens and validated by structural tests. This approach is appropriate but structural tests sometimes involve uncertainties of their own. For example, for complex structures subjected to thermal loads, estimation of strain distribution itself is a matter of research and development. One thing that can be proposed here is that the test that will be performed for the development of the SMT approach can be used to validate creep-fatigue evaluation methods other than the SMT approach. It is because the

tests to be conducted to develop the SMT approach must reproduce elastic follow-up and geometrical concentration behaviors under perfectly controlled “known” conditions.

### 4.4.3 Incorporation of safety factors

How to incorporate safety factors in the newly proposed methods is not determined yet. It would be useful to select parameters to which safety factors are to be applied based on the sensitivity analysis performed in 4.1.1. It is reasonable that safety factors are applied to parameters to which respective method is most sensitive. This could reduce the number of safety factors.

In the case of the modified ductility exhaustion method, tensile and creep rupture ductility could be the parameters to which safety factors are to be applied. In the case of strain range separation method, safety factors could be incorporated so that the Coffin-Manson type relationship for plastic and creep strain ranges are shifted towards a conservative direction. One more possibility is to apply some form of safety factors to Monkman-Grant relationship to account for the “additive stress”. For the approach for pressure vessel application, it is considered that creep rupture time $T_r$ would be one possibility and the other is $\beta$ which represents the extent of creep-fatigue interaction. In the case of Hybrid method, safety factors could be applied to both creep rupture time and ductility. The SMT approach can apply safety factors to the trend of the test data that will be generated newly.

### 4.4.4 Changes to the ASME-NH code

Apart from the necessary changes in code provisions regarding the creep-fatigue damage evaluation procedure itself, the following changes would be necessary to implement the new methods.

For the modified ductility exhaustion method, creep rupture strain as a function of strain rate should be implemented in the code. For the hybrid method, reduction of area or ductility should be implemented. The strain separation method may not require any particular new information. The approach for pressure vessel application needs to implement creep rupture time $T_r$ and stress-strain curves that allow estimation of plastic strain amplitude. The connection between the SMT approach and the current NH provisions is elastically calculated strain range and may not require additional provisions. On the contrary, the introduction of the SMT approach would greatly contribute to simplification of NH.

### 4.4.5 Technical readiness in 2009

The modified ductility exhaustion method, the strain range separation method, the hybrid method and the approach for pressure vessel application are almost ready for deployment (Of course, long-term tests and number of validation tests are desirable but this point is excluded when evaluating technical readiness). Small amount of investigation would be necessary to determine properties that are to be codified (relationship between inelastic strain range and ductility is an example for the modified ductility exhaustion method). The simplified model test approach would require a fairly large amount of small structural tests to establish the relationship between creep-fatigue life and elastically calculated strain range. Therefore, this approach is yet to be ready for deployment at this point.

## 4.5 Recommendations

This section summarizes recommendations of the author for the improvement of Subsection NH based on the investigations described in previous sections.

Five new methodologies have been investigated and it was clarified that each of them has technical advantage over the current time fraction rule and offers technical insights which should be thought much of in the improvement of creep-fatigue evaluation procedures. As described in the previous sections, the advantages that the modified ductility exhaustion method, the strain range separation method, the hybrid method and the approach for pressure vessel applications could be incorporated by modification of the current time fraction rule in a manner the main point each of the method raises is relevantly assessed in the procedure. On the contrary, the advantage that the simplified mode test approach offers is fundamental and wholly and if this method could replace the current time fraction rule, it would achieve a leap of progress in creep-fatigue evaluation in terms of robustness and simplicity. However, the simplified model test approach is not ready for deployment at this point.

Therefore, the author recommends the following two steps as a way to improve NH.

The first step is to modify existing time fraction rule by incorporating technical advantages and technical insights exhibited by the newly proposed method in a peace-by-peace manner. This would contribute to minimize disadvantages (or deficiencies) that are recognized on the current method in short term. And concurrently, for long-term improvement, pursue materialization of the SMT approach. Once the SMT approach become mature enough including data acquisition necessary for validation, it could replace the current time fraction rule. The fact that the time fraction rule generally gives conservative predictions in long-term regions justifies the first step which precludes immediate change of the time fraction rule as a basic methodology.

A rough sketch of the first step is as follows. The modified ductility exhaustion method gives good life prediction in regions where experimental results exist. Therefore predicted creep-fatigue life by this method could be referenced as something to be compared with other methods. Because there is no scientific (theoretical) way to determine the relevance of creep-fatigue life prediction in long term regions, comparison of predicted results acknowledging the bias which respective method

might have could be the only basis for discussion on the relevance of prediction. The modified ductility exhaustion method could be used for this purpose. The strain range separation method rises the point that the accounting for the effect of cyclic softening to creep properties. This point could be further investigated in connection with the examination of creep properties that are used in evaluation of creep damage. An option to be investigated is to use creep strength of cyclically softened material for creep damage evaluation. The hybrid method offers caution that each of the investigated method could have bias in creep-fatigue life prediction and they can be pronounced contradictory in long-term regions leading to completely different creep-fatigue prediction depending on method. This point should always be kept in mind when we discuss the relevance of creep-fatigue evaluation procedures. An approach for Pressure Vessels Application suggests that the degree of creep-fatigue interaction depends on loading conditions. This point is related to the discussion on the interception of creep-fatigue damage envelope of Mod.9Cr-1Mo steel where (0.3, 0.3) is going to be adopted instead of current (0.1, 0.01). It would be useful in this kind of discussion to recognize that there is possibility that an interception point could vary according to loading conditions. If so, the discussion is not a matter of drawing “average trend” but drawing something that bounds the conditions expected in practical applications.

The points raised in the previous paragraph generally coincide with those that have been discussed in the reports of DOE/ASME Tasks 3 and 5, and they are being investigated within the Task Force on Creep-Fatigue of the Subgroup on Elevated Temperature Design of the Standards Committee of the ASME Boiler and Pressure Vessel Committee Section III. The recommendations of this report could be reflected to the work scope of the Task Force to ensure that it is necessary and sufficient for short-term improvement with newly proposed concepts being incorporated.

The second step corresponds to long term, where the simplified test approach is most promising particularly from the viewpoint of simplicity which is of prime importance in the application to actual design performed in various elevated temperature fields by various designers some of whom may not be as familiar with academic and technical details of creep-fatigue phenomena as those currently involved in writing creep-fatigue rules in a highly sophisticated society. A road map is to be prepared to further investigate the approach and materialize it by gathering available resources effectively.

# 5. Conclusions

This report described the results of investigation on Task 10 of DOE/ASME Materials NGNP/Generation IV Project based on a contract between ASME Standards Technology, LLC (ASME ST-LLC) and Japan Atomic Energy Agency (JAEA). Task 10 is to Update and Improve Subsection NH – Alternative Simplified Creep-Fatigue Design Methods.

Five newly proposed promising creep-fatigue evaluation methods were investigated. Those are 1) modified ductility exhaustion method, 2) strain range separation method, 3) approach for pressure vessel application, 4) hybrid method of time fraction and ductility exhaustion, and 5) simplified model test approach.

The outlines of those methods are presented first, and predictability of experimental results of these methods is demonstrated using the creep-fatigue data collected in previous Tasks 3 and 5. All the methods (except the simplified model test approach which is not ready for application) predicted experimental results fairly accurately. On the other hand, predicted creep-fatigue life in long-term regions showed considerable differences among the methodologies. These differences come from the concepts each method is based on.

All the new methods investigated in this report have advantages over the currently employed time fraction rule and offer technical insights that should be thought much of in the improvement of creep-fatigue evaluation procedures.

The main points of the modified ductility exhaustion method, the strain range separation method, the approach for pressure vessel application and the hybrid method can be reflected in the improvement of the current time fraction rule. The simplified mode test approach would offer a whole new advantage including robustness and simplicity which are definitely attractive but this approach is yet to be validated for implementation at this point.

Therefore, this report recommends the following two steps as a course of improvement of NH based on newly proposed creep-fatigue evaluation methodologies. The first step is to modify the current approach by incorporating the partial advantages the new method offer, and the second step is to replace the current method by the simplified test approach when it has become technically mature

enough.

The recommendations are basically in line with the work scope of the Task Force on Creep-Fatigue of the Subgroup on Elevated Temperature Design of the Standards Committee of the ASME Boiler and Pressure Vessel Committee Section III.

## References


1. ASME Boiler and Pressure Vessel Code, Division 1 Subsection NH, 2007
2. DOE/ASME Generation IV Materials Project Task 3 Report
3. DOE/ASME Generation IV Materials Project Task 5 Report
4. Kawasaki, N. et al., Recent Design Improvements of Elevated Temperature Structural Design Guide for DFBR in Japan, Transactions of the 15th International Conference on Structural Mechanics in Reactor Technology, Volume IV (1999) 161.
5. RCC-MR 2002, Design and Construction Rules for Mechanical components of FBR nuclear islands and high temperature applications, AFCEN, 2002 Edition
6. Takahashi, Y., Study on creep-fatigue evaluation procedures for high-chromium steels – Part I: Test results and life prediction based on measured stress relaxation, International Journal of Pressure Vessels and Piping, 85 (2008) 406-422.
7. Hoffelner, W., A Strain Range Partitioning type approach for the determination of creep-fatigue (cyclic creep) in modified 9Cr 1Mo steel, RWH/Oberrohrdorf, March 2008
8. Spera, D. A., The calculation of elevated-temperature cyclic life considering low-cycle fatigue and creep, NASA Technical Note, NASA TN D-5317, 1969.
9. Prager, M., ASME ST-LLC Research Project Extended Low Chrome Steel Fatigue Rules BPVC(#2) – RFP-ASME ST-07-04, An Approach for Pressure Vessel Applications of 2 1/4 Cr-1Mo-V and Similar Materials
10. High Pressure Institute of Japan, Creep-Fatigue Life Evaluation Scheme for Ferritic Component at Elevated Temperature, HPIS C107 TR 2005 (2005)
11. Jetter, R. (1998) “An Alternate Approach to Evaluation of Creep-Fatigue Damage for High Temperature Structural Design Criteria” PVP-Vol. 5 Fatigue , Fracture, and High Temperature Design Methods in Pressure Vessel and Piping, Book No. H01146 – 1998
12. “Companion Guide to the ASME Boiler & Pressure Vessel Code, Volume 1” Second Edition, 2006, Edited by K. R. Rao, ASME Press
13. Jetter, R. (1998) “An Alternate Approach to Evaluation of Creep-Fatigue Damage for High Temperature Structural Design Criteria” PVP-Vol. 5 Fatigue , Fracture, and High Temperature Design Methods in Pressure Vessel and Piping, Book No. H01146 – 1998
14. Kasahara, N., Nagata, T., Iwata, K., and Negishi, H., Advanced Creep-Fatigue Evaluation Rule for Fast Breeder Reactor Components: Generalization of Elastic Follow-up Model,” Nuclear Engineering and Design 155 499-518, Elsevier Science S. A.

15. Takakura, K., Ueta, M., Dosaki, K., Wada, H., Hayashi, M., Ozaki, H., and Ooka, Y., 1995, “Elevated Temperature Structural Design Guide for DFBR in Japan,” Transactions of the 13th International Conference on Structural Mechanics in Reactor Technology
16. Takakura, K., Ueta, M., Dosaki, K., Wada, H., Hayashi, M., Ozaki, H., and Ooka, Y., 1993, “Improvement of Elevated Temperature Structural Design Guide for DFBR in Japan,” SMiRT-12, Elsevier Science Publishers B. V.
17. Tanaka, C., Watashi, K., Umeda, H., Kikuchi, M., Iwata, K., 1993, “Creep-fatigue failure test and analysis of a vessel-type structure subjected to cyclic thermal transients” Nuclear Engineering and Design 140 349-372, Elsevier Science S. A.
18. Nickel, H., Schubert, F., Breitling, H., Bodmann, E., “Development and Qualification of Materials for Structural Components for High-Temperature Gas-Cooled Reactor” 1990 Nuclear Engineering and Design 121 183-192 Elsevier Science Publishers B. V.
19. Kobatake, K., Ohta, H., Ishiyama, H., Ueno, O., "Simplified Model Tests of SUS304 Stainless Steel for an Alternate Approach to Creep-Fatigue Damage Evaluation of High Temperature Structural Design" (!999) PVP Conf. Boston, MA
20. Asayama, T. and Jetter, R., An Overview of Creep-Fatigue Damage Evaluation Methods and an Alternative Approach, (2008) PVP Conf. Chicago, IL

# Appendix A

TableA.1 Creep fatigue experiment data of Mod.9Cr-1Mo

| Heat treatment | Test Condition | Controle | Temperature (℃) | strain range (%) | Hold time Ten.(hr) | Hold time Comp.(hr) | Strain rate (%/sec) | Plastic strain | Nf (cycles) | The authority |
|---|---|---|---|---|---|---|---|---|---|---|
| NT | Air | Strain | 482 | 1 | 0.01 | | 0.4 | 0.59 | 3599 | ORNL-JAPC-USDOE |
| NT+SR | Air | Strain | 500 | 0.500 | 0.0167 | | 0.100 | 0.22 | 19468 | JAEA |
| NT+SR | Air | Strain | 500 | 1.510 | 0.0167 | | 0.100 | 1.17 | 1232 | JAEA |
| NT+SR | Air | Strain | 500 | 0.700 | 0.167 | | 0.100 | 0.42 | 6485 | JAEA |
| NT+SR | Air | Strain | 500 | 1.000 | 0.167 | | 0.100 | 0.74 | 2070 | JAEA |
| NT+SR | Air | Strain | 500 | 0.507 | 1 | | 0.100 | 0.254 | 20686 | JAEA |
| NT+SR | Air | Strain | 500 | 0.500 | | 0.0167 | 0.100 | 0.23 | 8958 | JAEA |
| NT+SR | Air | Strain | 500 | 0.500 | | 0.05 | 0.100 | 0.23 | 6717 | JAEA |
| NT+SR | Air | Strain | 500 | 1.010 | | 0.083 | 0.100 | | 1404 | JAEA |
| NT | Air | Strain | 550 | 1.2 | 0.0167 | | 0.1 | 1.01 | 771 | IGCAR |
| NT+SR | Air | Strain | 550 | 0.345 | 0.1 | | 0.001 | 0.151 | 56097 | JAEA |
| NT+SR | Air | Strain | 550 | 0.498 | 0.1 | | 0.100 | 0.255 | 16093 | JAEA |
| NT+SR | Air | Strain | 550 | 0.693 | 0.1 | | 0.100 | 0.433 | 3568 | JAEA |
| NT+SR | Air | Strain | 550 | 0.991 | 0.1 | | 0.100 | 0.768 | 1749 | JAEA |
| NT+SR | Air | Strain | 550 | 1.94 | 0.1 | | 0.5 | 1.64 | 339 | NRIMP1 |
| NT+SR | Air | Strain | 550 | 1.52 | 0.1 | | 0.5 | 1.2 | 743 | NRIMP1 |
| NT+SR | Air | Strain | 550 | 1.08 | 0.1 | | 0.5 | 0.78 | 1180 | NRIMP1 |
| NT+SR | Air | Strain | 550 | 0.84 | 0.1 | | 0.5 | 0.58 | 2550 | NRIMP1 |
| NT+SR | Air | Strain | 550 | 0.7 | 0.1 | | 0.5 | 0.44 | 3410 | NRIMP1 |
| NT+SR | Air | Strain | 550 | 0.52 | 0.1 | | 0.5 | 0.26 | 13100 | NRIMP1 |
| NT+SR | Air | Strain | 550 | 1.490 | 0.167 | | 0.100 | 1.229 | 1065 | JAEA |
| NT+SR | Air | Strain | 550 | 1.001 | 0.167 | | 0.100 | 0.768 | 1067 | JAEA |
| NT+SR | Air | Strain | 550 | 1.001 | 0.167 | | 0.100 | 0.766 | 1197 | JAEA |
| NT | Air | Strain | 550 | 1.2 | 0.167 | | 0.1 | 0.96 | 736 | IGCAR |
| NTA | Air | Strain | 550 | 1 | 0.167 | | 0.1 | 0.786 | 1968 | EPRI/CRIEPI |
| NTA | Air | Strain | 550 | 0.5 | 0.167 | | 0.1 | 0.294 | 10120 | EPRI/CRIEPI |
| NT | Air | Strain | 550 | 0.7 | 0.167 | | 0.1 | | 2751 | CEA |
| NT | Air | Strain | 538 | 0.78 | 0.25 | | 0.4 | 0.52 | 3537 | ORNL-JAPC-USDOE |
| NT+SR | Air | Strain | 550 | 1.500 | 0.333 | | 0.100 | 1.188 | 1184 | JAEA |
| NT+SR | Air | Strain | 550 | 0.998 | 0.333 | | 0.100 | 0.775 | 2290 | JAEA |
| NT | Air | Strain | 538 | 0.5 | 0.5 | | 0.4 | 0.24 | 6975 | ORNL-JAPC-USDOE |
| NT | Air | Strain | 538 | 0.79 | 0.5 | | 0.4 | 0.56 | 1530 | ORNL-JAPC-USDOE |
| NT | Air | Strain | 538 | 0.51 | 0.5 | | 0.4 | 0.25 | 7770 | ORNL |
| NT | Air | Strain | 550 | 1 | 0.5 | | 0.1 | | 1920 | CEA |
| NT | Air | Strain | 550 | 0.7 | 0.5 | | 0.1 | | 3778 | CEA |
| NT | Air | Strain | 550 | 0.6 | 0.5 | | 0.1 | | 4046 | CEA |
| NT | Air | Strain | 550 | 0.6 | 0.5 | | 0.1 | | 4802 | CEA |
| NT | Air | Strain | 538 | 1 | 1 | | 0.4 | 0.67 | 1734 | ORNL-JAPC-USDOE |
| NT | Air | Strain | 538 | 1 | 1 | | 0.4 | 0.55 | 2654 | ORNL-JAPC-USDOE |
| NT | Air | Strain | 538 | 0.5 | 1 | | 0.4 | 0.22 | 6787 | ORNL-JAPC-USDOE |
| NTA | Air | Strain | 550 | 1 | 1 | | 0.1 | 0.788 | 1885 | EPRI/CRIEPI |
| NT+SR | Air | Strain | 550 | 0.361 | 1 | | 0.002 | 0.171 | 13012 | JAEA |
| NT+SR | Air | Strain | 550 | 0.494 | 1 | | 0.100 | 0.252 | 6453 | JAEA |
| NT+SR | Air | Strain | 550 | 0.692 | 1 | | 0.100 | 0.446 | 2623 | JAEA |
| NT+SR | Air | Strain | 550 | 1.003 | 1 | | 0.100 | 0.747 | 1266 | JAEA |
| NT+SR | Air | Strain | 550 | 0.72 | 1 | | 0.5 | 0.52 | 2420 | NRIMP1 |
| NT+SR | Air | Strain | 550 | 1.94 | 1 | | 0.5 | 1.66 | 360 | NRIMP1 |
| NT+SR | Air | Strain | 550 | 1.46 | 1 | | 0.5 | 1.18 | 491 | NRIMP1 |
| NT+SR | Air | Strain | 550 | 0.98 | 1 | | 0.5 | 0.72 | 944 | NRIMP1 |
| NT | Air | Strain | 550 | 0.6 | 1.5 | | 0.1 | | 3560 | CEA |
| NT | Air | Strain | 538 | 0.5 | 3 | | 0.4 | 0.33 | 3113 | ORNL-JAPC-USDOE |
| NT | Air | Strain | 550 | 1.2 | | 0.0167 | 0.1 | 0.96 | 600 | IGCAR |
| NTA | Air | Strain | 550 | 1 | | 0.167 | 0.1 | 0.745 | 1006 | EPRI/CRIEPI |
| NTA | Air | Strain | 550 | 0.5 | | 0.167 | 0.1 | 0.297 | 2822 | EPRI/CRIEPI |
| NT | Air | Strain | 550 | 0.7 | | 0.167 | 0.1 | | 2121 | CEA |
| NT | Air | Strain | 538 | 0.5 | | 0.25 | 0.4 | 0.24 | 8840 | ORNL |
| NT | Air | Strain | 550 | 0.6 | | 0.5 | 0.1 | | 3362 | CEA |
| NTA | Air | Strain | 550 | 1 | | 1 | 0.1 | 0.745 | 956 | EPRI/CRIEPI |
| NT+SR | Air | Strain | 550 | 0.373 | | 1 | 0.002 | 0.187 | 7347 | JAEA |
| NT+SR | Air | Strain | 550 | 0.505 | | 1 | 0.100 | 0.18 | 3293 | JAEA |
| NT | Air | Strain | 550 | 0.6 | | 1.5 | 0.1 | | 3677 | CEA |
| NT | Air | Strain | 550 | 1 | | 2 | 0.1 | | 964 | CEA |
| NT+SR | Air | Strain | 550 | 0.724 | | 10 | 0.002 | 0.536 | 1428 | JAEA |
| NTA | Air | Strain | 550 | 1 | 0.167 | 0.167 | 0.1 | 0.864 | 1142 | EPRI/CRIEPI |
| NTA | Air | Strain | 550 | 0.5 | 0.167 | 0.167 | 0.1 | 0.331 | 3871 | EPRI/CRIEPI |
| NTA | Air | Strain | 550 | 1 | 1 | 1 | 0.1 | 0.868 | 734 | EPRI/CRIEPI |
| NT | Air | Strain | 593 | 0.51 | 1 | | 0.4 | 0.18 | 2926 | ORNL-JAPC-USDOE |
| NT | Air | Strain | 593 | 1 | 1 | | 0.4 | 0.73 | 1081 | ORNL-JAPC-USDOE |
| NT | Air | Strain | 593 | 1 | 1 | | 0.4 | 0.18 | 400 | ORNL-JAPC-USDOE |
| NT | Air | Strain | 593 | 0.5 | 0.5 | | 0.4 | 0.28 | 4202 | ORNL-JAPC-USDOE |
| NT | Air | Strain | 593 | 0.5 | 0.5 | | 0.4 | 0.3 | 3360 | ORNL-JAPC-USDOE |
| NT | Air | Strain | 593 | 0.5 | 1 | | 0.4 | 0.32 | 2882 | ORNL-JAPC-USDOE |
| NT | Air | Strain | 593 | 0.4 | 2 | | 0.4 | 0.17 | 2958 | ORNL-JAPC-USDOE |

| | | | | | | | | | | |
|---|---|---|---|---|---|---|---|---|---|---|
| NT | Air | Strain | 593 | 0.51 | 2 | | 0.4 | 0.34 | 3352 | ORNL-JAPC-USDOE |
| NT | Air | Strain | 593 | 0.5 | 1 | | 0.4 | 0.32 | 3207 | ORNL |
| NT | Air | Strain | 593 | 0.5 | 1 | | 0.4 | 0.37 | 2870 | ORNL |
| NT | Air | Strain | 600 | 1.2 | 0.0167 | | 0.1 | 0.8 | 657 | IGCAR |
| NT | Air | Strain | 600 | 1.2 | 0.167 | | 0.1 | 1.04 | 545 | IGCAR |
| NT | Air | Strain | 600 | 1.2 | 0.5 | | 0.1 | 0.99 | 506 | IGCAR |
| NT+SR | Air | Strain | 600 | 0.996 | 0.333 | | 0.100 | 0.85 | 1452 | JAEA |
| NT+SR | Air | Strain | 600 | 0.518 | 1 | | 0.100 | 0.34 | 3630 | JAEA |
| NT+SR | Air | Strain | 600 | 1.86 | 0.1 | | 0.5 | 1.62 | 361 | NRIMP1 |
| NT+SR | Air | Strain | 600 | 1.52 | 0.1 | | 0.5 | 1.32 | 580 | NRIMP1 |
| NT+SR | Air | Strain | 600 | 1.4 | 0.1 | | 0.5 | 1.16 | 596 | NRIMP1 |
| NT+SR | Air | Strain | 600 | 1.04 | 0.1 | | 0.5 | 0.82 | 1180 | NRIMP1 |
| NT+SR | Air | Strain | 600 | 0.8 | 0.1 | | 0.5 | 0.6 | 1340 | NRIMP1 |
| NT+SR | Air | Strain | 600 | 0.52 | 0.1 | | 0.5 | 0.3 | 3910 | NRIMP1 |
| NT+SR | Air | Strain | 600 | 0.46 | 0.1 | | 0.5 | 0.26 | 5840 | NRIMP1 |
| NT+SR | Air | Strain | 600 | 2.02 | 1 | | 0.5 | 1.82 | 291 | NRIMP1 |
| NT+SR | Air | Strain | 600 | 1.48 | 1 | | 0.5 | 1.24 | 398 | NRIMP1 |
| NT+SR | Air | Strain | 600 | 1.04 | 1 | | 0.5 | 0.84 | 1000 | NRIMP1 |
| NT+SR | Air | Strain | 600 | 0.82 | 1 | | 0.5 | 0.62 | 1090 | NRIMP1 |
| NT+SR | Air | Strain | 600 | 0.74 | 1 | | 0.5 | 0.56 | 954 | NRIMP1 |
| NT+SR | Air | Strain | 600 | 1.001 | | 0.333 | 0.100 | 0.501 | 589 | JAEA |
| NT aged 50kh | Air | Strain | 538 | 0.51 | 0.25 | | 0.4 | 0.29 | 4791 | ORNL-JAPC-USDOE |
| NT aged 75kh | Air | Strain | 538 | 0.51 | 0.5 | | 0.4 | 0.35 | 3535 | ORNL-JAPC-USDOE |
| NT aged 50kh | Air | Strain | 538 | 0.78 | 0.5 | | 0.4 | 0.54 | 2590 | ORNL-JAPC-USDOE |
| NT aged 50kh | Air | Strain | 538 | 0.76 | 0.25 | | 0.4 | 0.55 | 2894 | ORNL-JAPC-USDOE |
| NT aged 50kh | Air | Strain | 593 | 0.5 | 0.5 | | 0.4 | 0.38 | 1652 | ORNL-JAPC-USDOE |
| NT aged 50kh | Air | Strain | 593 | 0.51 | 0.5 | | 0.4 | 0.37 | 1221 | ORNL-JAPC-USDOE |
| NT aged 50kh | Air | Strain | 593 | 0.5 | 1 | | 0.4 | 0.37 | 2303 | ORNL-JAPC-USDOE |
| NT | vacuum | Strain | 593 | 0.5 | 0.5 | | 0.4 | 0.24 | 4150 | ORNL-JAPC-USDOE |
| NT | vacuum | Strain | 593 | 0.5 | 1 | | 0.4 | 0.27 | 2900 | ORNL-JAPC-USDOE |
| NT+SR | vacuum | Strain | 600 | 0.978 | 0.167 | | 0.1 | 0.693 | 6627 | TOKYO Univ. |
| NT+SR | vacuum | Strain | 600 | 1.972 | 0.167 | | 0.1 | 1.663 | 2547 | TOKYO Univ. |
| NT+SR | vacuum | Strain | 600 | 1.988 | | 0.017 | 0.1 | 0.994 | 1674 | TOKYO Univ. |
| NT+SR | Na | Strain | 550 | 0.504 | 1 | 0 | 0.1 | | 3346 | JAEA |
| NT+SR | Na | Strain | 550 | 0.5 | 0 | 1 | 0.1 | | 12120 | JAEA |
| NT | Air | Stress | 550 | 0.7 | 0.0083 | | 0.1 | 0.18 | 2533 | CEA |
| NT | Air | Stress | 550 | 0.7 | 0.0167 | | 0.1 | 0.23 | 1900 | CEA |
| NT | Air | Stress | 550 | 0.7 | 0.05 | | 0.1 | 0.31 | 2050 | CEA |
| NT | Air | Stress | 550 | 0.7 | 0.1 | | 0.1 | 0.39 | 1094 | CEA |
| NT | Air | Stress | 550 | 0.7 | 0.1667 | | 0.1 | 0.44 | 1270 | CEA |
| NT | Air | Stress | 550 | 0.7 | 0.5 | | 0.1 | 0.7 | 880 | CEA |
| NT | Air | Stress | 550 | 1 | 0.0063 | | 0.1 | 0.3 | 999 | CEA |
| NT | Air | Stress | 550 | 0.5 | 0.0125 | | 0.1 | 0.1 | 5550 | CEA |
| NT | Air | Stress | 550 | 0.5 | 0.0175 | | 0.1 | 0.1 | 6995 | CEA |
| NT | Air | Stress | 550 | 0.7 | 0.0528 | | 0.1 | 0.3 | 1600 | CEA |
| NT | Air | Stress | 550 | 0.4 | 0.0972 | | 0.1 | 0.1 | 8836 | CEA |
| NT | Air | Stress | 550 | 0.5 | 0.1497 | | 0.1 | 0.2 | 4032 | CEA |
| NT | Air | Stress | 550 | 1 | | 0.0081 | 0.1 | 0.3 | 849 | CEA |
| NT | Air | Stress | 550 | 0.5 | | 0.0161 | 0.1 | 0.1 | 3170 | CEA |
| NT | Air | Stress | 550 | 0.5 | | 0.0169 | 0.1 | 0.1 | 2260 | CEA |
| NT | Air | Stress | 550 | 0.7 | | 0.0667 | 0.1 | 0.3 | 1415 | CEA |
| NT | Air | Stress | 550 | 0.4 | | 0.0908 | 0.1 | 0.1 | 4300 | CEA |
| NT | Air | Stress | 550 | 0.5 | | 0.1858 | 0.1 | 0.2 | 1676 | CEA |